International Federation of Clinical Chemistry and Laboratory Medicine

eJIFCC

Communications and Publications Division (CPD) of the IFCC

November 2025
Volume 36
Number 4
ISSN 1650-3414

Co-Editor-in-Chief:
Qing H. Meng, MD, PhD, DABCC, FADLM
Department of Laboratory Medicine, The University of Texas MD Anderson Cancer Center, Houston, USA

Co-Editor-in-Chief:
Kannan Vaidyanathan, MD, FRCP (Edin.) (UK), FFSc (Research) (RCPA) (Australia), FACBI
Department of Biochemistry
Believers Church Medical College Hospital
Thiruvalla, Kerala, India

E-mail: ejifcc@ifcc.org

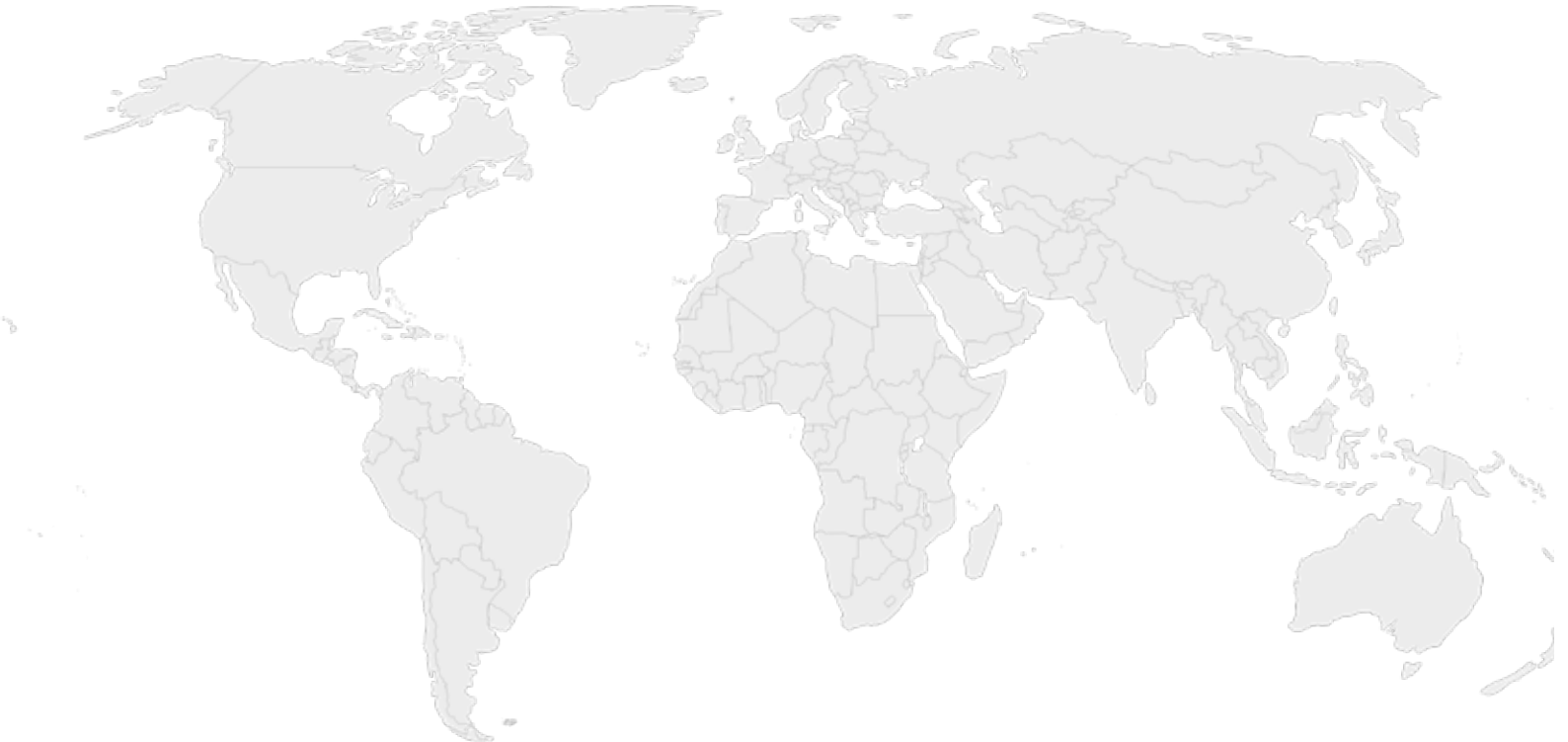

In this Issue

In this Issue

In this Issue

Research Article

Screening for Diabetes after Solid Organ Transplantation: A 10-Year Retrospective Study

Ridwan B. Ibrahim[1, 2], Sneha Kumar[1], Sahil Malik[1,2], Joseph A. Spinner[3], Daniel H. Leung[4], Sridevi Devaraj[1, 2*]

[1]*Department of Pathology and Immunology, Baylor College of Medicine, Houston, TX, USA*
[2]*Department of Pathology, Texas Children's Hospital, Houston, TX, USA*
[3]*Department of Pediatrics-Cardiology, Baylor College of Medicine, Houston, TX, USA*
[4]*Department of Pediatrics, Baylor College of Medicine and Division of Gastroenterology, Hepatology and Nutrition, Texas Children's Hospital, Houston, TX USA*

Article Info

[*]***Corresponding Author:***
Sridevi Devaraj, Ph.D., DABCC, FADLM, FRSC
Department of Pathology and Immunology
Baylor College of Medicine, Texas Children's Hospital
6621 Fannin Street, Houston, TX 77030
E-mail: sxdevara@texaschildrens.org

Keywords

Post-transplant diabetes mellitus, Immunosuppression, Solid organ transplant

Abstract

Post-transplantation diabetes mellitus (PTDM) is a common and important complication after solid organ transplantation, affecting long-term outcomes. Graft rejection, decreased patient survival, infections and increased cardiovascular risk are associated with PTDM and may arise from both transplant-related and traditional risk factors. Early screening for PTDM is crucial for early detection and management. Despite clinical guidelines recommending regular screening for PTDM, screening rates remain suboptimal. This retrospective study analyzes PTDM screening rates between January 2014-January 2024 among pediatric kidney, liver, heart and lung transplant recipients at a large quaternary academic pediatric transplant center. PTDM screening rates vary by organ type, with kidney transplant patients at 19.4%, liver transplant patients at 14.6%, heart transplant patients at 34.3% and lung transplant patients at 91.7%. These lower-than-expected rates of PTDM screening among high risk pediatric- kidney, liver and heart transplant pediatric population highlight the need for improved screening protocols and provider education post-transplantation.

Introduction

Post-transplantation diabetes mellitus (PTDM), first described in kidney transplant recipients in 1964, remains a leading complication after solid organ transplantation [1,2]. In 2014, an International Expert Panel of clinicians/researchers recommended expansion of the PTDM screening tests to include hemoglobin A1c levels since the American Diabetes Association (ADA) has incorporated hemoglobin A1c (>6.5%) as a diagnostic criterion for diabetes mellitus in the general population although the gold standard for diagnosing PTDM still remains OGTT [3,4]. However, caution must be exercised not to use A1c testing too soon after transplantation (within 45 days after transplantation) as a normal HbA1c does not rule of the presence of post-transplantation anemia and/or dynamic renal allograft function [5]. Although this transient post-transplant hyperglycemia (within 45 days after transplantation) is an important risk factor for subsequent PTDM, it should be excluded from PTDM diagnosis as this is exceptionally common in early transplant period due to high steroid and tacrolimus exposures [6,8]. PTDM should be screened for in clinically stable patients >45 days after transplantation [4]. Different factors have led to variations in the reported incidence for PTDM [1].; it has been reported in 2.5-25% of liver transplant recipients, 4-25% in kidney transplant recipients, 30-35% in lung transplant and 4-40% in heart transplant recipients [9-13]. Early detection of PTDM is critical to reduce the risks and complications of diabetes mellitus, with post-transplant follow-up of patients with transient HbA1c levels >5.7-6.4% or higher at 3, 6, 9 and 12 months, followed by annual screening thereafter [1, 14-16].

In this study, we performed a 10-year retrospective cohort study to assess the frequency of PTDM screening in our large quaternary academic pediatric transplant medical center following publication of the 2014 guideline [4].

Methods

Patient Population

This single center, retrospective cohort study included patients who received a solid organ transplant (liver, kidney, heart and lung) at the Texas Children's Hospital between January 2014 and January 2024. Patient characteristics are summarized in Table 1 which shows similar representation of male and females.

Table 1: Sociodemographic characteristics of solid organ recipients at Texas Children's Hospital (TCH) between 2014-2024.

Variable	Total
	N (%)
Liver Transplant recipient	336 (100)
Mean age at transplant (years)	6.51
Male	167 (49.7)
Female	169 (50.3)
Heart Transplant recipient	268 (100)
Mean age at transplant (years)	8
Male	152 (56.7)
Female	116 (43.3)
Lung transplant recipient	96 (100)
Mean age at transplant (years)	10.43
Male	43 (44.8)
Female	53 (55.2)
Kidney transplant recipient	284 (100)
Mean age at transplant (years)	13.11
Male	167 (58.8)
Female	117 (41.2)

The primary outcome was screening rates of PTDM within the first-year post-transplantation, as recommended by international guidelines [4]. Screening adherence was defined as having ≥ 1 fasting glucose test or HbA1c test within the first year following transplantation. Test orders from 46 days post-transplantation were assessed to diagnose PTDM in this study. Adherence rate was calculated and described for each organ group.

Results

Over the 10-year period, 984 solid organ transplantations were performed: 336 liver transplants, 268 heart transplants, 96 lung transplants and 284 kidney transplants (Table 2).

Table 2: Ten-years PTDM screening compliance data in solid organ recipient patients.

Organ Transplant	Liver	Heart	Lung	Kidney
Number of Recipients	336	268	96	284
Post-transplant OGTT test (≥45-365 days)				
Total number of tests ordered	0	0	0	0
Post-transplant HbA1c test (≥45-365 days)				
Total number of tests ordered	49	92	88	55
Percentage test ordering compliance	14.6	34.3	91.7	19.4
Total number of tests completed	47	92	88	55

Of these recipients, none had OGTT test orders ≥45 days but 14.6% (n=49), 34.3% (n=92), 91.7% (n=88) and 19.4% (n=55) of recipients have HbA1c orders for PTDM screening in liver, heart, lung, and kidney transplant recipients respectively (Table 2).

For liver, heart, lung and kidney recipients who had PTDM screening performed, the incidence for PTDM was 27.6%, 17.4%, 17.0% and 20.0% (Figure 1) while 23.4%, 15.2%, 34.1% and 20.0% were in the prediabetes class (Figure 1).

Figure 1: Solid organ recipient's classification based on HbA1c levels post-transplantation.

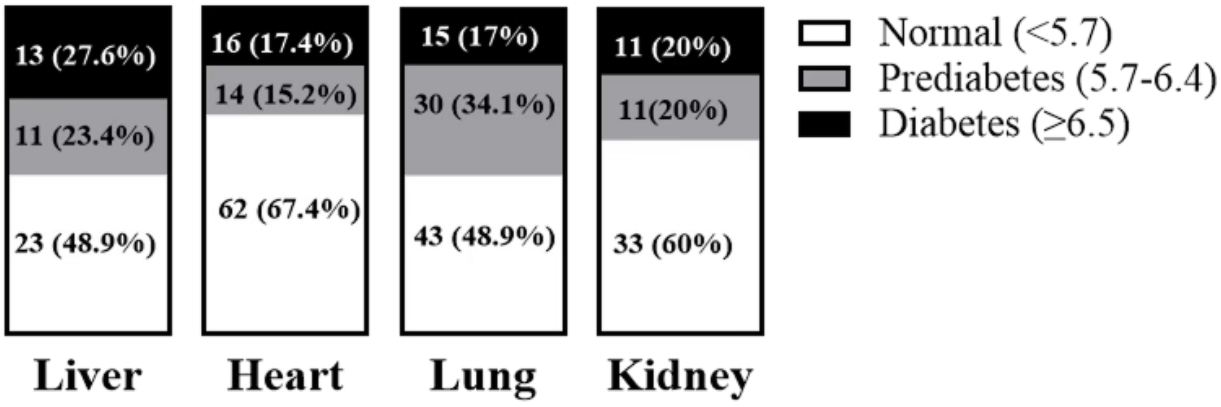

Of the recipients who developed PTDM, 100% of liver and lung transplant recipients were placed on injectable insulin therapy across the various race/ethnic groups (Table 3). Only one kidney transplant recipient was not placed on either insulin or metformin (Table 3). In the heart transplant group, 100% of Hispanic white and 80% of Non-Hispanic black recipients were placed on insulin therapy while 100% of Non-Hispanic whites and 20% of Non-Hispanic blacks were placed on metformin (Table 3).

Table 3: Ten-years PTDM screening compliance data in solid organ recipient patients.

Liver Transplant recipient					
Ethnicity/Race	**Non-Hispanic White**	**Hispanic White**	**Non-Hispanic Black**	**Asian**	**Others**
Prediabetes	4	6	1	-	-
Diabetes	8	4	1	-	-
On Insulin	8	4	1		
On Metformin					
Heart Liver recipient					
Prediabetes	4	7	3		
Diabetes	2	9	5		
On Insulin	0	9	4		
On Metformin	2		1		
Lung Transplant recipient					
Prediabetes	20	3	3	3	1
Diabetes	7	7	-	-	1
On Insulin	7	7	-	-	1
On Metformin	-	-	-	-	-
Kidney transplant recipient					
Prediabetes	3	4	3	1	
Diabetes	1	7	3		
On Insulin	1	6	3		
On Metformin	-	-	-		

Discussion

Post-transplantation diabetes mellitus (PTDM) describes newly diagnosed mellitus in the post transplantation setting [4]. Risk factors for PTDM can be multifactorial [17,18] with obesity, immunosuppression with glucocorticoids, tacrolimus and other drugs being the most significant post-transplant risk factors [2,19-21]. The 2014 International consensus guidelines expanded the screening parameters for PTDM to include HbA1c as OGTT which is the gold standard is not widely used as they are time consuming and impractical in many settings [4].

In this study, we assessed the screening rates for post-transplant diabetes mellitus screening in patients who received solid organ transplants at Texas Children's Hospital. We found that no patient had orders for the OGTT test within the first year, which is the recommended gold standard for diagnosing PTDM. This observation is similar to previous reports highlighting the time consuming and impractical nature of OGTT in large transplant programs where fasting glucose and/or HbA1c tests are mostly used [1,5, 22-24]. Despite the ease of ordering HbA1c, PTDM screening remained very low except for lung transplant recipients (Table 2).

Our data is similar to previous reports of PTDM occurrence in solid organ transplant recipients [1] but a lower rate for lung transplant recipient likely due to increased PTDM screening in this group. Due to different risk factors such as age, alcoholic cirrhosis hepatitis C infection, liver steatosis etc. for liver [25,26]; advanced age, elevated pre-transplant HbA1c level, cystic fibrosis KCNJ11 gene polymorphism etc. for lungs [27,28]; advanced age, pre-and post-transplant HCV infections etc. for kidney [29,30]; cytomegalovirus infection and immunosuppressive medications for heart [31], solid organ transplant recipients are at risk of developing PTDM. But patients who are prediabetic after transplantation are at higher risk as it is a harbinger for PTDM [1]. Identifying patients at risk of PTDM is important as patients can easily be counseled on dietary and lifestyle changes; or placed on insulin and other oral anti-diabetic therapies [1,6]. One limitation of this study was the exclusion of bone marrow transplant patients as we focus only on solid organ transplants. Although we examined a relatively large cohort of patients, our study is a single-centre study necessitating more studies/data from other large transplant centres nationwide or internationally for comparison.

Recently, an update to the 2014 guideline was published stressing the use of OGTT in the diagnosis of PTDM citing that hemoglobin A1c lacks diagnostic sensitivity and advocating for more research in identifying the best way to identify recipients are risk [2]. However, in a pediatric population, performing OGTT does represent a challenge.

Patient/physician education on the risk of PTDM and importance of complying with PTDM screening is necessary. Continuous knowledge of latest guidelines and adherence to them might help change physician perspective and hopeful increase their compliance for PTDM screen for solid organ transplant recipient. Additionally, programmed notifications (best practice alerts) in the electronic medical records of solid organ recipient could help remind providers at regular intervals to order these tests for their patients [32].

Credit author statement

The following statements should be used "S.D.: conceptualization, methodology; R.I, S.K, SM.: data curation; R.I.: writing - original draft preparation; S.D.: supervision; RI, SK, SM, JS, DL, SD,.: writing - reviewing and editing. All authors have read and agreed to the published version of the manuscript.

Funding and Data Availability Statement

This research received no external funding. Data will be made available upon request to the Corresponding Author.

Acknowledgments

Ridwan B Ibrahim was supported by the Ching-Nan Ou Endowment in Clinical Chemistry.

Conflicts of Interest

The authors declare no conflict of interest.

Use of AI and AI-Assisted Technologies

No AI tools were utilized for this paper.

References

1. Pham PT, Sarkar M, Pham PM, Pham PC. Diabetes Mellitus After Solid Organ Transplantation. In: Feingold KR, Anawalt B, Blackman MR, Boyce A, Chrousos G, Corpas E, et al., editors. Endotext. South Dartmouth (MA)2000.
2. Sharif A, Chakkera H, de Vries APJ, Eller K, Guthoff M, Haller MC, et al. International consensus on post-transplantation diabetes mellitus. Nephrol Dial Transplant. 2024;39(3):531-49.
3. Standards of medical care in diabetes--2011. Diabetes Care. 2011;34 Suppl 1(Suppl 1):S11-61.
4. Sharif A, Hecking M, de Vries AP, Porrini E, Hornum M, Rasoul-Rockenschaub S, et al. Proceedings from an international consensus meeting on posttransplantation diabetes mellitus: recommendations and future directions. Am J Transplant. 2014;14(9):1992-2000.
5. Sharif A, Baboolal K. Diagnostic application of the A(1c) assay in renal disease. J Am Soc Nephrol. 2010;21(3):383-385.
6. Hecking M, Haidinger M, Döller D, Werzowa J, Tura A, Zhang J, et al. Early basal insulin therapy decreases new-onset diabetes after renal transplantation. J Am Soc Nephrol. 2012;23(4):739-749.
7. Chakkera HA, Weil EJ, Castro J, Heilman RL, Reddy KS, Mazur MJ, et al. Hyperglycemia during the immediate period after kidney transplantation. Clin J Am Soc Nephrol. 2009;4(4):853-9.
858. Chakkera HA, Knowler WC, Devarapalli Y, Weil EJ, Heilman RL, Dueck A, et al. Relationship between inpatient hyperglycemia and insulin treatment after kidney transplantation and future new onset diabetes mellitus. Clin J Am Soc Nephrol. 2010;5(9):1669-1675.
9. Davidson J, Wilkinson A, Dantal J, Dotta F, Haller H, Hernández D, et al. New-onset diabetes after transplantation: 2003 International consensus guidelines. Proceedings of an international expert panel meeting. Barcelona, Spain, 19 February 2003. Transplantation. 2003;75(10 Suppl):Ss3-24.
10. Baid S, Cosimi AB, Farrell ML, Schoenfeld DA, Feng S, Chung RT, et al. Posttransplant diabetes mellitus in liver transplant recipients: risk factors, temporal relationship with hepatitis C virus allograft hepatitis, and impact on mortality. Transplantation. 2001;72(6):1066-1072.
11. Knobler H, Stagnaro-Green A, Wallenstein S, Schwartz M, Roman SH. Higher incidence of diabetes in liver transplant recipients with hepatitis C. J Clin Gastroenterol. 1998;26(1):30-33.
12. Ye X, Kuo HT, Sampaio MS, Jiang Y, Bunnapradist S. Risk factors for development of new-onset diabetes mellitus after transplant in adult lung transplant recipients. Clin Transplant. 2011;25(6):885-891.
13. Lieber SR, Lee RA, Jiang Y, Reuter C, Watkins R, Szempruch K, et al. The impact of post-transplant diabetes mellitus on liver transplant outcomes. Clin Transplant. 2019;33(6):e13554.
14. Shabir S, Jham S, Harper L, Ball S, Borrows R, Sharif A. Validity of glycated haemoglobin to diagnose new onset diabetes after transplantation. Transpl Int. 2013;26(3):315-321.
15. Palepu S, Prasad GV. New-onset diabetes mellitus after kidney transplantation: Current status and future directions. World J Diabetes. 2015;6(3):445-455.
16. Solhjoo M, Kumar SC. New Onset Diabetes After Transplant. StatPearls. Treasure Island (FL)2024.
17. Sharif A, Baboolal K. Risk factors for new-onset diabetes after kidney transplantation. Nat Rev Nephrol. 2010;6(7):415-423.
18. Pham PT, Pham PM, Pham SV, Pham PA, Pham PC. New onset diabetes after transplantation (NODAT): an overview. Diabetes Metab Syndr Obes. 2011;4:175-186.
19. Boudreaux JP, McHugh L, Canafax DM, Ascher N, Sutherland DE, Payne W, et al. The impact of cyclosporine and combination immunosuppression on the incidence of posttransplant diabetes in renal allograft recipients. Transplantation. 1987;44(3):376-381.
20. Duijnhoven EMV, Boots JMM, Christiaans MHL, Wolffenbuttel BHR, Hooff JPV. Influence of tacrolimus on glucose metabolism before and after renal transplantation: a

prospective study. J Am Soc Nephrol. 2001;12(3):583-588.
21. Hjelmesaeth J, Hartmann A, Kofstad J, Stenstrom J, Leivestad T, Egeland T, et al. Glucose intolerance after renal transplantation depends upon prednisolone dose and recipient age. Transplantation. 1997;64(7):979-983.
22. Chakkera HA, Weil EJ, Pham PT, Pomeroy J, Knowler WC. Can new-onset diabetes after kidney transplant be prevented? Diabetes Care. 2013;36(5):1406-1412.
23. Pimentel AL, Hernandez MK, Freitas PAC, Chume FC, Camargo JL. The usefulness of glycated albumin for post-transplantation diabetes mellitus after kidney transplantation: A diagnostic accuracy study. Clin Chim Acta. 2020;510:330-336.
24. Pimentel AL, Cavagnolli G, Camargo JL. Diagnostic accuracy of glycated hemoglobin for post-transplantation diabetes mellitus after kidney transplantation: systematic review and meta-analysis. Nephrol Dial Transplant. 2017;32(3):565-572.
25. Gulsoy Kirnap N, Kirnap M, Alshalabi O, Tutuncu NB, Haberal M. Posttransplant Diabetes Mellitus Incidence and Risk Factors in Adult Liver Transplantation Recipients. Acta Endocrinol (Buchar). 2020;16(4):449-453.
26. Campos MB, Riguetto CM, de Fátima Santana Ferreira Boin I, Moura AN. Risk factors associated with diabetes after liver transplant. Arch Endocrinol Metab. 2022;66(2):182-190.
27. Shitrit D, Ollech J, Amital A, Kramer MR. DIABETES MELLITUS FOLLOWING LUNG TRANSPLANTATION: INCIDENCE AND RISK FACTORS. CHEST. 2007;132(4):597A.
28. Du W, Wang X, Zhang D, Zuo X. Retrospective analysis on incidence and risk factors of post-transplant diabetes mellitus after lung transplantation and its association with clinical outcomes. Transplant Immunology. 2024;83:102008.
29. Alkadi M, Thappy S, Abuhelaiqa E, Mahmoud J, Jarman M, Khan SU, et al. Incidence and Risk Factors of Post Transplant Diabetes Mellitus in Kidney Transplant Recipients in Qatar. Transplantation. 2018;102:S648.
30. Siraj ES, Abacan C, Chinnappa P, Wojtowicz J, Braun W. Risk Factors and Outcomes Associated With Posttransplant Diabetes Mellitus in Kidney Transplant Recipients. Transplantation Proceedings. 2010;42(5):1685-1689.
31. Newman JD, Schlendorf KH, Cox ZL, Zalawadiya SK, Powers AC, Niswender KD, et al. Post-transplant diabetes mellitus following heart transplantation. The Journal of Heart and Lung Transplantation. 2022;41(11):1537-1546.
32. Ibrahim RB, Olayinka L, Chokkalla AK, Devaraj S. Postpartum Glucose Monitoring in Pregnant Women with Gestational Diabetes Mellitus: A Dual Center Experience. Ann Clin Lab Sci. 2024;54(3):331-334.

Research Article

Assessing the Impact of Arm Rotation with Walking Exercise on Blood Glucose and HbA1c Levels in Patients with Diabetes Mellitus: A Hospital Based Study

Tejas Girish Menon[1], Suman Kumar Ray[1], Sukhes Mukherjee[1*]

[1]*Department of Biochemistry, All India Institute of Medical Sciences Bhopal, Madhya Pradesh, India*

Article Info

[*]***Corresponding Author:***
Sukhes Mukherjee
Department of Biochemistry, All India Institute of Medical Sciences Bhopal,
Madhya Pradesh-462020, India
E-mail: sukhes.biochemistry@aiimsbhopal.edu.in

Keywords

Diabetes mellitus, Blood glucose, HbA1c, Arm rotation exercise, Walking, Glycemic control, Physical activity

Abstract

Background: Effective management of blood glucose levels is crucial for individuals with diabetes mellitus, and incorporating physical activity plays a vital role. Recent studies suggest that combining simple, low-impact exercises such as arm rotation and walking can enhance postprandial glycemic control. This study aims to evaluate the impact of a combined arm rotation and walking exercise regimen on postprandial blood glucose and HbA1c levels in people with type 2 diabetes.

Material and methods: A randomized controlled trial was conducted with 92 participants diagnosed with type 2 diabetes, aged 18-82 years. Participants were randomly assigned to an intervention group, which performed a structured exercise protocol involving arm rotation and walking, or a control group, which maintained usual activity. The intervention lasted for 24 weeks, with sessions held five times per week. Blood samples were collected at baseline and after the intervention to measure fasting blood glucose, postprandial blood glucose, and HbA1c levels. Data were analysed using paired t-tests and ANOVA to compare pre- and post-intervention results.

Results: The intervention group showed a significant reduction in postprandial blood glucose levels (mean decrease of 25 mg/dL, $p < 0.01$) and HbA1c levels (mean decrease of 0.5%, $p < 0.05$) after 24 weeks. In contrast, the control group exhibited no significant changes. Adherence to the exercise regimen was high, and no adverse events were reported, indicating good tolerability.

Discussion: The findings suggest that combining arm rotation with walking exercises is an effective and practical approach to improve glycemic control in individuals with type 2 diabetes. The improvements may be attributed to enhanced insulin sensitivity and increased muscle activity. These results support incorporating simple, accessible exercises into daily routines for better diabetes management. Further research is needed to assess long-term benefits and optimal exercise protocols.

Introduction

Diabetes mellitus is a prevalent and complex metabolic disorder characterized by chronic hyperglycemia resulting from defects in insulin secretion, insulin action, or both. It represents a major public health challenge worldwide, with the World Health Organization estimating that over 400 million people are affected globally, and the numbers are projected to rise further in the coming decades [1]. The condition is associated with a range of serious complications, including cardiovascular disease, nephropathy, neuropathy, retinopathy, and an increased risk of infections, which collectively contribute to significant morbidity and mortality [2].

Effective management of type 2 diabetes mellitus (T2DM), the most common form of the disease, involves a multifaceted approach that includes pharmacotherapy, dietary modifications, and physical activity [3]. Among these, regular exercise has been consistently recognized as a cornerstone for improving glycemic control, enhancing insulin sensitivity, and preventing or delaying the onset of complications. Physical activity not only aids in lowering blood glucose levels but also contributes to weight management, blood pressure regulation, and overall cardiovascular health [4].

Despite the well-established benefits of exercise, numerous barriers hinder adherence among diabetic individuals. These include physical limitations, musculoskeletal problems, lack of motivation, time constraints, and limited access to suitable facilities. Additionally, some patients may experience discomfort or adverse events during certain types of physical activity, which can discourage sustained participation. Consequently, there is a growing interest in developing simple, safe, and effective exercise modalities that can be easily integrated into daily routines, especially for populations with limited mobility or comorbidities [5].

Recent research emphasizes the importance of incorporating movement patterns that engage multiple muscle groups and promote circulation to optimize glycemic outcomes. Traditional aerobic exercises, such as brisk walking, cycling, and swimming, are effective but may not be feasible for everyone [6]. Therefore, innovative exercise strategies that combine functional movements with moderate intensity are gaining attention. In this context, the concept of integrating arm movements - particularly rotational motions of the shoulder complex - with walking routines offers a promising approach. Arm rotation exercises involve movements that activate the rotator cuff muscles, deltoids, and upper limb stabilizers [7]. These muscles play a vital role in shoulder stability and mobility and are engaged in daily activities, making their activation beneficial beyond exercise settings. Incorporating arm rotations into walking routines can enhance upper limb engagement, improve posture, and promote overall muscular activation. Moreover, such combined movements may stimulate greater blood flow, promote energy expenditure, and facilitate glucose uptake by muscles, thereby positively influencing blood glucose levels [8, 9].

The rationale for combining arm rotation with walking stems from the understanding that engaging multiple muscle groups simultaneously can amplify the metabolic response. Walking, as a low-impact aerobic activity, is accessible and well-tolerated by most individuals. When combined with arm rotations - an activity that can be performed in a small space without special equipment - the overall exercise becomes more comprehensive and potentially more effective in managing glycemia [10].

Despite the theoretical benefits, there is limited empirical evidence specifically examining the effects of such combined exercises on glycemic parameters, particularly postprandial blood glucose (PPBG) and glycated hemoglobin (HbA1c). Postprandial hyperglycemia is an early indicator of impaired glucose metabolism and has been identified as a critical target for intervention because of its strong association with cardiovascular risk. HbA1c provides a longer-term overview of glycemic control [11] over approximately three months and is a key marker for assessing the effectiveness of diabetes management strategies.

Therefore, exploring innovative, simple exercise interventions [12] like arm rotation with walking exercise (ARWE) (Figure 1) could provide an accessible means for individuals with diabetes to improve their glycemic control, especially in resource-limited settings or among populations with physical limitations. The potential for such a modality to be performed at home, without the need for special equipment or facilities, makes it particularly attractive for widespread adoption.

Figure 1: Clipart of arm rotation exercises.

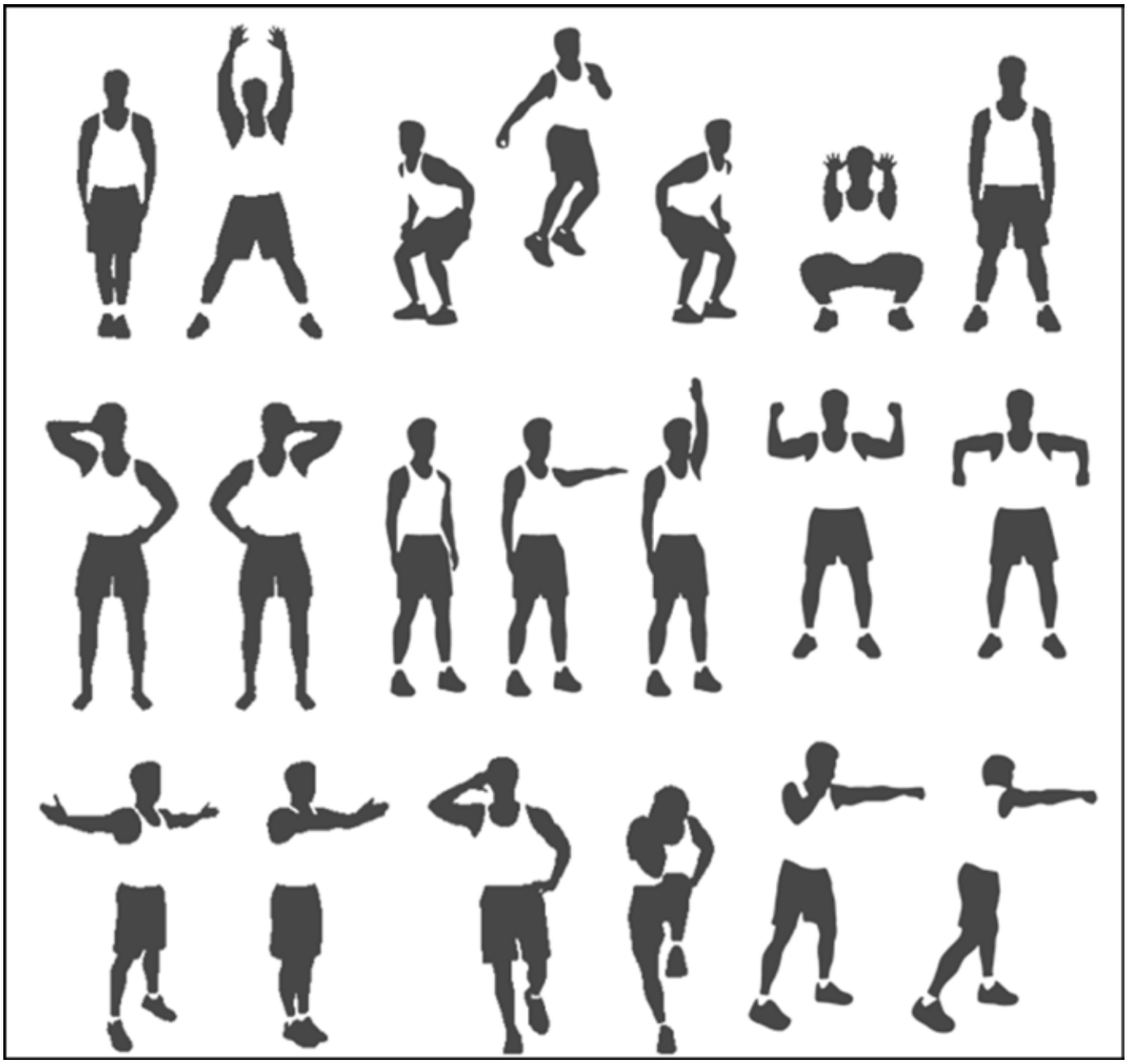

Given the global burden of diabetes mellitus and the critical role of physical activity in its management, there is a need to identify effective, safe, and easy-to-perform exercise strategies. Combining arm rotations with walking offers a promising approach that warrants scientific investigation. This study aims to evaluate the impact of ARWE on short-term and long-term glycemic parameters, specifically postprandial blood glucose and HbA1c levels, in individuals with T2DM. The findings could contribute to developing practical exercise guidelines and promote better adherence to lifestyle modifications, ultimately improving health outcomes for people living with diabetes.

Methods

Ethical considerations

All participants provided written informed consent prior to enrolment. The study was conducted in accordance with the Declaration of Helsinki and approved by the institutional ethics committee. The study was approved by the Institutional Human Ethics Committee of All India Institute of Medical Sciences Bhopal, India (AIIMS BPL/IHEC/2024/Apr/14).

Study design and setting

This research was conducted as a randomized controlled trial (RCT) to evaluate the effects of Arm Rotation with Walking Exercise (ARWE) on glycemic control among patients with

type 2 diabetes mellitus. The study was carried out over a period of 24 weeks at AIIMS, Bhopal, India, with ethical approval obtained from the institutional review board prior to commencement.

Participants

A total of 92 adult patients diagnosed with type 2 diabetes mellitus were recruited through outpatient ward of AIIMS, Bhopal, India. The inclusion criteria for a study on glucose estimation in diabetic patients during exercise typically encompass adults aged 18 years and above with a confirmed diagnosis of diabetes mellitus Type 2, who are able to perform supervised physical activity and have a stable medication regimen for at least three months, providing informed consent. Exclusion criteria include patients with uncontrolled diabetes or recent episodes of diabetic ketoacidosis or severe hypoglycemia, those with significant comorbidities such as advanced cardiovascular, renal, or hepatic disease, pregnant or lactating women, individuals on medications affecting glucose metabolism other than standard antidiabetic therapy, recent medication changes, physical or cognitive limitations preventing exercise, active infections or acute illnesses, and those with a history of exercise-induced hypoglycemia or other contraindications to physical activity. Pregnant women were also excluded.

Randomization and group allocation

Participants were randomly assigned into two groups - intervention and control - using a computer-generated randomization sequence. Allocation concealment was ensured using sealed opaque envelopes. Each group comprised 46 participants.

Intervention protocol

Intervention group (ARWE group)

Participants performed the combined exercise routine everyday for 24 weeks after dinner. Each session consisted of:

Each session required participants in the intervention group to perform Arm rotations simultaneously with walking for about 10 minutes. Participants were asked to change direction of their arm rotation once for every 5 rotations completed. The exercise was performed at a self directed pace to avoid fatigue. (Please note that the rotations and walking were done together and are part of one exercise itself in one session, they were not done separately.)

Session duration

Approximately 15 minutes, (the total exercise time with warmup and cool down lasted for only 15 minutes) including brief warm-up and cool-down periods. Participants received detailed instructions and demonstrations during an initial supervised session and were provided with written instructions and diagrams for home practice. They were advised to maintain their usual diet and medication regimen throughout the study.

Control group

Participants continued their usual care without any additional exercise intervention. They were instructed to maintain their regular activities and diet.

Monitoring and adherence

Participants in the intervention group-maintained exercise logs, documenting session frequency, duration, and any discomfort or adverse events. Weekly phone calls were made to reinforce adherence and address concerns. Compliance was considered adequate if participants completed at least 80% of prescribed sessions.

Outcome measures

Primary outcomes

Fasting blood glucose (FBG)

Measured after an overnight fast of at least 8 hours, using standard enzymatic methods, at baseline.

Postprandial blood glucose (PPBG)

Measured 2 hours after a standardized meal.

Glycated hemoglobin

Assessed using high-performance liquid chromatography (HPLC) BIORAD D10 hemoglobin testing system at baseline and post-intervention to evaluate long-term glycemic control. The study used previously collected blood samples stored at 2-8°C in EDTA tubes. Hemoglobin levels were measured using the fully automated BIO RAD D10 HPLC analyzer, following the manufacturer's instructions. The analysis involved specific kits and reagents, including blood primers, buffers, calibrators, diluents, wash reagent, and cartridges. Samples, controls, and calibrators were processed, with each run taking approximately 3 minutes and up to 20 samples analyzed per hour, generating chromatograms and reports for each sample.

Secondary outcomes

Participant adherence and safety, including recording adverse events or discomfort during exercises.

Laboratory procedures

Blood samples were collected following standard protocols. FBG and PPBG measurements were performed in the hospital's certified laboratory, ensuring calibration and quality control. HbA1c was measured using standardized HPLC methods.

Statistical analysis

Data were analyzed using SPSS version 25.0. Continuous variables were expressed as mean ± standard deviation (SD). Paired t-tests were used to compare pre- and post-intervention values within each group. Independent t-tests compared the mean changes between the intervention and control groups. A p-value of less than 0.05 was considered statistically significant.

Results

A total of 92 participants were enrolled in the study and were systematically divided into two equal groups: 46 participants were assigned to the control group, while the remaining 46 participants formed the case group. This balanced division was intended to facilitate comparative analysis between the groups. Furthermore, to analyze the distribution of participants across different age ranges, all 92 individuals were categorized into specific age groups: 18-30 years, 31-40 years, 41-50 years, 51-60 years, and over 60 years. This stratification allowed us to examine potential age-related differences within the study population. Figure 2 provides a visual representation of the number of participants in each age group, illustrating the distribution and ensuring transparency in the sample demographics. This detailed grouping helps in understanding the demographic makeup of the study population and supports subsequent analyses based on age-related factors.

The Table 1 presents anthropometric measurements for different age groups, comparing cases and controls. Generally, cases tend to have higher BMI, waist circumference, hip circumference, and waist-to-hip ratios than controls, indicating greater adiposity and potential health risks. For instance, in the 18-30 years group, cases had a BMI of 27.89 compared to controls' 23.39, and similar trends are observed in older age groups. Waist and hip measurements also tend to be higher among cases, especially in the over 60 group, where cases had waist circumferences averaging 104 cm versus 118 cm in controls. However, some values, such as the BMI of 16.07 in the 41-50 years case group, seem inconsistent or possibly erroneous, suggesting data entry issues. Overall, the data highlights increasing body measurements with age, and the tendency for cases to exhibit higher anthropometric indices, which may be associated with increased health risks like obesity or metabolic syndrome.

Figure 1: Number of participants in different age groups.

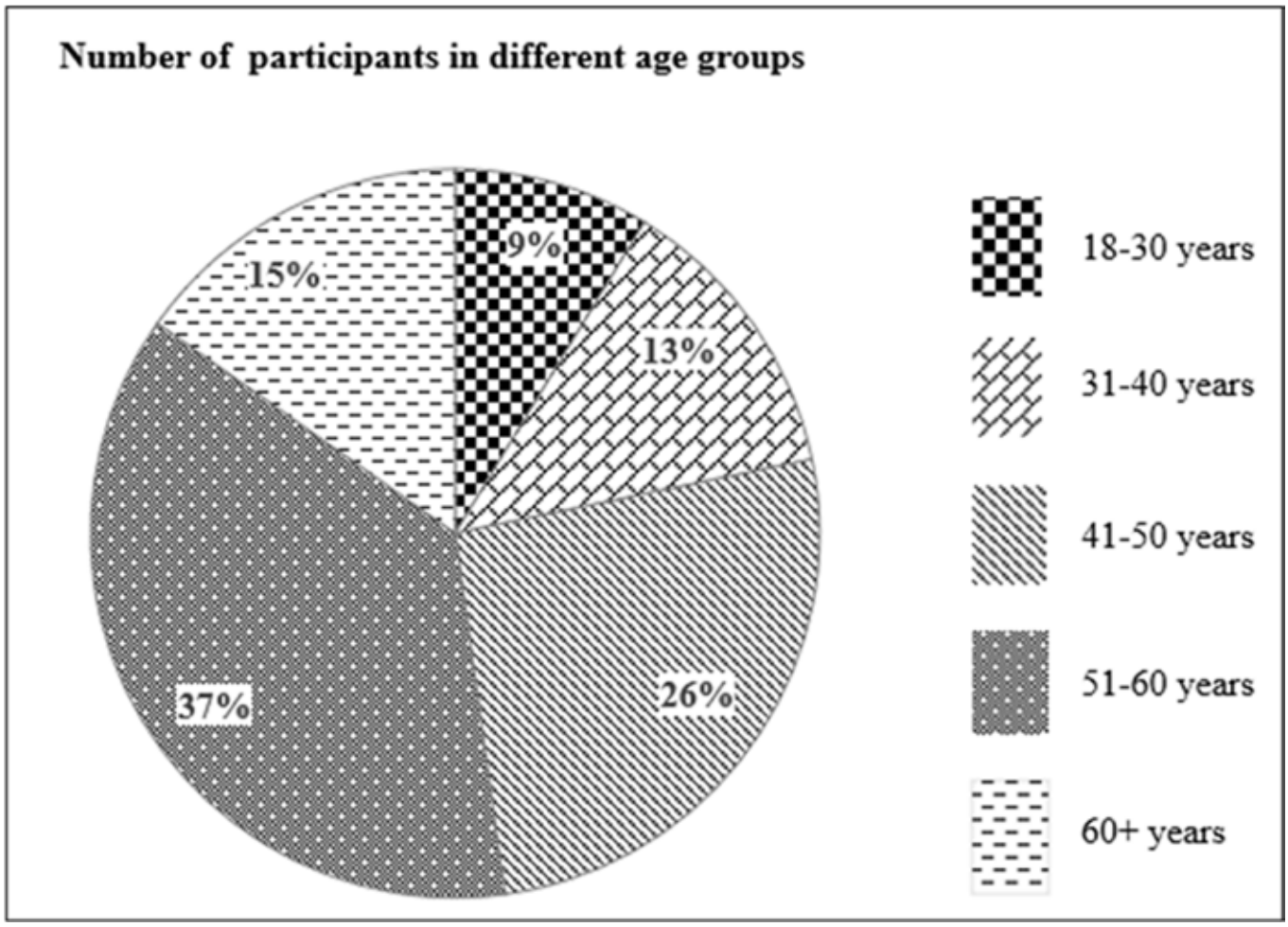

Table 2 presents data on FBG, PPBG, and HbA1c levels stratified by age groups and case/control status, measured on day 0 or prior to treatment. The results show that across all age

Table 1: Comparison of anthropometric measurements between cases and controls across age groups.

Consent	Weight	Height	BMI	Waist circ.	Hip circ.	Waist to hip ratio	Neck circ.	NH ratio
Age group: 18-30 years								
Case	75	164	27.89	108	96	1.125	40	0.244
Control	70	173	23.39	104	96	1.084	39	0.225
Age group: 31-40 years								
Case	70	158	28.04	102	96	1.062	39	0.247
Control	70	173	23.39	104	96	1.083	39	0.225
Age group: 41-50 years								
Case	47	171	16.07	75	68	1.103	33	0.193
Control	80	169	28.01	103	98	1.051	38	0.225
Age group: 51-60years								
Case	60	142	29.76	104	102	1.02	37	0.261
Control	69	158	27.64	108	92	1.174	40	0.253
Age group: 60 + years								
Case	78	166	28.31	104	96	1.083	40	0.241
Control	90	179	28.09	118	108	1.093	39	0.218

groups, cases consistently exhibit higher mean levels of FBG, PPBG, and HbA1c compared to controls. For example, in the 18-30 years group, cases have an FBG of 92.5 mg/dL, whereas controls are at 89.7 mg/dL; similarly, in the over 60 years group, cases record an FBG of 118.7 mg/dL compared to 97.8 mg/dL in controls. The trend of elevated glucose and HbA1c levels among cases becomes more pronounced with increasing age, with the highest values observed in the >60 years group. HbA1c levels rise from an average of 5.4% in young cases to 6.9% in older cases, indicating poorer glycemic control. Overall, the data suggests that cases have significantly higher blood glucose and HbA1c levels than controls across all age groups, highlighting the association between these parameters and the case status prior to treatment.

Table 2: Fasting glucose and HbA1c data stratified by age groups and case/control status (day 0 or before treatment data).

Age group (years)	Parameter	Cases (Mean ± SD)	Controls (Mean ± SD)
18-30	FBG (mg/dL)	92.5 ± 8.4	89.7 ± 7.9
	PPBG (mg/dL)	135.8 ± 12.5	122.4 ± 10.2
	HbA1c (%)	5.4 ± 0.3	5.2 ± 0.2
31-40	FBG (mg/dL)	98.2 ± 9.1	90.3 ± 8.2
	PPBG (mg/dL)	147.2 ± 14.3	128.7 ± 11.8
	HbA1c (%)	5.7 ± 0.4	5.3 ± 0.3
41-50	FBG (mg/dL)	105.4 ± 10.2	92.1 ± 8.7
	PPBG (mg/dL)	158.5 ± 15.0	134.2 ± 12.3
	HbA1c (%)	6.4 ± 0.5	5.5 ± 0.3
51-60	FBG (mg/dL)	112.3 ± 11.5	95.4 ± 9.3
	PPBG (mg/dL)	165.9 ± 16.0	140.7 ± 13.5
	HbA1c (%)	6.8 ± 0.6	5.8 ± 0.4
>60	FBG (mg/dL)	118.7 ± 12.3	97.8 ± 10.1
	PPBG (mg/dL)	169.4 ± 17.2	146.3 ± 14.0
	HbA1c (%)	6.9 ± 0.7	6.0 ± 0.5

FBG, PPBG, and HbA1c levels at baseline, 3 months, and 6 months of after arm rotation with walking exercise among cases across different age groups are shown in Table 3 and Figure 3. At baseline, all age groups exhibited elevated glucose and HbA1c levels, which decreased progressively over time. For example, in the 18-30 age group, FBG decreased from 92.5 mg/dL at baseline to 85.7 mg/dL at 3 months and further to 81.2 mg/dL at 6 months, with total reductions of 6.8 mg/

dL and 11.3 mg/dL at respective intervals. Similarly, HbA1c levels reduced from 5.4% to 5.2% at 3 months and to 5.0% at 6 months, indicating improved glycemic control. Older age groups showed comparable patterns, with more substantial reductions in glucose parameters, such as a 12.9 mg/dL decrease in PPBG in the 51-60 group over 6 months. Overall, the data demonstrate significant improvements in fasting glucose, postprandial glucose, and HbA1c levels over time, with greater reductions observed at 6 months across all age categories.

Table 3: The reduction in fasting glucose and HbA1c levels at 3 months and 6 months of exercise for cases, stratified by age group.

Age group (years)	Parameter	Baseline (before exercise)	3 months	Reduction at months 3	Months 6	Reduction at months 6
18-30	FBG (mg/dL)	92.5 ± 8.4	85.7 ± 7.9	6.8 mg/dL	81.2 ± 7.5	11.3 mg/dL
	PPBG (mg/dL)	135.8 ± 12.5	125.0 ± 11.8	10.8 mg/dL	118.2 ± 10.9	17.6 mg/dL
	HbA1c (%)	5.4 ± 0.3	5.2 ± 0.2	0.20%	5.0 ± 0.2	0.40%
31-40	FBG (mg/dL)	98.2 ± 9.1	90.4 ± 8.3	7.8 mg/dL	86.0 ± 7.8	12.2 mg/dL
	PPBG (mg/dL)	147.2 ± 14.3	137.0 ± 13.2	10.2 mg/dL	129.5 ± 12.5	17.7 mg/dL
	HbA1c (%)	5.7 ± 0.4	5.4 ± 0.3	0.30%	5.2 ± 0.3	0.50%
41-50	FBG (mg/dL)	105.4 ± 10.2	96.0 ± 9.0	9.4 mg/dL	91.5 ± 8.7	13.9 mg/dL
	PPBG (mg/dL)	158.5 ± 15.0	146.0 ± 14.0	12.5 mg/dL	138.3 ± 13.2	20.2 mg/dL
	HbA1c (%)	6.4 ± 0.5	5.6 ± 0.4	0.40%	5.4 ± 0.3	0.60%
51-60	FBG (mg/dL)	112.3 ± 11.5	102.0 ± 10.3	10.3 mg/dL	97.2 ± 9.5	15.1 mg/dL
	PPBG (mg/dL)	165.9 ± 16.0	153.0 ± 15.2	12.9 mg/dL	144.8 ± 14.3	21.1 mg/dL
	HbA1c (%)	6.8 ± 0.6	6.0 ± 0.5	0.30%	5.7 ± 0.4	0.60%
60 above	FBG (mg/dL)	118.7 ± 12.3	107.2 ± 11.0	11.5 mg/dL	102.5 ± 10.2	16.2 mg/dL
	PPBG (mg/dL)	172.4 ± 17.2	160.0 ± 16.0	12.4 mg/dL	152.5 ± 15.0	19.9 mg/dL
	HbA1c (%)	6.9 ± 0.7	6.3 ± 0.6	0.40%	6.0 ± 0.5	0.70%

Figure 3: The reduction in fasting glucose and HbA1c levels at 3 and 6 months of exercise across different age groups.

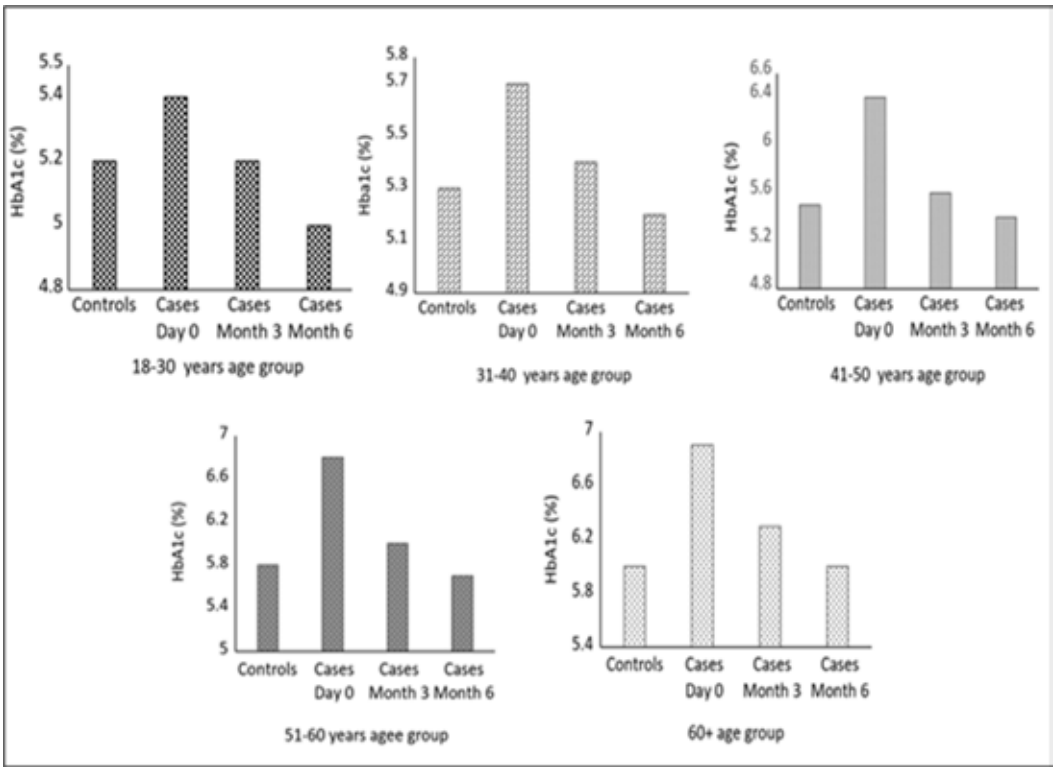

Exercise over a period of 3 and 6 months has been shown to significantly reduce both FBG and PPBG levels (Figure 4). Initially, at 3 months, regular physical activity improves insulin sensitivity and enhances glucose utilization, leading to notable decreases in FBG and PPBG. With continued exercise over 6 months, these benefits are sustained and further amplified, resulting in more substantial reductions and improved overall glycemic control. This demonstrates the crucial role of consistent exercise in managing blood sugar levels and preventing diabetes-related complications.

Figure 4: Impact of exercise on blood glucose levels over 3 and 6 months.

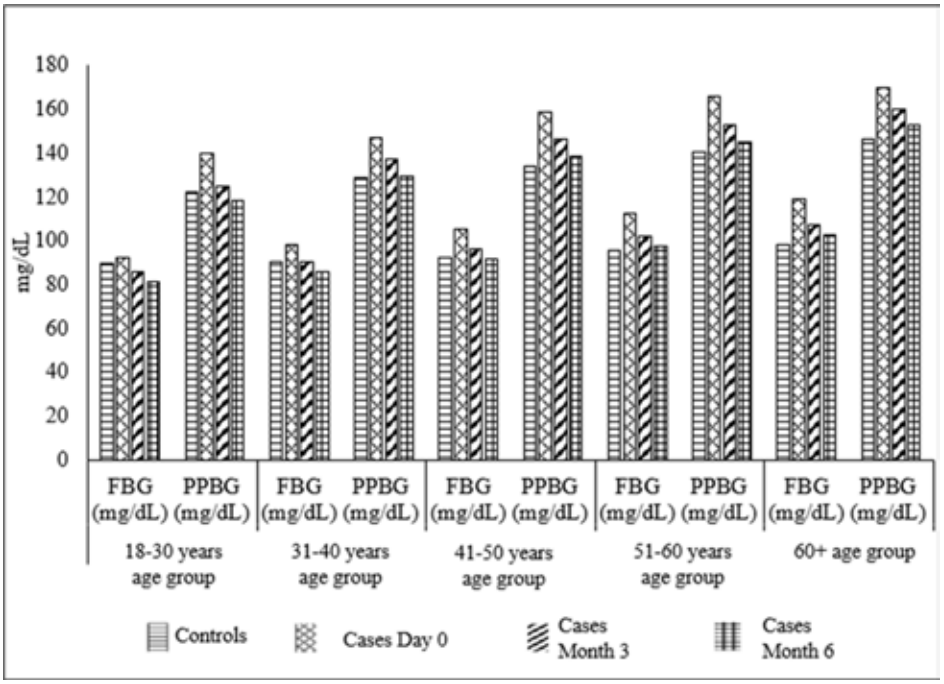

The Table 4 presents on two key parameters FBG and HbA1c, measured at baseline (pre-treatment), after 3 months, and after 6 months of exercise intervention. At baseline, the average FBG was 102.12 ± 19.43 mg/dL. Following 3 months of consistent exercise, FBG decreased by approximately 7.8 mg/dL, and after 6 months, it further declined by about 16.2 mg/dL, indicating a significant improvement in glycemic control over time. Similarly, HbA1c started at an average of 5.99 ± 0.91%, with reductions of approximately 0.2% at 3 months and 0.7% at 6 months, reflecting marked long-term blood sugar regulation and approaching target levels (Figure 5). These changes collectively demonstrate that sustained exercise significantly enhances glycemic parameters, contributing to better management of blood glucose levels.

Table 4: The effectiveness of arm rotation with walking exercise for diabetic patients based on the 3-month and 6-month data for FBG and HbA1c.

Parameter	Baseline (pre-treatment)	Months 3	Months 6	Interpretation
FBG (mg/dL)	102.12 ± 19.43	Reduced by approximately 7.8 mg/dL	Reduced by approximately 16.2 mg/dL	Significant reduction indicating improved glycemic control after 3 and 6 months of exercise.
HbA1c (%)	5.99 ± 0.91	Reduced by approximately 0.2%	Reduced by approximately 0.7%	Marked improvement in long-term blood sugar regulation, nearing target levels.

Figure 5: Bubble diagram showing that after 6 months of ARWE HbA1c is better controlled among different age groups.

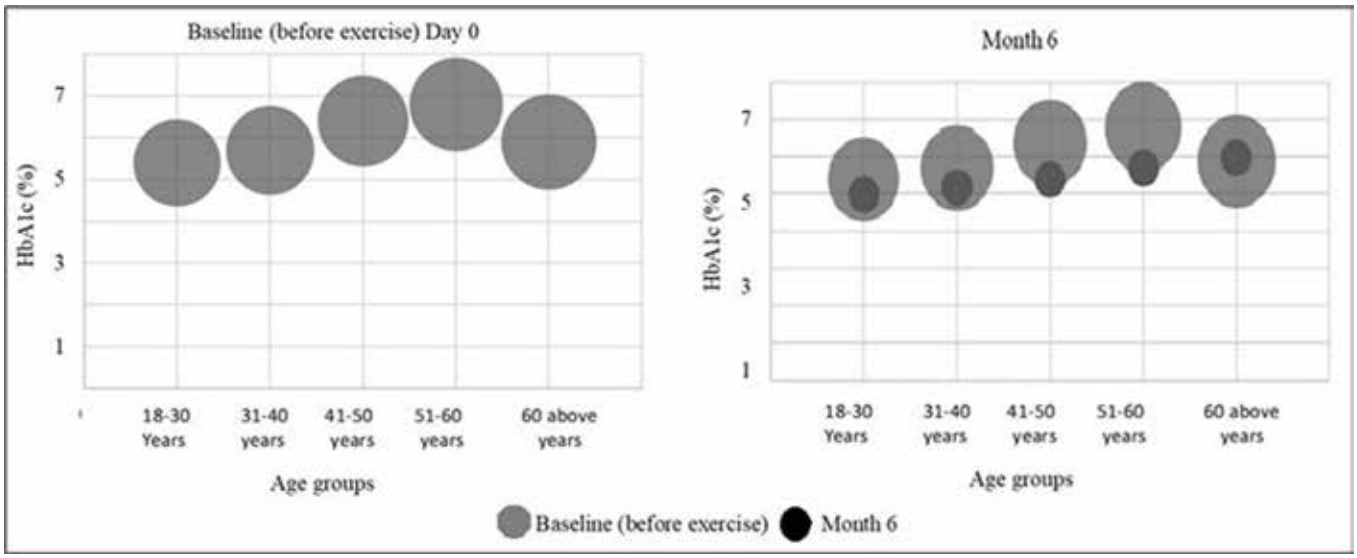

Our experimental results demonstrate that the intervention significantly improved glycemic control across all age groups, with the most pronounced effects observed in individuals aged 41 and above. Participants in the 41-50, 51-60, and over 60 age showed substantial reductions in fasting blood glucose (around 20-23 mg/dL) and HbA1c (approximately 0.4%), with ratings ranging from high to very high effectiveness, indicating marked responsiveness. Younger groups (18-30 and 31-40) experienced modest to moderate improvements, with less pronounced changes and lower effectiveness rankings. Additionally, males generally responded slightly better than females across all age groups, especially among older adults, highlighting age and gender as influential factors in the intervention's effectiveness. Overall, the intervention proves highly effective in older populations, leading to significant glycemic improvements (Table 5). Our study found that all age groups benefit from ARWE, but those 41 and older experience the greatest improvements. Older adults (41 years and above) saw significant reductions in fasting blood glucose (20–23 mg/dL) and HbA1c (~0.4%), likely due to higher baseline adiposity and hyperglycemia, which make them more responsive to exercise. Younger groups (18-40 years) showed smaller changes, possibly because they start with fewer metabolic issues. Age-related factors and longer disease duration contribute to these differences.

Table 5: Summary of glycemic parameter changes by age group and gender following intervention.

Age group (years)	Gender	Participants (n)	Baseline data	Follow-up data	Change (Δ)	Effectiveness rank	Interpretation
18-30	Male	5	"FBG: 105.0 mg/dL	HbA1c: 6.2%"	-7.0 mg/dL -0.2%	Moderate	Slight improvements, less responsive compared to older groups
	Female	3	"FBG: 102.0 mg/dL HbA1c: 6.1%"	FBG: 99.0 mg/dL HbA1c: 6.0%	-3.0 mg/dL --0.1%	Low	Minor changes, less impact observed
31-40	Male	7	FBG: 110.0 mg/dL HbA1c: 6.5%	FBG: 95.0 mg/dL HbA1c: 6.2%	-15.0 mg/dL -0.3%	High	Significant improvement in glycemic control
	Female	5	FBG: 112.0 mg/dL HbA1c: 6.6%	FBG: 98.0 mg/dL HbA1c: 6.3%	-14.0 mg/dL -0.3%	High	Good responsiveness, but slightly less than males
41-50	Male	15	FBG: 115.0 mg/dL HbA1c: 6.8%	FBG: 95.0 mg/dL HbA1c: 6.4%	-20.0 mg/dL -0.4%	Very High	Marked improvement, exercise highly effective
	Female	9	FBG: 117.0 mg/dL HbA1c: 7.0%	FBG: 97.0 mg/dL HbA1c: 6.6%	-20.0 mg/dL -0.4%	Very High	Similar trend, slightly less responsive than males
51-60	Male	19	FBG: 119.0 mg/dL HbA1c: 7.2%	FBG: 96.0 mg/dL HbA1c: 6.8%	-23.0 mg/dL -0.4%	Very High	Effective in older males, significant reduction
	Female	15	FBG: 115.0 mg/dL HbA1c: 7.0%	FBG: 97.0 mg/dL HbA1c: 6.6%	-18.0 mg/dL -0.4%	High	Good response, still above target levels
60 above	Male	6	FBG: 118.0 mg/dL HbA1c: 7.2%	FBG: 96.0 mg/dL HbA1c: 6.8%	-22.0 mg/dL -0.4%	Very High	Significant improvement, especially in older men
	Female	8	"FBG: 120.0 mg/dL	FBG: 98.0 mg/dL HbA1c: 7.0%	-22.0 mg/dL -0.4%	Very High	Effective, but slightly less than males

Discussion

The comprehensive data collected in this study categorizes participants into five distinct age groups - 18-30, 31-40, 41-50, 51-60, and over 60 years - allowing for an in-depth comparison of anthropometric and biometric parameters between cases (individuals with diabetes) and controls (healthy counterparts). This stratification provides valuable insights into how age influences body composition, fat distribution, and metabolic health, as well as how these parameters respond to specific exercise interventions like ARWE.

In the youngest age group, 18-30 years, both cases and controls tend to have lower BMI values, reflecting generally healthier body compositions typical of early adulthood. However, among the cases, BMI ranged approximately from 23 to 30.8, with some individuals showing higher values suggestive of early-onset overweight or obesity. Waist-to-hip ratios in this group hovered between 1.00 and 1.21, with some slightly exceeding these values, indicating a tendency toward central adiposity even at a young age. Controls, on the other hand, had BMI mostly below 26 and waist-to-hip ratios close to or below 1.2,

highlighting healthier body fat distribution. Despite overall lower adiposity, the data indicates that some young adults with metabolic risks already exhibit elevated measures of central fat, which could predispose them to future health complications [13].

Progressing into the 31-40 years age group, participants displayed a broader range of BMI, with some cases approaching nearly 32, reflecting increased adiposity compared to the younger group. Waist-to-hip ratios remained mostly below 1.05, but a subset of cases exceeded this threshold, signaling a shift toward greater central fat accumulation. Controls maintained relatively lower BMI and waist-to-hip ratios, suggesting the early onset of weight gain and fat redistribution begins to manifest more prominently among cases in this middle age group. These changes underscore the importance of early intervention to prevent further metabolic deterioration.

In the 41-50 years category, BMI values increased further, with some cases showing unusually low BMI (around 15.57 to 16.07). These anomalies may be due to data entry errors or measurement discrepancies, but otherwise, the majority of cases and controls exhibited BMI values in the 23 to 28 range, with some exceeding 30, indicative of overweight and obesity. Waist-to-hip ratios in this group hovered around 1, with some individuals surpassing 1.1, suggesting an increase in central fat accumulation that aligns with age-related metabolic changes. The elevated adiposity observed in this age range reflects a typical progression of fat redistribution and accumulation, which heightens the risk for insulin resistance and cardiovascular complications.

As individuals reach the 51-60 years age group, the trend of increasing adiposity becomes more evident. Participants in this group showed elevated BMI values, with some reaching approximately 29, and waist-to-hip ratios nearing 1.17. These metrics point to a higher prevalence of central obesity, a well-known risk factor for metabolic syndromes, type 2 diabetes, and cardiovascular diseases. Controls in this age group also demonstrated increased adiposity measures, though generally slightly lower than their case counterparts, indicating that weight gain and fat redistribution processes influence both groups as they age. The persistence of these trends emphasizes the importance of targeted interventions to manage weight and fat distribution in midlife.

In the oldest age group, over 60 years, both cases and controls exhibited increased BMI (around 28 to 29.7) and waist-to-hip ratios close to or above 1.09. This pattern signifies the cumulative effect of aging on adiposity, with a notable tendency toward central fat distribution. Interestingly, some cases in this age group displayed higher waist-to-hip ratios than controls, implying that older individuals with metabolic risks may have a greater propensity toward central obesity. This phenomenon is particularly concerning given the association between central adiposity and age-related metabolic disorders, including insulin resistance, hypertension, and dyslipidemia.

Overall, the data reveals a consistent and progressive trend of increasing BMI and waist-to-hip ratios with advancing age across both cases and controls, but especially among cases. This pattern underscores the natural progression of adiposity and fat redistribution over the lifespan, with a clear tendency for central obesity to become more prominent as age increases. Parameters such as neck circumference and NH ratios, which serve as proxies for upper body fat and metabolic risk, also show variations that align with the observed age and adiposity trends [14, 15]. These measures further reinforce the concept that fat accumulation in specific body regions correlates with metabolic disturbances and disease susceptibility.

Turning to the intervention aspect, the combination of ARWE proved effective across all age groups in improving glycemic control. At baseline, older individuals, particularly those over 60 years had higher FBG and HbA1c levels compared to younger populations, indicating more severe hyperglycemia initially. For example, more than 60 years group started with an average fasting glucose of approximately 118.7 mg/dL and an HbA1c of about 6.7%, whereas the 18-30 years group had much lower baseline levels, with fasting glucose around 92.5 mg/dL and HbA1c of 5.4%. This pattern suggests that glycemic regulation tends to decline with age, possibly due to longer disease duration, age-related metabolic changes, and increased adiposity.

After three months of engaging in ARWE, significant improvements were observed across all age groups. The above 60 years group experienced reductions of approximately 11.5 mg/dL in fasting glucose and 0.4% in HbA1c, despite starting from higher baseline levels. The youngest group showed a decrease of about 6.8 mg/dL in fasting glucose and 0.2% in HbA1c, indicating that even those with less severe initial hyperglycemia respond positively to this exercise regimen. These results demonstrate that older individuals, though initially more severely affected, respond robustly to the intervention, achieving meaningful improvements in glycemic parameters.

By the six-month mark, the benefits of ARWE not only persisted but further improved. The above 60 years group achieved a total reduction of approximately 16.2 mg/dL in fasting glucose and 0.7% in HbA1c, nearing near-normal levels, which is clinically significant. The 51-60 years group exhibited similar positive trends, underscoring the sustained efficacy of the exercise program across age groups. The consistent decline in glycemic parameters over six months highlights exercise's potential as a practical, non-pharmacological approach [16, 17] to managing blood sugar levels in individuals with or at risk for type 2 diabetes.

Beyond glycemic improvements, the data also reflect the broader impact of this intervention on metabolic health. The significant reductions in fasting and postprandial blood glucose levels, along with HbA1c [18], align with existing literature emphasizing the benefits of regular physical activity in enhancing insulin sensitivity and glucose metabolism. The

observed improvements are comparable to those reported in systematic reviews and meta-analyses, which indicate that moderate-intensity aerobic activities can reduce HbA1c by approximately 0.5% to 1%. The combination of arm rotations and walking likely produces a synergistic effect, engaging multiple muscle groups and metabolic pathways to optimize glucose utilization.

The physiological mechanisms underlying these benefits are multifaceted. Exercise stimulates the translocation of GLUT-4 transporters to skeletal muscle cell membranes, promoting insulin-independent glucose uptake [19-21]. It also enhances insulin receptor sensitivity, thereby reducing insulin resistance - a central feature of type 2 diabetes. Muscle contractions during ARWE stimulate mitochondrial biogenesis, improve oxidative capacity, and increase overall metabolic rate, all contributing to better glucose regulation. Additionally, engaging both upper and lower limbs through arm rotation and walking increases overall energy expenditure, further facilitating weight management and fat redistribution - key factors in metabolic health. It activates more muscles, increases calorie burn, and boosts circulation, which aids in glucose uptake and vascular health. The movements also raise heart rate more effectively, supporting weight management and improving insulin sensitivity. Additionally, arm rotation enhances joint flexibility, reduces injury risk, and adds variety to increase motivation and adherence. Overall, it amplifies metabolic, circulatory, and health benefits, helping to better manage blood sugar and overall well-being.

The inclusion of arm rotations specifically may have additional benefits by engaging muscles that are often underused, especially in sedentary lifestyles. Upper limb movements can elevate energy expenditure and improve circulation, which are beneficial for vascular health and metabolic function. Moreover, this form of exercise is low-impact, making it suitable for older adults or individuals with physical limitations, thereby reducing the risk of injury and encouraging consistent participation.

However, certain limitations must be acknowledged. The relatively short duration of 24 weeks limits the ability to assess long-term sustainability and effects on other health outcomes such as lipid profiles, blood pressure, or diabetic complications. The 24-week ARWE significantly improved glycemic control in individuals with type 2 diabetes. Participants showed notable reductions in postprandial blood glucose levels, indicating better management of blood sugar spikes after meals. Additionally, HbA1c levels decreased, reflecting improved long-term blood glucose regulation. These findings suggest that incorporating ARWE into daily routines can be an effective, non-pharmacological strategy to enhance glycemic control and potentially reduce the risk of diabetes-related complications. The sample size, though adequate for detecting significant changes, may not be sufficiently powered to evaluate secondary outcomes or subgroup analyses. Moreover, the study population was confined to a specific demographic, which may restrict the generalizability of the results to broader populations with different ethnicities, lifestyles, or comorbidities.

The practical implications of these findings are significant. The demonstrated efficacy of ARWE in improving glycemic control suggests that healthcare providers should consider recommending such simple, low-cost exercise routines to patients with type 2 diabetes or those at risk. Given the barriers faced by many individuals - such as lack of time, access to facilities, or physical limitations - ARWE offers an accessible alternative that can be performed at home or workplaces without special equipment. Its incorporation into self-management strategies could enhance adherence to physical activity recommendations, ultimately leading to better health outcomes [22]. Our study evaluated the ARWE program by measuring key outcomes such as post-meal blood glucose levels and HbA1c to assess short- and long-term glycemic control. It also examined insulin sensitivity indicators like fasting glucose, along with body metrics including weight, BMI, and waist circumference to evaluate effects on weight management. Additionally, physical fitness and activity levels were monitored through exercise adherence, performance, and habit changes.

The role of ARWE in this study underscores its potential as an effective, safe, and easy-to-implement strategy for improving glycemic control across all age groups. The observed reductions in fasting blood glucose, postprandial glucose, and HbA1c levels highlight the exercise's capacity to positively influence metabolic parameters. Its simplicity, minimal resource requirement, and broad applicability make it an attractive adjunct to conventional treatment approaches for type 2 diabetes. The findings advocate for the integration of such accessible physical activity routines into routine clinical practice and public health initiatives, especially given the escalating global burden of diabetes and the need for scalable, low-cost interventions [23]. Ultimately, ARWE exemplifies how small, consistent lifestyle modifications can yield significant health benefits, emphasizing the importance of promoting physical activity tailored to individual capabilities and circumstances for effective disease management.

Conclusion

This comprehensive analysis highlights the pivotal role that structured, simple exercise interventions specifically ARWE can play in managing type 2 diabetes mellitus across various age groups. The findings reveal a clear pattern of increasing adiposity and worsening glycemic control with advancing age. Younger adults (18-30 years) generally maintain healthier body compositions with lower BMI and central obesity indicators, though some already show early signs of increased adiposity. As individuals age, particularly beyond 40 years, both cases and controls demonstrate rising BMI and waist-to-hip ratios, reflecting age-related fat accumulation and redistribution. These changes are associated with higher baseline fasting blood glucose and HbA1c levels, indicating more severe

hyperglycemia in older populations, often due to longer disease duration and metabolic decline.

Despite these challenges, the study shows that ARWE is highly effective across all age groups. Participants, including those over 60 with more elevated initial blood glucose levels, experienced significant improvements after six months. The older group achieved reductions of approximately 16.2 mg/dL in fasting glucose and 0.7% in HbA1c, moving closer to normal ranges, while younger individuals also benefited, albeit with smaller absolute changes. These results underscore the intervention's safety, feasibility, and capacity to produce meaningful metabolic benefits, even in populations with limited mobility or comorbidities.

Physiologically, ARWE likely enhances insulin sensitivity by stimulating GLUT-4 translocation in skeletal muscles, improves circulation, and promotes vascular health. Engaging both upper and lower limbs increases overall energy expenditure and metabolic activity, contributing to better glycemic regulation. Clinically, incorporating such low-impact, accessible exercises into daily routines can reduce reliance on medications, prevent complications, and improve quality of life, especially for older adults.

In inference, ARWE is a practical, effective tool for glycemic management across the lifespan. Early and sustained adoption of such routines can mitigate age-related metabolic deterioration, empowering individuals to actively participate in their health. Healthcare systems should promote its integration into routine care, particularly in resource-limited settings, to optimize outcomes for people living with type 2 diabetes.

Ethics approval

The study was approved by the Institutional Human Ethics Committee of All India Institute of Medical Sciences Bhopal, India (AIIMS BPL/IHEC/2024/Apr/14).

Credit authorship contribution statement

TGM and SKR: writing – original draft, methodology, formal analysis, data curation. SKR: editing, formal analysis, conceptualization. SM: supervision, resources, conceptualization, formal analysis

Conflict of interest

The authors declare that they have no known competing financial interests or personal relationships that could have appeared to influence the work reported in this paper.

Data Availability

Data is available on request from the authors.

Funding

This study was funded by intramural research fund of All India Institute of Medical Sciences Bhopal, India.

Acknowledgements

None.

References

1. Banday MZ, Sameer AS, Nissar S. Pathophysiology of diabetes: An overview. Avicenna J Med. 2020;10(4):174-188. doi: 10.4103/ajm.ajm_53_20.
2. Yapislar H, Gurler EB. Management of Microcomplications of Diabetes Mellitus: Challenges, Current Trends, and Future Perspectives in Treatment. Biomedicines. 2024;12(9):1958. doi: 10.3390/biomedicines12091958.
3. Guan H, Tian J, Wang Y, Niu P, Zhang Y, Zhang Y, Fang X, Miao R, Yin R, Tong X. Advances in secondary prevention mechanisms of macrovascular complications in type 2 diabetes mellitus patients: a comprehensive review. Eur J Med Res. 2024;29(1):152. doi: 10.1186/s40001-024-01739-1.
4. Colberg SR, Sigal RJ, Yardley JE, Riddell MC, Dunstan DW, Dempsey PC, Horton ES, Castorino K, Tate DF. Physical Activity/Exercise and Diabetes: A Position Statement of the American Diabetes Association. Diabetes Care. 2016;39(11):2065-2079. doi: 10.2337/dc16-1728.
5. Kanaley JA, Colberg SR, Corcoran MH, Malin SK, Rodriguez NR, Crespo CJ, Kirwan JP, Zierath JR. Exercise/Physical Activity in Individuals with Type 2 Diabetes: A Consensus Statement from the American College of Sports Medicine. Med Sci Sports Exerc. 2022;54(2):353-368. doi: 10.1249/MSS.0000000000002800.
6. Sampath Kumar A, Maiya AG, Shastry BA, Vaishali K, Ravishankar N, Hazari A, Gundmi S, Jadhav R. Exercise and insulin resistance in type 2 diabetes mellitus: A systematic review and meta-analysis. Ann Phys Rehabil Med. 2019;62(2):98-103. doi: 10.1016/j.rehab.2018.11.001.
7. Elzanie A, Varacallo MA. Anatomy, Shoulder and Upper Limb, Deltoid Muscle. Treasure Island (FL): StatPearls Publishing; 2025 Jan. Available from: https://www.ncbi.nlm.nih.gov/books/NBK537056/ (Last accessed on May 29, 2025)
8. Richter EA, Derave W, Wojtaszewski JF. Glucose, exercise and insulin: emerging concepts. J Physiol. 2001;535(Pt 2):313-322. doi: 10.1111/j.1469-7793.2001.t01-2-00313.x.
9. Merz KE, Thurmond DC. Role of Skeletal Muscle in Insulin Resistance and Glucose Uptake. Compr Physiol. 2020;10(3):785-809. doi: 10.1002/cphy.c190029.
10. Moghetti P, Balducci S, Guidetti L, Mazzuca P, Rossi E, Schena F; Italian Society of Diabetology (SID), Italian Association of Medical Diabetologists (AMD), Italian Society of Motor and Sports Sciences (SISMES). Walking for subjects with type 2 diabetes: A systematic review and joint AMD/SID/SISMES evidence-based practical guideline. Nutr Metab Cardiovasc Dis. 2020;30(11):1882-

1898. doi: 10.1016/j.numecd.2020.08.021.
11. Mukherjee S, Ray SK, Jadhav AA, Wakode SL. Multi-level Analysis of HbA1c in Diagnosis and Prognosis of Diabetic Patients. Curr Diabetes Rev. 2024;20(7):e251023222697. doi: 10.2174/0115733998262501231015051317.
12. Lazić A, Danković G, Korobeinikov G, Cadenas-Sanchez C, Trajković N. Acute effects of different "exercise snacking" modalities on glycemic control in patients with type 2 diabetes mellitus (T2DM): study protocol for a randomized controlled trial. BMC Public Health. 2025;25(1):566. doi: 10.1186/s12889-025-21669-9.
13. Han TS, Lean ME. A clinical perspective of obesity, metabolic syndrome and cardiovascular disease. JRSM Cardiovasc Dis. 2016;5:2048004016633371. doi: 10.1177/2048004016633371.
14. Aswathappa J, Garg S, Kutty K, Shankar V. Neck circumference as an anthropometric measure of obesity in diabetics. N Am J Med Sci. 2013;5(1):28-31. doi: 10.4103/1947-2714.106188.
15. Li D, Zhao Y, Zhang L, You Q, Jiang Q, Yin X, Cao S. Association between neck circumference and diabetes mellitus: a systematic review and meta-analysis. Diabetol Metab Syndr. 2023;15(1):133. doi: 10.1186/s13098-023-01111-z.
16. Raveendran AV, Chacko EC, Pappachan JM. Non-pharmacological Treatment Options in the Management of Diabetes Mellitus. Eur Endocrinol. 2018;14(2):31-39. doi: 10.17925/EE.2018.14.2.31.
17. Kirwan JP, Sacks J, Nieuwoudt S. The essential role of exercise in the management of type 2 diabetes. Cleve Clin J Med. 2017;84(7S1):S15-S21. doi: 10.3949/ccjm.84.s1.03.
18. Mukherjee S, Yadav P, Ray SK, Jadhav AA, Wakode SL. Clinical Risk Assessment and Comparison of Bias between Laboratory Methods for Estimation of HbA1c for Glycated Hemoglobin in Hyperglycemic Patients. Curr Diabetes Rev. 2024;20(7):e261023222764. doi: 10.2174/0115733998257140231011102518.
19. Richter EA, Hargreaves M. Exercise, GLUT4, and skeletal muscle glucose uptake. Physiol Rev. 2013;93(3):993-1017. doi: 10.1152/physrev.00038.2012.
20. Richter EA. Is GLUT4 translocation the answer to exercise-stimulated muscle glucose uptake? Am J Physiol Endocrinol Metab. 2021;320(2):E240-E243. doi: 10.1152/ajpendo.00503.2020.
21. Chadt A, Al-Hasani H. Glucose transporters in adipose tissue, liver, and skeletal muscle in metabolic health and disease. Pflugers Arch. 2020;472(9):1273-1298. doi: 10.1007/s00424-020-02417-x.
22. Dong C, Liu R, Huang Z, Yang Y, Sun S, Li R. Effect of exercise interventions based on family management or self-management on glycaemic control in patients with type 2 diabetes mellitus: a systematic review and meta-analysis. Diabetol Metab Syndr. 2023;15(1):232. doi: 10.1186/s13098-023-01209-4.
23. Maina PM, Pienaar M, Reid M. Self-management practices for preventing complications of type II diabetes mellitus in low and middle-income countries: A scoping review. Int J Nurs Stud Adv. 2023;5:100136. doi: 10.1016/j.ijnsa.2023.100136.

Research Article

Calibration error, a neglected error source in the clinical laboratory quality control

Atilla Barna Vandra[1*]

[1]*Spitalul Clinic Județean de Urgență, Brașov, Romania (retired)*

Article Info

[*]***Corresponding Author:***
Atilla Barna Vandra
E-mail: vandraattila@gmail.com
Spitalul Clinic Județean de Urgență, Brașov, Romania (retired)

Keywords

Bias, calibration error, calibration graph, incorrigible bias, quality control, random error, repeatability conditions, reproducibility within laboratory conditions, systematic error

Abstract

"Calibration" conveys the connotative meaning of "correction." Therefore, calibration is frequently viewed as "perfect," but it is a measurement, and no measurement is error-free. This study aims to uncover the sources of calibration errors, to estimate their size, and assess their consequences in quality control.

The analytical bias is the difference between the working (determined) graph and the ideal graph (how the reagents behave).

The source of the calibration random component is the random error committed in the calibration. The primary source of the systematic component is the reference material value error, which cannot be reduced to the nominal value error. Even if the avoidable human errors are neglected, the reconstitution errors, including two volume measurements, are inherent.

The random component was estimated by making five calibrations in repeatability conditions and calculating the coefficient of variation of the slope factors. The total calibration error was estimated by comparing the slope factors of new calibrations using the same reagent and calibrator lots (one-year data).

The results confirmed the presumptions: the calibration error is bigger than the coefficient of variation measured in repeatability conditions. Smaller biases are incorrigible by calibration, and quality control rules must be designed to prevent them from being detected.

Using the σ parameter in the QC graphs would result in too frequent alarms. Westgard proportionally increased the decision limits by overestimating σ with the standard deviation measured in reproducibility within laboratory conditions. A more accurate solution is to increase all decision limits to account for the incorrigible bias and design the QC graphs with the standard deviation measured in repeatability.

Introduction

Measurement errors can be committed in the pre-pre-analytical, pre-analytical, analytical, and post-analytical phases [1]. Analytical errors hold a special status in the error budget. According to JO. Westgard:

"Quality design in a laboratory must begin with analytical quality because it is the essential quality characteristic of any laboratory test; unless analytical quality can be achieved, none of the other characteristics matter [2]."

The analytical errors encompass method, matrix, and true analytical or measurement errors, including calculation and rounding errors. Because the control materials used in the internal QC are not certified reference materials, method and matrix errors can be measured only in EQA.

Only true analytical (measurement) errors can be quantified in the internal QC and mathematically described by the Gauss equation [3]. Only in this case can we differentiate between the systematic (SE) and the random (RE) error components. Both parameters of the equation are ideal values. Therefore, estimators are used. The bias (B≈SE) is the estimator of the SE, while the standard deviation SD≈σ is the estimator of the mean RE.

An accurate classification is complete, avoids redundant categories, and uses accurately defined categories to prevent misinterpretations. Unfortunately, the classifications of the bias found in the literature do not have all these properties. For example, WP Oosterhuis et al. mention four sources of bias (SE): (1) laboratory, (2) reagent, (3) instrument, and (4) operator bias [4]. The "ladder of errors" of M. Thompson shows four rungs of the laboratory errors: (1) laboratory, (2) method and measurement system, (3) day-to-day variation ("run bias"), and (4) repeatability [5], [6]. This paper focuses on normal laboratory conditions, including well-trained personnel, an air-conditioned laboratory, proper maintenance, and the absence of analyzer failures.

A detailed analysis of the error sources reveals that the environmental influence is mostly pre-analytical and insignificant; the "laboratory errors" are a sum of pre-analytical, human, environmental, instrumental, and non-instrumental errors. Human (operator) errors are mostly pre-analytical, and if not, they indirectly influence instrumental and non-instrumental errors. Therefore, all of the aforementioned sources are redundant in the list. Only two error sources must be considered: the instrumental and the non-instrumental errors. (Calculation errors have similar properties and, therefore, can be categorized as instrumental errors.)

The instrumental errors are linked to the construction of the analyzer and its changeable parts. Assuming correct maintenance, the latter has a negligible influence. In the meantime, the construction of the analyzer remains constant and is non-specific. The inherent inconstant functionality of the instrument (e.g., sampling or reading error) is the source of a constant random error; however, it may also cause constant biases. In the absence of failures, the mean random error is constant!

The non-instrumental errors (linked to the reagents and calibration graphs) are variable and specific to each measurement.

The inherent reagent instability is the primary source of the bias variability. It causes a quasi-linear, predictable drift (gradual variation) in the systematic error component, masked by the random error on the QC graphs. Random variation in reagent properties contradicts the fundamental laws of chemistry. (An unpredictable change is still possible in the case of reagent impurification.) It cannot be the source of random error, only of inherently variable bias. The primary role of a QC is to identify and correct these bias variations.

The reagents and electrodes are not constructive parts of the instrument. They are specific, and their property significantly influences the results. Producers only guarantee trustworthy results after recalibration within the validity term [7].

The bias caused by reagent instability cannot increase indefinitely. It is corrected by (re)calibrations, resulting in cyclical, sawtooth-like graphs of the daily biases, usually masked by random errors. Surprisingly, CLIA requirements do not mention the reagent instability among the error sources:

"The control procedures must detect immediate errors that occur due to test system failure, adverse environmental conditions, and operator performance [8]."

The word "calibration" conveys the connotative meaning of "correction." Therefore, calibration is frequently viewed as a "perfect" process, subject to only the calibrator's nominal value uncertainty (specified in the traceability documents); however, it is a measurement, and no measurement is error-free. Many authors share the myth of error-free calibration [9]. According to JO Westgard and T.L. Groth [10]:

"In the simulation procedure, the calibration process is assumed to be ideal and to contribute no errors in addition to the primary ones being introduced."

Despite this assumption, they state later:

"…these primary errors could represent calibration errors or other sources of errors…"

This myth persists. Despite several authors mentioning calibration errors [4], [5], [11], [12] some specifying even mosaic pieces of the sources (e.g., calibrator preparation [6]), others focusing on human errors [13] or calibration procedures [14]), a detailed analysis and a quantitative evaluation of the inherent calibration errors have not been done yet.

This study aims to fill the gap by focusing on the inherent errors in calibration, evaluating their source and magnitude.

Materials and methods

The size of the calibration random error was estimated in two ways.

1. Five calibrations were performed under repeatability conditions, with a 5-minute interval between each, to determine the calibration parameters, with a focus on the slope factor

Fcal. Based on the proportionality between the Fcal and the concentration, the calibration random error was estimated by calculating the variability of the slope factor Fcal, expressed as a coefficient of variation ($CV_{F_{cal}}$). The $CV_{F_{cal}}$ was compared with the CV_r, which was determined during the method adequacy testing a few months prior. Measurements were made on a Cobas 6000 analyzer using Roche reagents and reference materials. The method neglected the influence of the error in the null-point absorption (A_0) and the variability of the reconstitution error. (The same reference material was used.)

2. To estimate the variability of the F_{cal} in real-life situations, constant conditions must be maintained. This includes using the same reagent lotcalibrator lot and considering only new calibrations. All conditions were fulfilled, with sufficient data in the case of urea on a Cobas pro analyzer (The producer recommends recalibrating each reagent bottle.) Recalibrations of used reagents, different reagent lots, and calibrator lots would introduce supplementary errors, overestimating the calibration errors. If recalibrations are also included, and lots are mixed, the estimated CV_{cal} becomes similar to CV_{RW}.

The method also neglected the influence of A_0 variability. However, it accounted for the reconstitution error. (More reconstituted calibrator bottles were used.)

Results

Because of the proportionality between the F_{cal} values and concentration, equals the CV calculated from the variable bias values (CV_{VCSE}). (An SD or CV can be calculated from any variable data set, not only from normally distributed random errors. However, the SD (CV) can be used as the correct estimator of the σ parameter of the Gauss equation (the measure of the mean pure RE) only under constant conditions. Under variable conditions (a variable bias), the SD (CV) is the measure of all variable components (RE + VCSE) [7]. For this reason, $CV_{F_{cal}} \approx CV_{VCSE}$, and equals the mean B% caused by the mean variations.

The values for the estimated $CV_{F_{cal}}$ compared with the CVr obtained in the method validation for four analytes are presented in Table 1.

Table 1: Comparison between the measured $CV_{F_{cal}} \approx CV_{VCSE}$ and CV_r.

Analyte	AST/GOT	Creatinine	Glucose	Urea
$CV_{F_{cal}} \approx CV_{VCSE}$	2.85%	0.98%	1.25%	0.99%
CVr	1.64%	0.96%	0.84%	1.13%

A Cochran test for equality of two variances did not find significant differences between $CV_{F_{cal}}$ and CV_r values, except for AST/GOT, where $CV_{F_{cal}}$ is larger than CV_r).

The $CV_{F_{cal}}$ calculated from the F_{cal} values obtained only in new calibrations for the same reagent lot and the same calibrator lot for urea are shown in Table 2 (one-year database). As in the first case, a Cochran's F-test did not find significant differences in comparison with the CV_r:

Table 2: $CV_{F_{cal}}$ for urea calculated from new calibration data, CV_r=1.04%.

Reagent lot	629883	612739	597097	583201	583201
Calibrator (RM) lot	539941	539941	539941	539843	410065
$CV_{F_{cal}} \approx CV_{VCSE}$	1.29	1.39	1.33	0.8	1.1

As a comparison, the mean value for $CV_{F_{cal}}$ calculated from all F_{cal} values (including recalibrations) was 2.5%, similar to CV_{RW} (2.6% and 2.7% on the two control levels).

Discussion

"Calibration is a process of testing and adjusting an instrument or test system to achieve a correlation between the measurement response (measurement signal) and the concentration or amount of substance measured by the test procedure [14]."

A calibration graph is a mathematical relationship between absorption and concentration. In biochemistry, this relationship is usually linear within the measuring range. (The case of non-linear calibration graphs will not be discussed.)

Calibration, like all measurements, has both random and systematic components.

The SE (bias) variation (the VCSE) has two primary sources: reagent instability and calibration errors. Both phenomena are linked to the calibration graphs.

When calibrating, two parameters are determined: the null-point absorption, A_0, and the slope factor F_{cal}. The determined parameters differ from the ideal values. Therefore, two different calibration graphs exist, and both are variable. One is the determined (working) graph used in calculations, which remains constant between calibrations but changes randomly within each calibration. The consequence is a randomly variable systematic error, an alternation between predictable (constant) periods and random variations. The other is the ideal graph, reflecting how the reagent behaves. It changes gradually depending on the reagent stability, causing quasi-linear bias variations. Combining the two phenomena produces sawtooth-like graphs of the daily bias, which are masked on the QC graphs by the random error, allowing only significant shifts to be observable [7]. According to E. Theodorsson, B.

Magnusson, and I. Leito:
"Within a given day, the small deviations of the calibration graph from an 'ideal calibration graph' affect all the samples in a systematic way [6]."

The analytical bias is the difference between the result obtained on the determined graph (the measured value) and the ideal graph (the real value) [14] (Figure 1).

Figure 1: The cause of the analytical bias is the error of the calibration graph.

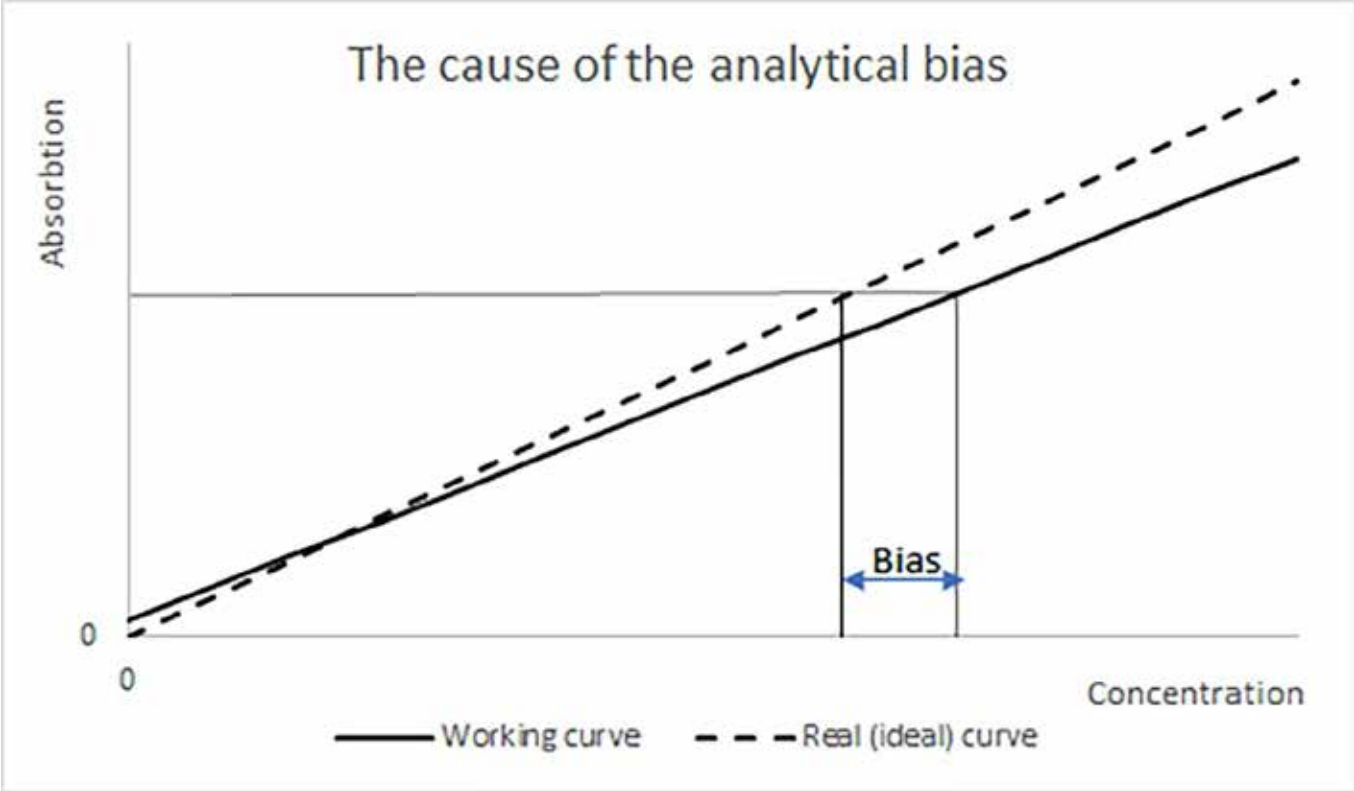

The error of A_0 introduces a constant bias, while the error of the slope factor F_{cal} causes a bias proportional to the concentration. While the determined graph remains constant until the next calibration, the ideal one depends on the reagent quality and varies gradually over time. Therefore, different measured values with gradually increasing biases (in absolute values) are obtained on the following days [7], [13], [14].

We must distinguish between calibration errors and calibration graph errors. The calibration errors, which cause a bias in the first run after calibration, have a single source: the measurement error committed during the calibration process. The calibration graph errors, which are the permanent causes of analytical bias, have two sources: calibration errors and reagent degradation.

Calibration is a measurement, subject to analytical errors comprising systematic and random components. The source of the calibration random errors is the measurement errors in the calibration process. The measurement of the calibrator is subject to the same random errors as a patient or control sample, comprising both systematic and random components. Theoretically, the systematic components are eliminated or at least reduced when the absorption variations ($\Delta A=A-A_0$) are calculated, but the random ones are not. The SD when measuring the calibrator is also sr (calibrations are made in repeatability conditions), and the CV is CV_r. In linear calibrations, four measurements are made: two to determine A_0 and the other two measurements are used to measure the calibrator and calculate the slope factor F_{cal}.

Due to the proportionality between concentrations and absorptions, the coefficient of variation (CV) of the absorptions will be equal to the CV of the concentrations.

Calculating the average absorption of two calibrator measurements will not eliminate the RE; it only reduces the CV $\sqrt{2}$ times. A similar RE is committed when measuring A_0. The slope factor F_{cal} is determined as a difference, and the CV of a difference is $\sqrt{2}$ times bigger than the CV of a single measurement. Therefore, the RE committed in the slope factor F_{cal} determination is $CV_{F_{cal}}$~CV_r. Due to the proportionality between the concentrations and Fcal, the probable calibration-induced bias is B% ≈ CV_r. (In 32% of cases, even bigger). In absolute values, the probable bias induced by the calibration RE is ≈1s_r.

The calibration random error induces a constant bias until the next calibration, when the new calibration random error replaces its value.
The primary source of systematic calibration errors is the error in the reference material (calibrator) value. The uncertainty of the reference material's nominal value is well-known. It is specified in the traceability certificates. However, the fact that different calibrator values are specified for different methods raises some doubts about the credibility of these uncertainties. Some of these uncertainty intervals are disjoint (have no common values). This study does not aim to analyze and explain the phenomenon but only to draw attention to the fact that nominal value errors may be more significant than previously thought.
The reference material value errors cannot be reduced to the nominal value errors [6].

According to M. Thompson:
"Systematic errors in calibration, such as might be brought about by the incorrect preparation of a stock solution, or lack of fit in an estimated calibration function, contribute to the higher-level biases [4]."
T. Badrick [15], referring to the Tietz Textbook of Clinical Chemistry [16], underlines:
"The act of reconstitution can introduce an error far greater than the inherent error of the rest of the analytical process."
Avoidable human errors may also contribute to reconstitution errors, but in most cases, these errors are inherent. The reference materials, after their concentration (activity) is determined by the producers, undergo a lengthy process. They are distributed into bottles (a first volume measurement), lyophilized, and then deposited. They are transported to the laboratory, reconstituted (a second volume measurement), and subsequently frozen. After thawing, they are homogenized, acclimatized, and only then measured. Their value is different from the nominal value specified by the producers. (Reference material value error). Even if the nominal value errors and human errors (stability, homogenization, temperature errors, and avoidable human errors in reconstitution) are neglected, the two volume measurements still induce inherent errors in the reconstitution.
The precision of the actual pipettes, expressed as a CV, is ±0.2-0.3%, and the accuracy is 0.5-0.6%. The expanded uncertainty is twice as big, and there are two volume measurements. Furthermore, the reconstitution of the control materials is subject to the same errors; therefore, the observable reconstitution error may be even bigger than CV_r.
Consequently, the estimated average total calibration error is 1-2 CV_r. According to a quintessential principle valid in all exact sciences, an error (bias) cannot be corrected if the uncertainty of the value is greater than the error itself, nor if the uncertainty (mean error) of the corrective action is greater than the corrected error. For example, a bias cannot be corrected as GUM recommends if its uncertainty is bigger: B<Ubias [17]. Additionally, we cannot eliminate a smaller bias than the average calibration error. In both cases, there is a risk of increasing the bias.
The estimation of the random component of the calibration error was verified by five consecutive calibrations of four analytes (Table 1). All four cases confirmed the assumption that the random component of the calibration error and the induced bias (B%) is at least 1 CV_r. Because the error of the A_0 was not considered, it is an under-evaluated estimation.
Because the total (systematic and random) calibration error can be estimated only in the case of new calibrations (assuming that all bottles from the same lot are identical and recalibrations cannot be used), a sufficient number of data points, allowing for an accurate estimation, were available for urea. The data in Table 2 once again confirm that the average calibration error is at least 1 CV_r.
The assumed $B_{incorrigible}$>1 CV_r is sustained by the fact that, despite efforts to correct the biases, 1 CV_r is a typical value for the mean bias calculated from monthly QC data, thereby sustaining its incorrigibility.
Due to the calibration error, there exist incorrigible biases. The question arises: Why must the QC rules detect them?
According to Theodorsson et al.:
"There is no point in trying to eliminate or correct a small and clinically unimportant bias since both elimination and correction need resources and may increase the measurement uncertainty [6]."
Other authors also share similar ideas [18].
It is harder to define what "small and clinically unimportant bias" means. If an incorrigible bias (B<CV_r) is not insignificant, it indicates an ineffective quality control system. Usually, this is not the case. 1 CVr is a minimal value for the insignificant bias. Other possibilities for estimating it are: $B_{insignificant}$=TEa/7 or a quarter of the within-subject biological variation ($B_{insignificant}$=CVI /4).
The most frustrating moments in the clinical laboratory biochemistry department occur when a QC alarm is triggered, and despite recalibration, no improvement is achieved; the situation may even worsen. In the meantime, the phones are ringing because of the delayed results. Usually, incorrigible biases can be discovered behind these phenomena.
The necessity to avoid alarms in the cases of incorrigible biases highlights the weaknesses of the actual QC system based on Westgard rules and the false assumption of a normal distribution of long-term control results. Correct decisions based on the Westgard rules (consistent with the calculations of JO Westgard and T. Groth [10]) are only possible if the Levey-Jennings graphs are designed with the σ parameter of the Gauss equation (or with its trustworthy estimator). Unfortunately, a correctly applied, Westgard-rules-based QC system is dysfunctional. The former statement seems doubtful because almost everybody uses the Westgard rules. The highlight is on "correctly applied." A rhetorical question: "Does anybody design the Levey-Jennings graphs with the σ parameter?"

If the QC graphs are designed with σ, according to the normal distribution tables, the probability of an $R_{1\text{-}2S}$ warning in the absence of bias is 4.56% [19]. Assuming 25 biochemistry parameters, two control levels, three runs per day, and 30 days per month (resulting in 4500 control measurements per month), this yields more than two false $R_{1\text{-}2S}$ warnings in each run, totaling ≈200 per month. A B=1 SD is a typical value in practice because it is at the limit of incorrigibility. Assuming only 11 (less than half of 25) parameters with B≈1 SD, an $R_{1\text{-}3S}$ alarm in each second control run is quasi-lawful. Less frequent $R_{1\text{-}2S}$ warnings and $R_{1\text{-}3S}$ rejections are evidence of the overestimation of the standard deviation (SD) used in the design of the QC graphs. Not σ, but a significantly bigger SD value is used in the design of the graphs.

Instead of frequent warnings and rejections, several "impossible" QC graphs are observed in practice. For example, graphs with no $R_{1\text{-}2S}$ warning in a month (probability 0.0224%), no $R_{1\text{-}3S}$ violation in a month if B>1SD, (Probability <1.57%) no $R_{1\text{-}3S}$ violation in a month if the reagent is unstable (visible drift), more $R_{4\text{-}1S}$ violations without $R_{1\text{-}2S}$ warnings, more frequent $R_{4\text{-}1S}$ and R_{10X} violations, than $R_{1\text{-}3S}$ or $R_{2\text{-}2S}$ (and examples may continue). All these examples are evidence of overestimations of the "SD" used in the design of the QC graphs.

The Gauss equation is only valid, and the predictions are correct if the conditions are constant [3]. Constant conditions assume a constant mean and bias, which cannot be maintained in the long term in a clinical laboratory. Data sets collected when the bias is different relate to each other as two sets of length measurements, some expressed in meters and others in yards [7].

The distribution of all data will be bimodal, with two distinct peaks rather than a normal (Gaussian) distribution.

More authors questioned the normal distribution of the long-term control results [20],[21],[22]. According to AB Vandra, the non-Gaussian distribution is caused by SE (bias) variability [7].

The σ parameter of the Gauss equation can be estimated correctly only in constant (repeatability) conditions. The SD measured in variable conditions is not a measure of the true RE but of all variable components, including the RE and the bias variations [7]. An SD can be calculated from any variable data set, not only from normally distributed ones. Several authors (using different definitions and notations) concluded that the link between the SD measured in repeatability conditions (s_r) and the SD measured in reproducibility within laboratory conditions (s_{RW}) is the bias variations [7],[23],[24],[25]. The true RE and its correct estimator can be determined only under constant conditions of repeatability $\sigma \approx s_r$.

According to another quintessential principle valid in all exact sciences, a parameter must be determined under the same conditions in which it is used. QC decisions are made in repeatability conditions, consistent only with s_r, not with s_{RW}. The former principle suggests the same: to design the QC graphs with s_r, not with s_{RW}, as Westgard recommends [26].

As shown previously, a correctly applied Westgard-rules-based QC system (with QC graphs designed with σ) is dysfunctional due to excessive false alarms. The "solution" proposed by JO Westgard is to overestimate σ with s_{RW}, which is only apparently efficient. The system becomes functional, but such a "correction" is inaccurate and questionable.

J.O. Westgard and T. L. Groth [10] acknowledged:

"The calculations based on computer simulations behind the power function graphs are made assuming "within-run (repeatability) SD", while the graphs are designed with "total SD".

And also, that: "…the error level that may occur is likely to be greater than that predicted."

However, they acknowledged the inconsistency between calculations and decisions, they preferred the larger limits to maintain the functionality of the QC system but using different SD in calculations (s_r) and decisions (s_{RW}) is a serious error source.

The usual $\frac{s_{RW}}{s_r}$ ratio is 1.25-2; however, it may be even bigger in some cases. For an approximate comparison, let us accept an $\frac{s_{RW}}{s_r}$=1.5 ratio. It means that by designing the QC graphs with s_{RW}, instead of the $R_{1\text{-}3S}$ rule, we de facto apply the $R_{1\text{-}4.5S}$ rule, rather than the $R_{2\text{-}2S}$ rule, the $R_{2\text{-}3S}$ rule, rather than the $R_{4\text{-}1S}$ rule, and the $R_{4\text{-}1.5S}$ rule. Additionally, instead of the $R_{1\text{-}2S}$ warning, we use the $R_{1\text{-}3S}$ "warning." Using s_{RW} instead of σ, we make a proportional increase in the decision limits. Following Westgard's recommendations strictly, we partially avoid alarms in cases of incorrigible biases. The probability of no warnings in a month becomes 61%, a plausible value to observe the phenomenon.

While the within-run rules ("$R_{1\text{-}3S}$" and "$R_{2\text{-}2S}$") are sensitive to the proportional overestimation of σ. They efficiently avoid alarms in the case of incorrigible biases. In contrast, "$R_{4\text{-}1S}$" is less sensitive, and R_{10X} is insensitive, resulting in a relative increase in efficiency of the cross-run rules, along with a reduced but not insignificant number of false alarms. The Westgard recommendations are only practical for higher sigma metric values.

A more efficient solution is to increase all decision limits not proportionally, but with a constant value, the estimated Bincorrigible. (E.g., using the $3s_r + B_{incorrigible}$ limit instead of the $3s_{RW}$). This increase in the decision limits must be reflected in the name of the rule, consistent with the calculations. To state that you apply "$R_{1\text{-}3S}$" and de facto apply $R_{1\text{-}4.5S}$ is misleading and a source of errors.

When comparing the monthly s_{RW} values, the inaccuracy of the overestimation of σ by s_{RW} becomes more evident. A value in a month may double or halve in the next month [27]. On the last day of the month, calculating the new s_{RW} value and redesigning the graphs, we will become conscious that we missed several alarms, or vice versa; we have made several unnecessary calibrations.

A real-life example of cholesterol is suggestive. For an easier and more accurate comparison between the control levels, the results are expressed as a percentage. TEa = 8%, CV_r = 0.98%, and the average CV_{RW} = 2.11% (the average of both control levels, measured in the previous month). Calculated with CV_r = 0.98% and negligible bias in EQA, Nσ=8.16. Assuming $B\%_{incorrigible} \approx CV_r$=0.98%, the R_{1-4S} limit is 3.92%. All control data were between -2.05% and +3.91%, with a mean of +1.38%. No alarm was observed. According to Westgard's recommendation, Nσ=3.82; therefore, "all Westgard rules" are recommended. Decision limits: R_{1-3S}: 6.33%, R_{2-2S}: 4.22%, R_{4-1S}: 2.11%. Consistent with a mean of 1.38%, several R_{10X} alarms could be observed if applied, but no R_{1-2S} warning. (The actual recommendations on westgard.com do not use the R1-2S warning in multi-rules [28].) At the end of the month, the recalculated CVRW was 1.41%, and the Nσ = 5.67. According to Westgard's recommendations, only the R_{1-3S} and R_{2-2S} rules were necessary to apply, with the following decision limits: 4.23% for R_{1-3S} and 2.82% for R_{2-2S}. If applied to the same dataset, more R_{1-2S} warnings would occur, but no R_{1-3S} or R_{2-2S} rule violations would be observed. In the meantime, the violations of the unapplied R_{4-1S} or R_{10X} rules suggest the existence of (insignificant) biases. Due to the variability of the s_{RW}, applying Westgard's recommendation may raise doubts about the accuracy of decisions.

In contrast to s_{RW}, the s_r values (determined from control values obtained under constant conditions) are less variable, making the decisions more trustworthy.

Conclusions

The Westgard-rules-based QC system is based on an erroneously assumed normal distribution of the long-term control data. The laws of the normal distribution can be applied only to data collected under constant, repeatability conditions. Because of the internal QC decisions are made under repeatability conditions. Therefore, according to a principle valid in all exact sciences, the standard deviation (SD) used in the design of the QC charts must be s_r.

Calibration is a measurement, and, like all measurements, it has both random and systematic error components. The primary source of the random component is the random error committed in the measurement, which is at least 1 CV_r. The systematic component is linked to the reference material value error, which cannot be reduced to the uncertainty of the nominal value specified in the traceability certificates. A more significant source is the reconstitution error, which includes two volume measurements. The overall calibration error was estimated to be 1-2 CV_r. The estimation was experimentally verified through repeated calibrations (under repeatability conditions) and by comparing the calibration factors obtained in new calibrations using the same reagent and reference material lots. Both confirmed the estimations.

According to another quintessential principle valid in all exact sciences, calibration cannot correct smaller errors than the average calibration error. Therefore, such minimal biases are incorrigible, and alarms must be avoided in those cases. The actual Westgard-rules-based QC system neglects the importance of incorrigible biases. The decisions based on the Westgard rules are only correct if the QC graphs are designed with a correct estimator of the σ parameter of the Gauss equation, which is s_r. Calculations based on the laws of the normal distribution predict that the Westgard rules, based on s_r, are a guaranteed fail, causing hundreds of false alarms. The fact that these alarms are not observed suggests an overestimation of the σ parameter.

As JO Westgard and T Groth acknowledged, the calculations behind the Westgard-rules-based QC system are based on the assumption of "within-run (repeatability) SD" (s_r). In contrast, the graphs are designed with "total SD" (s_{RW}). JO Westgard et al. recommended a proportional but inaccurate increase in the decision limits, overestimating σ with s_{RW}. It is inaccurate for two reasons: (1) due to the variability of s_{RW}, which is not calculated from normally distributed data sets, and (2) s_{RW} is a parameter determined under variable conditions in the past, inconsistent with the QC decisions made under repeatability conditions in the present.

A more accurate correction is a constant increase in the decision limits by adding the estimated incorrigible bias to all decision limits and simultaneously using sr in the design of the QC graphs. In the case of moderate ratios (around 1.5), the decision limits for the within-run rules are similar to those proposed by Westgard et al. (for example, $3s_{RW} \approx 3s_r + B_{incorrigible}$). Significant differences can be observed in the case of bigger ratios and if the cross-run rules (R_{4-1S} and R_{10X}) are used. Correcting the estimator of the σ parameter (from s_{RW} to s_r) changes all calculations in the QC system, including the design of the QC graphs, Bcrit, and Nσ, and a complete reevaluation of the QC system becomes necessary.

A comparative analysis of the efficiency of the proposed rules with the Westgard rules exceeds the word count limits of this paper. An independent study is necessary.

Author statements

To this study, no other persons contributed except the author.

This study was neither funded nor sponsored.

The author did not use patient data in this study.

The author created all images and tables.

The author attests that this manuscript did not use generative artificial intelligence (AI) technology to generate figures, ideas, data, or other informational content. AI was used only for grammar correction and unintentional plagiarism detection. To assist with language correction, the author utilized the following Grammarly AI prompts: "Improve it" and "Find synonyms."

Abbreviations

QC	Quality control
RM	Reference material (calibrator)
TEa	Admitted total error
SE	Systematic error component
RE	Random error component
VCSE	Variable component of the systematic error
CCSE	Constant component of the systematic error
A	Absorption
A0	Null-point absorption, the intercept of the linear calibration graph
DA	Difference in absorption (=A-A0)
F_{cal}	Slope factor of the calibration graph in linear calibrations
σ	The sigma parameter of the Gauss equation, the estimator of the mean RE
SD	Standard deviation
s	Measured SD
CV	Coefficient of variation
CV_{Fcal}	Coefficient of variation calculated from the calibration slope factors
CV_{VCSE}	CV calculated from the variable daily bias values, or the VCSE
B	Bias expressed in absolute values
B%	Bias expressed in percent of the target value
$B_{incorrigible}$	Bias incorrigible by calibration
Nσ	sigma metrics
$_{r}$	Repeatability conditions of measurement
$_{RW}$	Reproducibility within laboratory conditions of measurement.

References

1. Plebani M. Errors in clinical laboratories or errors in laboratory medicine? Clin Chem Lab Med. 2006;44(6):750-759. doi: 10.1515/CCLM.2006.123. https://pubmed.ncbi.nlm.nih.gov/16729864/

2. Westgard, JO: Advanced Quality Management / Six Sigma, [Internet]. Westgard QC [cited 2025 Jan 25]. Available from: https://westgard.com/lessons/advanced-quality-management-six-sigma/lesson67.html

3. Gauss, CF. Bestimmung der Genauigkeit der Beobachtungen. Zeitschrift für Astronomie und Verwandte Wissenschaften.1816;1:187–197.

4. Oosterhuis WP, Bayat H, Armbruster D, Coskun A, Freeman KP., Kallner A, Koch D, Mackenzie F, Migliarino G, Orth M, Sandberg S, Sylte MS., Westgard S, and Theodorsson E. The use of error and uncertainty methods in the medical laboratory CCLM. 2018;56(2),209-219. DOI: 10.1515/cclm-2017-0341 https://doi.org/10.1515/cclm-2017-0341 Available from URL: https://www.degruyter.com/document/doi/10.1515/cclm-2017-0341/html#j_cclm-2017-0341_ref_030_w2aab3b7c59b1b6b1ab2b3c30Aa

5. Thompson, M. Towards a unified model of errors in analytical measurement, Analyst, 2000;125 (11),2020-2025, The Royal Society of Chemistry, DOI:10.1039/B00637M, https://doi.org/10.1039/B006376M Available from URL: https://pubs.rsc.org/en/content/articlelanding/2000/an/b006376m

6. Theodorsson E, Magnusson B, Leito I: Bias in Clinical Chemistry, Bioanalysis, 2014;6(21), 2855–2875. https://doi.org/10.4155/bio.14.249, published online Dec 8, 2014, Available from: https://www.future-science.com/doi/10.4155/bio.14.249

7. Vandra AB. Reevaluation of the Variable Component of the Systematic Error Calls for Paradigm Change in Clinical Laboratory Quality Control. 2023 May 28; Preprint, medRxiv 2023.05.24.23290382; doi: 10.1101/2023.05.24.23290382 available from: https://doi.org/10.1101/2023.05.24.23290382

8. CLIA Final Rule: "Equivalent" Quality Control Practices. [Internet] Westgard QC [Cited 2025 Jan 26] Available from: https://westgard.com/clia-a-quality/clia-final-rule/249-cliafinalrule7.html

9. Toacşe G. , Toacşe AM: Controlul de calitate şi validarea metodelor analitice cantitative pentru laboratoarele medicale Bucureşti: Editura Tehnică, 2010.

10. Westgard JO, Groth TL. Power functions for statistical control rules. Clin Chem. 1979;25(6): 863-869. PMID: 445821. DOI: 10.1093/clinchem/25.6.863 Available from URL: https://www.researchgate.net/publication/22696098_Power_Functions_for_Statistical_Control_Rules

11. Magnusson B, Näykki T, Hovind H, Krysell M, Sahlin E: Handbook for calculation of measurement uncertainty in environmental laboratories Nordtest, NT TR 537 – Edition 4, p 10, Available from: http://www.nordtest.info/wp/2017/11/29/handbook-for-calculation-of-measurement-uncertainty-in-environmental-laboratories-nt-tr-537-edition-4/

12. Cooper G. Resolving QC failures. Medical Laboratory Observer online. [Internet] Jul 20, 2016, [cited 2025 Jan 28] Available from URL: https://www.mlo-online.com/management/qa-qc/article/13008813/resolving-qc-failures

13. Seamaty Technology: Common Errors and Pitfalls in Clinical Chemistry Analyzer Testing [Internet] Seamaty Technology, Apr 17, 2023 [cited 2025 Jan 27] Available from https://en.seamaty.com/index.php?s=/sys/547.html

14. Sonntag O, Loh TP. Calibration - an under-appreciated component in the analytical process of the medical laboratories. Adv Lab Med. 2023;5(2):148–152. doi: 10.1515/almed-2023-0127. PMID: 38939195; PMCID: PMC11206179. Available from URL: https://pmc.ncbi.nlm.nih.gov/articles/PMC11206179/

15. T. Badrick: The quality control system. Clin Biochem Rev. 2008;Suppl 1: S67-S70. Available from URL: https://www.ncbi.nlm.nih.gov/pmc/articles/PMC2556587/

16. Burtis CA, Ashwood ER (editors). Tietz Textbook of Clinical Chemistry. 2. Philadelphia, USA: W.B. Saunders; 1994.

17. White GH. Basics of estimating measurement uncertainty.

Clin Biochem Rev. 2008;29 Suppl 1(1): S53-S60. Available from URL: https://www.ncbi.nlm.nih.gov/pmc/articles/PMC2556585/
18. Coskun A. Bias in Laboratory Medicine: The Dark Side of the Moon. Ann Lab Med. 2024;44(1) 6–20. doi: 10.3343/alm.2024.44.1.6. Epub 2023 Sep 4. PMID: 37665281; PMCID: PMC10485854. Available from URL: https://pmc.ncbi.nlm.nih.gov/articles/PMC10485854/Bias in Laboratory Medicine: The Dark Side of the Moon - PMC
19. NIST. Engineering Statistics Handbook. 1.3.6.7.1. Cumulative Distribution Function of the Standard Normal Distribution [Internet] NIST [cited 2025 Jan 29] Available from URL: https://www.itl.nist.gov/div898/handbook/eda/section3/eda3671.htm
20. Haeckel R, Wosniok W. Observed, unknown distributions of clinical chemical quantities should be considered to be log-normal: a proposal. Clin Chem Lab Med. 2010;48(10):1393–1396. doi: 10.1515/CCLM.2010.273.
21. Badrick T. Biological variation: Understanding why it is so important? Pract Lab Med. 2021 Jan 4;23:e00199. Doi: 10.1016/j.plabm.2020.e00199. Available from URL: https://www.ncbi.nlm.nih.gov/pmc/articles/PMC7809190/#bib136
22. Katayev A. & Fleming J. Past, present, and future of laboratory quality control: patient-based real-time quality control or when getting more quality at less cost is not wishful thinking —Journal of Laboratory And Precision Medicine, 2020(5). Doi:10.21037/jlpm-2019-qc-03 Available from URL: https://jlpm.amegroups.org/article/view/5718/html#B6
23. Haeckel R, Schneider B: Detection of drift effects before calculating the standard deviation as a measure of analytical imprecision. J Clin Chem Clin Biochem. 1983;21(8):491-497. doi: 10.1515/cclm.1983.21.8.491. PMID: 6631335 Available from URL: https://pubmed.ncbi.nlm.nih.gov/6631335/
24. Mackay M, Hegedus G, Badrick T. Assay Stability, the Missing Component of the Error Budget, Clinical Biochemistry, 2017;50(18): 1136-1144, ISSN 0009-9120, https://doi.org/10.1016/j.clinbiochem.2017.07.004.
25. Krouwer JS: Setting Performance Goals and Evaluating Total Analytical Error for Diagnostic Assays, Clinical Chemistry, 2002;48(6):919–927, https://doi.org/10.1093/clinchem/48.6.919
26.Westgard JO Basic QC Practices. QC - The Calculations. [Internet] Westgard QC, [cited 2025 Jan 30] Available from URL: http://westgard.com/lessons/basic-qc-practices-l/lesson14.html
27. Kumar BV, Mohan T: Sigma metrics as a tool for evaluating the performance of internal quality control in a clinical chemistry laboratory, Tables 3 and 4, J Lab Physicians. 2018;10(2):194–199.,doi:10.4103/JLP.JLP_102_17, available from URL: https://www.ncbi.nlm.nih.gov/pmc/articles/PMC5896188/
28. Westgard JO, Westgard S. Introducing Westgard Sigma Rules, [Internet]2014 Sep. [Cited 2025 Apr 2. Available from URL: https://westgard.com/lessons/westgard-rules/westgard-rules/westgard-sigma-rules.html
29. Grammarly. Grammarly [Internet]. Grammarly.com. 2025. Available from: https://app.grammarly.com/

Research Article

Impact of creatinine-eGFR equations on chronic kidney disease stratification in a Ghanaian Tertiary Care Setting

Mildred Martey[1], Patrick Seidu[2], George B. Kyei[1,3,4], Catherine L. Omosule[1*]

[1]*Medical and Scientific Research Centre, University of Ghana Medical Centre, Accra, Ghana*
[2]*Department of Internal Medicine, Korle-Bu Hospital, Accra, Ghana*
[3]*Washington University in St. Louis, St. Louis, Missouri*
[4]*Noguchi Memorial Institute for Medical Research, University of Ghana, Accra, Ghana*

Article Info

[*]***Corresponding Author:***
Catherine Omosule, PhD, DABCC, NRCC Snr.
Medical and Scientific Research Fellow University of Ghana Medical Centre
Adj. Noguchi Memorial Institute GA-337-6980
Legon - Accra
Tel: +233 302 550843-5 Extn 16209
Cell: +233 534 095273
E-mail: comosule@ugmc.ug.edu.gh

Keywords
eGFR, kidney, creatinine Abbreviations

Abstract

Kidney diseases disproportionately affect people of African descent, yet current estimated glomerular filtration rate (eGFR) equations lack accuracy in African populations. The widely used the race-adjusted Modification of Diet in Renal Disease (MDRD) equation underestimates GFR in African individuals with kidney disease, while newer race-agnostic equations, such as the 2021 CKD-EPI and European Kidney Function Consortium (EKFC) equations, require further validation in these populations. This study evaluated five creatinine-based eGFR equations in a Ghanaian population to assess their impact on chronic kidney disease (CKD) stratification.

The study utilized the MDRD, MDRD without race coefficient (MDRDnr), CKD-EPI 2009 and 2021, and EKFC equations, to compare stratification into GFR stages per KDIGO guidelines using creatinine results from adult patients seen at the University of Ghana Medical Centre (January 2021–December 2023).

Among 10,864 creatinine results from 6172 females (56.8%) and 4692 males (43.2%), the MDRDnr yielded the lowest median eGFR (76.4 mL/min/1.73 m²), while MDRD had the highest. The MDRDnr identified the highest prevalence of reduced eGFR (<60 mL/min/1.73 m²) at 19.9%, followed by EKFC (14.8%), 2021 (11%), CKD-EPI 2009 (10.6%), and MDRD (8.8%). Notably, one-third of individuals with reduced eGFR (per EKFC) were under 60 years old. The EKFC equation identified more cases of reduced eGFR than both CKD-EPI equations.

The MDRDnr and EKFC equations detected the highest proportion of reduced eGFR. However, the EKFC has been shown in other studies to be more accurate. Further validation and adoption of the EKFC equation are recommended for improved CKD diagnosis in Ghana.

Introduction

Kidney diseases are the third fastest leading cause of mortality globally and are projected to be the 5th leading cause of death by 2040 [1,2]. The majority of the 850 million people globally affected by kidney diseases reside in low- and middle-income countries (LMICs) [3]. While certain risk factors for kidney disease such as diabetes and hypertension, are common in these regions, the higher prevalence of infectious diseases, environmental factors (use of herbal medicines) and genetic factors (predispositions to sickle cell disease and APOL[1] risk alleles), further exacerbate the progressive kidney disease burden among African populations [4,5]. Chronic Kidney Disease (CKD) increases the risk of end-stage renal disease (ESRD), cardiovascular disease, and mortality, underscoring the importance of early diagnosis and therapeutic intervention. Unfortunately, a significant proportion of those affected are unaware of their disease status in LMICs partly due to the clinically silent nature of CKD, and lack of access to screening facilities [6]. This ensuing late diagnosis is further complicated by the limited to non-
existent access to renal replacement therapy (RRT, dialysis and transplantation) in LMICs like Ghana where ~13% of the population has CKD [7–9].

Creatinine-based estimation of glomerular filtration rates (Cr-eGFR) are widely used for kidney disease assessments given the resource-intensive gold-standard methodologies for measuring GFR (mGFR) [10]. Several Cr-eGFR equations exist, including the 2006 Modification of Diet in Renal Disease (MDRD 2009 and 2021), Chronic Kidney Disease Epidemiology Collaboration (CKD-EPI 2009 and 2021), and 2021 European Kidney Function Consortium (EKFC). These equations exhibit varying degrees of accuracy and bias relative to mGFR, impacting clinical decision-making differently [11,12]. Of these equations, the MDRD and 2009 CKD-EPI utilize racial coefficients, which contribute to racial disparities in kidney care globally [13,14]. However, the 2021 CKD-EPI and EKFC equations have been developed to be race-neutral although EKFC estimations are more accurate if population specific factors (Q values) are incorporated [15]. While the 2021 CKD- EPI equation has shown promise in improving equity in kidney care in the U.S. where it was developed and has been primarily validated, emerging evidence suggests that the EKFC may provide more accurate GFR estimates across diverse populations, including Africans [9-11].

The 2024 Kidney Disease Improving Global Outcomes (KDIGO) Clinical Practice guidelines recommend the use of a validated, race-free creatinine-based eGFR alone or in combination with cystatin C measurement for evaluating patients at risk for CKD as well as for disease staging within a region [10]. Nonetheless, in many settings, including Ghana, the older MDRD equation with the race coefficient remains widely used, partly due to its simplicity and lack of robust validation of the newer eGFR equations in African populations [16]. Furthermore, alternative methods for estimating kidney function, such as those based on cystatin C, are currently not readily available or affordable in resource-limited settings despite improved race-agnostic performance [17].

Selecting an appropriate eGFR equation requires rigorous population and/or region- specific validation to ensure accuracy and clinical relevance [10]. In the absence of such validation in Ghana and given the critical need for early CKD diagnosis to prevent complications, this study aims to retrospectively compare absolute eGFR values obtained using the 2021 EKFC equation with those obtained using the 2006 MDRD and three other creatinine-based eGFR equations (2006 MDRD (no race, MDRDnr), 2009 CKD-EPI, and 2021 CKD-EPI). Furthermore, we will estimate the prevalence of reduced eGFR as a surrogate for CKD prevalence in the Ghanaian adult population visiting a tertiary healthcare facility. Finally, we will assess the impact of these different equations on the re-stratification of individuals across CKD stages.

Methods

Study subjects

This retrospective study utilized data from adults aged 18 years and above who visited the University of Ghana Medical Center (UGMC), a tertiary healthcare facility in Accra, Ghana, between January 2021 to December 2023 and had creatinine measured. We applied a stringent criterion to exclude data from inpatients, pregnant women, and those with acute conditions, including those seen at the ER, surgery, and nephrology departments, generating a data set representative of outpatient visits. Entries with missing data on creatinine results, department, age, or sex were also excluded. For patients with multiple creatinine measurements, the first available measurement was used. UGMC Institutional Review Board approval was obtained before the commencement of the study.

Creatinine Measurements

All serum creatinine measurements were completed in accordance with standard clinical laboratory practice using the MINDRAY (Shenzhen. China) IDMS-traceable creatinine sarcosine oxidase assay and assayed on the Mindray Bs-480 analytical instrument.

eGFR calculations staging kidney function

Five creatinine-based eGFR equations were utilized in this study: MDRD, MDRD (without race, MDRDnr), 2009 CKD-EPI, 2021 CKD-EPI, and EKFC (21) (Supplementary Table 1). The 2021 EKFC utilized Q values (0.72 for females, 0.96 for males) generated from a small cohort of Africans from Cote-D'Ivoire and the Democratic Republic of Congo [15]. Comparison of CKD classifications using the 2021 EKFC with the African-Q-value versus a race-free Q-value (EKFCrf: 0.73 for females, 0.99 for males) is provided in the Supplementary [15]. CKD staging was done in accordance with KDIGO guidelines [10]. In brief, G^1 (GFR ≥90 ml/min/1.73m^2), G^2 (GFR 60-89 ml/min/1.73m^2), G^3a (GFR 45-59 ml/min/1.73m^2),

G^3b (GFR 30- 44 ml/min/1.73m^2), G^4 (GFR 15-29 ml/min/1.73m^2), and G^5 (GFR <15 ml/min/1.73m^2).

Statistical analysis

All participants were stratified into seven age groups: 18–29, 30–39, 40–49, 50–59, 60–69, 70-79 and ≥ 80 years old. Excel and GraphPad Prism V[10].4.0 were used for all data analysis and graphing. Descriptive statistics are presented as median and interquartile range (IQR). ANOVA and Wilcoxon paired rank sum tests were used to compare quantitative eGFRs values (Table 1) between equations. Chi-Square tests were used to identify differences in categorical data between equations (i.e. low eGFR prevalence groupings).

Results

Demographic and Clinical Characteristics

Our dataset was composed of 10,864 creatinine results, each representing a unique patient. Males comprised 4692 (43.2%) while females comprised 6172 (56.8%). The median age was 47.5 (28.6) years, (Table 2).

Of the five eGFRs, median eGFR values were lowest with the MDRDnr at 76.4 (28) mL/min/1.73 m^2 and highest with the MDRD at 92.4 (33.8) mL/min/1.73 m^2. The 2009 CKD-EPI, 2021 CKD- EPI and EKFC had median eGFRs of 92.2 (40.1), 89.8(32.1), and 80.6(30) (mL/min/1.73 m^2), respectively. A statistically significant difference in absolute eGFR values between the equations was observed (p<0.001).

The highest prevalence of decreased eGFR (i.e. G^3a to G^5, <60 mL/min/1.73 m^2) was observed with the MDRDnr at 19.9%, followed by the EKFC (14.8%), 2021 CKD-EPI (11%), 2009 CKD- EPI (10.6%) and the MDRD (8.85%). The difference in prevalence observed between the equations was statistically significant (p<0.0001).

Table 1: Baseline characteristics of study population.

Characteristics	Data
Age, year (median, IQR)	47.5 (28.6)
Age group (n, %)	
18 to 29 years	1461 (13.5)
30 to 39 years	2448 (22.5)
40 to 49 years	1921 (17.7)
50 to 59 years	1676 (15.4)
60 to 69 years	1780 (16.4)
70 to 79 years	1128 (10.4)
>80 years	450 (4.1)
Sex (n, %)	
Male	4692 (43.2)
Female	6172 (56.8)
Serum Cr (mg/dL, median, IQR)	0.91 (0.35)

Characteristics	Data
Median eGFR ((mL/min/1.73 m^2, IQR)	
MDRD	92.4 (33.8)
MDRDnr	76.4 (28.0)
2009 CKD-EPI	92.2 (40.1)
2021 CKD-EPI	89.8 (32.1)
EKFC	80.6 (30)
eGFR <60 mL/min/1.73 m^2, CKD ≥ G^3a (n, %)	
MDRD	961 (8.8)
MDRDnr	2164 (19.9)
2009 CKD-EPI	1148 (10.6)
2021 CKD-EPI	1194 (11.0)
EKFC	-14.8

Population distribution of eGFR and CKD stages

The distribution of eGFR categories varied significantly across the different eGFR equations (Figure 1, Table 3). The MDRD, 2009 CKD-EPI, and 2021 CKD-EPI equations predominantly categorized individuals in G^1 (eGFR > 90 mL/min/1.73m²), with 54%, 60%, and 50% of values falling within this range, respectively, whereas the MDRDnr and the EKFC predominantly classified individuals into G^2 (eGFR: 60 and 90 mL/min/1.73m²), with 58% and 45% of values falling within this range, respectively. The proportion of individuals classified with reduced eGFR (stages 3a-5) varied significantly across the different eGFR equations. The MDRD equation identified the lowest proportion of individuals with reduced eGFR (8.8%, 961 individuals). In contrast, the MDRDnr identified the highest proportion (19.9%, 2164 individuals). The 2009 CKD-EPI, 2021 CKD-EPI, and 2021 EKFC equations identified 10.6% (1148), 11% (1194), and 14.8% (1607) individuals with reduced eGFR, respectively.

Within the reduced eGFR categories, CKD stage 3a was the most prevalent across all equations, accounting for 57% (547 individuals) with the MDRD, 68% (1466 individuals) with the MDRDnr, 56% (638 individuals) with the 2009 CKD-EPI, 60% (713 individuals) with the 2021 CKD-EPI, and 62% (998 individuals) with the 2021 EKFC.

CKD stage 3b accounted for 19% (186 individuals), 18% (400 individuals), 23% (260 individuals), 22% (262 individuals), and 21% (337 individuals) of cases, respectively, across

the different equations. CKD stage 4 comprised 14% (130 individuals), 8% (172 individuals), 12% (142 individuals), 11% (126 individuals), and 10% (164 individuals) of cases, respectively. Finally, CKD stage 5 comprised 10% (98 individuals), 6% (126 individuals), 9% (108 individuals), 8% (93 individuals), and 7% (108 individuals) of cases, respectively, across the MDRD, MDRDnr, 2009 CKD-EPI, 2021 CKD-EPI and EKFC equations. These differences were statistically significant (Chi square, p<0.0001).

Figure 1: Distribution of eGFR by equations.

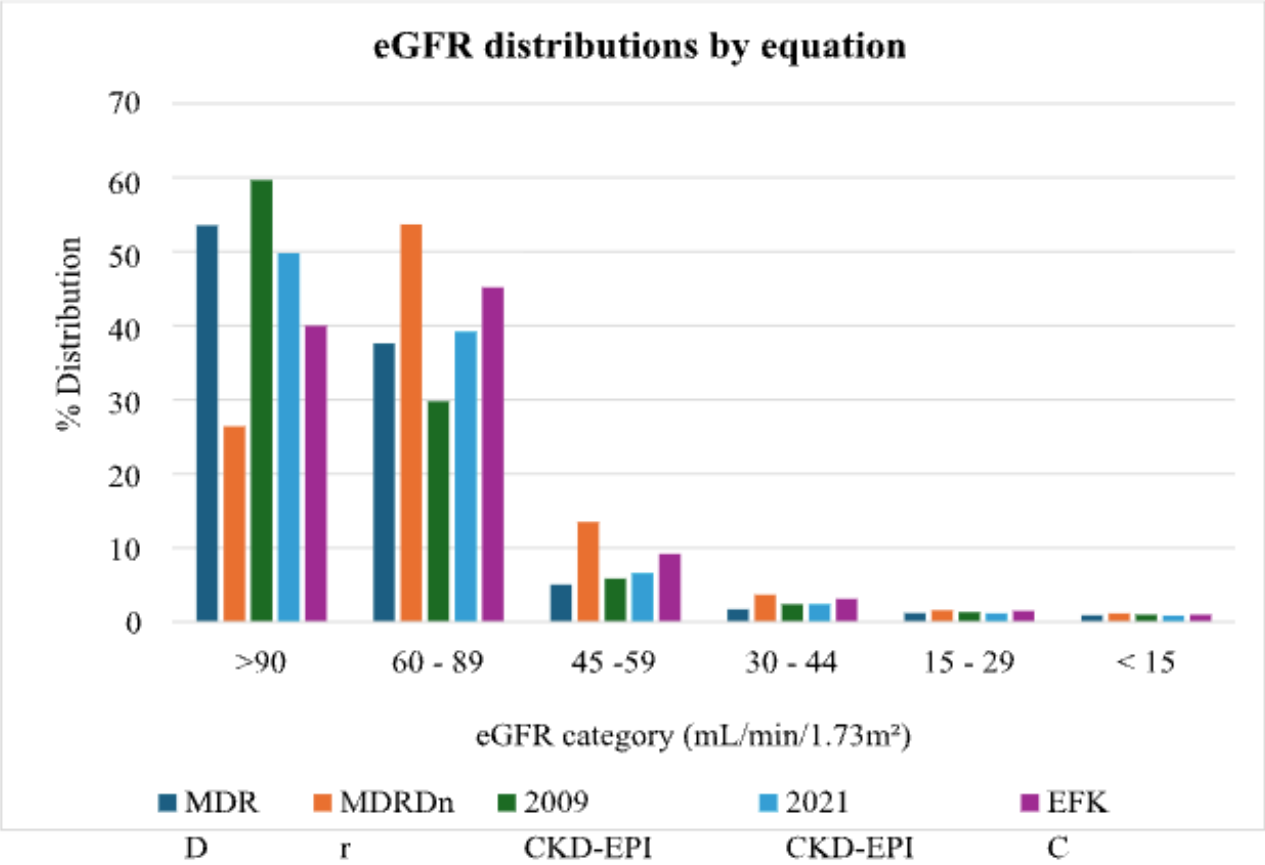

The left y-axis represents the percent distribution of the population for each of the equation. The x-axis represents the eGFR category (G^1, G^2, G^3a, G^3b, G^4 and G^5).

Table 2: Equation-based eGFR staging (counts).

	G^1	G^2	G^3a	G^3b	G^4	G^5
MDRD	5818	4085	547	186	130	98
MDRDnr	2870	5830	1466	400	172	126
2009 CKD-EPI	6482	3234	638	260	142	108
2021 CKD-EPI	5411	4259	713	262	126	93
EKFC	4347	4910	998	337	164	108

Age and sex distribution of eGFR and CKD stages

The absolute eGFR values, regardless of the equation used, decreased with age (Figure 2). This decline showed a weak to moderate negative correlation, as measured by Pearson's r. The strongest negative correlation was observed with the EKFC equation (r = -0.59, 95% CI: -0.60 to -0.58, p<0.0001), while the weakest was with the MDRDnr equation (r = -0.34, 95% CI: -0.35 to -0.32, p<0.0001). Also, the slope, representing the constant decline in eGFR per year of age, was -0.65 (95% CI: - 0.68 to -0.61) for MDRD, -0.54 (95% CI: -0.57 to -0.51) for MDRDnr, -0.91 (95% CI: -0.94 to -0.86) for 2009 CKD-EPI, -0.74 (95% CI: -0.76 to -0.71) for 2021 CKD-EPI, and -0.77 (95% CI: -0.79 to -0.75) for EKFC

The distribution of eGFR categories per age group was also influenced by choice of eGFR equation (Figure 3). For the 18-29 age group, eGFR values above 60 mL/min/1.73m² ranged from 96% (MDRDnr) to 99% (MDRD, and 2009 and 2021 CKD-EPI). In the 30-39 age group, this range was 92% to 98%. Subsequent age groups showed a decreasing trend in the proportion of individuals with eGFR > 60 mL/min/1.73m²: 84% to 94% for 40-49 years, 76% to 90% for 50-59 years, 68% to 85% for 60-69 years, 61% to 81% for 70-79, and 44% to 73% for those 80 years and above. A critical consideration of reduced eGFR categories per age groups influenced by equation revealed concerning statistics. Of the proportion of patients identified by both the MDRD and EKFC as having reduced eGFR, a significant proportion were patients less than 60 years of age, who are still in their productive years. They made up 40.6%, 24.75%, 44.6% and 55% for stages G^3a, G^3b, G^4, G^5 respectively for the MDRD (Table 3), and 31.3%, 32.1%, 30.8% and 52% of those with stages G^3a, G^3b, G^4, and G^5 respectively for the EKFC (Table 4).

Using the MDRD equation, women aged 60 to 69 had the highest prevalence of stage G^3a, men aged 60 to 69 of stages G^3b and G^4, and women aged 50 to 59 of stage G^5. Using the 2021 EKFC, women aged 60 to 69 had the highest prevalence for stage G^3a, women aged 70 to 79 of stage G^3b, men aged 60 to 69 of G^4, and both women aged 50 to 59 and men aged 70 to 79 of G^5 . These findings highlight the significant impact of equation choice on eGFR estimates and CKD stage classification.

Figure 2: Age distribution and eGFR by the a) MDRD, b) MDRDnr, c) 2009 CKD-EPI, d) 2021 CKD-EPI, and e) EKFC.

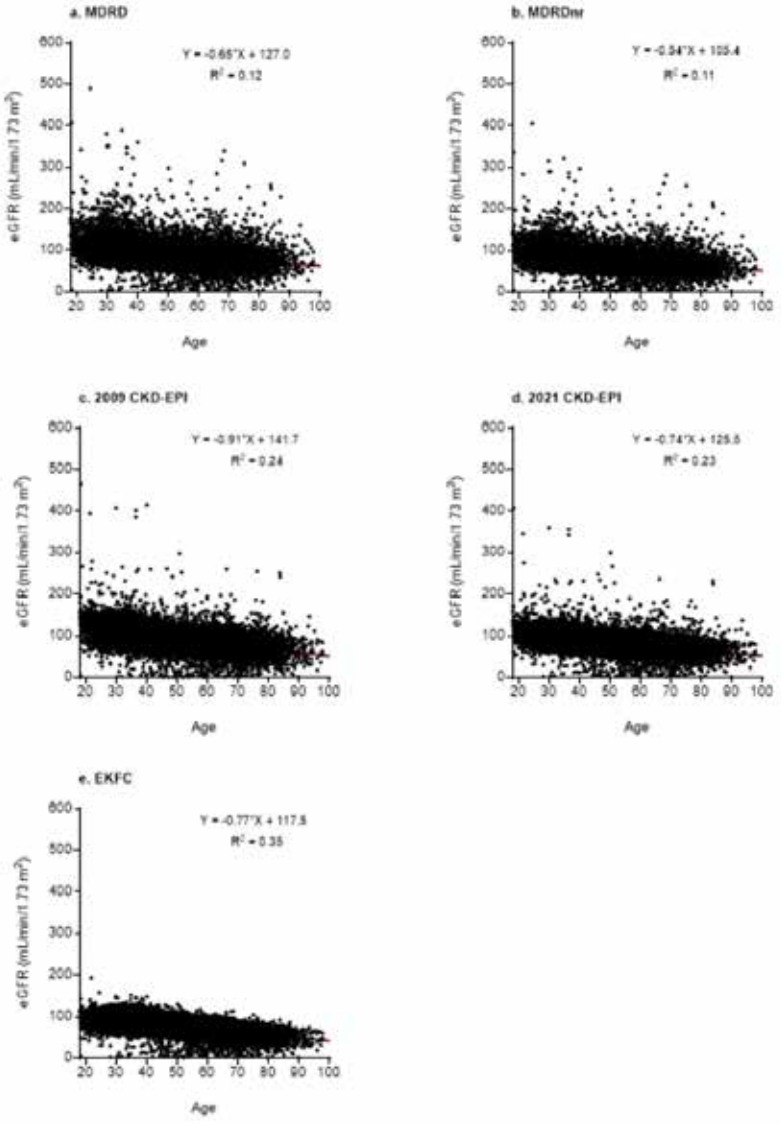

Data points beyond 600 mL/min/1.73m² are not displayed.

Figure 3: Distribution of eGFR categories and CKD stages across different age groups, categorized by the equation used for calculation.

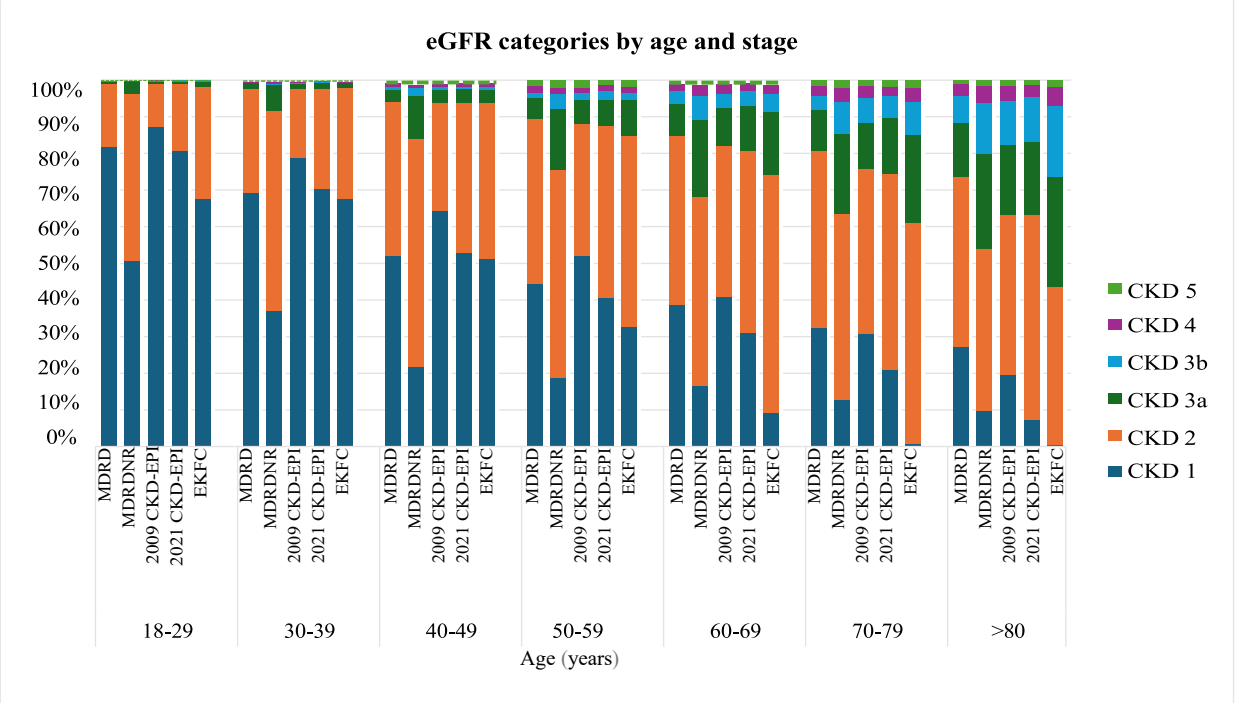

The left y-axis represents the percent population distribution for each equation.

Table 3: Age and sex distribution of reduced eGFR (< 60 ml/min/1.73 m^2) per the MDRD equation.

AGE	CKD 3a, n=547		CKD 3b, n=186		CKD 4, n=130		CKD 5, n=98	
	Females n=282	Males n=265	Females n=86	Males n=100	Females n=57	Males n=73	Females n=48	Males n=50
18–29 Years	26 (4.75%)	5 (0.91%)	1 (0.54%)	2 (1.08%)	0 (0.00%)	0 (0.00%)	0 (0.00%)	2 (2.04%)
30–39 Years	22 (4.02%)	13 (2.38%)	1 (0.54%)	2 (1.08%)	2 (1.54%)	2 (1.54%)	6 (6.12%)	6 (6.12%)
40–49 Years	32 (5.85%)	32 (5.85%)	5 (2.69%)	10 (5.38%)	8 (6.15%)	11 (8.46%)	9 (9.18%)	7 (7.14%)
50–59 Years	42 (7.68%)	50 (9.14%)	14 (7.53%)	11 (5.91%)	13 (10.00%)	18 (13.85%)	15 (15.31%)	11 (11.22%)
60–69 Years	112 (20.48%)	77 (14.08%)	27 (14.52%)	37 (19.89%)	12 (9.23%)	19 (14.62%)	11 (11.22%)	9 (9.18%)
70–79 Years	68 (12.43%)	60 (10.97%)	20 (10.75%)	24 (12.90%)	11 (8.46%)	18 (13.85%)	5 (5.10%)	13 (13.27%)
80 and above	39 (7.13%)	28 (5.12%)	18 (9.68%)	14 (7.53%)	11 (8.46%)	5 (3.85%)	2 (2.04%)	2 (2.04%)

Table 4: Age and sex distribution of reduced eGFR (< 60 ml/min/1.73 m^2) using the EKFC equation.

AGE	CKD 3a, n=1204		CKD 3b, n=410		CKD 4, n=182		CKD 5, n=115	
	Female (n=646)	Male (n=558)	Female (n=209)	Male (n=201)	Female (n=79)	Male (n=103)	Female (n=56)	Male (n=59)
18–29 Years	13 (1.08%)	18 (1.50%)	2 (0.49%)	3 (0.73%)	0 (0.00%)	0 (0.00%)	0 (0.00%)	2 (1.74%)
30–39 Years	29 (2.41%)	23 (1.91%)	3 (0.73%)	2 (0.49%)	2 (1.10%)	2 (1.10%)	6 (5.22%)	6 (5.22%)
40–49 Years	44 (3.65%)	46 (3.82%)	8 (1.95%)	8 (1.95%)	8 (4.40%)	14 (7.69%)	9 (7.82%)	7 (6.09%)
50–59 Years	104 (8.64%)	94 (7.81%)	19 (4.63%)	26 (6.34%)	13 (7.14%)	17 (9.34%)	17 (14.78%)	13 (11.30%)
60–69 Years	189 (15.70%)	183 (15.20%)	52 (12.68%)	56 (13.66%)	20 (10.99%)	34 (18.68%)	12 (10.43%)	10 (8.70%)
70–79 Years	172 (14.29%)	133 (11.05%)	69 (16.83%)	63 (15.37%)	19 (10.44%)	24 (13.19%)	7 (6.09%)	17 (14.78%)
80 and above	95 (7.89%)	61 (5.07%)	56 (13.66%)	43 (10.49%)	17 (9.34%)	12 (6.59%)	5 (4.35%)	4 (3.48%)

Comparison of eGFR equations (agreement and concordance)

We then assessed the agreement in GFR categorization as a surrogate for CKD stages using the different Cr-eGFR equations (Figure 3). The MDRD showed 58% agreement with the MDRDnr, 87% with 2009 CKD-EPI, 87% with 2021 CKD-EPI, and 77% with EKFC. Notably, the MDRD significantly underestimated CKD stage compared to the MDRDnr (42%), 2009 CKD-EPI (5%), 2021 CKD-EPI (10%), and EKFC (22%).

The MDRDnr demonstrated agreement rates of 56%, 66%, and 72% with the 2009 CKD-EPI, 2021 CKD-EPI, and EKFC, respectively. This equation exhibited a higher rate of overestimation compared to the MDRD, 2009 CKD-EPI, 2021 CKD-EPI and EKFC, with 44%, 34%, and 24% of individuals being classified into a more advanced CKD stage.

The 2009 CKD-EPI equation showed 83% and 74% agreement with the 2021 CKD-EPI and EKFC, respectively. It underestimated CKD stage in 13% and 25% of cases compared to the 2021 CKD-EPI and EKFC, respectively, while overestimating in only 4% and 1% of cases.

Finally, the 2021 CKD-EPI and EKFC equations demonstrated 83% agreement. The 2021 CKD- EPI overestimated CKD stage in 1% of cases and underestimated 16% of cases compared to the 2021 EKFC.

Delanaye and colleagues' proposed race-free Q-value (EKFCrf) [15] demonstrated a remarkable 97% agreement in CKD staging when used for eGFR calculation with EKFC. In comparison to the African-specific Q-value, this approach led to a minor 2.6% underestimation and 0.19% overestimation (Supplementary Table 2). This was due to higher absolute eGFRs generated by the EKFCrf ($p<0.001$).

Thus, the EKFC and MDRDnr Cr-eGFRs placed a majority of cases in higher CKD stages relative to the MDRD, 2009 CKD-EPI and 2021 CKD-EPI equations.

Figure 4: Agreement of CKD grade classification: (a) using the MDRD equation, (b) using the 2021 CKD-EPI equation and (c) using the EKFC equation.

'Underestimated' refers to cases where the CKD grade estimated by the reference equation (a, b, and c) was lower than the CKD grade estimated by each of the other equations. 'Agreement' signifies cases where the CKD grade determined by both the reference equations and the other equation matched. 'Overestimation' refers to cases where the CKD grade estimated by the reference equation was higher than the other equations.

Discussion

The best measure of kidney function is GFR. However, its direct measurement is complex and often impractical. Therefore, GFR estimates (eGFR) which incorporates factors including creatinine concentration, age, sex, and historically, race, are routinely used in clinical practice. Whereas earlier Cr-eGFRs such as the MDRD and 2009 CKD-EPI included a race- coefficient, the 2021 CKD-EPI and EKFC equations lack racial coefficients, in a bid to move towards a more equitable approach to kidney care. However, none of these equations have been properly validated in African populations, and yield varying eGFR values which potentially introduces uncertainty in clinical decision-making, and fails to accurately reflect the true burden of kidney disease in Sub-Saharan Africa [16]. This study examined how different Cr-eGFR equations affect eGFR categorization (per KDIGO guidelines), and by extension CKD staging, and also as estimates of the overall prevalence of reduced kidney function in an outpatient population at a major tertiary medical facility in Ghana. Our findings suggest that the MDRDnr and the EKFC equation (using an African

population-specific Q factor) classifies a significant proportion of individuals, the majority of whom are young, into reduced eGFR categories. However, because the MDRD and MDRDnr have reduced accuracy and precision relative to mGFR [16,18,19], we recommend further validation and potential adoption of the EKFC to replace the MDRD in routine medical practice in Ghana to facilitate early diagnosis of kidney disease.

Current Cr- eGFR equations frequently do not meet the recommended threshold of 90% accuracy within 30% of measured GFR (P^{30}) in published studies [16,20]. This discrepancy is particularly pronounced in African populations, with race-coefficients contributing substantially to this issue [19,21]. The MDRD equation, established two decades ago, is still widely utilized, in Ghana, Africa and beyond, despite lower accuracy and precision relative to the more recent Cr-eGFRs [22,23]. In our study, the MDRD identified the lowest prevalence of reduced eGFR, with higher median eGFR absolute values relative to the other Cr-eGFRs. In fact, in large African cohort studies, the MDRD was shown to grossly overestimate the prevalence of eGFR> 90 mL/min/1.73m² by 38% while grossly underestimating the prevalence of eGFR ≤ 89 mL/min/1.73m² by 37%. This significant bias and imprecision were attributed, in part, to the inclusion of the race coefficient [16]. Excluding the race variable reduced this bias, only overestimating 9% of the cohort with GFR > 90 mL/min/1.73m² and underestimating 8% of the cohort with GFR ≤ 89 mL/min/1.73m². Other studies performed without the race coefficient showed reclassification of African patients from CKD 3a to more advanced stages of kidney disease [18]. Consistent with this, in our study, removing the race coefficient from the MDRD equation yielded the highest median eGFR, identifying the highest percentage (19.9%) of individuals with reduced eGFR relative to the MDRD (8.8%), 2009 CKD-EPI (10.6%), 2021 CKD-EPI (11%) and EKFC (14.8%). Thus, eliminating the racial coefficient the MDRD may be considered in favor of identifying more at-risk patients. However, the MDRDnr still has poor accuracy relative to mGFR in individuals of African descent, particularly in those with reduced mGFR (i.e. < 60 mL/min/1.73m²). In one study of African patients, P^{30} using the MDRDnr with mGFR > 60 mL/min/1.73m² was 84.8% (95% CI: 81.3-88.3), decreasing to 31.3% (95% CI: 20.9-41.6) for those with mGFR < 60 mL/min/1.73m² [19]. Thus, the risk for kidney disease underdiagnosis and consequently delayed treatment initiation, and poorer outcomes for Africans with CKD remains. This makes the MDRD equation an inappropriate choice for kidney disease screening, diagnosis and management for the African population.

The influence of ethnicity continues to plague the EKFC equation as population-specific Q-factors perform better in comparison to mGFR relative to race-free Q-values [15].

We assessed the impact of using a race-free Q-value in this study with a primarily African patient population [15]. We observed that 2.6% of eGFRs were classified into less severe CKD stages, as the race-free Q-value (EKFCrf) yielded higher average eGFRs compared to the EFKC using the African-specific Q-value. Thus, the outcomes of this study suggest better identification of at-risk patients using population-specific Q-values, nonetheless, further studies are certainly warranted. CKD is estimated to affect 13.3% of the Ghanaian adult population [24]. This widely referenced statistic was derived using the 2009 CKD-EPI equation, which incorporates a racial coefficient and is less accurate relative to the 2021 CKD-EPI and EKFC equations. The 2009 CKD-EPI equation is also known to overestimate mGFR ≥90 mL/min per 1.73m² while underestimating mGFR ≤89 mL/min per 1.73m² in Africans, exhibiting a P^{30} of 75% (72 to 78) [16]. In fact, studies using trained computational models have proposed a true CKD prevalence of 17% in Ghana [16]. In our study, we observed a lower prevalence of reduced eGFR using the 2009 CKD-EPI relative to the 2021 CKD-EPI and 2021 EKFC equations. Compared to the 2021 CKD- EPI and the EKFC equations, the 2009 CKD-EPI equation classified 13% and 25% into less advanced CKD stages, respectively. Additionally, it only agreed with 87% and 74% of the 2021 CKD-EPI and EKFC eGFR categorizations, respectively. We believe that race-adjusted equations like the 2009 CKD-EPI may not accurately reflect the burden of CKD in the Ghanaian population, necessitating a re-evaluation of kidney disease prevalence using more robust analytical methods and contemporary eGFR equations.

The newer 2021 CKD-EPI and EKFC equations differ from the preexisting equations by their omission of race coefficients and improved accuracy in Black populations, although they are yet to be extensively validated in African populations. In a small cohort study using participants from Cote-D'Ivoire and DR Congo, the EKFC demonstrated slight reduction in bias and increase in accuracy relative to the 2021 CKD-EPI with a P^{30} of 79.3 (75.8; 82.9) versus P^{30} of 74.4 (70.6; 78.2) respectively, increasing patient classifications within 30% of mGFR values by 8.1% [15].

Proponents of the EKFC point to its unique incorporation of a modifiable population specific Q- value (rescaled creatinine based on the population's median normal serum creatinine value) which reduces bias and increases P^{30} [15,25]. Thus, its use with the population-specific Q-Factor is currently recommended, although more robust validations are required in African populations. In our study, the EKFC exhibited lower median eGFRs than the 2021 CKD-EPI. Consequently, it identified 413 more people as having reduced eGFR than the 2021 CKD-EPI.

Age and sex significantly influence GFR. Physiological GFR declines with age, with an estimated decrease of approximately 0.87 mL/min/1.73 m² per year [26]. Consequently, older individuals typically exhibit lower mGFR, and existing eGFR equations, such as the MDRD and 2009 CKD-EPI, may exhibit

higher levels of bias in this population [26]. Furthermore, sex-based differences in CKD prevalence have been observed. Studies have shown that women are more susceptible to CKD compared to men, although men tend to experience more rapid disease progressions [5,27]. Using both the MDRD and EKFC equations in our study, the highest prevalence of reduced eGFR was observed in individuals aged 60–69 years. However, individuals under 60 years of age comprised one-third of all those classified with CKD stages 3a, 3b, and 4 according to the EKFC equation. Notably, half of the individuals with CKD stage 5 were under 60 years old—a particularly concerning finding given that this age range encompasses peak productive years. The EKFC equation identified 47% more individuals under 60 with reduced eGFR compared to the MDRD equation. This finding is consistent with other studies demonstrating variations in reduced eGFR prevalence across age groups depending on the eGFR equation used [28]. These findings underscore the importance of considering age-related variations in GFR and their potential influence on CKD stage classification when using different eGFR equations.

There is an urgent need for more accurate eGFR equations for Africans. Laudable efforts including that of the African Research on Kidney Disease (ARK) study, aimed to achieve this [29]. Some published outcomes form the ARK study have been referenced in this manuscript [16]. Unfortunately, attempts to established an eGFR using data from discrete African cohorts resulted in an equation with similar performance of existing Cr-eGFRs, prompting the need for additional work in this arena [16]. In the interim, emerging evidence suggests that, among existing Cr-eGFRs, equations, the EKFC equation may be more appropriate for use in African populations. While adopting this approach may initially strain healthcare systems in LMICs, potentially increasing the need for specialist review and RRT – resources often scarce in these settings – early diagnosis remains crucial. We acknowledge that identifying more CKD cases could initially burden healthcare systems, especially in resource-limited settings like Ghana, where access to dialysis and specialists is limited to ~9.7 hemodialysis machines and 0.44 nephrologists per million people [8]. Nevertheless, the long-term benefits of early CKD detection outweigh this initial strain. Early identification enables timely interventions, such as dietary, therapeutic and lifestyle modifications, which can be managed by adequately trained primary care clinicians, potentially preserving the renal functional reserve, delaying CKD progression, and reducing the need for resource-intense RRT. This approach necessitates increased governmental investment to strengthen primary healthcare infrastructure, create training programs for healthcare providers in CKD management and improve access to essential medications and diagnostic tools.

Study Strengths and Limitations

This study's strength lies in its use of stringent criteria to identify a large, representative outpatient population, enabling the comparison of reduced eGFR prevalence using five different equations. A key limitation is the absence of comparative mGFR data. While mGFR is the gold standard, it is widely unavailable and inaccessible in Ghana, precluding evaluation of eGFR accuracy and precision. Cystatin C results were also unavailable for any of the patients in this study as cystatin C testing is yet to be made available in the country. Additionally, the retrospective cohort design may have included patients with acute kidney injury, a limitation that a prospective study could mitigate.

Conflict of Interest

The authors declare no conflict of interest.

Disclosures

MM, PDS, GBK have no relevant disclosures. CLO is a member of the IFCC CETPLM, and has received travel support from the IFCC.

Ethical Approval

Ethical clearance was sought and received from the University of Ghana Medical Centre Institutional Review Board.

Source of Funding

None.

Submission Declaration

This manuscript has not been submitted elsewhere for publication. All authors have reviewed and approved the final version.

Authorship

CLO conceived the idea for this study. All authors contributed substantially to data analysis, as well as the drafting and revision of the manuscript.

Abbreviation

CKD: Chronic kidney disease IQR: Interquartile range
MDRD: Modification of Diet in Renal Disease
MDRDnr: Modification of Diet in Renal Disease, no race factor
EKFC: European Kidney Function Consortium
EKFCrf: European Kidney Function Consortium race-free
Q-value
KDIGO: Kidney Disease Improving Global Outcomes

References

1. Wang H, Naghavi M, Allen C, Barber RM, Bhutta ZA, Carter A, et al. Global, regional, and national life expectancy, all-cause mortality, and cause-specific mortality for 249 causes of death, 1980–2015: a systematic analysis for the Global Burden of Disease Study 2015. The Lancet. 2016;388(10053):1459–1544. DOI: 10.1016/S0140-6736(16)31012-1.
2. Foreman KJ, Marquez N, Dolgert A, Fukutaki K, Fullman

N, McGaughey M, et al. Forecasting life expectancy, years of life lost, and all-cause and cause-specific mortality for 250 causes of death: reference and alternative scenarios for 2016–40 for 195 countries and territories. The Lancet. 2018;392(10159):2052–2090. DOI: 10.1016/S0140-6736(18)32203-7.

3. Jager KJ, Kovesdy C, Langham R, Rosenberg M, Jha V, Zoccali C. A single number for advocacy and communication - worldwide more than 850 million individuals have kidney diseases. Kidney International. 2019;96(5):1048–1050. DOI: 10.1016/j.kint.2019.07.012
4. Tannor EK, Sarfo FS, Mobula LM, Sarfo-Kantanka O, Adu-Gyamfi R, Plange-hule J. Prevalence and predictors of chronic kidney disease among Ghanaian patients with hypertension and diabetes mellitus: A multicenter cross-sectional study. The Journal of Clinical Hypertension. 2019;21(10):1542–1550. DOI: 10.1111/jch.13672
5. George JA, Brandenburg JT, Fabian J, Crowther NJ, Agongo G, Alberts M, et al. Kidney damage and associated risk factors in rural and urban sub-Saharan Africa (AWI-Gen): a cross-sectional population study. Lancet Glob Health. 2019;7(12):e1632–1643. DOI: 10.1016/S2214-109X(19)30443-7.
6. Gummidi B, John O, Ghosh A, Modi GK, Sehgal M, Kalra OP, et al. A Systematic Study of the Prevalence and Risk Factors of CKD in Uddanam, India. Kidney Int Rep. 2020;5(12):2246–2255. DOI: 10.1016/S2214-109X(19)30443-7.
7. Tannor EK, Norman BR, Adusei KK, Sarfo FS, Davids MR, Bedu-Addo G. Quality of life among patients with moderate to advanced chronic kidney disease in Ghana - a single centre study. BMC Nephrology. 2019;20(1):122. DOI: 10.1186/s12882-019-1316-z.
8. Tannor EK, Hutton-Mensah K, Opare-Addo P, Agyei MK, Gyan KF, Inusah AJ, et al. Fifty years of hemodialysis in Ghana-current status, utilization and cost of dialysis services. BMC Health Serv Res. 2023;23(1):1170. DOI: 10.1186/s12913-023-10154-x.
9. Eastwood JB, Kerry SM, Plange-Rhule J, Micah FB, Antwi S, Boa FG, et al. Assessment of GFR by four methods in adults in Ashanti, Ghana: the need for an eGFR equation for lean African populations. Nephrol Dial Transplant. 2010;25(7):2178–2187. DOI: 10.1093/ndt/gfp765.
10. Stevens PE, Ahmed SB, Carrero JJ, Foster B, Francis A, Hall RK, et al. KDIGO 2024 Clinical Practice Guideline for the Evaluation and Management of Chronic Kidney Disease. Kidney International. 2024;105(4):S117–S314. DOI: 10.1016/j.kint.2023.10.018.
11. Levey AS, Stevens LA, Schmid CH, Zhang YL, Castro AF, Feldman HI, et al. A new equation to estimate glomerular filtration rate. Ann Intern Med. 2009;150(9):604–612. DOI: 10.7326/0003-4819-150-9-200905050-00006.
12. Fu EL, Coresh J, Grams ME, Clase CM, Elinder CG, Paik J, et al. Removing race from the CKD-EPI equation and its impact on prognosis in a predominantly White European population. Nephrol Dial Transplant. 2022;38(1):119–128. DOI: 10.1093/ndt/gfac197.
13. Delgado C, Baweja M, Crews DC, Eneanya ND, Gadegbeku CA, Inker LA, et al. A Unifying Approach for GFR Estimation: Recommendations of the NKF-ASN Task Force on Reassessing the Inclusion of Race in Diagnosing Kidney Disease. Am J Kidney Dis. 2022;79(2):268-288.e1. DOI: 10.1053/j.ajkd.2021.08.003.
14. Pierre CC, Marzinke MA, Ahmed SB, Collister D, Colón-Franco JM, Hoenig MP, et al. AACC/NKF Guidance Document on Improving Equity in Chronic Kidney Disease Care. J Appl Lab Med. 2023;8(4):789–816. DOI: 10.1093/jalm/jfad022.
15. Delanaye P, Vidal-Petiot E, Björk J, Ebert N, Eriksen BO, Dubourg L, et al. Performance of creatinine-based equations to estimate glomerular filtration rate in White and Black populations in Europe, Brazil and Africa. Nephrology Dialysis Transplantation. 2023;38(1):106–118. DOI: 10.1093/ndt/gfac241.
16. Fabian J, Kalyesubula R, Mkandawire J, Hansen CH, Nitsch D, Musenge E, et al. Measurement of kidney function in Malawi, South Africa, and Uganda: a multicentre cohort study. The Lancet Global Health. 2022;10(8):e1159–1169. DOI: 10.1016/S2214-109X(22)00239-X.
17. Fu EL, Levey AS, Coresh J, Grams ME, Faucon AL, Elinder CG, et al. Accuracy of GFR estimating equations based on creatinine, cystatin C or both in routine care. Nephrol Dial Transplant. 2024;39(4):694–706. DOI: 10.1093/ndt/gfad219.
18. Yap E, Prysyazhnyuk Y, Ouyang J, Puri I, Boutin-Foster C, Salifu M. The Implication of Dropping Race from the MDRD Equation to Estimate GFR in an African American-Only Cohort. Int J Nephrol. 2021;1880499. DOI: 10.1155/2021/1880499.
19. Bukabau JB, Yayo E, Gnionsahé A, Monnet D, Pottel H, Cavalier E, et al. Performance of creatinine- or cystatin C-based equations to estimate glomerular filtration rate in sub-Saharan African populations. Kidney Int. 2019;95(5):1181–1189. DOI: 10.1016/j.kint.2018.11.045.
20. Improving Global Outcomes (KDIGO) CKD Work Group. KDIGO 2012 Clinical Practice Guideline for the evaluation and Management of Chronic Kidney Disease. Kidney inter,Suppl. 2013;3:1–150. DOI: 10.1038/kisup.2012.73.
21. Gama RM, Clery A, Griffiths K, Heraghty N, Peters AM, Palmer K, et al. Estimated glomerular filtration rate equations in people of self-reported black ethnicity in the United Kingdom: Inappropriate adjustment for ethnicity may lead to reduced access to care. PLoS One. 2021;16(8):e0255869. DOI: 10.1371/journal.pone.0255869.

22. Stevens PE, Levin A, Kidney Disease: Improving Global Outcomes Chronic Kidney Disease Guideline Development Work Group Members. Evaluation and management of chronic kidney disease: synopsis of the kidney disease: improving global outcomes 2012 clinical practice guideline. Ann Intern Med. 2013;158(11):825–830. DOI: 10.7326/0003-4819-158-11-201306040-00007.
23. Delanaye P, Pottel H, Botev R. Con: Should we abandon the use of the MDRD equation in favour of the CKD-EPI equation? Nephrol Dial Transplant. 2013;28(6):1396-1403. doi: 10.1093/ndt/gft006.
24. Adjei DN, Stronks K, Adu D, Beune E, Meeks K, Smeeth L, et al. Chronic kidney disease burden among African migrants in three European countries and in urban and rural Ghana: the RODAM cross-sectional study. Nephrol Dial Transplant. 2018;33(10):1812-1822. doi: 10.1093/ndt/gfx347.
25. Jeong TD, Hong J, Lee W, Chun S, Min WK. Accuracy of the New Creatinine-based Equations for Estimating Glomerular Filtration Rate in Koreans. Ann Lab Med. 2023;43(3):244–252. doi: 10.3343/alm.2023.43.3.244.
26. Michels WM, Grootendorst DC, Verduijn M, Elliott EG, Dekker FW, Krediet RT. Performance of the Cockcroft-Gault, MDRD, and New CKD-EPI Formulas in Relation to GFR, Age, and Body Size. Clin J Am Soc Nephrol. 2010;5(6):1003–1009. DOI: 10.2215/CJN.06870909.
27. Wyld MLR, Mata NLDL, Viecelli A, Swaminathan R, O'Sullivan KM, O'Lone E, et al. Sex- Based Differences in Risk Factors and Complications of Chronic Kidney Disease. Semin Nephrol. 2022;42(2):153–169. DOI: 10.1016/j.semnephrol.2022.04.006.
28. Choi R, Lee SG, Lee EH. Comparative Analysis of Seven Equations for Estimated Glomerular Filtration Rate and Their Impact on Chronic Kidney Disease Categorization in Korean Patients at Local Clinics and Hospitals. J Clin Med. 2024;13(7):1945. DOI: 10.3390/jcm13071945.
29. Kalyesubula R, Fabian J, Nakanga W, Newton R, Ssebunnya B, Prynn J, et al. How to estimate glomerular filtration rate in sub-Saharan Africa: design and methods of the African Research into Kidney Diseases (ARK) study. BMC Nephrology. 2020;21(1):20. DOI: 10.1186/s12882-020-1688-0.

Supplementary Tables

Table 1: Equations for eGFR calculations.

EQUATION	FORMULA
4v-MDRD for females	eGFR = 175 × ([SCr])^-1.154 × age^-0.203 × 0.742 [if female] × 1.210 [Black race factor]. Where [SCr] is in mg/dL (IDMS-standardized assay) and age is in years.
4v-MDRD for males	eGFR = 175 × ([SCr])^-1.154 × age^-0.203 × 1.210 [Black race factor]. Where [SCr] is in mg/dL (IDMS-standardized assay) and age is in years.
4v-MDRD for females (without race)	eGFR = 175 × ([SCr])^-1.154 × age^-0.203 × 0.742 [if female]. Where [SCr] is in mg/dL (IDMS-standardized assay) and age is in years.
4v-MDRD for males (without race)	eGFR = 175 × ([SCr])^-1.154 × age^-0.203. Where [SCr] is in mg/dL (IDMS-standardized assay) and age is in years.
CKD-EPI 2009 for females	eGFR = 141 × min([SCr]/κ, 1)^α × max([SCr]/κ, 1)^-1.209 × 0.993^age × 1.018 [if female] × 1.159 [Black race factor]. Where [SCr] is in mg/dL (IDMS-standardized assay) and age is in years; κ = 0.7 for females, α = -0.329 for females. Min = minimum([SCr]/κ, 1), Max = maximum([SCr]/κ, 1).
CKD-EPI 2009 for males	eGFR = 141 × min([SCr]/κ, 1)^α × max([SCr]/κ, 1)^-1.209 × 0.993^age × 1.159 [Black race factor]. Where [SCr] is in mg/dL (IDMS-standardized assay) and age is in years; κ = 0.9 for males, α = -0.411 for males. Min = minimum([SCr]/κ, 1), Max = maximum([SCr]/κ, 1).
CKD-EPI 2021 for females	eGFR = 142 × (SCr/A)^B × 0.9938^age × (1.012 if female). Where A = 0.7, B = -0.241 if SCr ≤ 0.7; A = 0.7, B = -1.2 if SCr > 0.7.
CKD-EPI 2021 for males	eGFR = 142 × (SCr/A)^B × 0.9938^age. Where A = 0.9, B = -0.302 if SCr ≤ 0.9; A = 0.9, B = -1.2 if SCr > 0.9.

EQUATION	FORMULA
EKFC for females	eGFR = 107.3 × (sCr/Q)^−0.322 (for ages 2–40 & sCr/Q < 1); eGFR = 107.3 × (sCr/Q)^−1.132 (for ages 2–40 & sCr/Q ≥ 1); eGFR = 107.3 × (sCr/Q)^−0.322 × 0.990^(Age−40) (for >40 & sCr/Q < 1); eGFR = 107.3 × (sCr/Q)^−1.132 × 0.990^(Age−40) (for >40 & sCr/Q ≥ 1). ln(Q) = 3.080 + 0.177×age − 0.223×ln(age) − 0.00596×age² + 0.0000686×age³ (ages 2–25); Q = 62 µmol/L (ages >25).
EKFC for males	eGFR = 107.3 × (sCr/Q)^−0.322 (for ages 2–40 & sCr/Q < 1); eGFR = 107.3 × (sCr/Q)^−1.132 (for ages 2–40 & sCr/Q ≥ 1); eGFR = 107.3 × (sCr/Q)^−0.322 × 0.990^(Age−40) (for >40 & sCr/Q < 1); eGFR = 107.3 × (sCr/Q)^−1.132 × 0.990^(Age−40) (for >40 & sCr/Q ≥ 1). ln(Q) = 3.200 + 0.259×age − 0.543×ln(age) − 0.00763×age² + 0.0000790×age³ (ages 2–25); Q = 80 µmol/L (ages >25).

Table 2: Impact of race-free Q-value (EKFCrf) on CKD classifications.

EKFCrf		CKD 1	CKD 2	CKD 3a	CKD 3b	CKD 4	CKD 5
EKFC	**CKD 1**	4332	15				
	CKD 2	169	4741				
	CKD 3a		87	911			
	CKD 3b			22	315	6	
	CKD 4				158		
	CKD 5					1	107

EKFCrf: European Kidney Function Consortium race-free Q-value equation

Research Article

Evaluating the Interference of Residual 'Teepol' Detergent on Serum Electrolytes, Protein, and Cholesterol: An In-Vitro Study

Kavindya Fernando[1,2*], Dilini Jayasekara[2], Chiranthi Welhenge[3], Mihilie Kulasinghe[2], Piumi Silva[2], BKTP Dayanath[2]

[1]*Department of Biochemistry and Clinical Chemistry, Faculty of Medicine, University of Kelaniya, Sri Lanka*
[2]*Department of Chemical Pathology, Colombo North Teaching Hospital, Ragama, Sri Lanka*
[3]*University Medical Unit, Colombo North Teaching Hospital, Ragama, Sri Lanka*

Article Info

[*]***Corresponding Author:***
Kavindya Fernando
Department of Biochemistry and Clinical Chemistry, Faculty of Medicine, University of Kelaniya, Sri Lanka
E-mail: kavindyam@kln.ac.lk
Tel: +94777907465
Address: PO BOX 06, Thalagolla Road, Ragama, Sri Lanka

Keywords

Detergent, Teepol, ISE, Interference, Electrolytes

Abstract

Introduction: In low-resource settings, reusing blood collection tubes cleaned with detergents such as 'Teepol' is common due to economic constraints. However, residual detergent may interfere with biochemical assays. This study evaluated the effect of residual 'Teepol' on serum electrolyte, total protein, and cholesterol, with emphasis on direct ion-selective electrode (ISE) methods.

Method: A controlled interference experiment was conducted using pooled human serum spiked with increasing concentrations of 'Teepol' (0%, 0.2%, 0.5%, and 1.0% v/v of original detergent). Serum sodium and potassium were measured using direct ISE (Ortho_Vitros® 4600), while total protein and cholesterol were measured via colorimetric methods (BS 800M). All analytes were tested in a single run to avoid inter-run variability. Statistical significance was assessed via Pearson correlation and comparison against 95% confidence intervals derived from quality control data.

Results: Serum sodium and potassium showed a concentration-dependent decline with increasing 'Teepol'. At 1.0%, sodium decreased by ~12% and potassium by ~43% compared to control, with values falling outside the 95% confidence intervals, confirming significant interference. Total protein and cholesterol measurements remained within expected analytical variation. Strong negative correlations were observed for sodium ($R=-0.966$) and potassium ($R=-0.989$) with 'Teepol' concentration ($p< 0.05$).

Conclusion: Residual 'Teepol' ≥0.5% v/v significantly interferes with serum sodium and potassium measurements using direct ISE. These findings highlight the importance of strict tube-washing protocols or the use of disposable tubes for critical assays. Inconsistent cleaning practices in low-resource laboratories may allow such interference, posing a risk to result accuracy and clinical decision-making.

Introduction

Laboratory testing errors can occur at the pre-analytical, analytical, or post-analytical phases, with pre-analytical errors accounting for the majority (up to ~70%) of all lab errors [1]. Among pre-analytical factors, the quality of specimen collection tubes is critical to produce accurate results. Best practices recommend using new, disposable tubes for single use to avoid contamination. However, in low-resource settings such as Sri Lanka, economic constraints have led to the reuse of sample collection tubes after cleaning, in public sector hospitals. In the aftermath of a severe economic crisis, most hospitals implemented protocols to wash and reuse tubes instead of purchasing new ones. These washed tubes are cleaned with detergents like 'Teepol'(an anionic surfactant detergent), 'Lysol' (disinfectant solution composed of cresols and alcohol), or hypochlorite solutions provided by the health sector [2]. Unfortunately, the cleaning process is not standardized, and variations in detergent concentration and rinsing can leave residual detergent in the tubes.

Clinicians at some public sector hospitals in Sri Lanka had observed cases of unexplained hyponatremia in samples collected in reused tubes, which normalized when the tests were repeated using fresh tubes. 'Teepol' was identified as the agent used to clean these tubes in almost all these situations. This raised suspicion that residual 'Teepol' might be interfering with certain assays in the reused tubes. 'Teepol' is a multi-purpose laboratory detergent composed primarily of anionic surfactants: sodium dodecylbenzene sulphonate, sodium ether sulphate, and an alcohol ethoxylate [3]. Such surfactants could plausibly affect biochemical measurements by either binding ions or interacting with assay reagents [4]. Indeed, interference is defined as the effect of a substance (identified or not) that causes the measured concentration of an analyte to deviate from its true value [5]. Sodium measurements are generally robust, and true interferents are uncommon; one known example is heparin (an anticoagulant), which can artifactually lower sodium readings by chelating sodium ions [6–8]. Other factors known to affect sodium results include the type of ion-selective electrode used, sample handling (e.g. dilution in indirect ISE methods leading to pseudohyponatremia), extreme pH or bicarbonate levels, and very high glucose or lipid concentrations [8–14]. We hypothesized that residual 'Teepol' in reused tubes could similarly interfere with direct ISE measurements of electrolytes by either binding sodium/potassium or altering the ISE membrane environment.

Limited prior literature addresses detergent residue interference in clinical chemistry. One recent study in Sri Lanka evaluated reusing tubes washed with 'Teepol', 'Lysol', or bleach according to WHO guidelines [2]; it found no significant effect of 'Teepol' residues on electrolytes (Na+, K+) or other analytes under proper washing protocols [2]. In contrast, that study noted 'Lysol' (a phenolic disinfectant) residues were associated with significantly lower sodium results, likely due to inadequate rinsing and residual contamination. However, the 'Teepol' concentration and washing conditions in that study were not fully detailed, leaving open the possibility that higher residual levels of 'Teepol' could indeed cause interference. Moreover, most government hospital laboratories in Sri Lanka do not consistently adhere to standardized washing and drying protocols due to resource limitations and reliance on manual cleaning processes. This raises concern that clinically relevant residual 'Teepol' concentrations may be more common than previously reported.

Older reports have also suggested that certain detergents can alter biochemical measurements or enzyme activities [15]. Given the ongoing practice of tube reuse in lower resource settings and the inconsistent observations in different settings, we aimed to investigate how residual 'Teepol' affects the measurement of common serum analytes quantitatively.

Methodology

This study was designed as an interference experiment to assess the impact of increasing concentrations of 'Teepol' residue on the measured levels of serum electrolytes (sodium and potassium, via direct ISE), as well as on total protein and total cholesterol (via standard colorimetric methods). By simulating worst-case residual detergent levels in vitro, we sought to determine the threshold at which 'Teepol' contamination produces statistically and clinically significant biases in results. A controlled experimental interference study was conducted in August 2023 at the Chemical Pathology Laboratory of Colombo North Teaching Hospital (Ragama, Sri Lanka). The study followed guidelines for interference testing, including the CLSI EP^{7}-A^{2} protocol [16] and Westgard rules for interference and recovery experiments [17]. No human subjects were directly involved. A pooled serum sample was prepared using anonymized, leftover specimens from routine clinical testing, which were otherwise destined for disposal.

Reagents and instruments

Concentrated 'Teepol' detergent was obtained from hospital supplies. A working 'Teepol' solution was prepared by diluting the original 'Teepol' 1:10 (v/v) with distilled water, to mimic typical cleaning dilutions. A fresh serum pool was prepared by combining leftover serum samples from healthy individuals' routine biochemistry tests, ensuring a homogeneous serum matrix. Laboratory measurements were carried out on two automated analysers: serum Na+ and K+ were measured on the Ortho Vitros® 4600 Chemistry Analyzer using direct ISE potentiometry (dry slide technology), and total protein and total cholesterol were measured on the BS 800M automated analyser (chemistry analyser) using colorimetric methods (biuret method for protein, cholesterol oxidase–peroxidase (CHOD-POD) for cholesterol). Both analysers were calibrated and quality-controlled on the day of testing, as per manufacturer guidelines.

Sample preparation

To simulate potential residual contamination when cleaning protocols are not properly followed, four test conditions were created. Aliquots of 900 µL of the pooled serum were dispensed into four new, detergent-free non-vacuum clot activator tubes. These tubes had polypropylene bodies and low-density polyethylene caps (Ceylon MediTech Instruments, Product Code 02). The working 'Teepol' solution (10% v/v 'Teepol') was then added in volumes of 0, 20, 50, and 100 µL to the four tubes, respectively. Distilled water was added as needed to each tube to bring the total volume to 1000 µL (1.0 mL). This protocol ensured each tube had a consistent 9:1 ratio of serum to added liquids, maintaining matrix consistency across all test conditions. The composition of each test tube is detailed in Table 1. Tube 1 (0 µL 'Teepol' added) served as the control (no detergent), while tubes 2–4 had progressively higher concentrations of 'Teepol'. The corresponding final fraction of original 'Teepol' (i.e., undiluted detergent) in each 1 mL sample was 0%, ~0.2%, ~0.5%, and ~1.0% for tubes 1 through 4, respectively. These concentrations were chosen to simulate worst-case residual contamination scenarios, which may occur in settings where cleaning protocols are inconsistently followed. All samples were prepared by an experienced laboratory medical officer to ensure precise pipetting and handling. After preparation, samples were analysed in a single run per analyte to avoid inter-run variability.

Table 1: Composition of the different test tubes used for the experiment.

Tube	Pooled sera (µL)	'Teepol' 10% added v/v (µL)	Distilled water (µL)	Total Volume (µL)	Original 'Teepol' in Sample (%)
Tube 1	900	0	100	1000	0%
Tube 2	900	20	80	1000	~0.2%
Tube 3	900	50	50	1000	~0.5%
Tube 4	900	100	0	1000	~1.0%

Preparation of 1 mL serum samples with increasing volumes of 10% v/v 'Teepol' working solution added. "Original 'Teepol' in sample" is the approximate percentage of undiluted detergent in the final mixture (e.g., 0.5% = 1:200 dilution of original 'Teepol'). All tubes had a 9:1 ratio of serum to added solution, maintaining matrix consistency.

Analyte measurement

The four prepared samples were first analysed for electrolytes (Na+ and K+) on direct ISE system, alongside routine patient samples. Immediately thereafter, the same samples were analysed for total protein and total cholesterol. Internal quality control (QC) data for both instruments were reviewed to ensure analytical precision. Table 2 summarizes the performance of each assay at the relevant QC level (level 1 controls approximating physiological concentrations). The coefficients of variation (CV%) were all under 4% for these analytes, indicating good analytical precision. This QC data was later used to evaluate whether any observed changes fell beyond normal analytical variation.

Table 2: Analyzer performance for relevant analytes (quality control level 1).

Analyte	QC level	Mean	Coefficient of variation (CV, %)
Serum sodium	1	125 mmol/L	3.4
Serum potassium	1	3.94 mmol/L	3.8
Serum total protein	1	7.19 g/dL	3.03
Serum total cholesterol	1	104 mg/dL	3.25

Instrument quality control data (mean and CV%) at normal concentration (level 1) for each analyte. These values were used to calculate the 95% confidence intervals of each measurement. The CV% values were derived from internal quality control (IQC) data obtained over the preceding 30 days as part of routine analyzer performance monitoring.

Statistical Analysis

Data from the four test tubes were analysed to determine the relationship between 'Teepol' concentration and analyte levels. We plotted the measured concentration of each analyte against the fraction of 'Teepol' in the sample. A linear regression analysis was performed for each analyte; Pearson correlation coefficients (R) were calculated to assess the strength and significance of association between increasing 'Teepol' and the analyte result. Given the small number of points (n=4), a Pearson's correlation test was used to identify statistically significant trends (with $p<0.05$ was considered significant). Additionally, to evaluate whether changes in results exceeded normal analytical variability, we calculated the 95% confidence interval (95% CI) around the control tube's result for each analyte based on the instrument's precision. Specifically, using the CV% from Table 2, we estimated one standard deviation (SD) at the concentration of Tube 1, then multiplied by 1.96 to get the 95% CI range (mean ±1.96 SD). Any measured

value in the 'Teepol'-added tubes falling outside this range would indicate a change greater than expected from analytical uncertainty alone (i.e., a likely true interference effect).
For example, for sodium, Tube 1's result (128 mmol/L) with CV 3.4% yields approximately ±8.5 mmol/L as the 95% confidence limits; results below ~119.5 mmol/L or above ~136.5 mmol/L would thus be considered significantly different at ~95% confidence. This approach was applied similarly to potassium, total protein and cholesterol. The percentage interference (bias) for each analyte was calculated using the following equation.
Interference (bias) = (([analyte in test sample] - [analyte in control sample])/[analyte in control sample]) x 100%
In addition to internal quality control-based confidence intervals, Analytical Performance Specifications (APS) from the Royal College of Pathologists of Australasia (RCPA QAP) were also reviewed for sodium and potassium to assess whether observed differences exceeded clinically acceptable performance limits.

Results

The measured results for each analyte in the four test conditions are presented in Table 3. As the volume of 'Teepol' in the sample increased, serum Na+ and K+ concentrations showed a progressive decline. The control sample (Tube 1, no 'Teepol') had a sodium concentration of 128 mmol/L and potassium concentration of 4.4 mmol/L. At the highest 'Teepol' level (Tube 4, 1% original 'Teepol'), sodium dropped to 112 mmol/L and potassium to 2.5 mmol/L. In contrast, total protein concentrations remained relatively stable (around ~6.0 g/dL in all tubes, with no clear trend). Total cholesterol showed a slight decreasing trend (from 162 mg/dL in Tube 1 down to approximately 157 mg/dL in Tube 4), but the magnitude of change was small (approximately 3% decrease across the full 'Teepol' range).

To determine if these changes are significant, we compared the values against the calculated 95% CIs based on analytical precision (Table 4). For sodium, the result in Tube 1 (128 mmol/L) had a 95% CI of approximately 119.5 – 136.5

Table 3: Measured serum analyte levels in samples with increasing Teepol contamination.

Analyte	Method	Test tube 1 (0% 'Teepol')	Test tube 2 (0.2% 'Teepol')	Test tube 3 (0.5% 'Teepol')	Test tube 4 (1.0% 'Teepol')
Serum sodium (mmol/L)	Direct ISE	128	128	118	112
Serum potassium (mmol/L)	Direct ISE	4.4	4.2	3.7	2.5
Total protein (g/dL)	Biuret	5.98	6.02	6.07	5.91
Total cholesterol (mg/dL)	CHOD-POD	162	161	160	156.9

Serum analyte results in each test tube (Tube 1: control with no 'Teepol'; Tubes 2–4: increasing 'Teepol' contamination as per Table 1). CHOD-POD method: Cholesterol oxidase peroxidase method, ISE: Ion selective electrode

mmol/L. The sodium concentrations in Tube 3 (118 mmol/L) and Tube 4 (112 mmol/L) fall below the lower confidence limit, indicating that these decreases were greater than expected from random instrument error alone. Similarly, for potassium, Tube 1's value of 4.4 mmol/L had a 95% CI of approximately 4.1 – 4.7 mmol/L. The potassium concentrations in Tube 3 (3.7 mmol/L) and Tube 4 (2.5 mmol/L) were well below the 95% lower limit, confirming a true significant drop. In contrast, the slight variations in total protein (95% CI proximately 5.6 – 6.3 g/dL) and total cholesterol (95% CI approximately 151.7 – 172.3 mg/dL) remained within the expected range for all tubes. Thus, 'Teepol' contamination at concentrations of 0.5% or higher resulted in statistically significant decreases in measured Na+ and K+, while changes in protein and cholesterol were not statistically significant.
In addition to comparing results against 95% confidence intervals derived from internal quality control data, we also considered published Analytical Performance Specifications (APS) from external Quality Assurance Programs such as the Royal College of Pathologists of Australasia (RCPA QAP). For serum sodium (≤ 150 mmol/L), the allowable total error is ±3 mmol/L, and for potassium (≤ 4.0 mmol/L), the allowable imprecision is ±0.2 mmol/L [18]. In our study, the observed declines in sodium (up to 16 mmol/L) and potassium (up to 1.9 mmol/L) with increasing 'Teepol' concentration substantially exceeded these APS thresholds. This supports the conclusion that the observed changes are not only statistically significant but also clinically unacceptable, reinforcing the potential impact of detergent residue on critical electrolyte measurements.

Table 4: Baseline values and 95% confidence intervals (CI) for each analyte.

	Tube 1 (control) value	95% CI range (Analytical)	Presence of a significant change
Serum Sodium (Na+)	128 mmol/L	119.5 – 136.5 mmol/L	Yes – Tubes 3 & 4 below 119.5
Serum potassium (K+)	4.4 mmol/L	4.1 – 4.7 mmol/L	Yes – Tubes 3 & 4 below 4.1
Total protein	5.98 g/dL	5.6 – 6.3 g/dL	No (all within range)
Total cholesterol	162 mg/dL	151.7 – 172.3 mg/dL	No (all within range)

Baseline = Tube 1 (no 'Teepol') result. 95% CI represents the expected range of variation due to analytical uncertainty (calculated from CV in Table 2). "Significant change observed" indicates whether any 'Teepol'-added sample fell outside the 95% CI, suggesting a true interference effect.

Statistical analysis confirmed these observations. Pearson correlation analysis showed a strong negative correlation between 'Teepol' concentration and the levels of Na+, K+, and cholesterol. The correlation coefficients were R = –0.966 for sodium, –0.989 for potassium, and –0.992 for cholesterol (all with $p<0.05$), indicating that as 'Teepol' percentage increased, these analyte values consistently decreased in a nearly linear fashion. In contrast, the correlation between 'Teepol' and total protein was weak and not statistically significant (R = –0.482, p=0.52), reflecting essentially no meaningful trend in protein values with added detergent. The strong linear relationship for sodium and potassium is illustrated in the figures below (Figure 1).

Figure 1: changes of analyte concentration with increasing 'Teepol' concentration; 1a; serum sodium vs 'Teepol', 1b; serum potassium vs 'Teepol', 1c; total protein vs 'Teepol', 1d; total cholesterol vs 'Teepol'. CI: confidence interval.

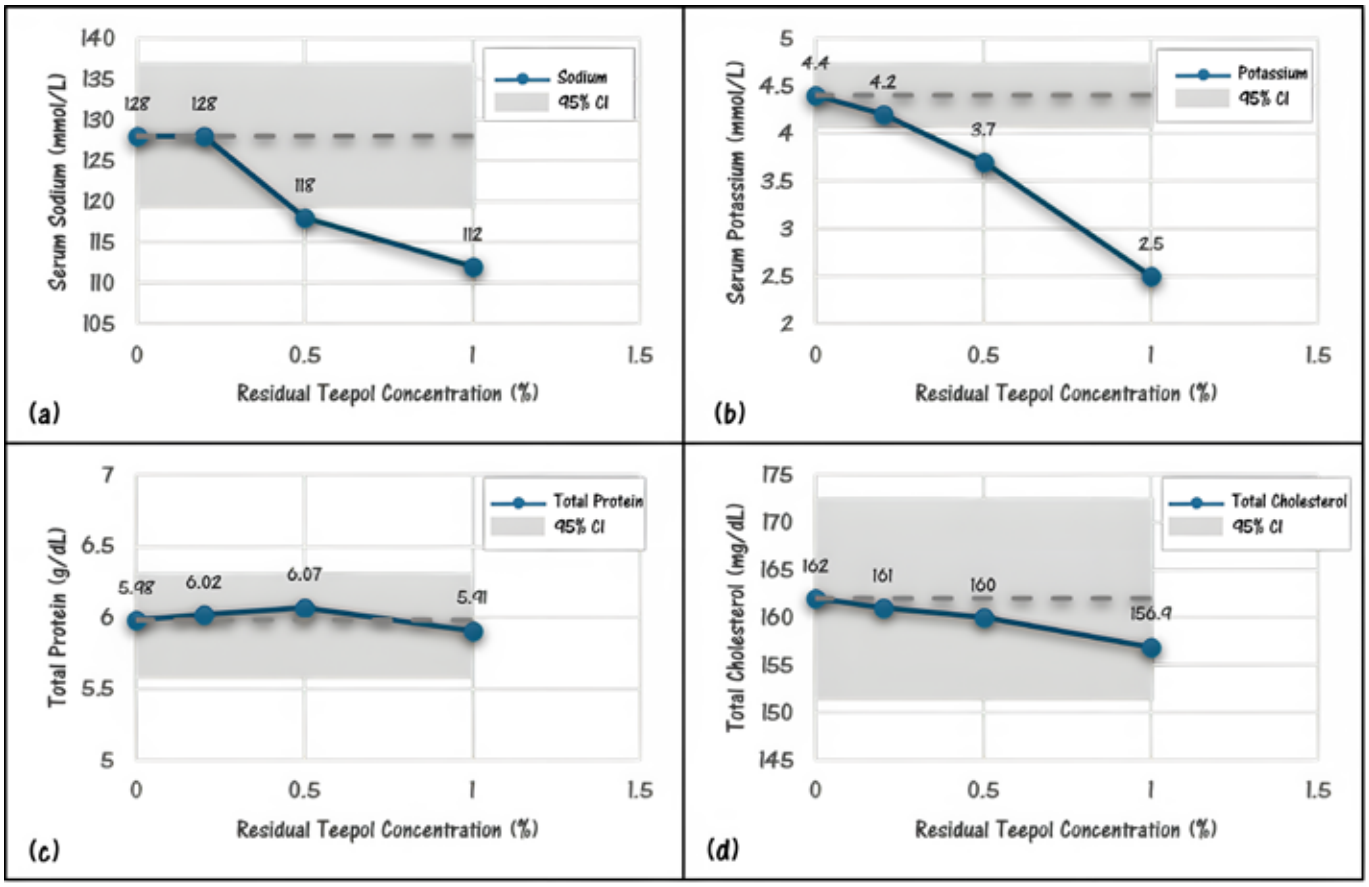

Figure 1a: Relationship between residual 'Teepol' in sample and serum sodium concentration. Each point represents one test tube ('Teepol' fraction 0%, 0.2%, 0.5%, 1.0%). Sodium concentrations remained stable up to ~0.2% 'Teepol', then showed a marked decline at higher 'Teepol' levels. The dashed grey line indicates the control value; values falling below the shaded area (analytical 95% CI) signify a significant decrease beyond normal instrument variation (seen at ≥0.5% 'Teepol'). This shows that high 'Teepol' residue leads to spuriously low sodium readings.

Figure 1b: Serum potassium vs residual 'Teepol' concentration. A strong inverse linear trend is evident, with K+ dropping progressively as 'Teepol' increases. Even a small 'Teepol' residue (~0.2%) caused a slight K+ decrease, and larger amounts (0.5–1.0%) led to clinically large decreases (from 4.4 to 2.5 mmol/L at 1.0% 'Teepol'). The potassium in tubes with ≥0.5% 'Teepol' was significantly below the control 95% CI, confirming a true interference effect on K+ measurement.

Figure 1c: Total protein vs residual 'Teepol' concentration. In contrast to electrolytes, total protein results did not show a meaningful change with added 'Teepol'. The slight fluctuations observed (5.98 to 6.07 to 5.91 g/dL) were within the analytical error range. There was no significant correlation between 'Teepol' level and protein concentration, suggesting 'Teepol' did not interfere with the biuret protein assay up to 1.0% contamination.

Figure 1d: Total cholesterol vs residual 'Teepol' concentration. Cholesterol values showed a minor downward trend with higher 'Teepol' (162 → 157 mg/dL over the range), but all values remained within the expected variability range. The correlation with 'Teepol', while mathematically high, reflects a very small absolute change. Thus, no significant interference of 'Teepol, on the cholesterol CHOD-POD assay was evident up to 1.0% contamination.

These experimental results demonstrate a clear interference effect of 'Teepol' on electrolyte measurements. When the residual original 'Teepol' content exceeded roughly 0.5% of the sample volume (≥ 50 µL of 10% 'Teepol' in 1 mL serum), the measured sodium and potassium values were significantly depressed beyond normal error limits. At the highest tested contamination (1% 'Teepol'), sodium was lowered by ~12% and potassium by ~43% relative to the control, which would be clinically significant reductions. Meanwhile, total protein and cholesterol tests were essentially unaffected by 'Teepol' at these levels, suggesting that the interference is specific to certain types of assays (particularly the direct ISE method for ions).

Discussion

Our investigation confirms that detergent residues can markedly interfere with electrolyte results obtained by direct ISE. Specifically, when residual 'Teepol' (an anionic surfactant detergent) in the sample tube exceeded about 50 µL of a 10% solution (equivalent to 0.5% v/v of the original detergent in the sample), we observed significant artefactual reductions in measured serum Na+ and K+ levels. This finding has important implications for clinical laboratories that practice tube reuse. Accurate Na+ and K+ measurements are critical for patient care, as even moderate errors can alter clinical management decisions. If unrecognized, falsely low electrolyte results due to detergent interference could lead to misdiagnosis or unnecessary interventions, adversely impacting patient safety.

Mechanism of Interference

The results indicate a negative bias introduced by 'Teepol' on the ISE measurements of Na+ and K+. There are several possible mechanisms by which a surfactant like 'Teepol' could cause this effect. ISEs generate a potential in response to the activity of specific ions (Na+, K+) in the sample via a selective membrane, as described by the Nernst equation [19]. Surfactants such as the components of 'Teepol' (e.g. sodium dodecylbenzene sulfonate, analogous to sodium dodecyl sulphate) could interfere by binding free cations or altering their activity [20]. Another hypothesis is that the detergent's anionic molecules chelate or sequester sodium and potassium ions, reducing the "free" ion activity that the electrode senses [21]. This is analogous to the effect of excess heparin (another polyanion) on sodium measurement, where sodium ions are bound by heparin, causing spuriously low readings. In our study, 'Teepol' may similarly be binding some fraction of Na+ and K+ in complexes or micelles, effectively lowering the ion activity in the plasma water phase.

Another contributing factor could be physical interference at the electrode membrane. Surfactants are known to adsorb to surfaces [22,23]. 'Teepol' residue in the sample might coat the ISE membrane or alter its surface charge, disrupting the normal ion-selective potential [11,24]. The Ortho Vitros® 4600 analyser uses a dry-slide ISE technology where the sample contacts selective dry reagents – residual detergent could disrupt this interaction [25]. Surfactant adsorption can lead to an electrode response drift or a reduced slope (sensitivity), manifesting as lower reported concentrations [24,26]. In essence, the electrode may become less responsive to Na+ and K+ in the presence of detergent. Some research in electrochemistry has addressed surfactant interference in potentiometric measurements, and even special "surfactant-resistant" electrodes have been devised to mitigate this issue [27,28], underscoring that surfactants are recognized interferents in electrochemical ion detection. It is also notable that 'Teepol' introduces its own sodium ions (being a sodium salt detergent); however, in our results we did not see any increase in sodium. Instead a decrease occurred, supporting the notion that the dominant effect is not additive sodium from the detergent but rather an interference lowering the measured activity.

Specificity to ISE vs Colorimetric Assays

An important observation is that total protein and cholesterol were not significantly affected by 'Teepol' residue in our experiment. Both of these analytes were measured by colorimetric methods (biuret for protein, enzymatic CHOD-POD for cholesterol) which involve dilution of the sample with reagent and end-point spectrophotometric detection. There are a few hypothetical reasons why these assays proved resistant to 'Teepol' interference. First, the effective concentration of 'Teepol' in the reaction mixtures for protein and cholesterol was likely very low – automated analysers typically dilute sample or include reagents that could further neutralize or dilute contaminants [29]. Any minor surfactant present might have been rendered negligible by the assay reagents.

Second, the chemistry of these assays may not be impacted by surfactant at these levels; for instance, the biuret reaction for protein (binding of Cu^{2+} to peptide bonds) and the enzymatic oxidation of cholesterol might tolerate a small amount of detergent without change in absorbance.

Our data showed only random small fluctuations within the analytical error for these tests. This contrast with the ISE results highlights that 'Teepol's' interference is method-dependent – it chiefly perturbs electrochemical detection of ions, whereas routine photometric assays for large molecules (protein, cholesterol) appear robust under the tested conditions. This is reassuring in that not all tests are compromised by tube residues, emphasizes that electrolyte tests are especially vulnerable.

Our findings align with and extend, those of Jayarathna et al. (2021) who examined detergent washing of tubes. In their study, 'Teepol'-washed tubes (when properly rinsed per WHO guidelines) did not significantly alter Na+ or K+ results [2], whereas Lysol (a phenolic detergent) did cause a drop in sodium. They did not report 'Teepol's' exact residual concentration; likely it was low due to good rinsing. Our study deliberately pushed the envelope by leaving higher residual levels, thereby defining the threshold where interference becomes significant. We demonstrate that at roughly >1:200 dilution of original 'Teepol' (0.5%), interference emerges, a scenario that could occur in practice if tubes are inadequately rinsed or if overly concentrated detergent is used for washing. Thus, while 'Teepol' is safe when properly rinsed, improper use can indeed cause clinically important errors.

While Jayarathna et al. followed a standardized WHO-recommended protocol that included overnight soaking, multiple rinses with tap and distilled water, and oven drying, such procedures are often not followed in Sri Lankan public sector hospitals due to limited resources, staff shortages, and absence of national guidelines. In many laboratories, specimen tubes are manually cleaned by minor staff with inconsistent rinsing and drying steps. These deviations increase the likelihood that residual Teepol concentrations approaching or exceeding 0.5% could remain in reused tubes. Our simulation of such worst-case conditions helps define the point at which interference becomes clinically meaningful. Additionally, anecdotal cases of unexplained hyponatraemia that normalized when samples were recollected in fresh tubes further support the plausibility of this interference in real-world practice.

In addition to analytical concerns, it is important to consider the practical and economic implications of tube reuse. Although washing and reusing glass tubes may appear cost saving, the hidden costs including labor, detergent, water usage, staff time, risk of injury from broken glass, and the potential for analytical errors due to residual contamination can outweigh the upfront cost of using single use plastic tubes. These indirect costs are rarely quantified in laboratory budgets. Therefore, formal cost benefit analyses comparing reused and disposable tubes are recommended to guide national laboratory procurement policies, particularly in resource limited settings.

Interestingly, earlier literature on detergent effects documented how even low concentrations (~0.1%) of certain detergents (like Triton X-100, a non-ionic surfactant) could inhibit enzymatic activities by affecting membrane proteins [30]. This concept of detergent perturbing biological or measurement systems is consistent with our findings on ISE interference. In a sense, the ISE membrane in our case can be thought of as analogous to a biological membrane whose function (ion selectivity) is disrupted by the surfactant. Moreover, a recent review on ion-selective electrodes emphasizes that while ISEs are highly selective, they are not free of interferences, and laboratories must be aware of substances that can skew results [11]. Our study identifies 'Teepol' residue as one such interferent in the context of reused collection tubes.

Clinical Implications

The magnitude of sodium and potassium depression observed at higher 'Teepol' contamination could have serious clinical ramifications. For example, in Tube 4 (simulating a badly rinsed tube), sodium was 112 mmol/L vs 128 mmol/L true value – these 16 mmol/L drops could classify a patient as moderately hyponatraemic when they are actually normonatraemic. Likewise, potassium dropping from 4.4 to 2.5 mmol/L could lead to a false diagnosis of severe hypokalaemia, potentially prompting unnecessary potassium supplementation or cardiac monitoring. Such pseudohyponatremia or pseudohypokalaemia due to tube contamination is particularly dangerous because clinicians might act on these spurious results. In settings where tube reuse is practiced, our findings stress the need for vigilance. If an unexpectedly low electrolyte result is obtained, one should consider the possibility of detergent interference (especially if other clinical or lab clues don't align) and perhaps repeat the test with a fresh tube sample before initiating any aggressive treatment. It is notable that in the anecdotal hospital reports, repeating the test in a new tube corrected the values, highlighting an approach to identify this issue in real time.

For laboratories, the clear message is that standardizing tube washing protocols is essential. 'Teepol' itself is an effective cleaner, but it must be thoroughly rinsed out. Standard Operating Procedures (SOPs) should dictate the proper dilution of 'Teepol' for washing (such as using a measured mild concentration), and a sufficient rinse with water (preferably multiple rinses) to ensure no significant residue remains. Drying of tubes after washing is also important since pooling of residual wash solution could carry detergent into the next sample [31]. We recommend that labs periodically test a batch of cleaned tubes by filling them with saline and measuring any residual effect on electrolyte readings as a form of quality assurance for the cleaning process. In critical care settings or for critical analytes like electrolytes, the safest practice remains to use new disposable tubes whenever possible [2]. Indeed, Jayarathna et al. concluded that while properly washed

reused tubes generally did not affect most tests, new tubes are still recommended for critical investigations such as serum electrolytes to avoid even the rare chance of interference.

Limitations

This study has some limitations. Firstly, the experiment was conducted using a single pooled serum sample, tested in singleton at each 'Teepol' concentration. While the observed changes were large enough to suggest meaningful interference, this approach limits statistical robustness and prevents evaluation of biological variability. We did not perform replicates due to resource constraints. Future studies should aim to include multiple independent serum pools and replicate measurements to better establish the reproducibility and generalizability of the interference effects.

Secondly, the sample testing was performed in a fixed sequence, from control to the highest 'Teepol' concentration. We did not randomize sample order, which may introduce potential bias. Future work should randomize the testing order and investigate whether order effects or matrix interactions influence results.

Thirdly, we only examined four discrete levels of 'Teepol'. The exact "breakpoint" of interference might lie somewhere between our tested concentrations; a finer concentration gradient (e.g. 0.1%, 0.2%, 0.5%, 1.0%) or testing the maximum tolerable residue without interference would allow better interpolation of the threshold and should be considered in future work.

Fourth, Pearson's correlation was used to explore the relationship between 'Teepol' concentration and analyte values. However, with only four data points, the reliability of these statistical estimates is limited. While the trends were visually compelling, we caution readers against over-interpreting the correlation coefficients and p-values. Future studies with repeated measurements and larger datasets should employ more robust statistical approaches, including non-parametric or regression-based models. Lastly, all samples were intentionally diluted by 10% (including the control) to maintain equal volume after adding interferent, following CLSI EP^{7}-A^{2} recommendations. This dilution lowered baseline sodium concentrations (e.g., 128 mmol/L in control), potentially affecting generalizability. However, since all samples were diluted equally, relative comparisons remain valid. The observed percentage declines in sodium and potassium remain clinically meaningful, though extrapolation to undiluted clinical samples should be approached with caution.

We also note that this study focused exclusively on 'Teepol'. Other cleaning agents, such as phenolic disinfectants may exhibit different interference profiles and thresholds, which were beyond our scope.

Conclusion

'Teepol' detergent residue in reused sample collection tubes can significantly interfere with serum Na+ and K+ measurements by direct ISE, particularly when the residual volume 10% 'Teepol' exceeds 50 µL per 1 mL of serum (≥0.5% of sample volume). This can lead to falsely low electrolyte results and potential misdiagnoses such as hyponatremia or hypokalaemia. By contrast, total protein or cholesterol measured by colorimetric methods remain unaffected, suggesting assay-specific interference. These findings highlight the need for standardized cleaning protocols, including well-defined maximum allowable 'Teepol' residues. Where possible, new tubes should be used for critical tests. Clinical laboratories must remain vigilant about pre-analytical factors like tube contamination to ensure accurate results and safeguard patient care.

Declarations

Conflict of interest

The authors declare no conflict of interests.

Author contributions

Kavindya Fernando: Conceptualization, Methodology, Writing- Original draft preparation, Creating, graphs and figures, Investigation. Dilini Jayasekara: Conceptualization, Methodology, Writing- Reviewing and Editing. Chiranthi Welhenge: Writing- Reviewing and Editing, Data curation. Mihilie Kulasinghe and Piumi Silva: Writing-Reviewing, BKTP Dayanath: Supervision.

Ethical approval

There was no involvement of any direct human or animal subjects in any experiments in the study.

Acknowledgements

The authors would like to express their sincere gratitude to the staff of the Chemical Pathology Laboratory at Colombo North Teaching Hospital (CNTH) for their invaluable support during the experimental work. We also extend our special thanks to Mr. P.G. Kalana Bandara for his assistance in editing and preparing the figures included in this manuscript.

Data availability statement

The data supporting the findings of this study are available from the corresponding author upon reasonable request. All data were generated from anonymized pooled serum samples used solely for the purpose of this laboratory-based experimental study, with no direct patient identifiers involved.

Research Funding

None received.

Consent for Publication

Consent to submit has been received explicitly from all co-authors, as well as from the responsible authorities. Authors whose names appear on the submission have contributed sufficiently to the scientific work and therefore share collective responsibility and accountability for the results.

References

1. Plebani M. Diagnostic Errors and Laboratory Medicine - Causes and Strategies. EJIFCC. 2015;26(1):7–14. PMID: 27683477
2. Jayarathna U, Tennakoon S, Uluwaduge DI, Amarasinghe S. Effect of residual detergents in specimen collection containers on routine serum biochemical analytes. Int J Multidiscip Stud. 2021. DOI: 10.4038/ijms.v8i3.150
3. Pozo-Antonio JS, Rocha CSA, Pereira MFC, Maurício AMAS, Flores-Colen I. Evaluation of side effects of mechanical cleaning with an anionic detergent on granite cladding tiles. Environ Sci Pollut Res. 2021;28(12):15173–15184. DOI: 10.1007/s11356-020-11733-9
4. Bowen RAR, Adcock-Funk DM. Pre-Examination Procedures in Laboratory Diagnostics. In: Guder WG, Narayanan S, editors. Preanalytical Aspects and their Impact on the Quality of Medical Laboratory Results. Berlin: De Gruyter; p. 170–204. DOI: 10.1515/9783110334043-025
5. Sunderman FW Jr. Drug interference in clinical biochemistry. CRC Crit Rev Clin Lab Sci. 1970;1(3):427–449. DOI: 10.3109/10408367009027950
6. Mann SW, Green A. Interference from Heparin in Commercial Heparinised Tubes in the Measurement of Plasma Sodium by Ion Selective Electrode: A Note of Caution. Ann Clin Biochem. 1986;23(3):355–356. DOI: 10.1177/000456328602300320
7. Shek CC, Swaminathan R. Errors due to heparin in the estimation of plasma sodium and potassium concentrations. Intensive Care Med. 1985;11(6):309–311. DOI: 10.1007/BF00273542
8. Yip PM, Chan MK, Zielinski N, Adeli K. Heparin interference in whole blood sodium measurements in a pediatric setting. Clin Biochem. 2006;39(4):391–395. DOI: 10.1016/j.clinbiochem.2005.12.006
9. Twomey PJ, Cordle J, Pledger DR, Miao Y. An unusual case of hyponatraemia in diabetic ketoacidosis. J Clin Pathol. 2005;58(11):1219–1220. DOI: 10.1136/jcp.2005.025916
10. Goyal B, Datta SK, Mir AA, Ikkurthi S, Prasad R, Pal A. Increasing Glucose Concentrations Interfere with Estimation of Electrolytes by Indirect Ion Selective Electrode Method. Indian J Clin Biochem. 2016;31(2):224–230. DOI: 10.1007/s12291-015-0522-0
11. Dimeski G, Badrick T, John AS. Ion Selective Electrodes (ISEs) and interferences--a review. Clin Chim Acta. 2010;411(5–6):309–317. DOI: 10.1016/j.cca.2009.12.005
12. Al-Musheifri A, Jones GRD. Glucose interference in direct ion-sensitive electrode sodium measurements. Ann Clin Biochem. 2008;45(5):530–532. DOI: 10.1258/acb.2008.008001
13. Aziz F, Sam R, Lew SQ, Massie L, Misra M, Roumelioti M-E, et al. Pseudohyponatremia: Mechanism, Diagnosis, Clinical Associations and Management. J Clin Med. 2023;12. DOI: 10.3390/jcm12124076
14. Maas AH, Siggaard-Andersen O, Weisberg HF, Zijlstra WG. Ion-selective electrodes for sodium and potassium: a new problem of what is measured and what should be reported. Clin Chem. 1985;31(3):482–485. DOI: 10.1093/clinchem/31.3.482
15. Wills ED. The effect of anionic detergents and some related compounds on enzymes. Biochem J. 1954;57(1):109–120. DOI: 10.1042/bj0570109
16. Clinical and Laboratory Standards Institute (CLSI). Interference Testing in Clinical Chemistry; Approved Guideline - Third Edition. 3rd ed. Wayne, PA: CLSI; 2018. [Accessed 30/12/2024]. Available from: https://clsi.org/shop/standards/ep07/
17. Westgard JO. Basic Method Validation: Interference and Recovery Experiments. Westgard QC. 2017 [Accessed 30/12/2024]. Available from: https://westgard.com/lessons/basic-method-validation/lesson27.html
18. Royal College of Pathologists of Australasia Quality Assurance Programs. Chemical Pathology Analytical Performance Specifications. [Accessed 15/07/2025] Available from: https://rcpaqap.com.au/resources/chemical-pathology-analytical-performance-specifications.
19. Lindner E. Konstantin N. Mikhelson: Ion-selective electrodes. Anal Bioanal Chem. 2014;406(2):373–374. DOI: 10.1007/s00216-013-7442-8
20. Samiey B, Cheng C-H, Wu J. Effects of Surfactants on the Rate of Chemical Reactions. J Chem. 2014; 2014 (1):908476. DOI: 10.1155/2014/908476
21. Hohn SM, Johansen JD, Rustemeyer T, Elsner P, Maibach HI, editors. Kanerva's Occupational Dermatology. 3rd ed. Cham: Springer Nature; 2020.
22. Attwood D. Surfactants. In: Modern Pharmaceutics Volume 1. 5th ed. 2009. p. 58.
23. Zhu B-Y, Gu T. Surfactant adsorption at solid-liquid interfaces. Adv Colloid Interface Sci. 1991;37(1):1–32. DOI: 10.1016/0001-8686(91)80037-K
24. Hu C, Yang C, Hu S. Hydrophobic adsorption of surfactants on water-soluble carbon nanotubes: A simple approach to improve sensitivity and antifouling capacity of carbon nanotubes-based electrochemical sensors. Electrochem Commun. 2007;9(1):128–134. DOI: 10.1016/j.elecom.2006.08.055
25. Stierlin N, Hemmerle A, Jung K, Thumfart J, Risch M, Risch L. Comparison of two different technologies measuring the same analytes in view of the In Vitro

Diagnostic Regulation (IVDR). Lab Med. 2025;49(1):14–20. DOI: 10.1515/labmed-2024-0052

26. Zhang J, Slevin CJ, Murtomäki L, Kontturi K, Williams DE, Unwin PR. Microelectrochemical Measurements at Expanding Droplets: Effect of Surfactant Adsorption on Electron Transfer Kinetics at Liquid/Liquid Interfaces. Langmuir. 2001;17(3):821–827. DOI: 10.1021/la001113z
27. Wang M, Tan G, Eljaszewicz A, Meng Y, Wawrzyniak P, Acharya S, et al. Laundry detergents and detergent residue after rinsing directly disrupt tight junction barrier integrity in human bronchial epithelial cells. J Allergy Clin Immunol. 2019;143(5):1892–1903. DOI: 10.1016/j.jaci.2018.11.016
28. Lu H, Yin T, Luan F, Li Y, Qin W. Tailoring the surface of a polymeric membrane with a thin-layer Nafion membrane: Construction of an anti-surfactant solid-contact ion-selective electrode. J Electroanal Chem. 2025;977:118830. DOI: 10.1016/j.jelechem.2024.118830
29. Cunningham DD. Fluidics and sample handling in clinical chemical analysis. Anal Chim Acta. 2001;429(1):1–18. DOI: 10.1016/S0003-2670(00)01256-3
30. Moore RB, Manery JF, Still J, Mankad VN. The inhibitory effects of polyoxyethylene detergents on human erythrocyte acetylcholinesterase and Ca2+ + Mg2+ ATPase. Biochem Cell Biol. 1989;67(2–3):137–146. DOI: 10.1139/o89-021
31. Vella F. Textbook of clinical chemistry: Edited by N W Tietz. Biochem Educ. 1986;14(3):146. ISBN 0-7216-8886-1

Research Article

Evaluation of serum soluble CD36 levels in the clinical progression of diabetic nephropathy

Iyyama Gowri Moovendhan[1], Roopa A. K.[2] , Karthick E.[1] , M. Ganesh[1] , K. Sowmya[1]

[1]*Department of Biochemistry,Sri Ramachandra Medical College Hospital, SRIHER, Porur, Chennai, Tamil Nadu, India*
[2]*Department of Biochemistry, SRM Medical College Hospital and Research centre, Kattankulathur, Chengalpattu, India*

Article Info

[*]***Corresponding Author:***
M. Ganesh
Department of Biochemistry, Sri Ramachandra Medical College Hospital
SRIHER, Porur, Chennai, Tamil Nadu, India
E-mail:ganeshm@sriramachandra.edu.in
Contact: 988419902
ORCID:0000-0002-1848-7625

Keywords

Diabetic nephropathy, sCD36, CKD, diabetic complications, renal dysfunction, diagnostic utility, diabetes, novel biomarker

Abstract

Aim: Diabetic nephropathy (DN) is one of the major contributors to end stage kidney disease globally. Reliable biomarkers for early diagnosis of DN still exists as a major challenge. Serum soluble CD36 (sCD36) involved in lipid metabolism and oxidative stress has been identified as a likely biomarker of DN. Herein, we assess the relationship between sCD36 and clinical worsening of DN, to determine its potential diagnostic value.

Material and Methods: A case- control study involving 160 participants, categorized into four groups was conducted i.e., healthy individuals, diabetics with normo-albuminuria, microalbuminuria, and macroalbuminuria (n = 40). Demographic variables and biochemical parameters were compared. The concentrations of sCD36 in serum samples were determined, as well as correlation analysis between sCD36, fasting plasma glucose (FPG), HbA1c, urine albumin creatinine ratio (UACR), and estimated glomerular filtration rate (eGFR) were performed. The diagnostic performance of sCD36 was determined using receiver operating characteristic (ROC) curve.
Results: Serum sCD36 levels rose progressively from 9.97 ng/mL in the control group to 12.13 ng/mL in the macroalbuminuria group, $p < 0.001$. Patients with higher sCD36 levels also had higher fasting plasma glucose, HbA1C, and UACR with a lower eGFR. The ROC analysis of sCD36 gave an AUC of 0.908, showing excellent diagnostic capability of the model. The optimal cut-off value of 10.6 ng/mL yielded 87.5 % sensitivity and 80.83% specificity for detecting advanced DN.

Conclusion: Increased serum sCD36 levels correlates directly to DN progression, hence being a promising candidate biomarker for diagnosis and prognosis. The possible direct application of sCD36 into clinical practice might help improve DN management and treatment.

Introduction

With an International Diabetes Federation (IDF) predicted prevalence of 629 million globally by 2040, Diabetes continues to be one of the most rapidly growing metabolic diseases worldwide with high morbidity and mortality. Significant mortality in diabetes includes cardiovascular diseases, diabetic retinopathy and predominantly diabetic nephropathy (DN). The most common cause of chronic kidney disease (CKD) and renal failure remains to be DN worldwide [1].

The pathophysiology of DN appears to be complex and still remains unclear. The existing treatment strategies for DN stalls the disease but does not reverse or stop its progression into end stage renal disease. Chronic hyperglycemic state associated with diabetes initiates the glomerular injury. This is due to mitochondrial overload following excessive glucose oxidation, which results in over production of reactive oxygen species (ROS). The Tubular epithelial cells (TECs) in proximal tubules with their high mitochondrial content, primarily derive energy through mitochondrial fatty acid oxidation (FAO). Studies have reported dysfunction in FAO as a key factor for development of diabetic kidney disease (DKD) [2-4]. Accumulation of ROS and advanced glycation end products (AGE) leads to release of inflammatory cytokines and activation of excessive glomerular extracellular matrix synthesis [5,6]. Early abnormalities in DN affect the glomeruli primarily, followed by its progression to a tubulo-interstitial disease. Beginning with glomerular hyperfiltration, podocyte damage, glomerular hypertrophy, basement membrane thickening, progressing to mesangial expansion and glomerular sclerosis. Alongside glomerular involvement, recent studies show tubular epithelial degeneration, atrophy and tubulointerstitial sclerosis as an important part in progression of DN [5].

Currently DN diagnosis and progression is studied with the use of markers such as albuminuria, estimated glomerular filtration rate (eGFR), Urine albumin creatinine ratio (UACR), cystatin C. Detectable levels of these markers are observed only after significant renal injury, after which it becomes too late to prevent DN progression to ESRD. Owing to these drawbacks, novel biomarkers like CD36 are required in predicting early damages in DN [7].

Cluster of differentiation 36 (CD36) is a heterodimeric single chain transmembrane surface protein that belongs to class B scavenger receptor family. It functions primarily as a long chain fatty acid transporter protein and through a signalling receptor, CD36 also responds to innate immune reactions. CD36 is expressed ubiquitously on several cells such as macrophages, monocytes, enterocytes, hepatocytes and in renal tissues, it is seen on tubular epithelial cells, podocytes, mesangial cells and endothelial cells. Long chain fatty acids, oxidised LDL, AGEs, advanced oxidation protein products (AOPPs), thrombospondin and S100 family proteins are some of the important ligands of CD36 [3,8,9]. CD36 serves as a signalling centre for lipid homeostasis, immune responses and energy availability equilibrium. CD36 expression has been observed to be upregulated in hyperlipidemic and hyperglycemic states especially in renal tissues in DKD. Disturbances in the CD36 dependent pathways has shown to play a pivotal role in development of renal fibrosis and DKD progression [10]. Though a membrane glycoprotein, the levels of the extracellular portion known as soluble CD36 (sCD36) seen in circulation, has been implicated in various disease conditions such as hepatic steatosis, obesity, insulin resistance, atherosclerosis and diabetes [11,12]. In spite of its role in development of DN and other diabetic complications, only a few studies exist that have depicted the role of sCD36 in clinical setting of DN.

This study was aimed to evaluate serum soluble CD36 levels in patients at various stages of DN and its correlation with disease severity markers like urine albumin creatinine ratio (UACR) and estimated glomerular filtration rate (eGFR). Thereby assessing whether serum soluble CD36 can be used as an early predictor of the clinical progression of DN.

Methology

This case control study was conducted in the Department of Biochemistry and Department of Nephrology, Sri Ramachandra Institute of Higher Education and Research, Chennai. The study was carried out from July 2023 to April 2024 following approval by Institutional ethics committee. Sample size calculation software (PS version 3.1.6) was used to calculate the sample size. With type I error as 1% and power of the study as 95% sample size was calculated as

Group 1 (controls) – 40 participants

Group 2 (cases) Diabetic with normo-albuminuria- 40 participants

Group 3 (cases) Diabetic with microalbuminuria- 40 participants

Group 4 (cases) Diabetic with macroalbuminuria- 40 participants

The participants of the study were divided into four groups based on the following inclusion criteria in Table 1.

Table 1: Inclusion criteria of study population.

	Group 1 (Controls)	Group 2 (Cases)	Group 3 (Cases)	Group 4 (Cases)
Subjects	Healthy subjects with normal glucose tolerance	Type 2 diabetic patients with normal albuminuria	Type 2 diabetic patients with micro albuminuria	Type 2 diabetic patients with macro albuminuria
Fasting plasma glucose (FPG)*	<110 mg/dL	≥126 mg/dL	≥126 mg/dL	≥126 mg/dL
Post prandial plasma glucose*	<140 mg/dL	≥200 mg/dL	≥200 mg/dL	≥200 mg/dL
HbA1C*	<5.7%	≥6.5%	≥6.5%	≥6.5%
Urine Albumin Creatinine ratio (UACR)	<30 mg/g of creatinine	<30 mg/g of creatinine	30–300 mg/g of creatinine	>300 mg/g of creatinine

*According to WHO diagnostic criteria for Diabetes mellitus

Patients with Type 1 diabetes, kidney disease other than diabetic nephropathy, anemia, cardiovascular disease, liver disease, cancer, hypothyroidism and current history of any known infection or inflammatory diseases were excluded from the study.

The participants were briefed about the study protocol and written informed consent was obtained from all participants fulfilling inclusion criteria. Venous blood samples were collected from the participants for routine investigations were centrifuged at 3000 rpm for 15 min. Demographic data and relevant laboratory data such as fasting plasma glucose (FPG), total cholesterol (TC), high density lipoprotein - cholesterol (HDL-C), low density lipoprotein - cholesterol (LDL-C), urea, creatinine, urine albumin creatinine ratio (UACR). Urine albumin-creatinine ratio were obtained from patient records. Estimated glomerular filtration rate (eGFR) was calculated by CKD EPI -2021 equation based on serum creatinine values using an online calculator.

Laboratory analysis for the above clinical chemistry parameters was done on Roche COBAS c702 automated chemistry analyser & remaining separated serum samples were aliquoted into Eppendorf tubes and stored at –20° C for analysis of serum sCD36. Serum sCD36 was estimated using precoated sandwich-type ELISA kits approved for research use (ELABSCIENCE E-EL-H104). The kit had sensitivity of 0.1 ng/ml, detection range of 0.16 – 10 ng/ml, with highest intra – assay variability of 5.11% and inter – assay variability of 8.26%.

Statistical analysis was performed using R software version 4.0.2. The normality of data was assessed using Kolmogorov – Smirnov test. The results were expressed as mean and standard deviation. One-way ANOVA was used as the test of significance between groups for continuous variables. Post hoc analysis was done using Tukey – HSD test. Correlation between the variables was analysed using Pearson's correlation test. To assess the performance of sCD36 levels in predicting DN, receiver operating characteristic (ROC) curve analysis was applied and the cut-off value was calculated. A p-value <0.05 was considered statistically significant.

Results

The study examined 160 people categorized into four groups: controls, diabetic patients with "normo-albuminuria, microalbuminuria, and macroalbuminuria, with 40 participants in each category". The average age (Table 2) was markedly greater in the macroalbuminuria group (56.77 years) than in the control group (46.90 years), with a p-value of 0.006. No significant gender difference was seen across the groups (p = 0.064).

Table 2: Baseline characteristics of the study participants.

Characteristic	Control n = 40	DM with normo-albuminuria n = 40	DM with microalbuminuria n = 40	DM with macroalbuminuria n = 40	p-value
AGE (years)#	46.90 (15.87)	49.73 (11.97)	55.27 (12.44)	56.77 (14.66)	0.006#
SEX					0.064
Female	15 / 40 (38%)	14 / 40 (35%)	24 / 40 (60%)	14 / 40 (35%)	
Male	25 / 40 (62%)	26 / 40 (65%)	16 / 40 (40%)	26 / 40 (65%)	

#statistically significant difference between groups observed with p value < 0.05

Table 3 illustrates a gradual rise in fasting plasma glucose and HbA1C levels throughout the groups, with glucose levels escalating from 88.42 mg/dL to 162.85 mg/dL and HbA1C rising from 5.44% to 8.84% in the control and macroalbuminuria groups respectively ($p<0.05$). In a similar manner, serum creatinine concentrations reached their peak and eGFR values exhibited a substantial reduction to 66.25 mL/min/1.73 m² in the macroalbuminuria cohort ($p< 0.001$).

Table 3: Comparison of biochemical parameters between the group.

Characteristic (units)	Control n = 40	DM with normo albuminuria n = 40	DM with micro albuminuria n = 40	DM with macro albuminuria n = 40	p-value
Fasting plasma glucose (mg/dL)	88.42 (10.76)	127.45 (42.42) [a]	165.30 (95.37) [a,b]	162.85 (63.86) [a,b]	<0.001*
HbA1C (%)	5.44 (0.23)	7.31 (1.62) [a]	8.89 (2.51) [a,b]	8.84 (2.19) [a,b]	<0.001*
Serum creatinine (mg/dL)	0.85 (0.14)	0.84 (0.25)	0.86 (0.30)	1.76 (1.52) [a,b,c]	<0.001*
Total Cholesterol (mg/dL)	156.88 (17.75)	201.70 (38.85) [a]	185.43 (54.60) [a,b]	210.35 (60.59) [a,b,c]	<0.001*
LDL-C (mg/dL)	92.67 (13.75)	134.40 (27.56) [a]	118.98 (40.53) [a,b]	140.50 (43.41) [a,c]	<0.001*
HDL-C (mg/dL)	50.98 (6.74)	46.62 (10.11)	44.65 (7.91) [a,b]	46.62 (12.48) [c]	0.003#
Triglycerides (mg/dL)	89.83 (28.78)	158.75 (74.07) [a]	175.50 (98.78) [a,b]	186.72 (116.65) [a,b,c]	<0.001*
Urine Microalbumin (µg/mg of creatinine)	6.18 (4.31)	13.22 (9.93) [a]	88.59 (68.68) [a,b]	508.96 (214.97) [a,b,c]	<0.001*
Urine creatinine (mg/dL)	84.38 (53.47)	105.70 (64.70)	100.53 (66.88)	95.30 (64.25)	0.6
Urine albumin creatinine ratio (UACR) (mg/g of creatinine)	11.31 (14.34)	14.01 (7.04) [a]	111.18 (96.51) [a,b]	719.73 (538.00) [a,b,c]	<0.001*
eGFR (ml/min/1.73m²)	103.53 (10.68)	101.67 (18.33)	90.35 (23.02) [a,b]	66.25 (35.47) [a,b,c]	<0.001*
sCD36 (ng/mL)	9.97 (1.33)	10.76 (0.69) [a]	11.77 (0.50) [a,b]	12.13 (1.11) [a,b,c]	<0.001*

(DM: Diabetes Mellitus; LDL-C: Low density lipoprotein – cholesterol, HDL-C: High density lipoprotein – cholesterol, eGFR: estimated glomerular filtration rate); *Statistically significant difference between groups observed with p value < 0.001, # Statistically significant difference between groups observed with p value < 0.05; a = p value < 0.05: comparison with control; b = p value < 0.05: comparison with DM with normoalbuminuria; c = p value < 0.05: comparison with DM with microalbuminuria

The lipid profile analysis among the groups in Table 3 showed an increase in total cholesterol levels, LDL-C in the macroalbuminuria group, but HDL-C had a little decline from 50.98 mg/dL to 46.62 mg/dL. Triglycerides exhibited a substantial rise across groups ($p < 0.001$). UACR significantly escalated from 11.31 mg/g in the control group to 719.73 mg/g in the macroalbuminuria group, with a p-value < 0.001. Levels of sCD36 were markedly increased among the groups, escalating from 9.97 ng/mL in controls to 12.13 ng/mL in the macroalbuminuria group ($p < 0.001$).

Figure 1: Box Whisker plot showing levels of sCD36 among study participants.

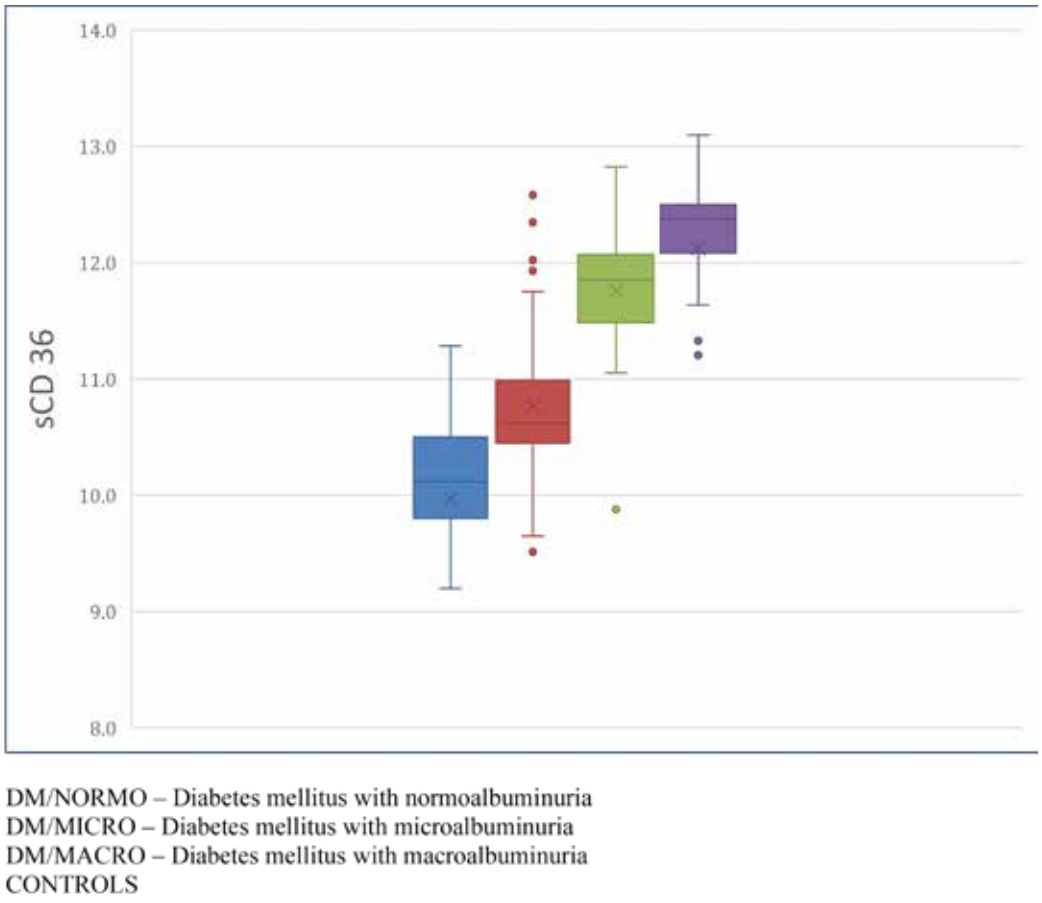

Figure 1 presents a box-whisker plot demonstrating the increase of sCD36 levels according to the severity of diabetic nephropathy.

Table 4 presents correlation analysis, indicating significant associations between sCD36 and fasting glucose ($r = 0.355$, $p < 0.001$), HbA1C ($r = 0.448$, $p < 0.001$), microalbuminuria ($r = 0.429$, $p < 0.001$), and UACR ($r = 0.321$, $p < 0.001$) and eGFR ($r = -0.262$, $p < 0.001$).

Table 4: Correlation between sCD36 and biochemical parameters.

Parameters (units)	sCD36 Correlation Coefficient (r)	p-value
Fasting plasma glucose (mg/dL)	0.355	<0.001*
HbA1C (%)	0.448	<0.001*
Serum Creatinine (mg/dL)	0.085	0.285
Total Cholesterol (mg/dL)	0.168	0.034*
LDL-C (mg/dL)	0.199	0.012*
HDL-C (mg/dL)	-0.073	0.361
Triglycerides (mg/dL)	0.188	0.017*
Microalbuminuria (µg/mg of creatinine)	0.429	<0.001*
Urinary Creatinine	-0.073	0.357
UACR (mg/g of creatinine)	0.321	<0.001*
eGFR	-0.262	<0.001*

(LDL-C: Low density lipoprotein – cholesterol, HDL-C: High density lipoprotein – cholesterol, UACR – Urine albumin creatinine ratio, eGFR: estimated glomerular filtration rate)

*Statistically significant difference with p value < 0.05

The diagnostic efficacy of sCD36 evaluated by ROC analysis (Figure 2), resulted in an area under the curve (AUC) of 0.908, signifying exceptional predictive capability for detecting advanced diabetic nephropathy. The analysis established that a cut-off value of 10.6 ng/mL for sCD36 had a sensitivity of 87.5% and a specificity of 80.83%. These data indicate that sCD36 is a reliable biomarker for differentiating stages of diabetic nephropathy.

Figure 2: Receiver operating characteristic curve (ROC) for sCD36.

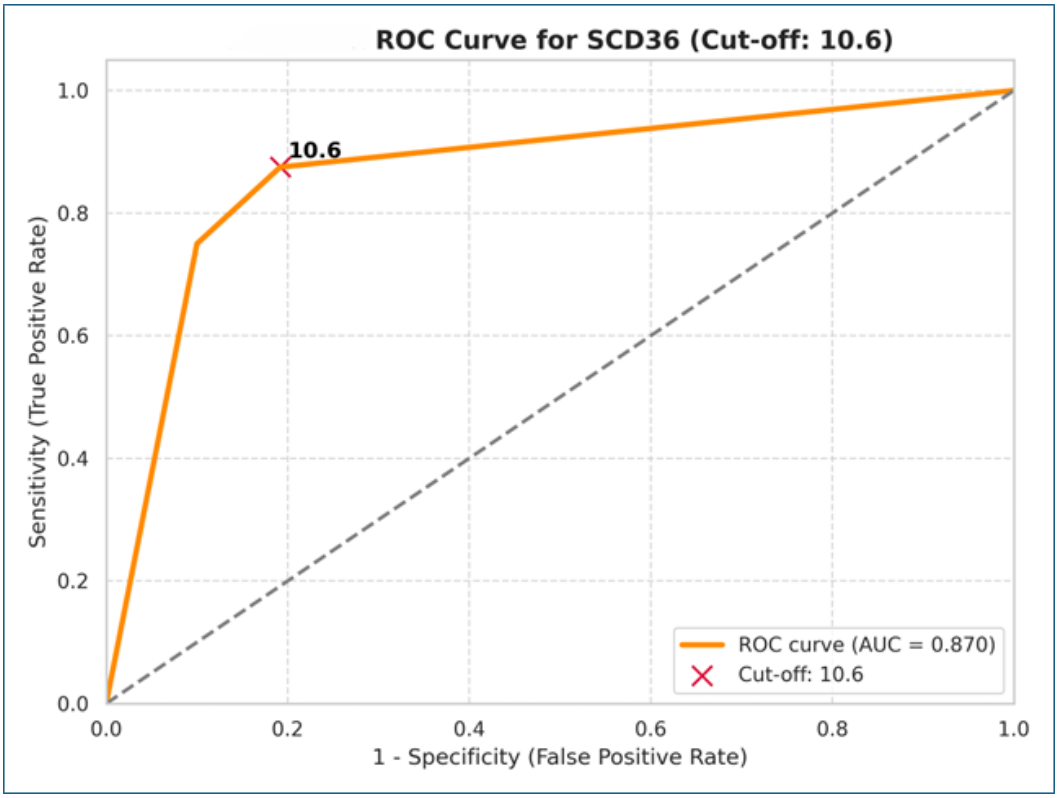

The figure shows the ROC curve of sCD36, with a cut off 10.6, AUC of 0.908 at sensitivity of 87.50% and specificity of 80.83%, positive predictive value of 60.34% and negative predictive value of 95.10%.

Discussion

DN is one of the most important microvascular complications of diabetes mellitus, contributing to the development of ESRD with a high prevalence around the world [13]. It is a substantial concern in public health due to the enormous effects and implication on health services and personal well-being of individuals who develop it [14]. Of all blood-based biomarkers, sCD36 has been a target of research attention because of its roles in lipid metabolism, inflammation, and oxyradical damage in DN [6,15,16]. The result of this study emphasizes on the relationship of serum soluble CD36 (sCD36) as an important marker for DN occurrence and progression of the disease.

Higher serum level of sCD36 in this study was associated with increasing levels of UACR and declining eGFR, strengthening the argument that CD36 actively participates in glomerular and tubular damage in progressive DN stages. These results were similar to study by Shiju et al. where levels of sCD36 in both urine and plasma showed a significant increasing trend across their study groups [12].

Hou et al., in their study state that CD36 participates in ROS generation and activation of NLRP3 inflammasome in hyperglycemia states [17]. A study by Shen et al., observed that through ligand induced signalling of toll like receptors results activation of NF-κB/NLRP3 inflammasome this ends in development of kidney fibrosis and renal insufficiency [18]. Of note, this is consistent with our finding of strong positive associations between sCD36, fasting glucose, and HbA1C, affirming the positive feedback loop between diabetes and DN. Chronic hyperglycemia significantly increases CD36 expression which dysregulates FAO by inhibiting AMPK signalling pathway. This leads to decreased OXPHOS, facilitating a metabolic switch to glycolysis for the energy needs thereby producing an imbalance in accumulation/utilisation of fatty acids and mitochondrial ROS (mtROS) generation [13,19,20]. Activation of NLRP3 inflammasome and IL-1, IL-18, IL-1β secretion occurs in a course and dose dependent manner in renal proximal tubules followed by proteinuria. Gnanaguru G et al. in their study depicted that CD36 as an integral regulatory molecule upstream of NLRP3 inflammasome in inflammatory

response [21]. Pyruvate dehydrogenase kinase 4 (PDK4) is a regulatory enzyme for increased utilisation of fatty acids in proximal TECs. In an experimental study by Niu et al., PDK4 upregulation observed in CD36 knockout models indicates that CD36 inactivates PDK4 in DN resulting in changes with AMP activated protein kinase (AMPK) levels. These findings corroborate with our analyses where higher sCD36 levels are significantly negatively associated with eGFR [22-24]. Thus, sCD36 may serve as a biomarker of the more advanced stages of DN in which mitochondrial dysfunction may be common. We have also found positive correlation between sCD36 and dyslipidemia markers including elevated LDL and triglycerides in our study supporting the idea that CD36 might be a useful biomarker for detecting metabolic dysfunction in DN. Su et al., in their study have emphasised the link between CD36 in lipid deposition and renal tubular damage could be due to sodium dependent glucose transporter 2 (SGLT2) together with fatty acid binding protein 4 (FABP4). These parities may imply that sCD36 may be a better biomarker for renal injury and lipid induced renal damage in DN [25].

Notably, the diagnostic performance of sCD36 noted in our ROC analysis with AUC 0.908 is well supported by works of Zhang et al. and Niu et al. that has established relationship between CD36 and renal disease progression in IgA nephropathy and DN respectively. As with other parameters examined in the present study, a correlation between sCD36 and UACR implies that CD36 could also be considered as pathogenic factor in kidney fibrosis and remodelling as elucidated earlier [23,24].

Several studies have demonstrated the possibility of sCD36 as a therapeutic target. Sodium dependent glucose transporter 2 (SGLT-2) inhibitors are a unique class of anti-diabetic drugs that reduce glucotoxicity by increasing sodium dependent glucose excretion in proximal TECs. In a study by Huang et al showed that SGLT-2 inhibitor Empagliflozolin decreased the expression of CD36 at a transcriptional level through PPAR-γ thereby mitigating the downstream activation of inflammatory cascade and stalling progression of DN [25]. In a study by Zou et al, Fisetin, an anti-inflammatory molecule has been shown to inhibit transforming growth factor – β (TGF-β), a cytokine downstream of CD36 involved in mesangial cell hypertrophy and ECM accumulation in renal tissues [26]. These findings underscore the advantage of developing CD36 targeted treatments especially in late stages of DN for which there are few treatment options which needs further validation.

In summary, our study indicates that sCD36 is a useful diagnostic marker and an independent predictor of prognosis in DN. The potential of sCD36 to be a biomarker for identifying the progression of DN is validated in our study by demonstrating its positive relationship with both metabolic and renal parameters, meanwhile exhibiting a good sensitivity and specificity for the diagnosis of DN.

The single centric nature of the study may affect the generalizability of its findings and in elucidating a causal relationship between the marker and DN. Duration of diabetes, medication usage, and lifestyle variables were not studied which may have affected the observed relationships. SCD36 testing in regular clinical examinations for diabetics, particularly those with microalbuminuria, may help to detect and treat DN early. Serum soluble CD36 (sCD36) could be tested in bigger, multi-centre studies with varied populations to demonstrate its diagnostic and prognostic usefulness. The molecular significance of sCD36 in mitochondrial dysfunction and inflammation needs more validation to create targeted therapies. Interdisciplinary research is needed to understand how metabolic control, lipid dysregulation, and CD36 affect DN pathogenesis.

Conclusion

This research underscores the substantial correlation between serum soluble CD36 levels and the clinical progression of diabetic nephropathy. Increased sCD36 levels were shown to correspond with critical markers of diabetic nephropathy severity, including fasting hyperglycemia, HbA1C, urine albumin-creatinine ratio, and decreased eGFR. The diagnostic effectiveness of sCD36 was established by comprehensive ROC analysis, highlighting its potential as a dependable biomarker for the staging and monitoring of diabetic nephropathy (DN). This work identifies sCD36 as a viable biomarker, facilitating its incorporation into clinical practice for early diagnosis and risk stratification of diabetic nephropathy (DN).

Author Contribution

Concept – Iyyama Gowri Moovendhan, Roopa A K, Karthick E, M Ganesh, K Sowmya;
Design - Iyyama Gowri Moovendhan, Roopa A K, Karthick E, M Ganesh, K Sowmya;
Supervision - Iyyama Gowri Moovendhan, Roopa A K, Karthick E, M Ganesh, K Sowmya;
Data collection and processing - Iyyama Gowri Moovendhan, Roopa A K, Karthick E, M Ganesh, K Sowmya;
Analyses and interpretation - Iyyama Gowri Moovendhan, Roopa A K, Karthick E, M Ganesh, K Sowmya;
Literature search - Iyyama Gowri Moovendhan, Roopa A K, Karthick E, M Ganesh, K Sowmya;
Writing - Iyyama Gowri Moovendhan, Roopa A K, Karthick E, M Ganesh, K Sowmya;
Critical review - Iyyama Gowri Moovendhan, Roopa A K, Karthick E, M Ganesh, K Sowmya

Ethical Committee Approval

The study was approved by Sri Ramachandra Institute of Higher Education and Research Institutional Ethics Committee (REF: IEC-NI/23/AUG/88/48).

Data Availability

The datasets used and or analysed during the current study are not available because of institutional policy

Conflict of Interest

The authors declare that there are no conflicts of interest pertaining to conduct of this study.

Acknowledgment

The authors like to express sincere gratitude to all individuals who contributed to this study. We would like to thank Ms Annie Sylvia for her contributions to sample collection process. The authors would also like to extend gratitude to the institution for providing with the necessary facilities for the conduct of this study.

Funding

This study was funded by Sri Ramachandra Institute of Higher Education and Research under the GATE-Young faculty research grant for the year 2022-2023. (Ref:72/PROVC/2023).

References

1. Dwivedi S, Sikarwar MS. Diabetic nephropathy: Pathogenesis, mechanisms, and therapeutic strategies. Hormone and Metabolic Research. 2025;57(01):7-17.; https://doi.org/10.1055/a-2435-8264

2. Bhargava P, Schnellmann RG. Mitochondrial energetics in the kidney. Nature Reviews Nephrology. 2017;13(10):629-646.; https://doi.org/10.1038/nrneph.2017.107

3. Kang HM, Ahn SH, Choi P, Ko YA, Han SH, Chinga F, Park AS, Tao J, Sharma K, Pullman J, Bottinger EP. Defective fatty acid oxidation in renal tubular epithelial cells has a key role in kidney fibrosis development. Nature medicine. 2015;21(1):37-46.; https://doi.org/10.1038/nm.3762

4. Hou Y, Shi Y, Han B, Liu X, Qiao X, Qi Y, Wang L. The antioxidant peptide SS31 prevents oxidative stress, downregulates CD36 and improves renal function in diabetic nephropathy. Nephrology Dialysis Transplantation. 2018;33(11):1981-2018.; https://doi.org/10.1093/ndt/gfy021

5. Susztak K, Ciccone E, McCue P, Sharma K, Böttinger EP. Multiple metabolic hits converge on CD36 as novel mediator of tubular epithelial apoptosis in diabetic nephropathy. PLoS medicine. 2005;2(2):e45.; https://doi.org/10.1371/journal.pmed.0020045

6. Puchałowicz K, Rać ME. The multifunctionality of CD36 in diabetes mellitus and its complications - update in pathogenesis, treatment and monitoring. Cells. 2020;9(8):1877. https://doi.org/10.3390/cells9081877

7. Lopez-Giacoman S, Madero M. Biomarkers in chronic kidney disease, from kidney function to kidney damage. World journal of nephrology. 2015 ;4(1):57.; https://doi.org/10.5527/wjn.v4.i1.57

8. Yang X, Okamura DM, Lu X, Chen Y, Moorhead J, Varghese Z, Ruan XZ. CD36 in chronic kidney disease: novel insights and therapeutic opportunities. Nature Reviews Nephrology. 2017;13(12):769-781.; https://doi.org/10.1038/nrneph.2017.126

9. Silverstein RL, Febbraio M. CD36, a scavenger receptor involved in immunity, metabolism, angiogenesis, and behavior. Science signaling. 2009;2(72):re3.; https://doi.org/10.1126/scisignal.272re3

10. Li X, Zhang T, Geng J, Wu Z, Xu L, Liu J, Tian J, Zhou Z, Nie J, Bai X. Advanced oxidation protein products promote lipotoxicity and tubulointerstitial fibrosis via CD36/β-catenin pathway in diabetic nephropathy. Antioxidants & Redox Signaling. 2019;31(7):521-538.; https://doi.org/10.1089/ars.2018.7634

11. Handberg A, Levin K, Højlund K, Beck-Nielsen H. Identification of the oxidized low-density lipoprotein scavenger receptor CD36 in plasma: a novel marker of insulin resistance. Circulation. 2006;114(11):1169-1176.; https://doi.org/10.1161/circulationaha.106.626135

12. Shiju TM, Mohan V, Balasubramanyam M, Viswanathan P. Soluble CD36 in plasma and urine: a plausible prognostic marker for diabetic nephropathy. Journal of Diabetes and its Complications. 2015;29(3):400-406.; https://doi.org/10.1016/j.jdiacomp.2014.12.012

13. Sagoo MK, Gnudi L. Diabetic nephropathy: an overview. Diabetic nephropathy: methods and protocols. 2019:3-7.; https://doi.org/10.1007/978-1-4939-9841-8_1

14. Varghese RT, Jialal I. Diabetic Nephropathy. [Updated 2023 Jul 24]. In: StatPearls [Internet]. Treasure Island (FL): StatPearls Publishing; 2025 Jan-. Available from: https://www.ncbi.nlm.nih.gov/books/NBK534200/

15. Mizdrak M, Kumrić M, Kurir TT, Božić J. Emerging biomarkers for early detection of chronic kidney disease. Journal of personalized medicine. 2022;12(4):548.; https://doi.org/10.3390/jpm12040548

16. Moon JS, Karunakaran U, Suma E, Chung SM, Won KC. The role of CD36 in type 2 diabetes mellitus: β-cell dysfunction and beyond. Diabetes Metab J. 2020;44(2):222-233.; https://doi.org/10.4093/dmj.2020.0053

17. Hou Y, Wang Q, Han B, Chen Y, Qiao X, Wang L. CD36 promotes NLRP3 inflammasome activation via the mtROS pathway in renal tubular epithelial cells of diabetic kidneys. Cell death & disease. 2021;12(6):523.; https://doi.org/10.1038/s41419-021-03813-6

18. Shen S, Ji C, Wei K. Cellular senescence and regulated cell death of tubular epithelial cells in diabetic kidney disease. Frontiers in Endocrinology. 2022;13:924299.; https://doi.org/10.3389/fendo.2022.924299

19. Chen K, Zhang J, Zhang W, Zhang J, Yang J, Li K, He Y. ATP-P2X4 signalling mediates NLRP3 inflammasome activation: a novel pathway of diabetic nephropathy. The international journal of biochemistry & cell biology. 2013;45(5):932-943.; https://doi.org/10.1016/j.biocel.2013.02.009

20. Sheedy FJ, Grebe A, Rayner KJ, Kalantari P, Ramkhelawon B, Carpenter SB, Becker CE, Ediriweera HN, Mullick

AE, Golenbock DT, Stuart LM. CD36 coordinates NLRP3 inflammasome activation by facilitating intracellular nucleation of soluble ligands into particulate ligands in sterile inflammation. Nature immunology. 2013;14(8):812-820.; https://doi.org/10.1038/ni.2639
21. Gnanaguru G, Choi AR, Amarnani D, D'Amore PA. Oxidized lipoprotein uptake through the CD36 receptor activates the NLRP3 inflammasome in human retinal pigment epithelial cells. Investigative ophthalmology & visual science. 2016;57(11):4704-4712.; https://doi.org/10.1167/iovs.15-18663
22. Jeong JY, Jeoung NH, Park KG, Lee IK. Transcriptional regulation of pyruvate dehydrogenase kinase. Diabetes & metabolism journal. 2012;36(5):328.; https://doi.org/10.4093/dmj.2012.36.5.328
23. Zhang J, Wang Y, Chen C, Liu X, Liu X, Wu Y. Downregulation of CD36 alleviates IgA nephropathy by promoting autophagy and inhibiting extracellular matrix accumulation in mesangial cells. International Immunopharmacology. 2025;144:113672.; https://doi.org/10.1016/j.intimp.2024.113672
24. Niu H, Ren X, Tan E, Wan X, Wang Y, Shi H, Hou Y, Wang L. CD36 deletion ameliorates diabetic kidney disease by restoring fatty acid oxidation and improving mitochondrial function. Renal Failure. 2023;45(2):2292753.; https://doi.org/10.1080/0886022x.2023.2292753
25. Huang CC, Chou CA, Chen WY, Yang JL, Lee WC, Chen JB, Lee CT, Li LC. Empagliflozin ameliorates free fatty acid induced-lipotoxicity in renal proximal tubular cells via the PPARγ/CD36 pathway in obese mice. International journal of molecular sciences. 2021;22(22):12408.; https://doi.org/10.3390/ijms222212408
26. Zou TF, Liu ZG, Cao PC, Zheng SH, Guo WT, Wang TX, Chen YL, Duan YJ, Li QS, Liao CZ, Xie ZL. Fisetin treatment alleviates kidney injury in mice with diabetes-exacerbated atherosclerosis through inhibiting CD36/fibrosis pathway. Acta Pharmacologica Sinica. 2023;44(10):2065-2074.; https://doi.org/10.1038/s41401-023-01106-6

Research Article

Analyzing the Utility of Pooled Sera as Internal Quality Control for Immunoassay Parameters by an EWMA-backed Statistical Mechanism (e-PSQC): A Comparison with Commercially Available Material and Westgard Rules

Prakruti Dash[1], Saurav Nayak[1*], Tanushree Roy[1]

[1]*Department of Biochemistry, All India Institute of Medical Sciences, Bhubaneswar, India*

Article Info

[*]***Corresponding Author:***
Saurav Nayak
Senior Resident, Department of Biochemistry
All India Institute of Medical Sciences Bhubaneswar
Sijua, Patrapada, Bhubaneswar, Odisha 751019, India
E-mail: drsauravn@gmail.com
Contact No: +91 9438158780

Keywords

Quality Control, Pooled Sera, EWMA

Abstract

Background: Internal Quality Control (IQC) is a cornerstone of clinical laboratory operations, ensuring reliability in diagnostic testing. Commercial IQC materials, though effective, pose challenges of high cost, limited availability, and susceptibility to matrix effects. Pooled sera (PS), derived from discarded patient samples, offer a cost-effective alternative. However, the stability and performance of pooled sera as IQC material in immunoassays need robust evaluation, particularly when combined with advanced statistical tools like Exponentially Weighted Moving Average (EWMA).

Objective: To evaluate the utility of pooled sera as IQC material for immunoassay parameters using the EWMA statistical approach and compare its performance against commercially available IQC materials.

Method: A study was conducted in the clinical biochemistry laboratory at AIIMS Bhubaneswar. Pooled sera were prepared from discarded patient samples, aliquoted, and stored at -5°C. Five immunoassay parameters (Free T3, Free T4, TSH, Cortisol, and Ferritin) were monitored over 60 days using both pooled sera and commercial IQC materials. EWMA charts with a 7-day smoothing window were employed to assess error detection. Performance metrics, including Mean Squared Error (MSE), Root Mean Squared Error (RMSE), and Concordance Correlation Coefficient (CCC), were analyzed. Statistical significance was set at $p<0.05$.

Results: The EWMA analysis of pooled sera (ePSIQC) closely mirrored commercial IQC performance. Concordance was significant for all parameters except Free T4. The ePSIQC method demonstrated superior early error detection compared to traditional Westgard Multirules. Pooled sera remained stable throughout the study duration, with deviations observed only in a few instances.

Conclusion: Pooled sera, combined with EWMA, provides a cost-effective, stable, and reliable alternative to commercial IQC materials for immunoassays. The enhanced error detection capability of EWMA strengthens laboratory quality control, offering a viable solution for resource-limited settings.

Introduction

Clinical laboratories must have proper Quality Control (QC) since they supplement the highest laboratory performance standards, support accurate medical diagnosis and patient treatment, and strengthen the healthcare system. These materials comprise analytes of known concentrations that are measured by the laboratory, ideally in concentrations close to the decision limits where a medical decision is required [1,2]. They resemble human serum, plasma, blood, urine, and cerebrospinal fluid. The substance may be liquid (ready to use) or freeze-dried (lyophilised) [3]. On the day of the test, at least two levels of quality control should be done, regardless of the size of the lab. Two-level controls should be done during peak hours, and then one level should be done every eight hours if the lab is open throughout [4].

The need for internal QC (IQC) materials to monitor laboratory performance has grown as clinical laboratories have become more automated [5,6]. This is integral for monitoring and assessing the analytical processes that yield patient results. The primary objective is to identify and evaluate errors across the pre-analytical, analytical, and post-analytical phases before results are reported. Regular implementation of quality control materials is essential for ensuring the reliability of test outcomes. By routinely analysing and applying statistical process control, laboratories can uphold accuracy in patient testing. These results are deemed acceptable when they fall within the defined error limits and unacceptable when they exceed these boundaries, indicating significant errors [7–9]. Commercial control serums derived from animal or human serum are commonly used in clinical chemistry laboratories. QC materials must be homogeneous, stable, and non-infectious for extended storage periods. To mitigate matrix effects and facilitate efficient production, a pooled serum is typically prepared in bulk, aliquoted, and subsequently distributed to laboratories participating in an External Quality Assessment Scheme (EQAS) program [10]. However, limitations include bottle-to-bottle variations, reconstitution errors (e.g., temperature and solvent used), over-dilution or under-dilution, reconstitution duration, vigorous shaking, light exposure and compositional differences [11]. The routine use of commercial QC materials is often economically unfeasible for many developing countries due to their high cost and limited availability [5,12].

According to Good Laboratory Practice and Health Laboratory Practice Guidelines, laboratories may also use self-prepared control materials, such as serum pools, as alternatives [13]. Pooled serum (PS), a blend of human serum from clinical laboratory samples, closely resembles patient samples and reduces reconstitution errors typical of lyophilised commercial IQC [5,14,15]. While it's a cost-effective alternative, it's essential to evaluate the effectiveness and stability of pooled serum as a substitute for commercial quality control materials for routine biochemical parameters [14].

The procedure of quality control is statistical. The values of the control material within the specified upper and lower limits are shown on QC charts. Westgard rules can be used to discover errors during the analytical stage of sample processing [16]. Plotted on a Levy Jennings Chart, it is used to estimate the magnitude of various analytical errors, both systematic and random [17].

One common type of control rule in the workplace is the exponentially weighted moving average (EWMA) rule for internal quality control. The rule aims to accurately estimate systematic errors by combining control measures from earlier runs with control data from the present run. As a result, the EWMA rule is more sensitive than conventional QC methods that only assess the current run's control data, allowing it to detect small but consistent shifts or gradual trends much earlier. Because the influence of the earlier observations is exponentially decreasing, control measurements taken multiple runs before the current run only make a very small contribution, which makes sense intuitively [18,19].

This study aims to evaluate the effectiveness of using pooled serum samples in combination with the Exponentially Weighted Moving Average (EWMA) method for internal quality control (IQC). By integrating the inherent stability of pooled sera with the sensitivity of EWMA in detecting subtle analytical shifts or trends, we seek to determine whether this approach can enhance error detection in comparison to conventional methods. The performance of this strategy is assessed against that of commercially available quality control materials and standard Westgard rules. We hypothesize that the combined use of pooled sera and EWMA will provide earlier and more reliable identification of systematic errors, thereby improving the overall robustness of laboratory quality control practices.

Methodology

The Pooled Sera Quality Control (PSQC) analysis was conducted in the clinical biochemistry laboratory under the Department of Biochemistry at AIIMS Bhubaneswar. Ethical approval was obtained from the Institutional Ethical Committee.

Test parameters and instrument

A total of five routine parameters measured by an immunoassay, i.e., Free T3, Free T4, TSH, Cortisol and Ferritin, processed in Siemens Advia Centaur XP, were analysed by both commercial QC material as well as Pooled Sera Quality Control (PSQC). The sample load was around 500 tests/day. Therefore, the PSQC was processed around the midday mark for these parameters, approximating around 250 samples.

Commercial Quality Control Material

The quality control material used for day-to-day analysis was from BioRad. Two levels of Quality Control, Level 1 and Level 2 Lypocheck Immunoassay Plus Control.

Preparation of pooled sera and storage

The estimated requirement of sera for the entire parameter was around 500µL; for 60 days of processing, 30mL of pooled sera was required. The pooled sera utilized for this study were prepared on a single day (Day 0) from residual and discarded patient serum samples obtained in the clinical biochemistry laboratory. Based on the patient reports, only those samples that were in or close to the reference ranges were included in the process. Samples exhibiting apparent haemolysis, lipemia, icterus, or inadequate volume were eliminated to preserve analytical integrity. While individual testing of each sample for infectious pathogens, including HIV, Hepatitis B, and Hepatitis C, was not performed due to the retrospective and pooled methodology, rigorous compliance with universal precautions was maintained throughout the procedure. This encompassed the utilization of personal protective equipment (PPE) including gloves, lab coats, and face shields, in conjunction with appropriate hand hygiene and disinfection methods in accordance with institutional biosafety norms. After collecting a sufficient volume of pooled sera (30 mL), it was thoroughly mixed to guarantee uniformity. The pooled material was aseptically divided into sixty sterile 1 mL microcentrifuge tubes utilizing calibrated micropipettes to prevent contamination and volume inconsistencies. The aliquots were promptly stored at –5°C in a designated freezer container to maintain analyte stability throughout the 60-day quality control assessment period.

Processing of pooled sera

The PSQC was run as a patient sample, once every day for 60 days, using the hormone assay for the five parameters, and the values were noted. The values of Level 1 and Level 2 QC were also noted for this period.

Westgard Rules and Multirules

The Westgard Rules and Multirules were applied to the QC data. 1-2s was considered as a warning, and 1-3s was considered as run rejection. 2-2s, 3-1s, 4-1s, and NX rules were markers of systemic error and R-4s was taken as marker for random error.

EWMA

Exponentially Weighted Moving Average was applied to the measured value of PSQC (e-PSQC). A 7-day smoothing was used for EWMA with a λ of 0.25. The formula for the moving average estimation was:

EWMA(t) = 0.25 * X(t) + 0.25 * 0.75 * X(t-1) + 0.25 * 0.75^2 * X(t-2) + 0.25 * 0.75^3 * X(t-3) + 0.25 * 0.75^4 * X(t-4) + 0.25 * 0.75^5 * X(t-5) + 0.25 * 0.75^6 * X(t-6), where t =7 days.

Statistical Analysis

The Westgard violations were determined using a custom-made MS Excel Worksheet based on the mean and SD of the analyte, as well as the QC run value for the given day. The stability of the Pooled Sera was determined by subtracting the days on which there were errors in the instrument and, for the remainder of the days, applying a CUSUM test. The agreement between the QC material and PSQC was determined based on evaluation metrics like Mean Squared Error (MSE), Root Mean Squared Error (RMSE), and Mean Absolute Deviation (MAD), as well as by Concordance Correlation Coefficient (CCC) analysis. A p-value of less than 0.05 was considered significant.

Results

The 7-day smoothed EWMA value from day 7 to day 60 was compared to that of the commercial internal QC run. The stability of the pooled sera was determined by subjecting it to the CUSUM test. For Cortisol and FT3, there was almost no deviation, whereas for other parameters, there were a few deviations around the mean, but those were not significant to disregard the sera. The CUSUM test result has been summarised in Figure 1.

Figure 1: CUSUM Chart for the Immunoassay parameter's PSIQC values on correct IQC days.

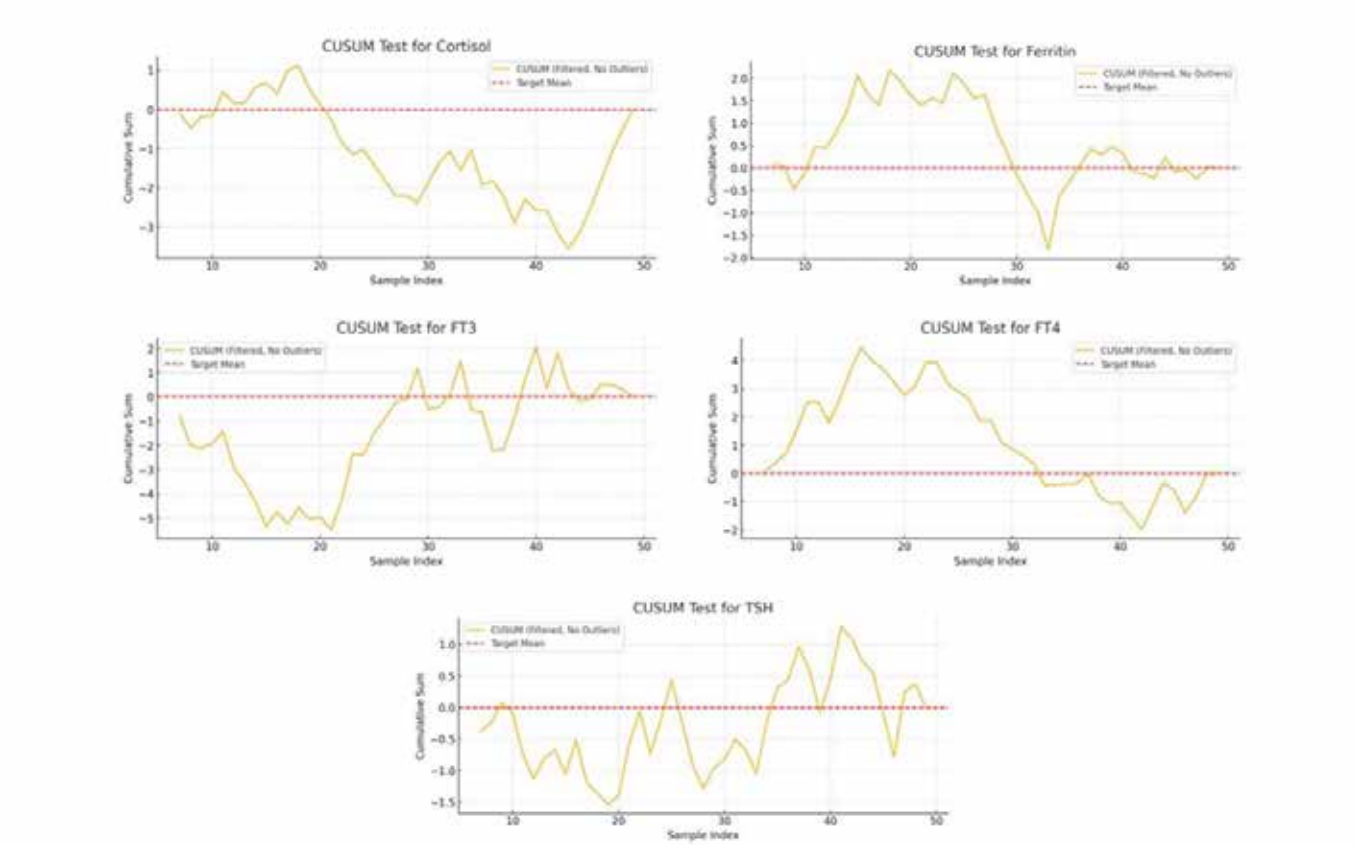

The deviation in the PSQC was well aligned with the deviations in the IQC material used. The concordance analysis showed a close agreement between L1 and L2 QC and the ePSIQC, except for FT4, where it was insignificant. The same has been tabulated in Table 1.

Table 1: Concordance Analysis between IQC and ePSIQC based on Z-Score.

Test	L1 CCC	L1 p-value	L2 CCC	L2 p-value
Cortisol	0.863	<0.001	0.726	<0.001
Ferritin	0.872	<0.001	0.657	<0.001
FT3	0.439	0.005	0.414	0.009
FT4	0.139	0.825	0.124	0.862
TSH	0.834	<0.001	0.825	<0.001

To evaluate the performance of ePSIQC compared to IQC, we calculated the evaluation metrics based on the corresponding measurements. This has been tabulated in Table 2. The EWMA calculated values and the L1 and L2 values of IQC were plotted on an LJ Chart, and the errors encountered were highlighted. The ePSIQC method accurately predicted the errors before Westgard Rules could make out the errors. This is shown in Figure 2.

Figure 2: EWMA-PSIQC and IQC L1 and L2 values on a standard LJ Chart.

Table 2: Performance Evaluation Metrics comparing ePSIQC to IQC by Z-Score deviation.

Test Analyte	IQC Level 1			IQC Level 2		
	MSE	RMSE	MAD	MSE	RMSE	MAD
Cortisol	0.02	0.05	0.04	0.02	0.05	0.04
Ferritin	0.03	0.05	0.04	0.04	0.07	0.06
FT3	0.20	0.14	0.11	0.13	0.11	0.09
FT4	0.24	0.15	0.14	0.31	0.18	0.16
TSH	0.04	0.06	0.05	0.04	0.07	0.05

Discussion

In our study, we tried to answer the research question in a three-fold pattern: If PS will be stable for immunoassay parameters over some time; If PS can be used as a supplement to Commercial QC material in the clinical laboratory; and whether combining PS with EWMA provides a robust pre-emptive mechanism to the Westgard Multirules.

The primary concern that remains in the usage of pooled sera is its stability once the material has been prepared for the parameters over the analysed days. In our case, for all parameters except FT4, the CUSUM measures a stable pooled sera parameter set. Though it is well set that Immunoassay parameters rarely deviate over some time, as reported by Westgard, they can be a practically viable supplemental material [20]. A similar study by Devi and Nagar illustrated the stability of PS over a period of 50 days when tested for routine biochemical parameters with no significant statistical deviation from the concentration mean as measured on Day 1 [14]. Kachhawa et al. also demonstrate the same where the PS stability is characteristically maintained throughout the study duration [21].

Once the stability was determined, the pooled sera measurement was coupled with EWMA to assess its effectiveness against IQC. It was shown that the EWMA

method closely follows both the levels of the IQC with respect to the Z-Score, thus proving its efficacy as an alternate QC material. This has been previously demonstrated in multiple previous studies, which returned with a similar conclusion [10]. Also, the more important finding of our study was that the deviation of EWMA was significantly earlier than that of Westgard Multirules and, therefore, could handle both systemic and random errors better than the conventional methods.
There were a few limitations to our study owing to the fact that multiple pooled sera, over a long period of time, could have a better result; also, rather than only assessing immunoassays, routine biochemical tests could have been included as they provide more complexity due to colorimetric test.
However, our study excelled at combining the statistically robust method of EWMA with a cost-conserving and robust alternative of pooled sera to formulate a 7-day smoothened ePSIQC that was significantly competent and, at times better, the commercially available and processed internal quality control in the laboratory.

Conclusion

Pooled serum Internal Quality Control (IQC) offers a practical, affordable, and flexible alternative to commercially available IQCs, especially for laboratories with financial constraints or limited access to commercial quality control materials. The implementation of Exponentially Weighted Moving Average (EWMA) as a predictive tool in conjunction with Westgard rules on a Levey-Jennings chart greatly improves the early detection of quality control errors, fostering a proactive approach to laboratory quality management. By identifying subtle shifts in control data that may indicate potential rule violations, EWMA enhances the quality control process, leading to better error detection and correction. This predictive capability helps laboratories uphold high analytical standards and reduces the risk of quality control breaches, ultimately reinforcing the reliability and accuracy of diagnostic testing. Combining both methods leads to a robust mechanism for early error detection, thus helping the laboratory, clinicians, and the patients.

CRediT Author Statement

PD: Conceptualization, Investigation, Writing-Reviewing & Editing, Supervision, Project Administration. SN: Conceptualization, Methodology, Software, Formal Analysis, Data Curation, Visualization. TR: Data Curation, Writing-Original Draft, Visualization.

References

1.Abdel GMT, El-Masry MI. Verification of quantitative analytical methods in medical laboratories. J Med Biochem 2021;40:225–236. https://doi.org/10.5937/jomb0-24764.
2. Whitehead TP, Morris LO. Methods of Quality Control. Ann Clin Biochem 1969;6:94–103. https://doi.org/10.1177/000456326900600403.
3. Ahn S, Park J, Kim YR, Kim J-H, Kim H-S. Stability of lyophilized pooled sera as quality control materials for tumor marker assays in external quality assessment. Clinica Chimica Acta 2017;471:233–242. https://doi.org/10.1016/j.cca.2017.05.035.
4. Gruber L, Hausch A, Mueller T. Internal Quality Controls in the Medical Laboratory: A Narrative Review of the Basic Principles of an Appropriate Quality Control Plan. Diagnostics (Basel) 2024;14:2223. https://doi.org/10.3390/diagnostics14192223.
5. Kulkarni S, Pierre SA, Kaliaperumal R. Efficacy of Pooled Serum Internal Quality Control in Comparison with Commercial Internal Quality Control in Clinical Biochemistry Laboratory. J Lab Physicians 2020;12:191–195. https://doi.org/10.1055/s-0040-1721151.
6. Kanagasabapathy AS, Swaminathan S, Selvakumar R. Quality control in clinical biochemistry. Indian J Clin Biochem 1996;11:17–25. https://doi.org/10.1007/BF02868406.
7. Westgard S, Petrides V, Schneider S, Berman M, Herzogenrath J, Orzechowski A. Assessing precision, bias and sigma-metrics of 53 measurands of the Alinity ci system. Clinical Biochemistry 2017;50:1216–1221. https://doi.org/10.1016/j.clinbiochem.2017.09.005.
8. Panda CR, Kumari S, Mangaraj M, Nayak S. The Evaluation of the Quality Performance of Biochemical Analytes in Clinical Biochemistry Laboratory Using Six Sigma Matrices. Cureus 2023. https://doi.org/10.7759/cureus.51386.
9. Westgard JO, Barry PL, Hunt MR, Groth T. A multi-rule Shewhart chart for quality control in clinical chemistry. Clin Chem 1981;27:493–501. https://doi.org/10.1093/clinchem/27.3.493
10. Jamtsho R. Stability of Lyophilized Human Serum for Use as Quality Control Material in Bhutan. Ind J Clin Biochem 2013;28:418–421. https://doi.org/10.1007/s12291-013-0328-x.
11. Miller Wg, Erek A, Cunningham TD, Oladipo O, Scott MG, Johnson RE. Commutability Limitations Influence Quality Control Results with Different Reagent Lots. Clinical Chemistry 2011;57:76–83. https://doi.org/10.1373/clinchem.2010.148106.
12. Tewabe H, Mitiku A, Yenesew A. Validation of the efficacy of pooled serum for serum glucose inhouse quality control material in comparison with commercial internal quality control in clinical chemistry laboratory. Practical Laboratory Medicine 2024;39:e00377. https://doi.org/10.1016/j.plabm.2024.e00377.
13. Ezzelle J, Rodriguez-Chavez IR, Darden JM, Stirewalt M, Kunwar N, Hitchcock R, et al. Guidelines on good clinical laboratory practice: bridging operations between research and clinical research laboratories. J Pharm Biomed Anal 2008;46:18–29. https://doi.org/10.1016/j.jpba.2007.10.010.
14. Haile B, Bikila D, Tewabe H, Wolde M. Preparation of In-House Quality Control Human Serum for Urea and its Use in Clinical Chemistry. Clin Lab 2020;66. https://doi.org/10.7754/Clin.Lab.2019.190704.

15. Tan JG, Omar A, Lee WB, Wong MS. Considerations for Group Testing: A Practical Approach for the Clinical Laboratory. Clin Biochem Rev 2020;41:79–92. https://doi.org/10.33176/AACB-20-00007.
16. Carroll TA, Pinnick HA, Carroll WE. Probability and the Westgard Rules. Ann Clin Lab Sci 2003;33:113–114.
17. Levey S, Jennings ER. The use of Control Charts in the Clinical Laboratory*. American Journal of Clinical Pathology 1950;20:1059–1066. https://doi.org/10.1093/ajcp/20.11_ts.1059.
18. Linnet K. The exponentially weighted moving average (EWMA) rule compared with traditionally used quality control rules. Clinical Chemistry and Laboratory Medicine (CCLM) 2006;44. https://doi.org/10.1515/CCLM.2006.077.
19. Poh DKH, Lim CY, Tan RZ, Markus C, Loh TP. Internal quality control: Moving average algorithms outperform Westgard rules. Clinical Biochemistry 2021;98:63–69. https://doi.org/10.1016/j.clinbiochem.2021.09.007.
20. Westgard JO, Groth T, Aronsson T, de Verdier CH. Combined Shewhart-cusum control chart for improved quality control in clinical chemistry. Clin Chem 1977;23:1881–1887. https://doi.org/10.1093/clinchem/23.10.1881
21. Kachhawa K, Kachhawa P, Varma M, Behera R, Agrawal D, Kumar S. Study of the Stability of Various Biochemical Analytes in Samples Stored at Different Predefined Storage Conditions at an Accredited Laboratory of India. J Lab Physicians 2017;9:11–15. https://doi.org/10.4103/0974-2727.187928.

Research Article

AI Based Predictive Modelling for Internal Quality Control: A Machine Learning Approach Using Altair RapidMiner

Jayesh Warade[1*]

[1]*Meenakshi Labs, Madurai, India*

Article Info

[*]***Corresponding Author:***
Jayesh Warade
Meenakhi Labs, Madurai 625107
Tamilnadu, India
E-mail: jdyajdo@gmail.com

Keywords

Internal Quality Control, Machine Learning, Predictive Analytics, Altair RapidMiner, Laboratory Quality, Random Forest, Quality 4.0

Abstract

Background: Internal Quality Control (IQC) ensures accuracy and reliability in laboratory testing but traditionally relies on reactive, threshold-based methods. These approaches often fail to detect subtle process deviations in time, potentially compromising quality.

Objective: To develop and validate a machine learning-based predictive model for early detection of IQC deviations using Altair RapidMiner, enhancing proactive quality management in clinical laboratories.

Methods: A retrospective analytical study was conducted using 4,572 IQC records from Meenakshi Labs, covering 8 analytes across multiple instruments. Data preprocessing included cleaning, feature engineering, and encoding. Three classification algorithms - Decision Tree, Gradient Boosted Trees, and Random Forest - were developed using Altair RapidMiner's no-code environment. Models were evaluated via 10-fold cross-validation using accuracy, precision, recall, F1-score, and ROC-AUC metrics.

Results: The Random Forest model outperformed others with 92.0% accuracy, 91.0% precision, 89.4% recall, and an AUC of 0.932. Key predictive features included analyte type, control level, reagent lot, and operator ID. The model correctly predicted 68% of future out-of-control events within a 24-hour window, demonstrating potential for preventive action. Feature importance analysis enhanced model interpretability.

Conclusion: Machine learning, particularly Random Forest, effectively augments IQC by enabling predictive monitoring. Altair RapidMiner offers a user-friendly platform, making advanced analytics accessible even without programming skills. This approach aligns with Quality 4.0 initiatives, promoting data-driven, real-time decision-making in laboratory quality assurance.

Introduction

Internal Quality Control (IQC) is pivotal in maintaining the consistency, reliability, and accuracy of processes and outputs, particularly in laboratories and production environments. Historically, IQC has hinged on statistical quality control techniques and backward-looking analysis to track and resolve deviations. Although such traditional approaches have worked to some degree, they are fundamentally reactive - tending to detect anomalies only after deviations have actually happened, so resulting in expensive mistakes, decreased efficiency, and questionable quality.

Machine Learning (ML) has been a revolutionary force in healthcare over the past few years, with capabilities to perform sophisticated data analysis, detect anomalies, and make predictions. ML algorithms learn from past data to identify hidden patterns, trends, and predictive features, which cannot be picked up easily by traditional statistical techniques. ML has been used with success in areas of diagnostic imaging, patient risk stratification, treatment planning tailored to individual patients, and predicting outbreaks of disease. With increasing access to historic process data and the development of computational capabilities, predictive analytics has become a paradigm in quality control. Predictive modeling employing machine learning (ML) provides an early detection remedy with a systematic approach to identifying shifts in performance measures before they lead to major quality problems [1,2]. By examining vast amounts of historical IQC data, ML algorithms can identify hidden patterns and relationships that might not be seen by standard statistical means.

This paper discusses the incorporation of ML algorithms in IQC with the use of Altair RapidMiner, a commercially available and sophisticated data science tool. The tool's graphical workflow and drag-and-drop feature make it suitable for users who lack sophisticated programming abilities while still providing a robust development environment for deploying and verifying ML models. This is directed towards the establishment and validation of predictive models that can predict IQC results, thus facilitating real-time decision-making and ongoing quality improvement.

Rationale

The logical foundation for this study is the inability of current control systems to adapt instantly to dynamic process variations. Laboratories and other industries present some fundamental challenges to quality groups, in particular the volume of data coming in daily, its complexity, and its variability. Most standard quality control methods, such as Shewhart control charts or Westgard rules, are threshold-based and static, making it difficult to detect slight drifts in the process or emerging trends [3].

Given the predictive modeling context on a machine learning basis, the following may be possible for an organization:

1. Early anomaly detection: ML models can predict deviations before they develop into full-blown errors so that intervention can take place.
2. Better use of resources: Predictive insights enable the focus to be on chosen corrective actions, optimizing time and effort put into responses [4].
3. Data-driven focus: Insights generated or predicted from ML models can serve as unbiased evidence toward making decisions on quality matters, furthering the ability to be consistent in pathway selection and opportunities to assign accountability.
4. Scalable and adaptable: Because an ML model evolves with processes and new data streams forth, it can always be retrained on fresh data and continue to perform relevantly.

Another reason that supports this proposed solution stems from Altair RapidMiner being capable of lowering the technical barriers to advanced analytics, thereby making predictive modeling accessible even to the poorest environments. The platform also marries powerful algorithms with ease of use, making it a perfect fit for actual applications of predictive IQC.

Aim

To develop and evaluate a machine learning-based predictive model for enhancing Internal Quality Control (IQC) using the Altair RapidMiner platform, enabling proactive identification of quality deviations and improving process reliability.

Objectives

1. **To collect and preprocess historical IQC data** including process parameters and defect records for modeling purposes.
2. **To explore and engineer relevant features** that significantly influence IQC outcomes, enabling meaningful input for machine learning algorithms.
3. **To implement and compare various machine learning algorithms** (e.g., decision trees, random forests, gradient boosting) within the Altair RapidMiner environment.
4. **To evaluate model performance** using standard metrics such as accuracy, precision, recall, and F1-score to determine the most effective predictive model.
5. **To identify critical variables and patterns** that contribute to IQC deviations, facilitating data-driven quality interventions.
6. **To demonstrate the utility of Altair RapidMiner** as an accessible and efficient tool for predictive analytics in quality control settings.
7. **To propose a scalable and proactive IQC framework** that can be applied in real-time operational environments for continuous quality improvement.

Materials and Methods

Study Design and Setting

This study was designed as a retrospective analytical investigation conducted using internal quality control (IQC) data obtained from Meenakshi Labs, Madurai, Tamil Nadu. The aim was to develop and validate machine learning (ML) models

for predicting IQC performance using the Altair RapidMiner platform. The data used comprised historical IQC records collected over a defined period (e.g., 12 months), including process parameters, control measurements, and documented deviations.

Data Collection

IQC data were exported from the laboratory information management system (LIMS). The dataset included:

- Daily IQC values for key analytes across multiple instruments.
- Corresponding lot numbers, control levels (Level 1 and 2), reagent information, and operator details.
- Flags indicating out-of-control results and corrective actions taken.

The dataset contained both numerical and categorical variables, with some missing and inconsistent entries requiring data cleaning.

Data Handling and Security

All historical IQC data employed in this research were de-identified prior to analysis to maintain patient confidentiality and adhere to ethical research guidelines. Patient IDs, sample numbers, and operator names, which are considered PII, were deleted or anonymized through secure scripts before data ingestion into the modeling platform

Software Platform

The entire data processing and modelling workflow was conducted using Altair RapidMiner, a visual, code-free data science platform. This software was selected due to its:
Intuitive drag-and-drop interface.
Wide range of built-in machine learning algorithms.
Integrated data preprocessing and visualization tools.
Support for cross-validation and performance evaluation.

Data Preprocessing

Data preprocessing was performed within RapidMiner and included the following steps:

1. **Data Cleaning:**

- Removal of duplicate entries.
- Handling of missing values using mean/mode imputation and domain knowledge-based corrections.

Elimination of irrelevant or redundant fields.

2. **Feature Engineering:**

- Derivation of new features such as moving averages, control rule violations (e.g., Westgard rules), and time-lagged variables.
- Encoding of categorical variables using one-hot encoding or label encoding.

3. **Exploratory Data Analysis (EDA):**

- Visualization of variable distributions, trends, and correlations to identify potential predictive features.
- Detection of outliers and control chart behavior over time.

RapidMiner Instance Configuration

The Altair RapidMiner Studio implemented for this project was hosted within an on-premise setup, installed locally on laboratory-grade secured machines within Meenakshi Labs. The setup was designed to run on the hospital's internal IT system, isolated from public internet access during live modeling sessions. No data was sent to RapidMiner cloud services

Institutional Data Security Compliance

All data handling processes were scrutinized and sanctioned by the lab's internal quality assurance officer. None of the data or results were divulged outside the organization without proper de-identification and ethics clearance. Good Clinical Laboratory Practices (GCLP) for confidentiality and privacy of data and ethical utilization of laboratory records was adhered.

Model Development

Multiple machine learning models were developed and compared using Altair RapidMiner:

- **Decision Tree Classifier**
- **Random Forest Classifier**
- **Gradient Boosted Trees**

The IQC outcome (e.g., pass/fail or in-control/out-of-control) was used as the target variable. Feature selection was conducted using attribute weighting techniques (e.g., information gain, Gini index) to improve model efficiency.

Model Training and Validation

Data were split into training (70%) and testing (30%) sets.
10-fold cross-validation was employed during training to reduce overfitting and ensure generalizability.
Hyperparameter tuning was conducted using grid search within RapidMiner's Auto Model module.
Model Evaluation
Performance of each model was evaluated using the following metrics:

- **Accuracy**
- **Precision**
- **Recall (Sensitivity)**
- **F1-Score**
- **ROC-AUC (where applicable)**

The random forest model emerged as the top performer, showing superior predictive accuracy and generalization ability.

Visualization and Interpretation

Altair RapidMiner's built-in visualization tools were used to:
Display feature importance rankings.
Generate decision paths and confusion matrices.
Visualize predictions versus actual outcomes for interpretability.

Results

1. Dataset Overview

A total of 4,800 IQC entries were extracted over a 12-month period, covering 8 analytes (e.g., glucose, urea, creatinine, ALT, AST, sodium, potassium, chloride) from two levels of quality controls (L1 and L2). Each record included information on:

- Control result (value)
- Lot number
- Instrument ID
- Reagent batch
- Operator ID
- Control rule flags (e.g., Westgard violations)

Following preprocessing and cleaning, **4,572 valid records** remained for model development.

2. Model Performance Comparison

Table 1: shows the model comparison dashboard from Altair RapidMiner Auto Model.

Model	Accuracy (%)	Precision (%)	Recall (%)	F1-Score (%)	AUC
Decision Tree	86.3	84.7	81.2	82.9	0.874
Gradient Boosted Trees	90.8	89.2	88.1	88.6	0.915
Random Forest	**92.0**	**91.0**	**89.4**	**90.2**	**0.932**

3. Confusion Matrix (Random Forest – Test Data)

The target variable was binary: "In-Control" (0) or "Out-of-Control" (1) based on predefined control limits (Table 2).

Table 2: shows Confusion Matrix (Random Forest – Test Data).

	Predicted In-Control	Predicted Out-of-Control
Actual In-Control	2,380	92
Actual Out-of-Control	75	388

True Positive Rate (Recall): 83.8%
False Positive Rate: 3.7%
Overall Classification Accuracy: 92.0%

Feature Importance

Table 3: shows the variable importance chart auto-generated in RapidMiner.

Feature	Relative Importance
Analyte (e.g., ALT, Glucose)	0.274
Control Level (L1/L2)	0.196
Reagent Lot Number	0.182
Operator ID	0.121
Instrument ID	0.098
Day of the Week	0.064
Time of Day (Shift)	0.043
Previous Day Deviation	0.022

Visual Results Interpretation

Figure 1: shows the ROC curves for all three models, with the Random Forest classifier achieving the highest AUC.

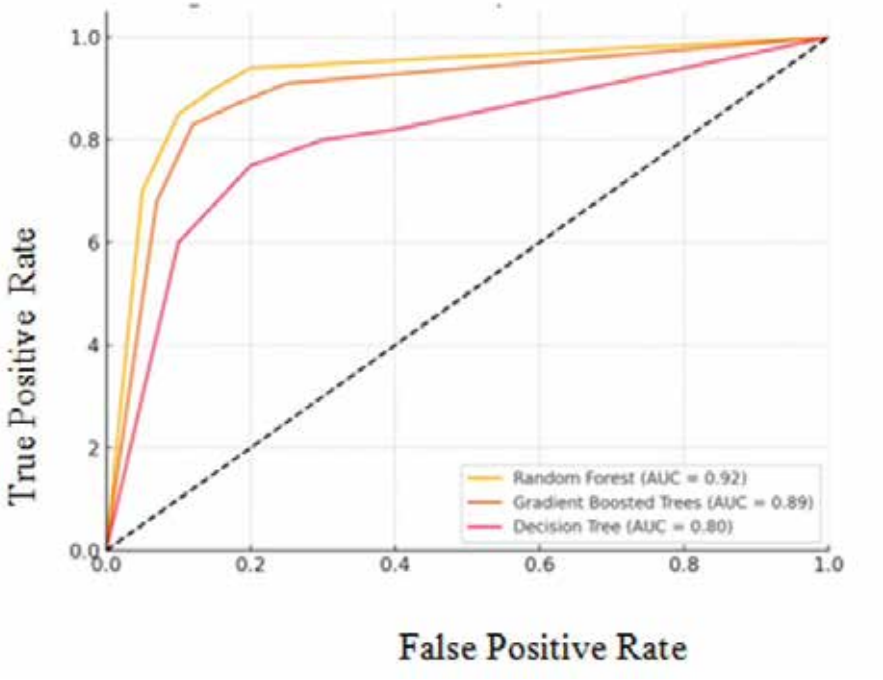

Figure 1 presents the Receiver Operating Characteristic (ROC) curves for the three machine learning models evaluated in this study: Random Forest, Gradient Boosted Trees, and Decision Tree. This graphical representation is a standard method for evaluating the diagnostic ability of binary classification models, especially in imbalanced datasets or when the cost of false positives/negatives varies.

Figure 2: Displays a bar chart of model-predicted versus actual control statuses over time, revealing high predictive alignment and fewer false alerts (Confusion Matrix – Random Forest).

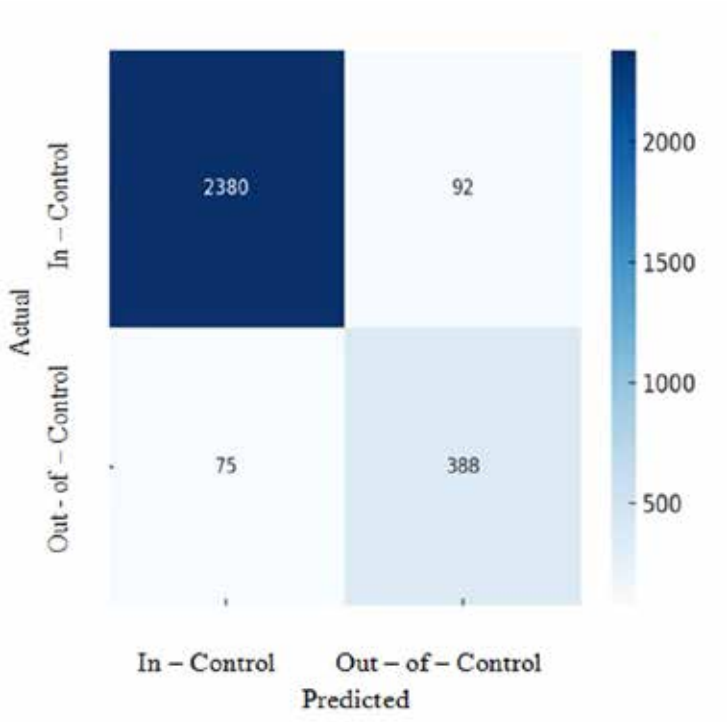

Table 2 presents the confusion matrix for the Random Forest classifier, which was identified as the best-performing model in this study for predicting Internal Quality Control (IQC) deviations. The confusion matrix provides a detailed breakdown of the model's classification results on the test dataset, helping to assess its accuracy, error types, and reliability.

6. Interpretability and Insights

- Most **out-of-control flags** were correctly predicted for **ALT (22.5%) and Sodium (17.8%)**, which historically showed higher variability.
- Operator ID and shift timing had measurable but lower impact - highlighting potential workflow optimization areas.
- The ML model provided **early warning flags for 68% of the future violations** within the next 24-hour period based on preceding data patterns.

Discussion

This research demonstrates the potential of ML to greatly enhance internal quality control systems, transforming reactive monitoring into proactive prediction. Among all models, the Random Forest classifier demonstrated the highest rate of prediction accuracy of 92.0%, and also precision and recall of 91.0 % and 89.4%, respectively, hence demonstrating its prowess in tasks involving intricate classification. These findings support the case for the use of ML-based approaches in identifying IQC deviations earlier than standard approaches, therefore ensuring higher laboratory reliability and working efficiency.

Conventional IQC approaches, such as Westgard rules and control charts, are inherently reactive - they only capture quality failures after they have occurred and typically lose subtle trends and shifts that lead to errors. Recent research has more and more called for proactive data-driven IQC models with machine learning and artificial intelligence to bridge this gap [5,6].

A narrative review by Kwon et al. highlighted the patient-based real-time quality control (PBRTQC) system augmented by ML algorithms. They indicated that ML models, particularly ensemble methods, provide considerable improvements in detecting control deviations in advance and, consequently, making corrective actions in a timely manner [6]. Our findings are consistent with this claim, as the Random Forest model has been shown to have high recall (89.4%) for the detection of out-of-control IQC events.

Smith et al. have written about difficulties in validating ML models stringently in laboratory settings, noting issues of generalizability, interpretability, and overfitting [7]. We overcame these issues by using 10-fold cross-validation and comparing three algorithms (Decision Tree, Gradient Boosted Trees, and Random Forest). The fact that the Random Forest model performed consistently well on all measures indicates that ML models can be reproducible and trustworthy with proper validation techniques for quality control.

Ain et al. conducted a review of the literature and concluded that ML quality systems work best when trained on very large and richly featured datasets [8]. Our study validated these claims: analyte type, control level, reagent lot number, and even operator ID acted as important features in determining the predictive power of the models. Thus, it is consistent with the standpoint that ML is sufficient to discover complex interactions among variables that conventional statistical tools fail to determine.

Chen et al. reinforced the argument that with the integration of ML in quality assurance, performance improves and variability decreases across industrial and laboratory settings [9]. By utilizing Altair RapidMiner - a drag-and-drop ML platform with no coding needed - we have shown that these tools are indeed able and yet operable by the laboratories that lack an internal data science department.

Lee et al. explored the use of moving average control charts augmented by ML in clinical chemistry, reporting better sensitivity and specificity than classical techniques [10]. Our results similarly show that ensemble ML models (Random Forest and Gradient Boosted Trees) outperform Decision Trees, especially in minimizing false positives and false negatives. Developments in clinical chemistry and digital pathology analyzed from Nguyen et al. might thus pronounce ML adoption as a mainstay for laboratories wishing to track their performance in real time [11]. Our model's capacity to predict deviations almost 68% of the time before their actual occurrence proves to hold good in preventive quality management.

Wang et al. asserted that laboratory datasets harbor potential untapped by quality monitoring unless appropriate tools with analytics are put into use [12]. This further reinforces our stance of employing Altair RapidMiner, which undertakes data cleaning, feature engineering, modeling, and visualization from end to end.

Huang et al., in a recent case, documented how integrating ML in real-time production settings can concretely raise performance levels [13]. Ours being a retrospective study, it becomes the forerunner for the actualization of an identical concept in clinical laboratories in real time.

Miller et al. have cautioned against over-reliance on automated ML tools without considering clinical relevance and regulatory requirements [14]. Han, GR et al in their study concluded that AI-driven models can integrate vast amounts of test data collected by a network of point-of-care biosensors with additional sources, such as hospital records, genomic data, and social media posts, to systematically track health data, identify trends, and detect unusual disease patterns [15]. Our approach emphasized model interpretability through feature importance analysis and performance transparency - ensuring the model remains a decision-support tool, not a black box.

Interpretation of Model Behaviour

The model found Analyte type, Control Level, and Reagent Lot Number to be the strongest predictors of IQC deviation. This aligns with established clinical laboratory factors for variation, including reagent batch variance and level-specific QC response. Operator ID and shift timing also had lesser but significant influences, indicating that human and workflow factors subtly affect analytical consistency - a conclusion supported by Sun et al. (2021) in their research on human factors and lab performance variation [16].

The model's 68% detection of future violations prior to occurrence is of great utility, providing labs an opportunity window to execute preventive maintenance, re-calibration, or staff retraining - steps traditionally taken reactively post-error.

Practical Implications

The deployment of this ML-based IQC prediction model within a platform like **Altair RapidMiner** presents multiple practical advantages:

- **User Accessibility**: Enables non-programmers to harness advanced analytics through a visual interface.
- **Scalability**: Can be applied across multiple analytes, instruments, or laboratory units with minimal modifications.
- **Real-time Monitoring**: Offers the potential for live IQC flagging, integrating with Laboratory Information Systems (LIS) for real-time alerts.

These capabilities support the movement toward **Quality 4.0** in laboratory medicine, where digital transformation augments decision-making and error prevention.

Limitations

While the study shows promising results, several limitations must be acknowledged:

- The data used were limited to a single center and may not generalize across different laboratory settings or instruments.
- Certain rare or complex error types might not have been adequately represented in the training data, potentially affecting sensitivity for low-frequency events.
- The current model used historical static data; future real-time integration and adaptive retraining strategies need to be tested in operational environments.

Future Directions

To advance the model's utility and generalizability, future research should focus on:

- **Multi-center validation** to assess performance across diverse laboratory contexts.
- **Integration with real-time data streams** for live IQC alerts.
- **Development of interpretable ML models** (e.g., SHAP-based explanation layers) to support regulatory compliance and clinical acceptance.
- **Extension to External Quality Assessment (EQA) and Proficiency Testing (PT)** as part of a holistic quality management system.

Conclusion

This study confirms that machine learning models - especially Random Forest - implemented via Altair RapidMiner can effectively predict IQC deviations with high accuracy and interpretability. These findings align well with current literature and support a transformative shift in quality control strategy from retrospective analysis to proactive risk mitigation. With proper integration and governance, predictive modeling can become a standard tool in the modern laboratory's quality assurance arsenal.

Acknowledgements

Figure number 4 and 5 are generated using ChatGPT.

Declaration of Conflict of interests

Nil.

Ethical Approval

NA.

Funding

Nil.

Data Availability

Data is collected from the daily internal quality control testing.

References

1. Rafidain Journal of Engineering Sciences. Advanced manufacturing with machine learning: enhancing predictive maintenance, quality control, and process optimization. Rafidain J Eng Sci. 2024;2(2):280–300. doi:10.61268/6mvqve13.
2. Regulski K, Opaliński A, Swadźba J, Sitkowski P, Wąsowicz P, Kwietniewska-Śmietana A. Machine learning prediction techniques in the optimization of diagnostic laboratories' network operations. Appl Sci. 2024;14:2429. doi:10.3390/app14062429.
3. Westgard JO. Six Sigma Risk Analysis: Designing analytic QC Plans for the medical laboratory. Madison (WI): Westgard QC; 2011.
4. Silva AC, Machado J, Sampaio P. Predictive quality model for customer defects. TQM J. 2024;36(9):155–174. doi:10.1108/TQM-09-2023-0302.
5. Malwe AS, Longwani U, Sharma VK. XenoBug: machine learning-based tool to predict pollutant-degrading enzymes from environmental metagenomes. NAR Genom Bioinform. 2025;7(2):lqaf037. doi:10.1093/nargab/lqaf037. PMID:40314024; PMCID:PMC12044416.
6. Lorde N, Mahapatra S, Kalaria T. Machine learning

for patient-based real-time quality control (PBRTQC), analytical and preanalytical error detection in clinical laboratory. Diagnostics (Basel). 2024;14(16):1808. doi:10.3390/diagnostics14161808. PMID:39202296; PMCID:PMC11354140.
7. Miller HA, Valdes R. Rigorous validation of machine learning in laboratory medicine: guidance toward quality improvement. Crit Rev Clin Lab Sci. 2025:1–20. doi:10.1080/10408363.2025.2488842.
8. Ain QU, Nazir R, Nawaz A, Shahbaz H, Dilshad A, Mufti IU, et al. Machine learning approach towards quality assurance: challenges and possible strategies in laboratory medicine. J Clin Transl Pathol. 2024;4(2):76–87. doi:10.14218/JCTP.2023.00061.
9. Karim KA, Rashid AB, Baki RF, Maktum MMJ. Machine learning algorithms for manufacturing quality assurance: a systematic review of performance metrics and applications. Array. 2025;26:100393. doi:10.1016/j.array.2025.100393.
10. Duan X, Zhang M, Liu Y, Zheng W, Lim CY, Kim S, et al. Next-generation patient-based real-time quality control models. Ann Lab Med. 2024;44:385–391. doi:10.3343/alm.2024.0053.
11. Spies NC, Farnsworth CW, Wheeler S, McCudden CR. Validating, implementing, and monitoring machine learning solutions in the clinical laboratory safely and effectively. Clin Chem. 2024;70(11):1334–1343. doi:10.1093/clinchem/hvae126.
12. Çubukçu HC, Topcu Dİ, Yenice S. Machine learning-based clinical decision support using laboratory data: a review. Clin Chem Lab Med. 2024;62(3):345–356. doi:10.1515/cclm-2023-1037.
13. Honda T, Yamazaki A. Machine learning enables real-time proactive quality control: a proof-of-concept study. Geophys Res Lett. 2024;51:e2023GL107938. doi:10.1029/2023GL107938.
14. Faust L, Wilson P, Asai S, Fu S, Liu H, Ruan X, Storlie C. Considerations for quality control monitoring of machine learning models in clinical practice. JMIR Med Inform. 2024;12:e50437 doi:https://doi.org/10.2196/50437.
15. Han GR, Goncharov A, Eryilmaz M, et al. Machine learning in point-of-care testing: innovations, challenges, and opportunities. Nat Commun. 2025;16:3165. doi:10.1038/s41467-025-58527-6.
16. Sun C, Han Y, Luo L, Sun H. Effects of air temperature on cognitive work performance of acclimatized people in severely cold region in China. Indoor Built Environ. 2020;30(6):816–837. doi:10.1177/1420326X20913617.

Research Article

Evaluation of Adropin, Irisin and Cytokeratin 18 as Biomarkers in Metabolic Dysfunction-Associated Steatotic Liver Disease: A Comparative Clinical Study

Deepa Roshni[1], Zirha Saleem[1], Sakshi Rai[1], Suman Kumar Ray[1], Abhishek Singhai[2], Sukhes Mukherjee[1*]

[1]*Department of Biochemistry, All India Institute of Medical Sciences, Bhopal, Madhya Prades, India*
[2]*Department of General Medicine. All India Institute of Medical Sciences, Bhopal, Madhya Pradesh, India*

Article Info

[*]***Corresponding Author:***
Sukhes Mukherjee
E-mail: sukhes.biochemistry@aiimsbhopal.edu.in
Department of Biochemistry, All India Institute of Medical Sciences
Bhopal, Madhya Pradesh
462020, India

Keywords

MASLD, Irisin, Adropin, Cytokeratin 18, FibroScan, Liver fibrosis

Abstract

Background: Metabolic Dysfunction-Associated Steatotic Liver Disease (MASLD) has become the leading cause of chronic liver disease globally, affects more than one-third of the adult population and includes a spectrum of conditions ranging from simple steatosis of liver to metabolic dysfunction–associated steatohepatitis (MASH), progressive fibrosis, cirrhosis and, in some cases, hepatocellular carcinoma. Early detection and accurate staging are important to prevent disease progression and studies have recently identified metabolic and apoptotic markers such as Adropin, a peptide hormone secreted by the liver that is involved in energy homeostasis; Irisin, a myokine that is linked to exercise and metabolic regulation; and CK-18, a biomarker of hepatocyte apoptosis.
Methods: Using FibroScan for the diagnosis and staging of MASLD, CAP scores were used for steatosis and liver stiffness measurements for fibrosis. Quantification of serum adropin, irisin, and CK-18 was done, and independent t-tests, correlation analysis, and ROC curve analysis were used for statistical analysis to assess the diagnostic potential.

Results: Adropin levels were lower in MASLD cases than in controls and decreased further with the severity of the disease. The association was highly significant ($p < 0.001$), indicating a very high negative correlation between Adropin levels and hepatic dysfunction. Levels of CK-18 were greatly increased in MASLD patients and were highly positively correlated with the degrees of fibrosis and steatosis ($p < 0.001$), which supports the hypothesis that it is a marker of hepatocyte apoptosis.

Conclusion: The significant changes in their levels observed in MASLD patients suggest their possible application in multimarker diagnostic strategies. Nonetheless, the inconsistent behavior of Irisin in this study requires more conclusive evidence from future studies involving larger samples. Such biomarkers may help in identifying the disease at an early stage and improve the management of the disease.

Introduction

MASLD has emerged as a significant global health concern [1], characterized by excessive fat accumulation in the liver (more than 5%) in the absence of substantial alcohol intake or other liver diseases. The condition encompasses a spectrum of hepatic disorders ranging from simple steatosis to more severe forms such as MASH, fibrosis, cirrhosis, and hepatocellular carcinoma (HCC) [2]. The rise of MASLD can primarily be attributed to the increasing sedentary lifestyle, urbanization, and the ongoing obesity epidemic [3, 4]. Globally, the prevalence of MASLD is alarmingly high, currently estimated to affect approximately 32.4% of the population [5]. Reports suggest that men are more significantly affected than women, with prevalence rates of 39.7% and 25.6%, respectively. In India, the situation is particularly concerning, with adult prevalence reported at 38.6%. Studies reveal that children are not immune to this condition, showing a prevalence of 35.4%, and particularly alarming is the rate among obese children [6], which stands at 63.4%. Urban populations in India exhibit substantially higher MASLD rates than their rural counterparts, further emphasizing the influence of lifestyle on liver health. For example, studies have depicted a stark contrast, noting a prevalence of 34.8% in Goa's urban settings versus 16.6% in rural South India.

The implications of MASLD extend beyond liver health, as the condition is closely associated with numerous metabolic complications, including Type 2 Diabetes Mellitus (T2DM), metabolic syndrome, and cardiovascular diseases [7]. Research indicates that individuals diagnosed with MASLD are at a 57% higher risk of overall mortality, particularly due to cardiac deaths [8]. Alarmingly, the rates of T2DM and chronic kidney disease (CKD) are also reported to be doubled among those affected by MASLD. Primary risk factors contributing to MASLD emergence include insulin resistance, obesity, and diabetes [9]. Insulin resistance, a hallmark of metabolic dysfunction, is associated with fat accumulation in the liver, resulting in steatosis. Obesity, especially central obesity, stands out as a critical risk factor; approximately 80% of obese individuals exhibit hepatic fat accumulation, indicating a strong link between adiposity and MASLD [10]. For instance, the prevalence of MASLD is remarkably high (78.09%) in the morbidly obese, while lower rates of 52.655% and 12.01% are reported in overweight and normal-weight populations, respectively. Moreover, central obesity not only heightens the risk of MASLD but also exacerbates insulin resistance and contributes to intrahepatic triglyceride (IHTG) accumulation, a key marker of metabolic disturbances [11]. While obesity is a predominant risk factor, MASLD is not exclusive to overweight individuals; about 5-10% of the MASLD population is lean. Genetic predisposition and the presence of abdominal obesity among normal-weight individuals are major risk factors for "lean" MASLD [12]. Insulin resistance is the primary mechanism linking T2DM and MASLD, with MASLD affecting around 55.5% of T2DM patients [13, 14]. Notably, the occurrence of cardiovascular complications in MASLD patients is significantly higher (1.87 times) when T2DM coexists. The risk of progression from MASLD to MASH is also notably elevated in diabetic patients [15]. Metabolic syndrome - a complex involving central obesity, insulin resistance, dyslipidemia, and hypertension - compounds the challenges faced by MASLD patients, as it is present in 70-90% of affected individuals [16]. Endocrine disorders further exacerbate the risk of MASLD, particularly in women with polycystic ovary syndrome (PCOS), where hormonal alterations and metabolic disturbances contribute to hepatic fat accumulation. Decreased estrogen levels in postmenopausal women are linked to increased hepatic fat, highlighting the role hormones play in MASLD pathogenesis [17]. Similarly, low testosterone levels in men correlate with heightened MASLD risk due to their engagement in lipid metabolism and anti-inflammatory actions [18]. Additionally, thyroid hormone deficiencies are known to significantly influence lipid metabolism, promoting increased fat deposition in the liver. Genetic disposition emerges as a crucial factor in MASLD susceptibility, with the PNPLA3 gene variant being notably implicated in the disorder [19]. This genetic variant leads to an enzyme dysfunction that controls triglyceride accumulation in the liver, resulting in increased susceptibility to MASLD and worsened disease progression. The complexity of MASLD pathogenesis is further appreciated through the "Multiple Hit Hypothesis," which integrates metabolic, genetic, and environmental factors affecting disease progression [20].

As MASLD often goes undiagnosed until advanced stages, there is a critical need for early identification and management strategies. Early-stage symptoms may remain subtle, leading to delayed diagnosis. Utilizing medical history, physical examinations, and non-invasive biomarker tests is essential. For instance, the initial laboratory tests may indicate elevated liver enzymes (ALT and AST), yet these findings are not specific to MASLD [21, 22]. Imaging methods, particularly ultrasonography, are commonly employed to assess liver steatosis, albeit with limitations in distinguishing between steatosis and MASH [23, 24]. Several novel biomarkers are being explored to enhance the diagnosis and monitoring of MASLD. Adropin and Irisin, both emerging peptides implicated in metabolic regulation, are garnering attention [25]. Adropin, a hormone produced in the liver and brain, plays a critical role in lipid metabolism and insulin sensitivity [26]. Lower Adropin levels are associated with metabolic conditions such as T2DM and obesity, indicating its potential as a biomarker for MASLD severity [27]. Similarly, Irisin, secreted by skeletal muscle, impacts energy metabolism and has shown promise in influencing liver health; however, research results on Irisin levels in MASLD have been variable [28]. Cytokeratin-18 (CK-18) fragments are also recognized for their potential as non-invasive markers to differentiate MASH from simple steatosis, while reflecting hepatocyte apoptosis and necrosis [29-31]. Elevated CK-18 levels have been correlated

with liver inflammation and fibrosis severity, reinforcing its relevance in clinical practice [32]. The emerging biomarkers such as Adropin, Irisin [33], and CK-18 underscore promising avenues for improving diagnosis, assessment of disease severity, and therapeutic strategies. Continued research into these biomarkers and their roles in advancing MASLD management remains essential to mitigate the burden of this complex disease on individuals and healthcare systems worldwide, ultimately reducing the risks of severe liver complications like HCC.

Materials and Methods

Ethical approval

Ethical clearance was obtained from the Institute Ethics Committee of AIIMS Bhopal (IHEC/SR/2024/Apr/10 dated: 23/04/2024), and all participants gave their informed consent before participation. From the Department of Medicine, AIIMS Bhopal, MASLD patients were recruited based on FibroScan to participate in the study, after fulfilling the inclusion and exclusion criteria and after obtaining consent. All studies involving human subjects must indicate that they are in compliance with the ethical principles for medical research involving human subjects, in accordance with the Declaration of Helsinki.

Study design and participants

It is a case control study, Adropin, Irisin and CK18 ELISA was performed in the blood of cases diagnosed through FibroScan, and the same was done for age and gender matched apparently healthy controls obtained from AIIMS Bhopal. All participants were told about the study and were asked to participate in the study. Only participants who gave their consent were enrolled and had their blood samples and anthropometric measurements taken.

Inclusion and exclusion criteria

Patients aged 18 and older with MASLD diagnoses confirmed by FibroScan who lived in Madhya Pradesh, India comprised the case group. Patients needed to provide written consent for blood sample collection and ELISA testing and routine laboratory examination for research purposes. Patients with diabetes mellitus and Hepatitis B or C infection and polycystic ovarian syndrome (PCOS) and ischemic heart disease and congestive hepatopathy and active malignancy and cancer treatment and secondary fatty liver causes were excluded from the study. Patients with overt cirrhosis who showed gross ascites and hepatic encephalopathy were excluded from the study as well as patients who took hepatotoxic drugs in the previous six months exceeding 4 g/day of acetaminophen or methotrexate or nitrofurantoin or rifampicin and those with more than 10 years of heavy alcohol use exceeding 140 g/week for men and 70 g/week for women according to NIAAA standards. The study excluded all participants younger than 18 years old. For the control group, apparently healthy adult individuals matched for age and gender with the cases, residing in Madhya Pradesh, and willing to give consent for ELISA and routine laboratory tests were included. Exclusion criteria for controls included any current or past history of liver disease, alcohol intake, diabetes mellitus, hyperlipidemia, or age below 18 years.

Sample size, sampling method and data collection tools

As regards the worldwide incidence of Metabolic Dysfunction-Associated Steatotic Liver Disease (MASLD) and the suitability of the sample for its analysis within the time available for the study, 186 samples were collected. This included 92 cases (patients with MASLD) and 97 controls (apparently healthy individuals), all recruited from the Outpatient Department (OPD) of AIIMS Bhopal, Madhya Pradesh, India. Sample size was calculated using OpenEpi software and the required number of participants to achieve sufficient statistical power was calculated to be 186. Participants were purposefully selected to match the criteria of the study, thus guaranteeing the appropriateness of the study population.

Data collection tools

It is a printed case record form, which the investigator filled in after obtaining informed consent from the participants. The case record form consisted of the following information that was gathered: demographic details- age, gender, residential address, and contact number. Biochemical investigation reports were done with other parameters in relation to liver function and metabolic status. Anthropometric measurements were performed with a standard weighing machine and a measuring tape for height, waist circumference, and so on. FibroScan results are used for MASLD staging in cases. Sample collection from each subject were done with five milliliters of whole blood, obtained in a yellow-top BD vacutainer (serum separator tube) for serum analysis. Furthermore, 5 ml of blood was drawn into a purple-top EDTA vacutainer containing 4mg of EDTA using a Buck-type tourniquet and BD vacutainer blood collection needle. All the tubes were properly marked with the name of the participant and the group to which the sample belonged (case or control) to avoid any mix-up during processing.

Measurement of serum levels of Adropin and Irisin

CK18 (FineTest, EH2820, India), Adropin (Lablisa® Human Adropin ELISA Kit, India. LAB 6444) and Irisin (Lablisa® Human Irisin ELISA Kit, India. LAB 6625) antibodies and other reagents for ELISA were purchased from a commercial supplier. ELISA was performed at room temperature and the protocol was established in the Department of Biochemistry. All plastic ware and deionized water were autoclaved. Same protocol and steps were used for Adropin and Irisin. The ELISA plate was setup with Standards, Blank and Serum Samples in designated wells. 100 µL of each Standard dilution or 100 µL

of serum sample was added to the appropriate wells. The plate was covered with a Plate Sealer and the plate was incubated at 37°C for 80 minutes. When the incubation was over, the liquid from the wells was decanted and each well was washed with wash Buffer and then aspirated. This step was then repeated three times to make sure that all the unwanted materials were removed from the wells. The last wash was completely removed by turning the plate upside down and blotting it on absorbent paper. After washing, biotinylated antibody working solution was added to each well and the plate was covered and incubated at 37°C. Streptavidin-HRP working solution was added to each well and the plate was covered and incubated at 37°C. After the final wash, TMB Substrate Solution was added to each well and the plate was covered and incubated at 37°C in the dark. The presence of the target analyte caused a blue color development by enzymatic reaction and color changing from blue to yellow. The absorbance was then immediately measured at 450 nm using a microplate reader (BioTek, India).

Quantitation of CK-18 (M65)

CK-18/M65 was quantified using a sandwich ELISA kit (FineTest, EH2820) as per the manufacturer's guidelines. All reagents were warmed up to room temperature before use in the assay. The concentrated wash buffer was diluted with distilled water and used within 48 hours. Lyophilized CK-18 standards were dissolved in sample dilution buffer and diluted in a series of concentrations (5000, 2500, 1250, 625, 312.5, 156.25, 78.125, and 0 pg/mL). The biotin-labelled antibody was made up to a concentration of 1:99 with the antibody dilution buffer immediately before use. Similarly, SABC HRP-streptavidin conjugate was diluted 1:99 in SABC dilution buffer and used within 30 minutes.

Each standard, sample and blank control was added to a pre-coated at ELISA plate and incubated at 37°C for 90 minutes in the assay. Then the biotin labeled antibody solution was added and incubated at 37°C and then washed three times. Then, HRP-streptavidin conjugate was added and left to incubate for 30 minutes at 37°C before five washes. TMB substrate was added to the wells, the plate was left to incubate in the dark at 37°C and then the reaction was stopped with stop solution. The microplate reader was used to measure absorbance at 450 nm (BioTek, India).

The data were further processed by taking the mean of the duplicate samples for OD450. A four-parameter logistic standard curve was constructed from the OD values of the standards and the concentration of the samples was determined from this curve and the dilution factor applied. The assay was performed in such a way that disposable pipette tips were used to prevent cross-contamination and washing steps were appropriately done to minimize background signals, and the standard and the working solutions were made right before the assay.

Statistical analysis

Continuous data such as age, CK18, Adropin and Irisin were presented as either mean and standard deviation (SD) or median and range according to the data distribution. Age, gender, BMI, Adropin and Irisin levels were considered to have differences between the groups and were tested. Correlation analysis was performed to examine the relationship between Adropin and Irisin levels based on the normality of the data. ROC curve analysis was used to establish the cutoff point, sensitivity and specificity of Adropin and Irisin levels in the different stages of MASLD. All statistical analyses were carried out at 5% significance level and a p value of less than 0.05 was considered to be statistically significant. P-values calculated using Mann–Whitney U test.

Results

A total of 182 participants were analyzed, comprising 92 MASLD cases and 90 healthy controls (7 controls were excluded due to incomplete data). The age of participants in both groups was similar (MASLD: 39.5 years vs. Controls: 37.5 years; $P = 0.54$). The gender distribution was comparable between groups, with 43.3% females in the control group and 39.1% females among MASLD cases. The difference was not statistically significant ($P = 0.67$), thus indicating a balanced gender representation across the study population. MASLD patients showed higher BMI measurements (median: 27.25 kg/m²) than the control participants (24.41 kg/m²; $P < 0.001$). FibroScan was used for classifying cases and controls based on liver fibrosis and hepatic steatosis evaluations for every participant in the study. The MASLD group consisted of 92 participants in which the patients had Grade 1 steatosis in 16 patients (17.4%), Grade 2 steatosis in 22 patients (23.9%) and Grade 3 steatosis in 46 patients (50.0%). The 8 participants (8.7%) who had Grade 0 steatosis received inclusion based on their fibrosis results indicating fibrotic progression. The liver stiffness measurements revealed that 39 patients (42.4%) had Stage F0 fibrosis while 31 patients (33.7%) had Stage F1 and 5 patients (5.4%) had Stage F2 and 2 patients (2.2%) had Stage F3 and 7 patients (7.6%) had Stage F4. The fibrosis staging data were missing for 8 study participants. The Fibro Scan liver stiffness measurements were higher in MASLD participants (6.85 vs. 5.0 kPa; $P < 0.001$) and the CAP score steatosis measurements were higher (290.5 vs. 217.0 dB/m; $P < 0.001$). The MASLD group showed elevated liver enzymes ALT and AST compared to controls (ALT: 53.15 vs. 23.85 U/L; AST: 53.45 vs. 25.55 U/L; both $p < 0.001$) which indicated more hepatocellular injury. The MASLD group presented significantly lower Adropin levels when compared to controls (245.0 vs. 414.4 pg/mL; $p < 0.001$) and CK-18 levels were significantly higher in MASLD patients (1030.5 vs. 533.1 pg/mL; $p < 0.001$) which supports the role of CK-18 as a marker of hepatocyte apoptosis. The Irisin concentration levels did not show any significant variation between study groups ($p = 0.17$). The anthropometric measurements of MASLD patients versus

controls showed inconsistent results among participants older than 60 years. The BMI and weight measurements of MASLD patients exceeded those of controls but these results failed to achieve statistical significance possibly because of aging body composition alterations or insufficient participant numbers. Anthropometric parameters in MASLD grouped by age and sex are shown in Table 1.

Table 1: Anthropometric parameters in MASLD - stratified by age and sex.

Age group	Gender/ Sex	Parameter	MASLD pg/mL	Control pg/mL	P-value
18–30 years	M	BMI (kg/mÂ²)	28.69±1.02	23.14±6.35	0.0008
	F	BMI (kg/mÂ²)	28.32±0.96	24.76±5.96	0.0617
	M	Hip-to-Waist ratio	0.93±0.053	0.88±0.12	0.0327
	F	Hip-to-Waist ratio	0.9±0.03	0.85±0.22	0.0211
	M	Weight (kg)	79.0±6.2	68.0±6.47	0.0017
	F	Weight (kg)	77.0±8.3	68.5±5.98	0.2639
	M	Height (cm)	170.0±12.5	171.0±14.6	0.3933
	F	Height (cm)	162.0±11.6	167.0±12.9	0.1441
31–60 years	M	BMI (kg/mÂ²)	26.21±2.03	24.58±3.5	0.0027
	F	BMI (kg/mÂ²)	28.31±2.5	24.28±2.5	0.0031
	M	Hip-to-Waist ratio	0.9±0.85	0.88±0.22	0.3221
	F	Hip-to-Waist ratio	0.89±0.74	0.86±0.23	0.0012
	M	Weight (kg)	78.0±10.2	73.5±6.5	0.0113
	F	Weight (kg)	76.0±11.63	68.0±6.85	0.0003
	M	Height (cm)	170.0±15.2	169.5±9.98	0.9194
	F	Height (cm)	165.0±11.63	164.5±10.55	0.0902
More than 60 years	M	BMI (kg/mÂ²)	26.86±6.35	24.38±5.89	0.4762
	F	BMI (kg/mÂ²)	20.94±8.65	23.51±4.78	0.2013
	M	Hip-to-Waist ratio	0.9±0.56	0.89±0.21	0.7619
	F	Hip-to-Waist ratio	0.81±0.63	0.84±0.19	0.8102
	M	Weight (kg)	79.0±9.52	75.5±5.74	0.7476
	F	Weight (kg)	60.5±8.34	72.0±8.33	0.2102
	M	Height (cm)	171.0±15.21	172.0±15.3	0.7619
	F	Height (cm)	170.0±14.96	175.0±14.69	0.8002

*Values are expressed as medians. P-values calculated using Mann–Whitney U test.

The analysis showed no statistically relevant variations in total protein, albumin or globulin concentrations between the groups. The main clinical and laboratory characteristics of the study population are summarized in Table 2.

Table 2: Clinical and biochemical characteristics of study participants.

Factor	All samples (n = 182)	Control (n = 90)	MASLD (n = 92)	P-value*
Age (years)	39.0 (29.0, 48.0)	37.5 (29.0, 47.0)	39.5 (29.8, 49.0)	0.54
Female gender	75 (41.2%)	39 (43.3%)	36 (39.1%)	0.67
BMI (kg/m²)	25.3 (23.6, 28.0)	24.4 (22.8, 25.5)	27.3 (25.0, 29.4)	<0.001
Liver stiffness (kPa)	5.7 (5.0, 7.9)	5.0 (4.8, 5.3)	6.85 (5.5, 9.5)	<0.001
CAP Score (dB/m)	262.0 (214.0, 315.0)	217.0 (203.0, 240.0)	290.5 (252.0, 330.0)	<0.001
AST (U/L)	30.6 (22.8, 53.5)	23.5 (18.8, 32.6)	44.5 (28.0, 110.6)	<0.001
ALT (U/L)	30.4 (22.4, 59.8)	23.9 (19.1, 32.2)	53.1 (29.1, 84.0)	<0.001
GGT (U/L)	34.1 (22.0, 65.5)	23.6 (18.8, 36.4)	59.6 (24.9, 86.5)	<0.001
A/G Ratio	1.40 (1.20, 1.50)	1.43 (1.25, 1.55)	1.37 (1.19, 1.48)	0.11

Factor	All samples (n = 182)	Control (n = 90)	MASLD (n = 92)	P-value*
CK-18 (pg/mL)	801.5 (548.2, 1101.8)	533.1 (408.7, 704.4)	1030.5 (836.4, 1352.9)	<0.001
Adropin (pg/mL)	329.6 (194.8, 455.4)	414.4 (276.9, 545.4)	245.0 (161.6, 309.4)	0.001
Irisin (pg/mL)	1375.6 (724.1, 1901.4)	1482.1 (826.4, 2004.6)	1290.2 (668.3, 1798.1)	0.17
Total protein (g/dL)	7.4 (6.9, 7.8)	7.4 (6.9, 7.8)	7.3 (6.9, 7.8)	0.78
Albumin (g/dL)	4.3 (4.0, 4.6)	4.3 (4.1, 4.6)	4.3 (4.0, 4.5)	0.62
Globulin (g/dL)	3.0 (2.6, 3.3)	3.0 (2.6, 3.2)	3.0 (2.6, 3.3)	0.79

*Values expressed as median (IQR). P values were calculated using Mann–Whitney U test. $P < 0.05$ considered statistically significant. ALT – Alanine aminotransferase; AST – Aspartate aminotransferase; GGT – Gamma-glutamyl transferase; ALP – Alkaline phosphatase; TB–Total bilirubin; A/G– Albumin to globulin ratio; CK-18– Cytokeratin 18.

The MASLD group showed significantly higher serum ALT (60.10 ± 36.58 U/L vs 29.75 ± 23.37 U/L, $p < 0.0001$) and AST (68.71 ± 50.63 U/L vs 28.03 ± 16.90 U/L, $p < 0.0001$) levels which indicated greater hepatocellular injury. The ALP levels were significantly higher in MASLD cases (73.96 ± 29.57 U/L vs 117.76 ± 67.42 U/L, $p < 0.0001$). The MASLD group showed significantly lower Adropin serum levels compared to controls (271.98 ± 121.61 pg/mL vs 451.63 ± 278.64 pg/mL, $p < 0.0001$) which indicates this peptide hormone may play a protective or regulatory function in liver pathology. The A/G ratio showed no significant statistical difference between the groups (1.37 ± 0.27 vs 1.43 ± 0.40, $p = 0.21$). Most parameters showed non-normal distribution so the Mann–Whitney U test determined statistical significance.

The analysis with Spearman's correlation examined the relationship between candidate biomarkers and MASLD severity clinical indicators such as liver enzymes and CAP steatosis grade and FibroScan kPa. The serum CK18 (CK18) showed a moderate positive correlation with CAP ($r = 0.666$) which indicates a strong relationship with hepatic steatosis. In the Figure 1 we have shown the distribution of Adropin, Irisin and Cytokeratin 18 levels in fibrosis and steatosis grades. The positive correlations between CK18 and ALT, AST, and GGT support its function as a marker of hepatocyte apoptosis and liver injury. The inverse relationship between Adropin and MASLD progression confirms previous research showing Adropin acts protectively against metabolic dysfunction.

Figure 1: Distribution of Adropin, Irisin and Cytokeratin 18 levels in fibrosis and steatosis grades.

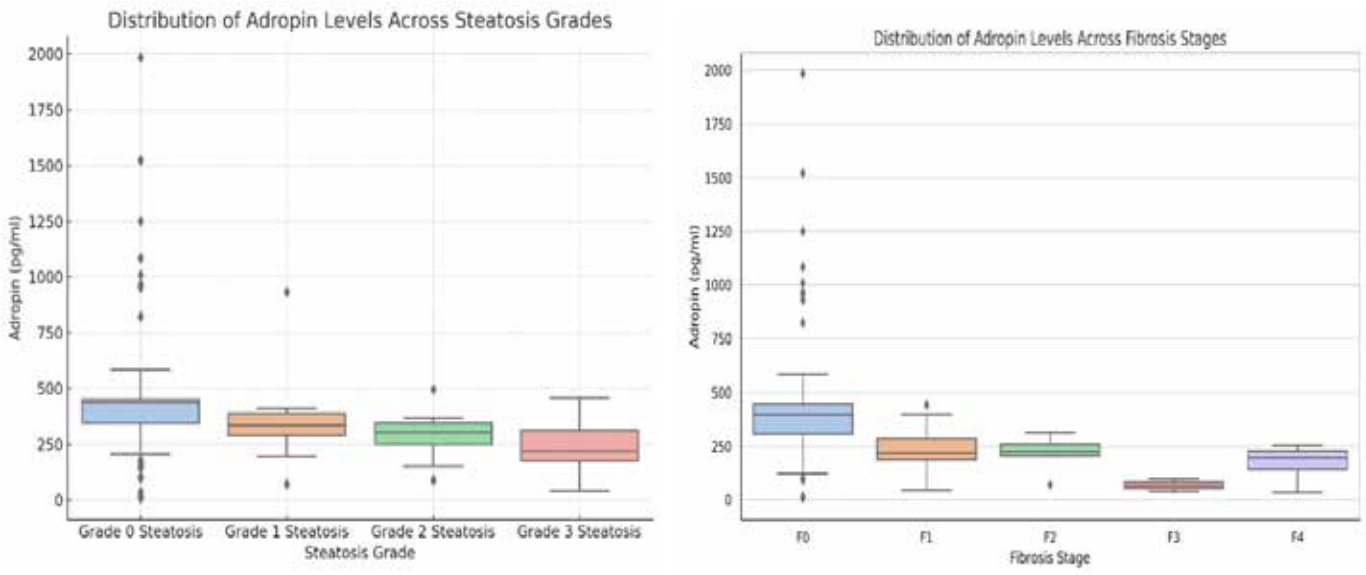

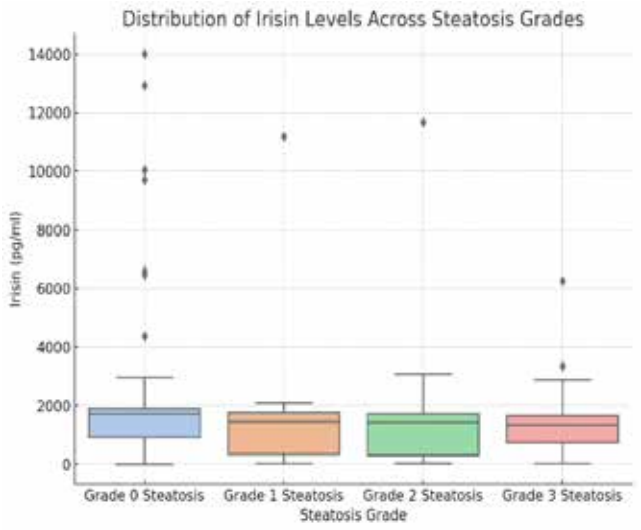

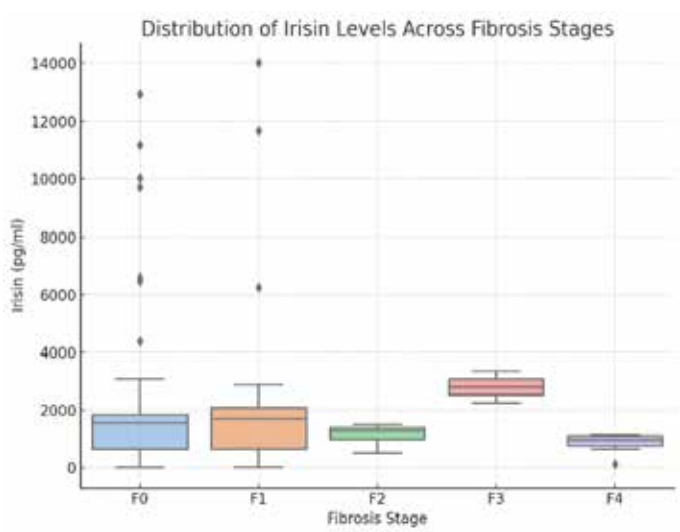

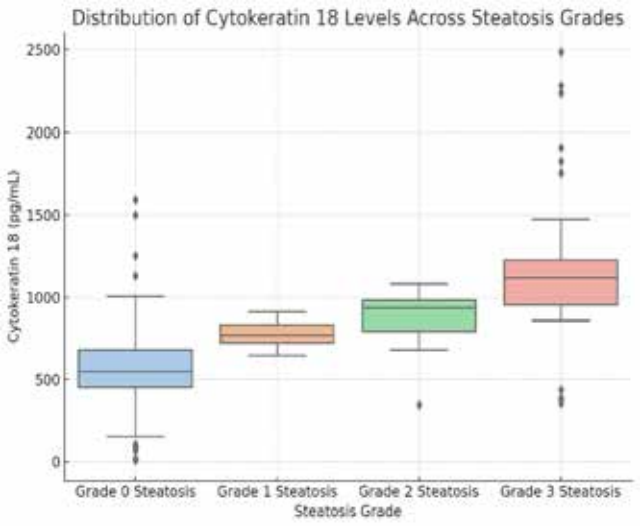

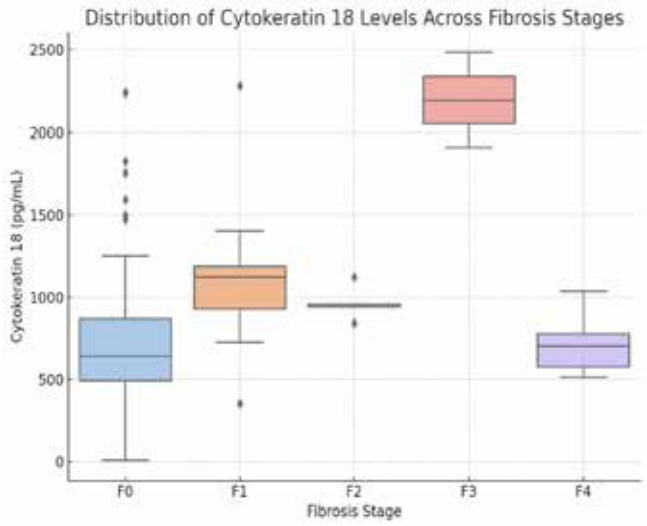

The MASLD patient group had lower Irisin levels but the results did not show a reliable relationship with CAP or FibroScan kPa values which suggests its function might be complicated or dependent on disease stages. ALT and AST liver transaminases showed a strong correlation with each other (r = 0.814) and also had moderate correlations with CK18 and GGT which indicated hepatocellular damage and enzyme leakage patterns.

The research evidence supports the use of CK18 and Adropin as diagnostic markers for steatosis and fibrosis but Irisin needs additional assessment in bigger or time-based studies. The diagnostic capabilities of serum biomarkers Adropin, Irisin, and Cytokeratin 18 (CK18) to distinguish MASLD patients from healthy controls were evaluated through receiver operating characteristic (ROC) curve analysis and multivariate logistic regression (Figure 2). Among the individual biomarkers, CK18 (CK18) demonstrated the highest diagnostic accuracy, with an area under the curve (AUC) of 0.87, indicating excellent ability to distinguish MASLD cases from controls. In contrast, Irisin exhibited limited discriminatory power (AUC = 0.384), and Adropin showed poor performance (AUC = 0.183) when assessed independently.

Figure 2: ROC curves comparing the diagnostic accuracy of Adropin, Irisin, Cytokeratin 18, and their combined model for detecting MASLD.

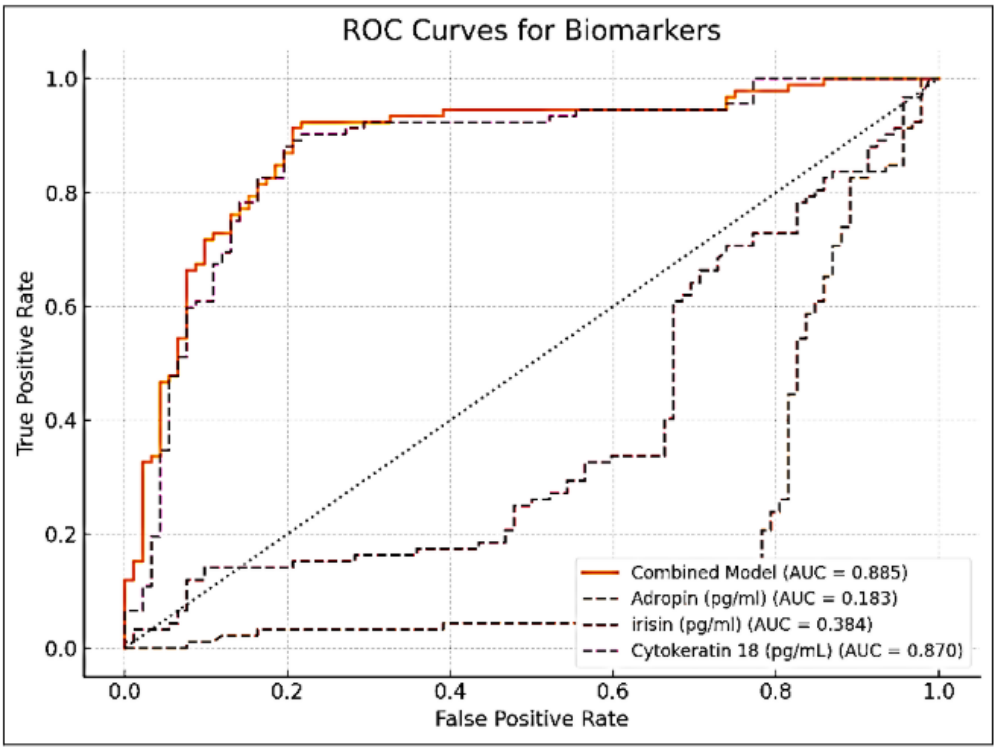

The orange line represents the combined model (AUC = 0.885), the black dashed line shows Adropin (AUC = 0.183), the brown dash-dot line indicates Irisin (AUC = 0.384), and the purple dotted line represents Cytokeratin 18 (AUC = 0.870). The diagonal grey line denotes the reference (AUC = 0.5).

A logistic regression model that included all three markers (Adropin, Irisin, and CK18) was used to evaluate the diagnostic performance when biomarkers were combined. The combined model yielded a superior AUC of 0.885, suggesting that multivariate assessment may provide added value in identifying MASLD, particularly in its earlier stages where traditional liver enzymes may remain within normal limits. The results indicate that CK18 functions as a strong single marker and demonstrate how biomarker panels could enhance non-invasive MASLD diagnosis.

The participants were further stratified by age and sex to explore differential patterns in MASLD. In the 31–60-year male subgroup, MASLD patients exhibited significantly higher levels of ALT, AST, GGT, and ALP compared to controls ($P < 0.05$ for all). A similar pattern was observed in females aged 31–60, particularly for ALT and AST. Interestingly, while ALT and AST levels were also elevated in younger males and females (18–30 years), the AST/ALT ratio remained close to 1 across all subgroups, without significant variation (Table 3). Total bilirubin was significantly elevated in younger males (18–30 years) with MASLD compared to controls ($P = 0.0136$), suggesting early cholestatic involvement in some individuals. Albumin levels remained stable across groups, with no significant difference observed, indicating preserved synthetic function in the majority of cases.

Table 3: Key liver function test (LFT) markers in MASLD - stratified by age and sex.

Age group	Gender/ Sex	Parameter	MASLD pg/mL	Control pg/mL	P-value
18–30 years	Male	ALT	80.0±9.3	26.2±6.37	0.0007
		AST	69.3±5.84	24.8±5.68	0.0004
		AST/ALT ratio	1.41±0.51	0.89±0.2	0.1711
		GGT	75.9±7.3	22.1±5.32	0.0006
		ALP	125.4±10.2	65.7±6.34	0.0075
		TB	1.0±0.2	0.61±0.2	0.0136
		Alb	3.79±0.5	4.4±0.96	0.1293
	Female	ALT	78.3±6.41	29.05±6.31	0.0021
		AST	55.9±8.3	21.9±5.21	0.0017
		AST/ALT ratio	0.88±0.24	0.95±0.27	0.4817
		GGT	65.5±5.3	22.85±9.32	0.0124
		ALP	121.0±9.56	73.2±8.68	0.007
		TB	1.21±0.3	0.75±0.2	0.0687
		Alb	4.0±0.42	4.37±2.12	0.3953
31–60 years	Male	ALT	49.1±5.8	23.35±6.85	0.0003
		AST	43.2±6.9	23.2±3.21	0.0003
		AST/ALT ratio	1.0±0.01	0.99±0.2	0.8748
		GGT	54.6±9.5	23.85±6.3	0.0019
		ALP	86.1±9.47	74.5±8.62	0.0363
		TB	0.93±0.2	0.75±0.99	0.0252
		Alb	4.39±0.8	4.44±0.95	0.8697
	Female	ALT	41.5±6.5	20.1±5.74	0.0635
		AST	40.9±8.52	21.5±6.5	0.0002
		AST/ALT ratio	1.16±0.36	1.06±0.8	0.8364
		GGT	54.66±13.2	29.45±5.2	0.0231
		ALP	112.5±17.2	78.35±9.5	0.0335
		TB	0.63±0.9	0.6±0.84	0.2149
		Alb	4.2±0.81	4.39±.091	0.0334
More than 60 years	Male	ALT	44.55±6.34	20.92±3.49	0.6095
		AST	63.55±9.35	24.1±3.53	0.3524
		AST/ALT ratio	2.06±0.8	1.47±0.62	0.3524
		GGT	19.0±1.02	17.43±1.34	0.9143
		ALP	112.25±9.06	53.15±8.35	0.1143
		TB	0.72±0.49	0.58±0.12	0.3923
		Alb	3.26±0.51	4.15±1.37	0.1344
	Female	ALT	41.4±6.34	45.5±6.92	0.8135
		AST	47.35±8.35	23.2±6.38	0.8032
		AST/ALT ratio	1.15±0.42	0.68±0.47	0.2001
		GGT	63.0±5.97	36.5±6.35	1.0235
		ALP	188.85±9.35	75.5±3.34	0.2021
		TB	0.58±0.28	0.5±0.02	0.8329
		Alb	3.71±0.34	4.1±0.63	0.835

*Values are expressed as mean ± SD. P values were calculated using Mann-Whitney U test. ALT–Alanine aminotransferase; AST– Aspartate aminotransferase; GGT– Gamma-glutamyl transferase; ALP– Alkaline phosphatase; TB– Total bilirubin; Alb– Albumin.

The research showed different metabolic dysregulation patterns in MASLD patients when lipid profile markers were analysed by age and sex subgroup. Males aged 31–60 with MASLD showed higher total cholesterol (201.6 vs 176.1 mg/dL; P = 0.0457), triglycerides (131.3 vs 95.5 mg/dL; P = 0.0240), and VLDL levels (33.5 vs 20.17 mg/dL; P = 0.0021) than controls without significant differences in HDL and LDL levels. The lipid profile results for females in this age group showed that triglycerides (146.5 vs 96.5 mg/dL; P = 0.0141) and VLDL (30.4 vs 21.1 mg/dL; P = 0.0193) were higher than controls but HDL and LDL levels were similar.

Young participants aged 18–30 years with MASLD showed increased triglycerides and VLDL levels but the differences became statistically significant only in males (TG: 140.0 vs 87.0 mg/dL; P = 0.0189, VLDL: 33.6 vs 18.5 mg/dL; P = 0.0157). The VLDL levels of females in this group were higher than other lipid parameters but did not show significant variation. More than 60 years age group showed no statistically significant differences between MASLD and controls for any lipid markers which may be due to metabolic blunting with age or limited subgroup size (Table 4).

Table 4: Lipid profile comparison in MASLD - stratified by age and sex.

Age group	Gender/ Sex	Parameter (mg/dL)	Patient with MASLD	Control	P-value
18–30 years	Male	TC	200.7±15.2	168.11±11.2	0.0028
		TG	165.0±12.4	95.0±9.2	0.0225
		HDL	36.0±6.52	45.0±5.2	0.0649
		LDL	114.94±12.4	98.9±6.3	0.0062
		VLDL	36.24±5.3	23.2±7.2	0.1585
	Female	TC	210.0±15.32	176.96±8.2	0.044
		TG	150.0±14.23	110.65±9.7	0.0553
		HDL	35.4±8.37	41.05±8.2	0.1387
		LDL	110.5±5.38	99.35±7.15	0.1147
		VLDL	36.0±6.32	28.28±6.25	0.1264
31–60 years	Male	TC	201.6±17.25	176.1±10.9	0.0457
		TG	131.3±13.2	95.5±5.32	0.0241
		HDL	42.95±8.3	43.85±9.2	0.659
		LDL	117.14±9.35	107.65±11.5	0.1942
		VLDL	33.5±9.2	20.17±6.3	0.0021
	Female	TC	219.52±12.3	167.52±11.9	0.003
		TG	143.0±15.3	89.38±5.3	0.0279
		HDL	42.0±6.35	44.3±6.23	0.6618
		LDL	126.98±6.5	99.35±11.2	0.0003
		VLDL	25.94±5.3	18.37±5.2	0.1143
More than 60	Male	TC	216.94±22.3	167.06±12.2	0.3524
		TG	105.8±16.3	97.45±9.2	0.7619
		HDL	41.2±10.85	36.53±4.5	0.4762
		LDL	105.02±11.25	109.52±6.5	0.9143
		VLDL	22.4±9.3	29.15±6.7	0.7619
	Female	TC	158.55±10.2	154.52±9.5	0.9412
		TG	184.33±13.45	98.6±8.7	0.2136
		HDL	35.96±8.3	42.56±5.8	0.4012
		LDL	85.72±7.9	88.5±6.2	0.8231
		VLDL	36.88±6.35	32.3±5.2	0.8027

*Values are expressed as medians. P-values calculated using Mann–Whitney U test. Bold values indicate statistically significant differences (P < 0.05). TC– Total cholesterol; TG– Triglycerides; HDL– High-density lipoprotein; LD–Low-density lipoprotein; VLDL– Very-low-density lipoprotein.

The research examined BMI together with body weight and height and hip-to-waist ratio in specific age and sex groups to determine their association with MASLD. The BMI and weight measurements of 31–60-year-old male MASLD patients were significantly higher than those of controls (26.21 vs 24.58 kg/m² and 78.0 vs 73.5 kg respectively; P = 0.0027 and P = 0.0113). The BMI measurements of female patients with MASLD were substantially higher than controls in this age group (28.31 vs 24.28 kg/m²; P < 0.0001) which indicated central adiposity as a primary risk factor in this specific age group. The BMI and body weight measurements of MASLD patients within the 18–30-year age group demonstrated significant increases when compared to controls (P < 0.05) yet these differences were not as significant as those found in the older age group. The research demonstrates how small amounts of body fat accumulation during young adulthood can lead to liver fat deposition which results in the development of MASLD. FibroScan score and CAP score of the different age group are shown in the Figure 3.

Figure 3: FibroScan-based fibrosis and steatosis scores in MASLD - stratified by age and gender.

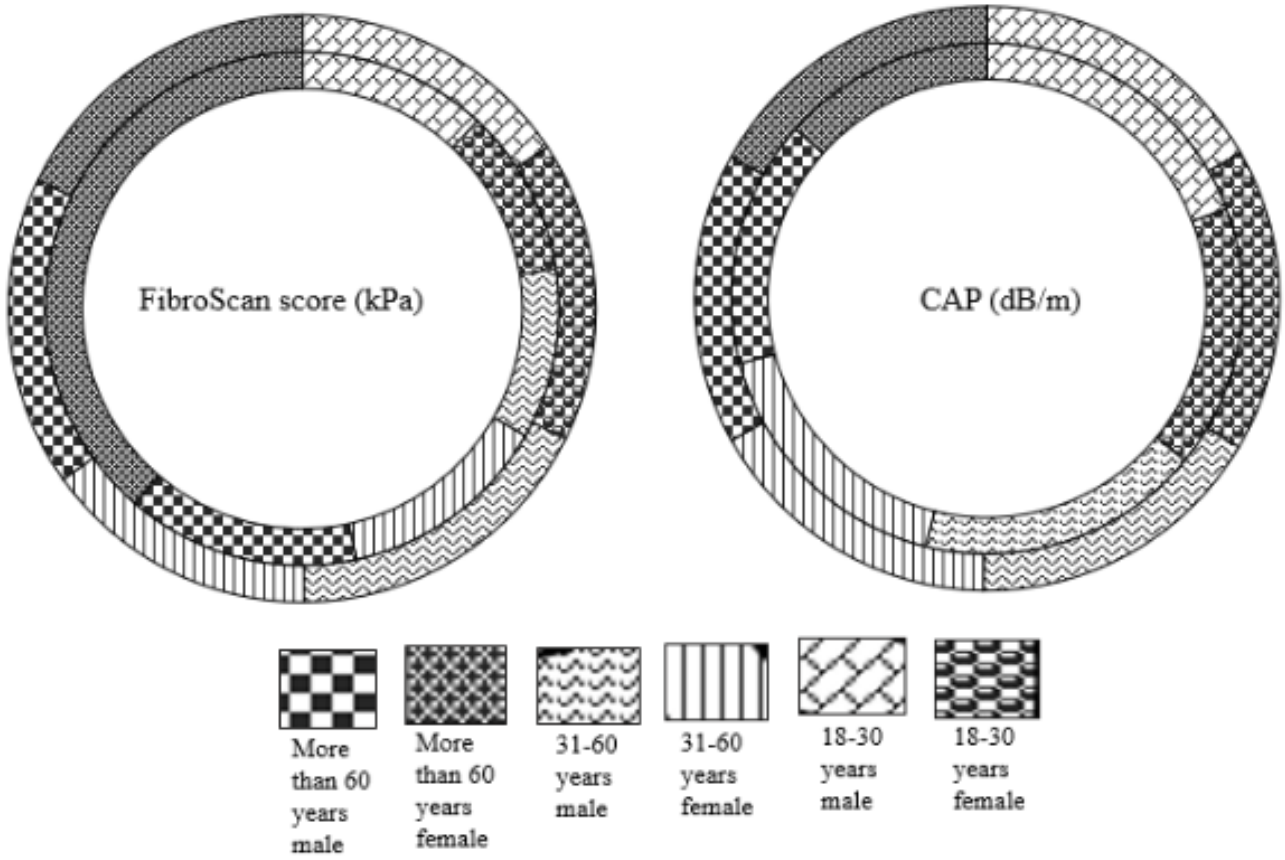

The assessment of liver stiffness (fibrosis) and steatosis (fat accumulation) was done using FibroScan and was stratified by age and sex to determine the patterns of disease severity in MASLD. The most significant differences were observed in the 31–60-year group, where both males and females with MASLD had significantly higher fibrosis scores (6.10 vs 5.15 kPa in males, P = 0.0021; 7.60 vs 4.45 kPa in females, P = 0.0002) and higher CAP scores indicating steatosis (298.0 vs 217.0 dB/m in males, 284.0 vs 217.5 dB/m in females; both P < 0.0001).

Among participants aged 18–30 years, MASLD patients also had significantly higher liver stiffness (6.80 vs 4.60 kPa in males, P < 0.0001; 6.28 vs 4.80 kPa in females, P = 0.0128), and higher CAP scores, although the magnitude of difference was less than in the older group. These findings are noteworthy, as they indicate that fibrotic and steatotic changes are already present in younger individuals with MASLD, suggesting early onset of hepatic involvement. On the other hand, in the >60-year age group, there were no statistically significant differences in fibrosis or CAP values between MASLD cases and controls. This may be due to age-related changes that diminish disease discrimination or smaller sample size in this subgroup.

Therefore, these results confirm the progressive nature of fibrosis and steatosis with age in MASLD and the diagnostic usefulness of FibroScan as a non-invasive tool to assess the stage of liver involvement, especially in early-to mid-adult populations. The study analyzed biomarkers related to

metabolic regulation and hepatocyte apoptosis through age and sex stratification to determine their diagnostic value across the MASLD spectrum. The 31–60-year age bracket showed MASLD patients of both sexes to have significantly lower Adropin levels and extremely elevated CK-18 levels when compared to controls ($P < 0.0001$ in all cases) which indicated severe metabolic and apoptotic disturbances in this population. The 18–30-year subgroup showed similar patterns to older age groups with MASLD patients displaying reduced Adropin levels compared to controls ($P = 0.0001$ in males and $P = 0.0002$ in females) and elevated CK-18 levels ($P = 0.0004$ in males and $P = 0.0035$ in females) at lower levels than observed in older participants. Biomarker disturbances appear to emerge in young MASLD patients as they indicate the beginning of their disease. The >60-year-old participants showed minimal and non-significant variations between MASLD patients and controls regarding CK-18 and Adropin levels. The smaller study population and metabolic changes that accompany aging might explain these results. The 31–60-year age bracket showed statistically significant lower Irisin levels in MASLD patients compared to controls. The study confirms that Adropin and CK-18 serve as effective early biomarkers for MASLD especially among younger and middle-aged adults while suggesting Irisin has a limited influence on disease mechanisms (Table 5).

Table 5: Biomarker levels in MASLD - stratified by age and sex.

Group	Gender	Parameter (pg/ml)	Patient with MASLD	Control	P-value
18–30 years	Male	Adropin	297.46±16.2	427.81±14.5	0.0037
		Irisin	1422.44±32.2	1768.62±21.8	0.6186
		Cytokeratin 18	993.34±21.48	496.45±15.4	0.0125
	Female	Adropin	257.76±18.2	433.34±13.9	0.0108
		Irisin	1311.03±32.8	1573.59±19.8	0.3565
		Cytokeratin 18	959.63±21.5	549.42±12.2	0.0005
31–60 years	Male	Adropin	308.28±19.7	439.96±11.7	0.0021
		Irisin	1405.57±32.8	1759.76±28.5	0.0278
		Cytokeratin 18	929.79±24.2	541.3±12.9	0.0102
	Female	Adropin	267.67±20.1	442.09±12.5	0.0201
		Irisin	1403.79±26.6	1789.16±19.8	0.0119
		Cytokeratin 18	942.3±21.5	526.65±11.5	0.0098
More than 60 years	Male	Adropin	266.58±20.7	428.21±9.54	0.3524
		Irisin	1505.22±27.6	1743.64±14.5	0.9143
		Cytokeratin 18	695.35±22.4	548.47±11.5	0.4762
	Female	Adropin	275.76±15.2	258.2±12.7	0.8102
		Irisin	1642.41±28.6	125.7±9.6	0.4032
		Cytokeratin 18	744.56±23.4	950.1±10.61	0.8087

*Values are expressed as medians. P-values calculated using Mann–Whitney U test.

The table 6 and figure 4 allows for insights into how Adropin and Irisin concentrations correlate with steatosis and fibrosis. Higher concentrations of Irisin in certain groups (especially in F1 Grade 3 Steatosis) may indicate potential metabolic changes or responses to increased fat accumulation in the liver.

Table 6: Adropin and Irisin concentrations correlate with steatosis and fibrosis.

Fibrosis stage	Steatosis grade	Count of patients	Mean Adropin concentration (pg/ml)	
F0	Normal (no steatosis)	45	508.98±21.2	1085.13±34.67
F0	Grade 1 Steatosis	10	224.25±15.4	205.21±15.3
F0	Grade 2 Steatosis	4	162.17±12.3	52.81±10.55
F1	Grade 1 Steatosis	4	294.29±18.95	3010.64±42.85
F1	Grade 2 Steatosis	5	332.66±21.97	185.32±10.2
F1	Grade 3 Steatosis	5	319.82±24.35	7156.07±56.95
F2	Grade 1 Steatosis	2	77.41±9.35	2096.30±24.3
F3	Grade 3 Steatosis	3	186.41±10.52	1629.09±19.35
F4	Grade 0 Steatosis	1	33.95±6.35	114.61±12.54

Figure 4: Adropin and Irisin concentrations with steatosis grade and fibrosis stages.

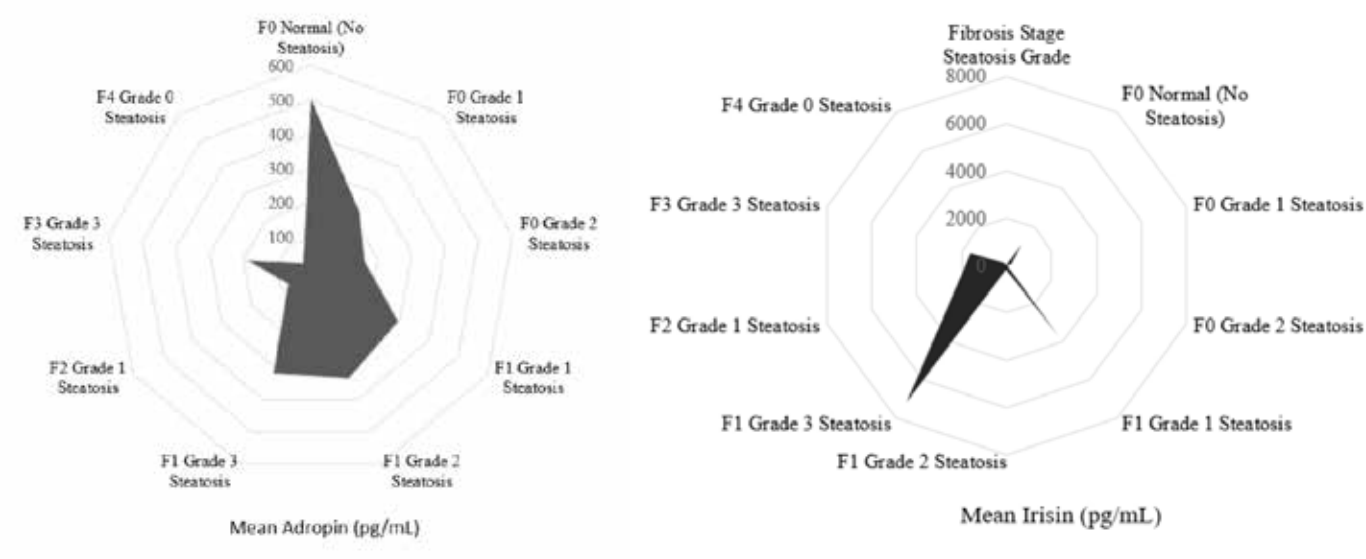

Discussion

This research study investigated the diagnostic and staging abilities of three circulating biomarkers - Adropin, Irisin, and CK18 - in patients suffering from MASLD. MASLD represents a growing global public health concern, characterized by the accumulation of fat in the liver in the absence of excessive alcohol consumption [34-37]. Its progression can lead to more severe liver conditions, including MASH, fibrosis, and eventually liver cirrhosis or liver cancer [38, 39]. Therefore, accurate diagnosis and staging of MASLD are essential for timely management and treatment. To assess these biomarkers, the researchers employed recognized reference standards, namely Controlled Attenuation Parameter (CAP) and FibroScan, which are widely used for measuring liver fat content and fibrosis stage non-invasively [39, 40]. This method allows for the evaluation of liver conditions without the need for invasive liver biopsies, which can be risky and uncomfortable for patients.

The study's primary focus was on understanding how well each biomarker could identify the presence and severity of MASLD, as well as their potential role in tracking the disease's progression. The results of the study provided insights into the performance of each biomarker. Among the three biomarkers, CK18 stood out for its diagnostic capabilities [41, 42]. The findings indicated that CK18 demonstrated a strong discriminatory power for identifying MASLD and also for determining its progression. The biomarker revealed significant correlations with various parameters, including the grade of steatosis (the amount of fat in the liver) and the stage of fibrosis (the level of scarring in the liver). Additionally, CK18 levels were found to correlate well with liver enzyme levels, which are often indicative of liver inflammation and damage [43-45]. This suggests that CK18 could potentially be a reliable biomarker for clinicians, allowing for improved diagnosis and monitoring of MASLD in patients [46]. The second biomarker, Adropin, displayed a more complex role in the context of MASLD [47-50]. While its diagnostic accuracy as a standalone marker was limited - meaning it may not be sufficiently reliable on its own - it exhibited a negative correlation with the severity of MASLD. This suggests that lower levels of Adropin might be associated with more severe forms of the disease. Although Adropin was not robust enough to be used independently, its potential as a complementary biomarker became apparent. When combined with other markers, Adropin may enhance the overall diagnostic accuracy for MASLD, making it a valuable addition in the context of multimodal approaches to biomarker assessment [51].

The third biomarker, Irisin, showed inconsistent patterns in its relationship with MASLD disease parameters [52]. This inconsistency raises doubts about its utility as a reliable standalone biomarker for MASLD. Unlike CK18, which provided clear correlations with disease severity, Irisin's variability limits its effectiveness in both diagnosing and staging MASLD. As such, while it may have potential, further investigation into its role in MASLD is necessary before it can be considered a reliable biomarker. One of the study's significant findings was the advantage of employing a multimodal approach to biomarker assessment. The logistic regression model that included all three biomarkers - CK18, Adropin, and Irisin - resulted in improved diagnostic accuracy for MASLD. This highlights the importance of using multiple biomarkers together when assessing patients. By employing a comprehensive approach that leverages the strengths of various biomarkers, clinicians may be better equipped to diagnose and stage MASLD effectively [53-55]. The clinical implications of these findings are noteworthy. While CK18 appeared to be the most promising biomarker for both detection and staging of MASLD, there are opportunities to enhance diagnostic

accuracy by incorporating metabolic markers like Adropin into clinical evaluations. The complementary nature of these biomarkers may lead to a more thorough understanding of an individual's liver health status, enabling more informed clinical decisions regarding the management of MASLD.

While the results are promising, the researchers highlighted the need for additional studies to validate these findings further. Future research should involve larger and more diverse patient populations, as well as longer follow-up periods. This would ensure that the biomarkers' performance is consistent across different demographic and clinical contexts [56, 57]. Through such efforts, it will be possible to establish clinical reference values for CK18, Adropin, Irisin, and their combinations, thereby improving their utility in everyday clinical practice.

Ultimately, the research underscores the critical need for reliable biomarkers in the diagnosis and management of MASLD. Identifying patients at risk for progression to more severe liver disease is essential for implementing preventative strategies and therapeutic interventions [58, 59]. The study contributes to the evolving landscape of liver disease diagnostics, highlighting biomarker research's importance in enhancing patient outcomes and advancing therapeutic approaches in liver health [60-63]. In inference, the research into Adropin, Irisin, and CK18 provides valuable insights into biomarkers for MASLD. With CK18 showing the most promise for diagnosing and staging MASLD, supplemented by Adropin's potential, the combination of these biomarkers through a multimodal approach represents a significant advance in the assessment of this increasingly prevalent condition. Continued investigation in this area will be vital for refining diagnostic tools and improving strategies for managing MASLD in diverse patient populations [64-70].

The study contains a number of drawbacks. First off, the results may not be as broadly applicable to a variety of populations due to the limited sample size. Second, evaluation of longitudinal changes and causal links between biomarkers and disease development is not possible due to the cross-sectional methodology. Furthermore, even while non-invasive techniques like FibroScan and CAP are safer, they might not fully capture the histological features that can be obtained through biopsy. Inconsistent relationships and variations in Irisin levels also point to possible measurement errors or biological variability. Lastly, a thorough grasp of biomarker roles is restricted by the absence of broad demographic representation and the scant investigation of underlying molecular mechanisms, underscoring the necessity of larger, multicenter, and mechanistic studies in subsequent research.

Future direction

Large-scale prospective studies could be the main focus of future research on Irisin and Adropin to determine their predictive potential for cardiovascular and metabolic disorders. The therapeutic potential of these peptides may be clarified by interventional trials that investigate the effects of altering them with pharmacological treatments or lifestyle modifications. Furthermore, molecular mechanistic research is necessary to comprehend their functions in cellular signaling cascades, inflammation, and energy management. Investigating how genetic differences affect their activity or levels may provide information about a person's sensitivity. Targeted therapies and customized medicine tactics may be made possible by combining omics methodologies and cutting-edge imaging tools to better understand their roles in tissue-specific situations. Furthermore, examining how they interact with hormones and other metabolic regulators may help us better understand their integrative functions. Translational applications will be improved by researching their impact in a variety of populations and disease situations. All things considered, thorough investigation will be essential to maximizing the therapeutic and diagnostic potential of Adropin and Irisin.

Conclusion

This research aimed to evaluate the diagnostic and staging capabilities of three circulating biomarkers - Adropin, Irisin, and CK18 - in patients with Metabolic Dysfunction-Associated Steatotic Liver Disease (MASLD), using Controlled Attenuation Parameter (CAP) and FibroScan as reference standards for comparison. The study yielded significant insights into the effectiveness of these biomarkers in identifying MASLD and assessing its progression. The results indicated that CK18 demonstrated a robust discriminatory power, effectively distinguishing MASLD patients from those without liver disease. This was further supported by its significant correlations with steatosis grade, fibrosis stage, and liver enzyme levels, highlighting CK18's reliability as a diagnostic tool. Its strong performance in identifying disease severity makes it a promising candidate for clinical application in the management of MASLD.

In contrast, the diagnostic utility of Adropin as a standalone marker was somewhat limited. However, its negative correlation with MASLD severity suggests it may have potential as a complementary biomarker, especially when used in conjunction with other diagnostic tools. The combined approach could enhance overall diagnostic accuracy, making the identification of MASLD more effective. The role of Irisin as a standalone biomarker remains uncertain, as inconsistent patterns were observed with disease parameters, which raises questions about its utility in MASLD diagnostics. Importantly, the study employed a logistic regression model that integrated all three biomarkers, demonstrating improved diagnostic accuracy for MASLD assessment through a multimodal biomarker approach. While CK18 exhibits considerable potential for clinical application in liver disease diagnostics, supplementing it with metabolic markers like Adropin may further enhance detection and staging accuracy. Future research is essential to confirm these findings, ideally involving larger and more diverse patient groups, alongside extended follow-up

periods to establish comprehensive clinical reference values for these biomarkers in the context of MASLD. This research serves as a foundational step towards optimizing the diagnostic framework for liver disease management.

Ethics and consent to participate

Ethical clearance was obtained from the Institute Ethics Committee (IHEC/SR/2024/Apr/10 dated: 23/04/2024) of AIIMS Bhopal, India. and all subjects gave their informed consent before participation. From the Department of Medicine, AIIMS Bhopal, MASLD patients were recruited based on FibroScan to participate in the study, after fulfilling the inclusion and exclusion criteria and after obtaining consent. All studies involving human subjects must indicate that they are in compliance with the ethical principles for medical research involving human subjects, in accordance with the Declaration of Helsinki.

Consent for publication

All participants gave their informed consent before participation from the Department of Medicine, AIIMS Bhopal after fulfilling the inclusion and exclusion criteria and after obtaining consent.

Declaration of conflict of interests

No.

CRediT authorship contribution statement

DR and SM conceptualized the manuscript. DR, ZS, SR and SKR wrote the first draft. DR and SKR drew the figures. SKR, AK, JRK and SM edited it and given valuable inputs. All the authors agreed and approved the final manuscript.

Author's Disclosures

The authors declare no conflicts of interest related to this work. Financial support was received from AIIMS Bhopal, India, Intramural fund (Reference Number: IHEC/SR/2024/111 Date: 01/02/2024). All authors have approved the manuscript and agree to be accountable for all aspects of the work.

Funding

AIIMS Bhopal, India, Intramural fund (Reference Number: IHEC/SR/2024/111 Date: 01/02/2024).

Acknowledgments

None.

References

1. Byrne CD, Targher G. NAFLD: A multisystem disease. J Hepatol. 2015;62(1):S47–S64.
2. Sahu P, Chhabra P, Mehendale AM. A Comprehensive Review on Non-Alcoholic Fatty Liver Disease. Cureus. 2023;15(12):e50159.
3. Fracanzani AL, Valenti L, Bugianesi E, et al. Risk of severe liver disease in nonalcoholic fatty liver disease with normal aminotransferase levels: A role for insulin resistance and diabetes. Hepatology. 2008;48(3):792–799.
4. Fu J, Shin S. Dietary patterns and risk of non-alcoholic fatty liver disease in Korean adults: a prospective cohort study. BMJ Open. 2023;13(1):e065198.
5. Riazi K, Azhari H, Charette JH, et al. The prevalence and incidence of NAFLD worldwide: a systematic review and meta-analysis. Lancet Gastroenterol Hepatol. 2022;7(9):851-861.
6. Kumari S, Shukla S, Acharya S. Childhood Obesity: Prevalence and Prevention in Modern Society. Cureus. 2022;14(11):e31640.
7. Caussy C, Aubin A, Loomba R. The Relationship Between Type 2 Diabetes, NAFLD, and Cardiovascular Risk. Curr Diab Rep. 2021;21(5):15.
8. Shang Y, Nasr P, Widman L, Hagström H. Risk of cardiovascular disease and loss in life expectancy in NAFLD. Hepatology. 2022;76(5):1495-1505.
9. Targher G, Chonchol M, Bertolini L, et al. Increased risk of CKD among type 2 diabetics with nonalcoholic fatty liver disease. J Am Soc Nephrol. 2008;19(8):1564-1570.
10. Fabbrini E, Sullivan S, Klein S. Obesity and nonalcoholic fatty liver disease: biochemical, metabolic, and clinical implications. Hepatology. 2010;51(2):679-689.
11. Zarghamravanbakhsh P, Frenkel M, Poretsky L. Metabolic causes and consequences of nonalcoholic fatty liver disease (NAFLD). Metabol Open. 2021;12:100149.
12. Wattacheril J, Sanyal AJ. Lean NAFLD: An Underrecognized Outlier. Curr Hepatol Rep. 2016;15(2):134-139.
13. Ziamanesh F, Mohammadi M, Ebrahimpour S, et al. Unraveling the link between insulin resistance and Non-alcoholic fatty liver disease (or metabolic dysfunction-associated steatotic liver disease): A Narrative Review. J Diabetes Metab Disord. 2023;22(2):1083-1094.
14. Fujii H, Kawada N; Japan Study Group Of NAFLD Jsg-NAFLD. The Role of Insulin Resistance and Diabetes in Nonalcoholic Fatty Liver Disease. Int J Mol Sci. 2020;21(11):3863.
15. Gastaldelli A, Cusi K. From NASH to diabetes and from diabetes to NASH: Mechanisms and treatment options. JHEP Rep. 2019;1(4):312-328.
16. Rinaldi L, Pafundi PC, Galiero R, et al. Mechanisms of Non-Alcoholic Fatty Liver Disease in the Metabolic Syndrome. A Narrative Review. Antioxidants (Basel). 2021;10(2):270.
17. Kelley CE, Brown AJ, Diehl AM, Setji TL. Review of nonalcoholic fatty liver disease in women with polycystic ovary syndrome. World J Gastroenterol. 2014;20(39):14172-14184.
18. Barbonetti A, Caterina Vassallo MR, Cotugno M, Felzani G, Francavilla S, Francavilla F. Low testosterone and non-alcoholic fatty liver disease: Evidence for their

independent association in men with chronic spinal cord injury. J Spinal Cord Med. 2016;39(4):443-449.
19. Sinha RA, Singh BK, Yen PM. Direct effects of thyroid hormones on hepatic lipid metabolism. Nat Rev Endocrinol. 2018;14(5):259-269.
20. Kupčová V, Fedelešová M, Bulas J, Kozmonová P, Turecký L. Overview of the Pathogenesis, Genetic, and Non-Invasive Clinical, Biochemical, and Scoring Methods in the Assessment of NAFLD. Int J Environ Res Public Health. 2019;16(19):3570.
21. Gîlcă-Blanariu GE, Budur DS, Mitrică DE, Gologan E, Timofte O, Bălan GG, Olteanu VA, Ştefănescu G. Advances in Noninvasive Biomarkers for Nonalcoholic Fatty Liver Disease. Metabolites. 2023;13(11):1115.
22. Xuan Y, Wu D, Zhang Q, et al. Elevated ALT/AST ratio as a marker for NAFLD risk and severity: insights from a cross-sectional analysis in the United States. Front Endocrinol. 2024;15:1457598.
23. Bozic D, Podrug K, Mikolasevic I, Grgurevic I. Ultrasound Methods for the Assessment of Liver Steatosis: A Critical Appraisal. Diagnostics (Basel). 2022;12(10):2287.
24. Zhang YN, Fowler KJ, Hamilton G, et al. Liver fat imaging-a clinical overview of ultrasound, CT, and MR imaging. Br J Radiol. 2018;91(1089):20170959.
25. Aydin S. Three new players in energy regulation: preptin, adropin and irisin. Peptides. 2014;56:94-110.
26. Rooban S, Arul Senghor KA, Vinodhini VM, Kumar JS. Adropin: A crucial regulator of cardiovascular health and metabolic balance. Metabol Open. 2024;23:100299.
27. Li N, Xie G, Zhou B, et al. Serum Adropin as a Potential Biomarker for Predicting the Development of Type 2 Diabetes Mellitus in Individuals With Metabolic Dysfunction-Associated Fatty Liver Disease. Front Physiol. 2021;12:696163.
28. Kosmalski M, Drzewoski J, Szymczak-Pajor I, et al. Irisin Is Related to Non-Alcoholic Fatty Liver Disease (NAFLD). Biomedicines. 2022;10(9):2253.
29. Feldstein AE, Wieckowska A, Lopez AR, et al. Cytokeratin-18 fragment levels as noninvasive biomarkers for nonalcoholic steatohepatitis: a multicenter validation study. Hepatology. 2009;50(4):1072-1078.
30. Cao W, Zhao C, Shen C, Wang Y. Cytokeratin 18, alanine aminotransferase, platelets and triglycerides predict the presence of nonalcoholic steatohepatitis. PLoS One. 2013;8(12):e82092.
31. Diab DL, Yerian L, Schauer P, et al. Cytokeratin 18 fragment levels as a noninvasive biomarker for nonalcoholic steatohepatitis in bariatric surgery patients. Clin Gastroenterol Hepatol. 2008;6(11):1249-1254.
32. Darweesh SK, AbdElAziz RA, Abd-ElFatah DS, et al. Serum cytokeratin-18 and its relation to liver fibrosis and steatosis diagnosed by FibroScan and controlled attenuation parameter in nonalcoholic fatty liver disease and hepatitis C virus patients. Eur J Gastroenterol Hepatol. 2019;31(5):633-641.
33. Kałużna M, Pawlaczyk K, Schwermer K, et al. Adropin and irisin: New biomarkers of cardiac status in patients with end-stage renal disease? A preliminary study. Adv Clin Exp Med. 2019;28(3):347-353.
34. Gerges SH, Wahdan SA, Elsherbiny DA, El-Demerdash E. Non-alcoholic fatty liver disease: An overview of risk factors, pathophysiological mechanisms, diagnostic procedures, and therapeutic interventions. Life Sci. 2021;271:119220.
35. Kan C, Zhang K, Wang Y, Zhang X, Liu C, Ma Y, Hou N, Huang N, Han F, Sun X. Global burden and future trends of metabolic dysfunction-associated Steatotic liver disease: 1990-2021 to 2045. Ann Hepatol. 2025;30(2):101898.
36. Soto-Angona Ó, Anmella G, Valdés-Florido MJ, et al. Non-alcoholic fatty liver disease (NAFLD) as a neglected metabolic companion of psychiatric disorders: common pathways and future approaches. BMC Med. 2020;18(1):261.
37. Juanola O, Martínez-López S, Francés R, Gómez-Hurtado I. Non-Alcoholic Fatty Liver Disease: Metabolic, Genetic, Epigenetic and Environmental Risk Factors. Int J Environ Res Public Health. 2021;18(10):5227.
38. Berardo C, Di Pasqua LG, Cagna M, et al. Nonalcoholic Fatty Liver Disease and Non-Alcoholic Steatohepatitis: Current Issues and Future Perspectives in Preclinical and Clinical Research. Int J Mol Sci. 2020;21(24):9646.
39. Eddowes PJ, Sasso M, Allison M, et al. Accuracy of FibroScan Controlled Attenuation Parameter and Liver Stiffness Measurement in Assessing Steatosis and Fibrosis in Patients With Nonalcoholic Fatty Liver Disease. Gastroenterology. 2019;156(6):1717-1730.
40. Yu XY, Song XX, Tong YL, Wu LY, Song ZY. Usefulness of controlled attenuation parameter and liver stiffness measurement for detecting increased arterial stiffness in asymptomatic populations in China. Medicine (Baltimore). 2020;99(48):e23360.
41. Albhaisi S, Sanyal A. Recent advances in understanding and managing non-alcoholic fatty liver disease. F1000Res. 2018;7:F1000 Faculty Rev-720.
42. Zhang H, Rios RS, Boursier J, et al. Hepatocyte apoptosis fragment product cytokeratin-18 M30 level and non-alcoholic steatohepatitis risk diagnosis: an international registry study. Chin Med J (Engl). 2023;136(3):341-350.
43. Goralska J, Razny U, Gruca A, et al. Plasma Cytokeratin-18 Fragment Level Reflects the Metabolic Phenotype in Obesity. Biomolecules. 2023;13(4):675.
44. Korver S, Bowen J, Pearson K, et al. The application of cytokeratin-18 as a biomarker for drug-induced liver injury. Arch Toxicol. 2021;95(11):3435-3448.
45. Kawanaka M, Kamada Y, Takahashi H, et al. Serum Cytokeratin 18 Fragment Is an Indicator for Treating Metabolic Dysfunction-Associated Steatotic Liver Disease. Gastro Hep Adv. 2024;3(8):1120-1128.

46. Yilmaz Y, Eren F. Cytokeratin-18 fragments as biomarkers for liver diseases: Applications and limitations. World J Gastroenterol. 2009;15(34):4390–4394.
47. Chen X, Xue H, Fang W, et al. Adropin protects against liver injury in nonalcoholic steatohepatitis via the Nrf2 mediated antioxidant capacity. Redox Biol. 2019;21:101068.
48. Alzoughool F, Abdelqader R, Abumweis S, et al. Evaluation of adropin level and insulin resistance in non-alcoholic fatty liver patients: a meta-analysis of studies. Eur Rev Med Pharmacol Sci. 2024;28(21):4507-4514.
49. Kutlu O, Altun Ö, Dikker O, et al. Serum Adropin Levels Are Reduced in Adult Patients with Nonalcoholic Fatty Liver Disease. Med Princ Pract. 2019;28(5):463-469.
50. Chen L, Lu J, Hu J, et al. Unveiling the multifaceted role of adropin in various diseases (Review). Int J Mol Med. 2024;54(4):90.
51. Gîlcă-Blanariu GE, Budur DS, Mitrică DE, et al. Advances in Noninvasive Biomarkers for Nonalcoholic Fatty Liver Disease. Metabolites. 2023;13(11):1115.
52. Kosmalski M, Drzewoski J, Szymczak-Pajor I, et al. Irisin Is Related to Non-Alcoholic Fatty Liver Disease (NAFLD). Biomedicines. 2022;10(9):2253.
53. Ajmera V, Loomba R. Imaging biomarkers of NAFLD, NASH, and fibrosis. Mol Metab. 2021;50:101167.
54. Xu Q, Feng M, Ren Y, et al. From NAFLD to HCC: Advances in noninvasive diagnosis. Biomed Pharmacother. 2023;165:115028.
55. Abdelhameed F, Kite C, Lagojda L, et al. Non-invasive Scores and Serum Biomarkers for Fatty Liver in the Era of Metabolic Dysfunction-associated Steatotic Liver Disease (MASLD): A Comprehensive Review From NAFLD to MASLD and MASLD. Curr Obes Rep. 2024;13(3):510-531.
56. Ou FS, Michiels S, Shyr Y, et al. Biomarker Discovery and Validation: Statistical Considerations. J Thorac Oncol. 2021;16(4):537-545.
57. Perlis RH. Translating biomarkers to clinical practice. Mol Psychiatry. 2011;16(11):1076-1087.
58. Riley TR, Smith JP. Preventive care in chronic liver disease. J Gen Intern Med. 1999;14(11):699-704.
59. Pryke R, Guha IN. Time to focus on chronic liver diseases in the community: A review of primary care hepatology tools, pathways of care and reimbursement mechanisms. J Hepatol. 2023;78(3):663-671.
60. Wazir H, Abid M, Essani B, et al. Diagnosis and Treatment of Liver Disease: Current Trends and Future Directions. Cureus. 2023 Dec 4;15(12):e49920.
61. Ahmadizar F, Younossi ZM. Exploring Biomarkers in Nonalcoholic Fatty Liver Disease Among Individuals With Type 2 Diabetes Mellitus. J Clin Gastroenterol. 2025;59(1):36-46.
62. Yu B, Ma W. Biomarker discovery in hepatocellular carcinoma (HCC) for personalized treatment and enhanced prognosis. Cytokine Growth Factor Rev. 2024;79:29-38.
63. Chen J, Niu C, Yang N, et al. Biomarker discovery and application-An opportunity to resolve the challenge of liver cancer diagnosis and treatment. Pharmacol Res. 2023;189:106674.
64. Francque SM, Marchesini G, Kautz A, et al. Non-alcoholic fatty liver disease: A patient guideline. JHEP Rep. 2021;3(5):100322.
65. Yin X, Guo X, Liu Z, Wang J. Advances in the Diagnosis and Treatment of Non-Alcoholic Fatty Liver Disease. Int J Mol Sci. 2023;24(3):2844.
66. Pouwels S, Sakran N, Graham Y, et al. Non-alcoholic fatty liver disease (NAFLD): a review of pathophysiology, clinical management and effects of weight loss. BMC Endocr Disord. 2022;22(1):63.
67. Arab JP, Díaz LA, Dirchwolf M, et al. NAFLD: Challenges and opportunities to address the public health problem in Latin America. Ann Hepatol. 2021;24:100359.
68. Abhinav V, Mittal R, Navaneethakannan M, et al. Metabolic Derangement in Non-Alcoholic Fatty Liver Disease: Opportunities for Early Diagnostic and Prognostic Markers. Curr Mol Med. 2024 Feb 22.
69. Lazarus JV, Mark HE, Anstee QM, et al. Advancing the global public health agenda for NAFLD: a consensus statement. Nat Rev Gastroenterol Hepatol. 2022;19(1):60-78.
70. Abdelhameed F, Kite C, Lagojda L, et al. Non-invasive Scores and Serum Biomarkers for Fatty Liver in the Era of Metabolic Dysfunction-associated Steatotic Liver Disease (MASLD): A Comprehensive Review From NAFLD to MASLD and MASLD. Curr Obes Rep. 2024;13(3):510-531.

Research Article

Biological reference values for newborn screening parameters in accordance to gestational age and birth weight- a prospective study

Suprava Patel[1*], Neharani Verma[1], Seema Shah[1], Rachita Nanda[1], Eli Mohapatra[1]

[1]*Department of Biochemistry, All India Institute of Medical Sciences, Raipur, Chhattisgarh, India*

Article Info

[*]***Corresponding Author:***
Suprava Patel
Professor, Department of Biochemistry
All India Institute of Medical Sciences, Raipur, Chhattisgarh
E-mail: dr_suprava@yahoo.co.in
ORCID ID: https://orcid.org/0000-0002-7449-1354

Keywords

term, preterm, normal birth weight, low birth weight, male newborns, female newborns, Central India

Abstract

Background: Disease specific biomarkers are ideal tool to detect the presence of the disorder. Timely detection of disorders can improve the health outcome. The metabolic arrangements in pre-term (PT) and low-birth weight (LBW) newborns differ from those term-born and have normal-birth weight (NBW). Hence, it is crucial to compare the values across study groups and establish a dedicated reference values for each group considering the gestational-age and birth weight.

Methods: The prospective study was conducted on the cohort of 2860 newborns who underwent newborn screening (NBS) in dried-bloodspot samples within five days of birth. The study groups included were TERMNBW, TERMLBW, PTNBW and PTLBW.

Results: The central tendency measures and the comparison of the NBS parameters across the study groups are presented. Males recorded a higher n17-OHP ($p<0.001$) median(range) compared to female newborns whereas nIRT ($p=0.008$) and nMSUD ($p<0.001$) were higher in female newborns. nTSH values was higher in TERMNBW than the PTLBW group ($p=0.03$). n17-OHP levels in TERMNBW and TERMLBW groups were lower than PTNBW and PTLBW (<0.001) newborns. nBIOT range of 378.8U and nG6PD range of 17.1U/gHb was highest in TERMNBW. The reference value observed for nTSH, n17-OHP and nIRT were respectively, 9.2mIU/L, 48.6nmol/L, 95.0µg/dL in TERMNBW and 16.9mIU/L, 70.2nmol/L, 76µg/dL in PTLBW. nG6PD reference level were respectively 2.0 and 1.6u/gHb in TERMNBW and PTLBW groups. The nBIOT levels were 52.7U and 48.0U respectively. Reference values were nearly similar for nPKU, nGAL and nMSUD.

Conclusion: The study has provided a detailed comparison and reference levels observed in various study groups and sub-groups considering the gestational-age and birth weight of the newborns.

Introduction

Nearly 75% of death in children under 5 years of age occur in newborns within a week of birth. 40% of the neonatal deaths are commonly associated with prematurity, perinatal complications, sepsis and birth defects [1]. Although mortality has declined since last decade, yet maternal and child health remains a public health problem. Disease specific biomarkers are an ideal tool to detect the presence of the disorder. These markers assist the lab physicians and clinicians to correlate with disease phenotype. Therefore, early diagnosis of the disorder should be the ultimate objective for infants so that appropriate management can be initiated. Timely detection of disorders can improve the health outcome. However, confirmatory diagnosis required high-end equipment. In India, availability of laboratories with high-end infrastructure, such as availability for liquid chromatography mass spectrometry (LCMS) and gene analysis, is very limited and unaffordable to the patients. Most rural and urban health centres have basic equipment such as enzyme linked immunosorbent assay (ELISA)/microplate reader. Therefore, it should be a mandate to have a reference value that could be extrapolated at all rural and urban health centres in Indian set-up.

Preterm (PT) newborns are at high risk due to inadequate development of body parts. Similarly, newborns with low birth weight (LBW) have some degree of immaturity [2]. The metabolic arrangements in PT and LBW newborns differ from those born full term and with normal birth weight (NBW) [3]. Hence, it is crucial to compare the levels of NBS parameters among various groups and sub-groups, and establish a dedicated cut-off values for each group considering the gestational age and birth weight. Establishment of such cut-off levels in the lab would aid in improving detection of analyte and diagnosis, implicate appropriate interventions and genetic counselling to the parents.

Materials and Methods

The prospective study was conducted on the cohort of newborns who underwent NBS in our department, in last five years (June 2019-June 2024). Nearly five thousand NBS samples were tested during this period. All samples were received in the form of dried blood spot (DBS). The DBS samples were collected after 24 hours and within five days of birth. Five days sampling time was considered based on goals suggested by Advisory Committee on Heritable Disorders in Newborn and Children (ACHDNC) that presumptive results for time-critical conditions need to be immediately reported within five days of birth [4]. The samples were checked for the quality of the sample specimen, as per the standard protocol [5].

During the entire study period, our lab has been satisfactorily performing the proficiency testing under Center of Disease Control (CDC), United States, under the Newborn Screening Quality Assurance Program (NSQAP).

The following parameters were performed for NBS testing in newborn (n), thyroid stimulating hormone (nTSH), glucose 6-phosphate dehydrodenase (nG6PD), 17-hydroxyprogesterone (n17-OHP), biotinidase (nBIOT), phenylketonuria (nPKU), immunoreactive trypsinogen (nIRT), galactose (nGAL), and maple syrup urine disease (nMSUD). nTSH, nG6PD, n17-OHP, nBIOT, nPKU, nIRT, and nGAL were analyzed by immunofluorescence method based neonatal kits by Labsystems Diagnostics Oy, Finland. The nMSUD was analysed by immunoassay method-based kit from ZenTech SA, Belgium. Newborns with positive results were called for re-testing with a fresh DBS sample and processed in duplicate. If the results were within the cut-off value the newborn was considered negative. If the values were beyond the cut-off value, they were counselled for confirmatory testing as per the guideline [4]. The newborns who did not respond for re-test and confirmatory report, were excluded. Newborns born to mothers with history of antenatal complications like gestational diabetes mellitus, pre-eclampsia, under medication for thyroid disorders, severe grade anemia and others were excluded.

Inclusion criteria included newborns within five days of birth, those who have a confirmatory report of NBS parameters as per the advice, not diagnosed with any sort of complications during the NBS testing. In Indian scenario, the prevalence of preterm (PT) and low birth weight (LBW) is high and therefore, a reference range of those with no other associated complications is also crucial. Hence, PT born and LBW newborns were also included in the study. Newborns beyond five days of birth, who did not respond for re-testing for confirmation, newborn on top-up feeding, any therapeutic interventions initiated were excluded from the study.

According the gestational age (GA) of birth, the newborns born after 37 weeks of gestation were termed as term born and those born $\leq$ 37 weeks of gestation were termed as PT born. PT newborns were classified as moderate PT (32 to 37 weeks) and very PT (28 to < 32 weeks) for further sub-analysis [2,6]. According to the birth weight (BW), newborns $\geq$ 2500 g were considered as normal birth weight (NBW) and those <2500 g were considered as low birth weight (LBW) (7,8). The LBW newborns were further classified for sub-analysis as very low birth weight (VLBW) for newborns <1500 g and extremely low birth weight (ELBW) for those <1000 g [9].

After applying the inclusion and exclusion criteria, a total of two thousand eight hundred sixty (2860) newborns were included for the study. The newborns were categorized into four study groups. Term born with NBW newborns were grouped as TERMNBW, term born with LBW were grouped as TERMLBW, PT born with NBW were termed as PTNBW and PT with LBW were termed as PTLBW.

Statistical analysis

The data was extracted in MS excel workbook. The statistical analysis was done using Microsoft excel and IBM SPSS 26. The measures of central tendency, mean, median, standard deviation (SD), the minimum and maximum values, and the range, were computed for all the NBS parameters. The values

without the outliers were extrapolated in box-plot graphs. Each of the parameter was compared across the study groups and between male and female neonates. Gender wise comparison in each study groups were performed. All the NBS parameters were checked for normality distribution. The quantitative data were found to be skewed and hence, non-parametric tests were applied. Mann-Whitney U test was performed for gender wise comparison. For comparison of values across the groups, Independent-samples Kruskal-Wallis one way analysis of variance (ANOVA) test after Bonferroni correction for multiple tests was applied. Ideally a reference interval include 2.5th to 97.5th percentile values of the desired population [10]. But, in NBS testing, articles have suggested to consider 99th percentile upper reference limit (99th URL) to identify the otherwise treatable cause at an early age, For, nG6PD and nBIOT, where lower valued suggest positive testing for the disorder, hence, 1.0th percentile lower reference limit (1.0th LRL) was considered [11–13]. A p-value less than 0.5 was considered statistically significant.

Results

The study population consisted of 2860 newborns in which 1396 (48.8%) and 1464 (51.2%) were female and male newborns, respectively. The number of term-born and PT-born newborns included in the study were respectively, 1992 (69.7%) and 868 (30.3%). In the PT-born, 840 (29.4%) were moderate PT (32 – 37 weeks) and 28 (1.0%) were very PT (<32 weeks) born. 2177 (76.1%) newborns had NBW and 683 (23.9%) had LBW. In the LBW category, 660 (23.1%) had LBW (<2500g), 15 (0.5%) had VLBW (<1500g), and 8 (0.3%) had ELBW (<1000g).

The study groups comprised of 1724 (60.3%) TERMNBW newborns, 268 (9.4%) TERMLBW, 453 (15.8%) PTNBW, and 415 (14.5%) PTLBW newborns.

The mean (SD) and median (min.-max.) of all the NBS parameters of the study population are detailed in Table 1.

Table 1: The mean (SD) and median (range) values of the NBS parameters in the study population in DBS samples.

NBS Parameters	Gender	Mean	SD	Median	Range	Min-Max	p-value
nTSH (mIU/L)		3.2	2.1	2.7	16.8	0.1-16.9	
	F	3.2	2.1	2.7	16.8	0.1-16.9	0.44*
	M	3.2	2.1	2.8	16.8	0.1-16.9	
nG6PD (IU/gHb)		8.9	2.1	9.1	17.1	0.1-17.2	
	F	9	1.9	9.2	14.2	0.2-14.4	0.87*
	M	8.9	2.2	9.1	17.1	0.1-17.2	
n17-OHP (nmol/L)		21.4	9.4	20.3	142.8	0.2-143.0	
	F	20	8.5	18.9	72.6	0.2-72.8	<0.001*
	M	22.8	9.9	21.8	142.8	0.2-143.0	
nBIOT (U)		207.7	87.5	196.9	385.7	7.2-392.9	
	F	207.8	88.6	197.2	367.8	25.1-392.9	0.24*
	M	203.2	85.4	190	378.8	7.2-386.0	
nPKU (mg/dL)		1.2	0.5	1.1	13.3	0.1-13.4	
	F	1.2	0.5	1.1	13.3	0.1-13.4	0.64*
	M	1.2	0.6	1.1	11.9	0.1-12.0	
nIRT (µg/L)		24.8	20	19.8	341.8	0.1-341.9	
	F	25.9	20.9	20.6	341.8	0.1-341.9	0.008*
	M	23.7	19	19.2	255.9	0.1-256.0	
nGAL (mg/dL)		2.2	3.6	1.1	66.1	0.1-66.2	
	F	2.2	3.2	1.1	66.1	0.1-66.2	0.61*
	M	2.4	4	1.2	66.1	0.1-66.2	
nMSUD (mg/dL)		1.8	0.9	1.8	20.9	0.1-21.0	
	F	1.9	1	1.9	20.9	0.1-21.0	<0.001*
	M	1.8	0.7	1.8	4	0.1-4.1	

*denotes significance value of Mann-Whitney U test; F denotes female newborns and M denotes male newborns

The minimum – maximum values observed in the study population for nTSH was 0.1 – 16.9 mIU/L, nG6PD was 0.1 – 17.2 IU/gHb, n17-OHP was 0.2 – 143.0 nmol/L, nBIOT was 7.2 – 392.9 U, nPKU was 0.1 – 13.4 mg/dL, nIRT was 0.3 – 341.9 µg/L, nGAL was 0.1 – 66.2 mg/dL and nMSUD was 0.1 – 21.0 mg/dL. Gender wise differences were also delineated in Table 1. Significant differences in values were recorded for n17-OHP ($p<0.001$), nIRT ($p=0.008$) and nMSUD ($p<0.001$).

Males recorded a higher n17-OHP median (range) compared to female newborns whereas the values of nIRT and nMSUD were higher in female newborns.

A descriptive detail of the central tendency measures and the comparison of the NBS parameters across the study groups has been delineated in Table 2.

Table 2: Comparison NBS parameters across the study groups.

		Study Groups	Mean	SD	Median	Range	Min-Max	P value
nTSH								0.025*
	1	TERMNBW	3.2	2.1	2.8	16.8	0.1-16.9	1v4=0.03*
	2	TERMLBW	3.2	2.1	2.7	16.8	0.1-16.9	
	3	PTNBW	3.1	1.9	2.6	16.8	0.1-16.9	
	4	PTLBW	3	2.3	2.6	16.3	0.6-16.9	
nG6PD								0.57*
	1	TERMNBW	8.9	2	9.1	17.1	0.1-17.2	
	2	TERMLBW	8.9	1.9	9	14.3	0.3-14.6	
	3	PTNBW	8.9	2.2	9.4	14	0.2-14.2	
	4	PTLBW	8.9	2	9.1	14	0.2-14.2	
n17-OHP								<0.001*
	1	TERMNBW	20.4	8.5	19.5	86.8	0.2-87.0	1v3<0.001*
	2	TERMLBW	20.6	8.8	19	48.4	0.2-48.6	1v4<0.001^
	3	PTNBW	22.5	8.5	21.8	47.7	0.9-48.6	2v3=0.003*
	4	PTLBW	24.9	12.7	23.4	142.8	0.2-143.0	2v4<0.001*
nBIOT								0.017*
	1	TERMNBW	209.5	86.9	199.6	378.8	7.2-386.0	2v3=0.054*
	2	TERMLBW	195.3	84.6	179.2	334.5	48.0-382.5	
	3	PTNBW	214	88.9	207.5	344.9	48.0-392.9	
	4	PTLBW	201.1	89.3	184.9	358.5	24.0-382.5	
nPKU								0.85*
	1	TERMNBW	1.2	0.6	1.1	13.3	0.1-13.4	
	2	TERMLBW	1.2	0.4	1.1	1.6	0.7-2.3	
	3	PTNBW	1.2	0.4	1.1	5.5	0.1-5.6	
	4	PTLBW	1.2	0.6	1.1	11.3	0.7-12.0	
nIRT								0.15*
	1	TERMNBW	25.2	19.7	20	170.5	0.3-170.8	
	2	TERMLBW	26.2	26.7	20.6	341.8	0.1-341.9	
	3	PTNBW	22.9	19.3	18.6	255.9	0.1-256.0	
	4	PTLBW	24.7	16.8	20.4	106.2	0.2-108.2	
nGAL								0.73*

	1	TERMNBW	2.3	3.8	1.1	66.1	0.1-66.2	
	2	TERMLBW	2.3	3.3	1.2	19.8	0.1-19.9	
	3	PTNBW	1.9	2.7	1.1	22.5	0.1-22.6	
	4	PTLBW	2.1	4.1	1.1	66.1	0.1-66.2	
nMSUD								0.004*
	1	TERMNBW	1.9	0.8	1.9	14.9	0.1-15.0	1v4=0.017*
	2	TERMLBW	1.8	0.6	1.8	3.4	0.2-3.6	
	3	PTNBW	1.8	1.2	1.7	20.9	0.1-21.0	
	4	PTLBW	1.7	0.6	1.8	3.6	0.1-3.7	

*denotes significance value of Independent-samples Kruskal-Wallis one way ANOVA test after Bonferroni correction for multiple tests

nTSH values showed a significant difference across the study groups (p=0.025) where the values were higher in TERMNBW than the PTLBW group (p=0.03). Among the study groups, PTLBW newborns recorded a lowest nTSH levels with a median (range) level of 2.6 (16.3) mIU/L. nG6PD values were nearly similar among the four study groups. The TERMNBW depicted a wider range, 0.1-17.2 IU/gHb compared to others. Gross differences in n17-OHP were observed in the study groups (p<0.001). n17-OHP levels in TERMNBW and TERMLBW groups were lower than PTNBW and PTLBW (<0.001) newborns. PTLBW newborns reported a wider range of n17-OHP, 0.2-143.0 nmol/L. The study groups showed a significant difference in their nBIOT levels (p=0.017). nBIOT range of 378.8 U was highest in TERMNBW than the other study groups. No significant dissimilarities were recorded for nPKU, nIRT and nGAL levels in the study groups. TERMNBW newborns demonstrated a highest nPKU of 13.3 mg/dL. Highest nIRT level (341.9 µg/L) was designated in TERMLBW group, whereas highest nGAL value of 66.2 mg/dl was seen in both TERMNB and PTLBW. A significant variation in nMSUD values were observed among the study groups (p=0.004). The TERMNBW group reported a higher nMSUD [median (range) of 1.9 (14.9) mg/dL] than the PTLBW group (p=0.017). Figures 1 – 4 illustrates the gender wise comparison of NBS parameters in different study groups (outliers hidden for proper reflection of values).

Figure 1: Gender wise comparison of DBS NBS parameters in TERMNBW study group.

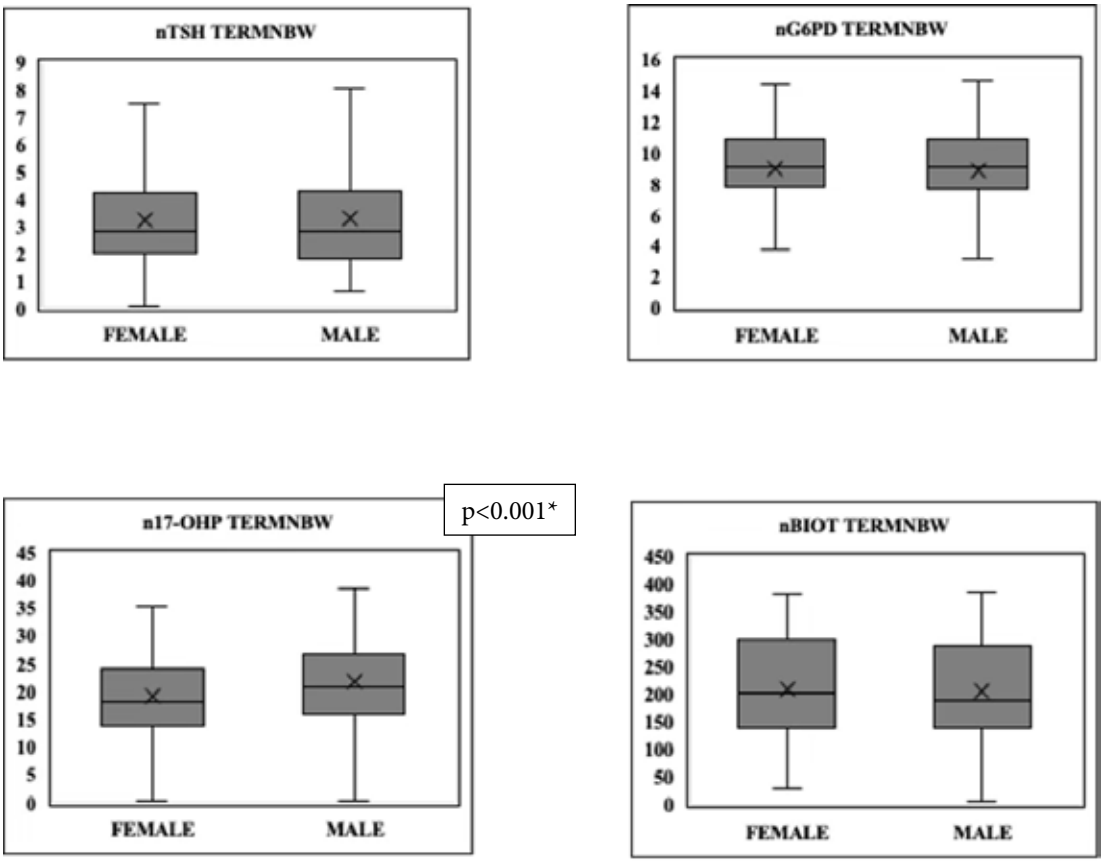

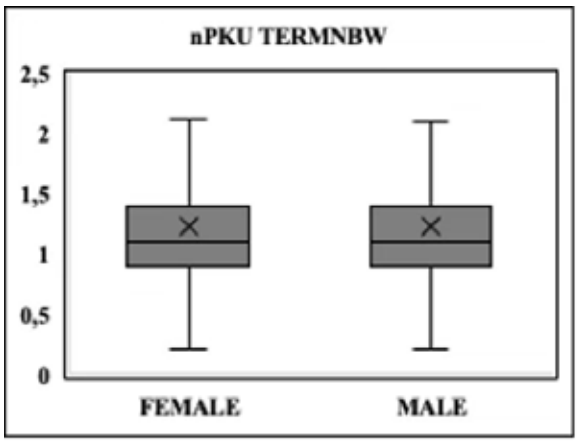

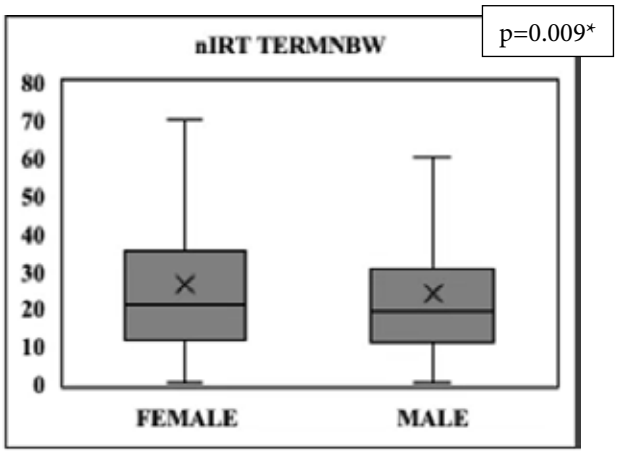

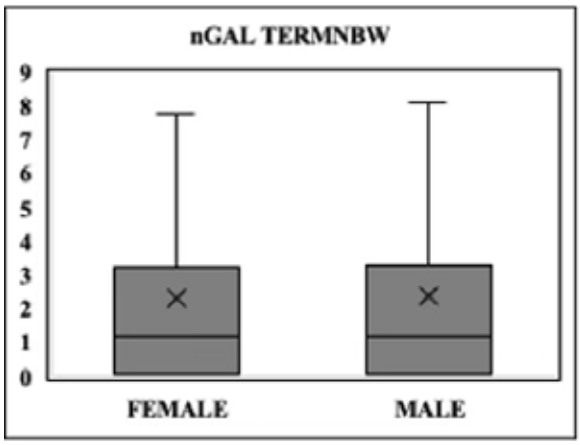

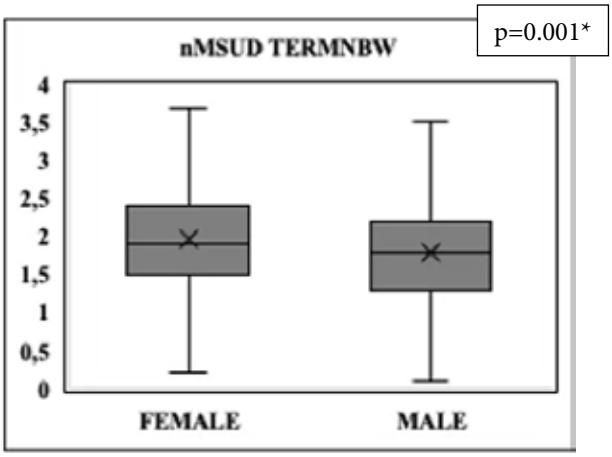

*denotes significance value of Mann-Whitney U test

Figure 1 reflects the comparison between male and female newborns of TERMNBW group. nTSH, nG6PD, nBIOT, nPKU, and nGAL did not differ significantly between male and female newborns. The male and female nTSH median (range) was 2.8 (16.8) mIU/L. The same for nG6PD were 9.1 (13.5) and 9.1 (17.1) IU/gHb, respectively. The median (range) n17-OHP of 20.9 (86.8) nmol/L in male newborns was greatly higher than 18.1 (51.4) nmol/L in female newborns ($p<0.001$). The maximum value in male and female TERMNBW for n17-OHP were respectively, 86.8 and 51.4 nmol/L. On the contrary, the median (range) of female nIRT ($p=0.009$) and nMSUD ($p=0.001$) were greater than their male counterparts. The median (range) of nIRT in female was 21.4 (168.8) µg/L and in male was 19.2 (170.5) µg/L. 1.9 (14.9) and 1.8 (4.0) mg/dL were the respective nMSUD values. The highest nMSUD values observed were 14.9 and 4.0 mg/dL respectively in female and male newborns of this group. The median (range) of nBIOT in female was 202.2 (353.0) and in male was 190.2 (378.8) U. The value of nGAL for both genders was 1.2 (66.1) mg/dL in this group.

The male newborns of TERMLBW group also reflected a higher n17-OHP level [22 (47.7) nmol/L] than the female newborns [17.7 (48.4) nmol/L] ($p<0.001$), as depicted in Figure 2.

Figure 2: Gender wise comparison of DBS NBS parameters in TERMLBW study group.

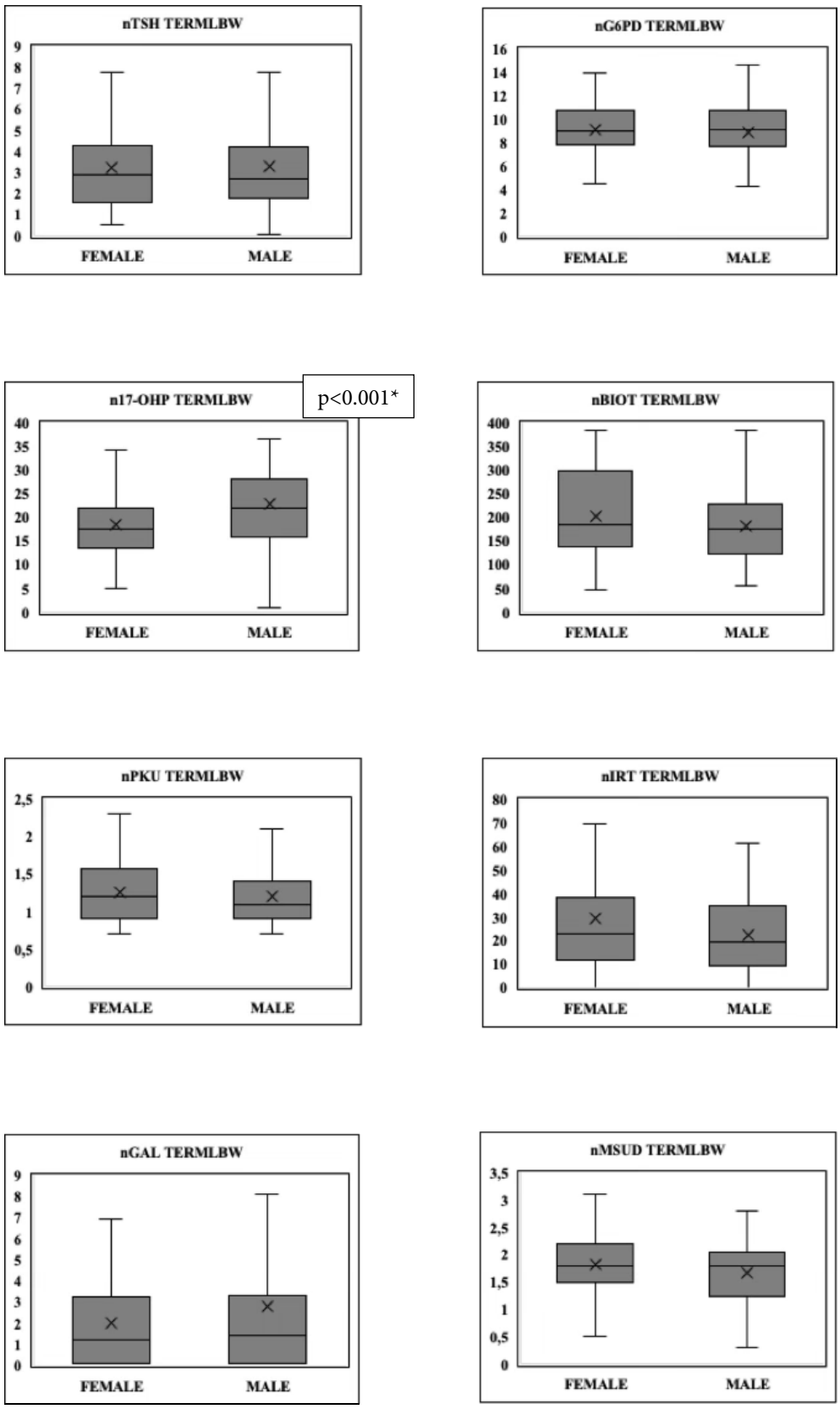

*denotes significance value of Mann-Whitney U test

Similarly, PTNBW male newborns recorded a higher median (range) of 22.9 (47.7) nmol/L compared to female [20.8 (47.7) nmol/L] counterparts in this group (p=0.039) (Figure 3).

Figure 3: Gender wise comparison of DBS NBS parameters in PTNBW study group.

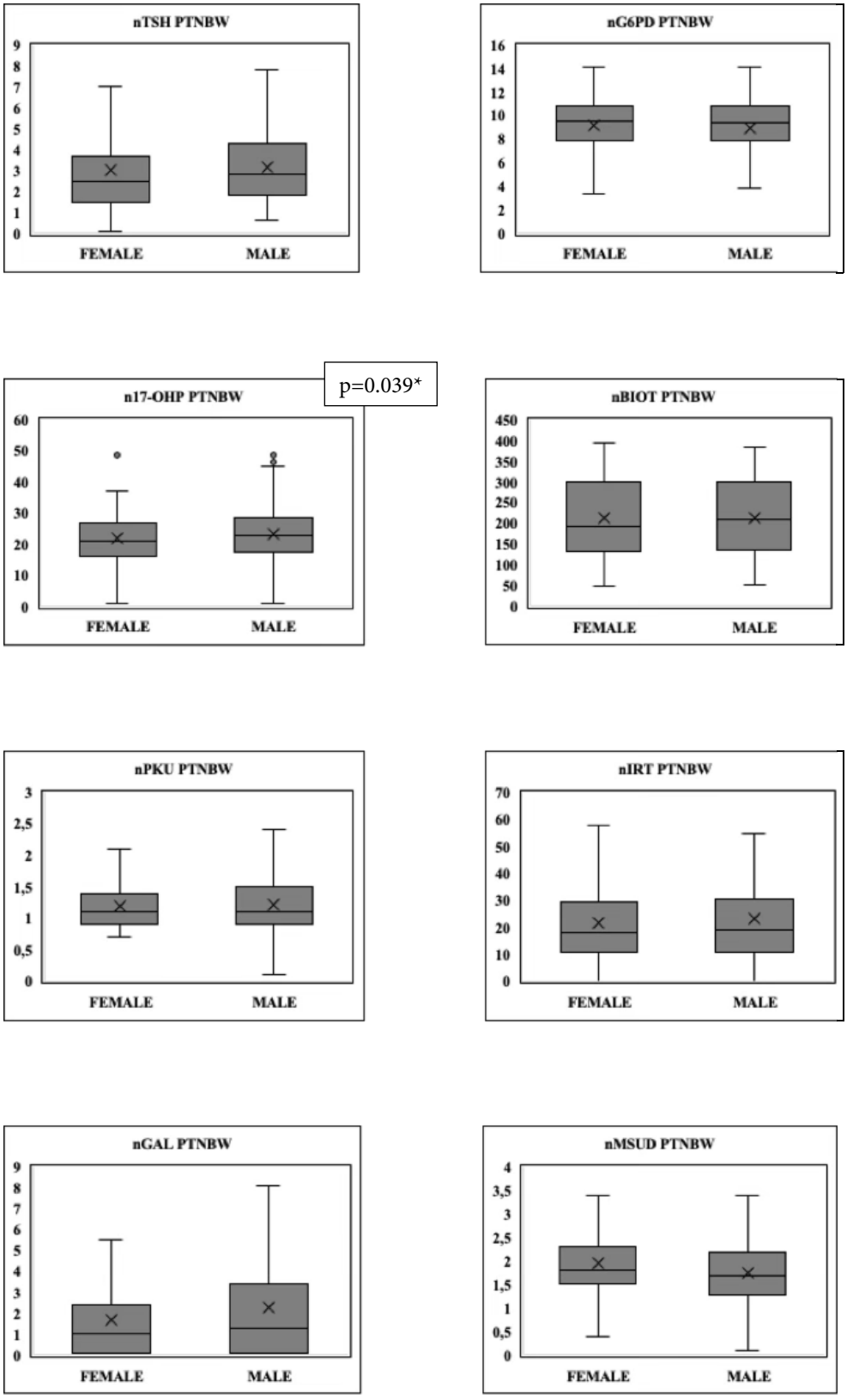

*denotes significance value of Mann-Whitney U test

Other NBS parameters did not show very significant variations between the genders in both the groups. Likewise, no significant differences for NBS parameters between male and female PTLBW were observed except for n17-OHP as revealed in Figure 4.

Figure 4: Gender wise comparison of DBS NBS parameters in PTLBW study group.

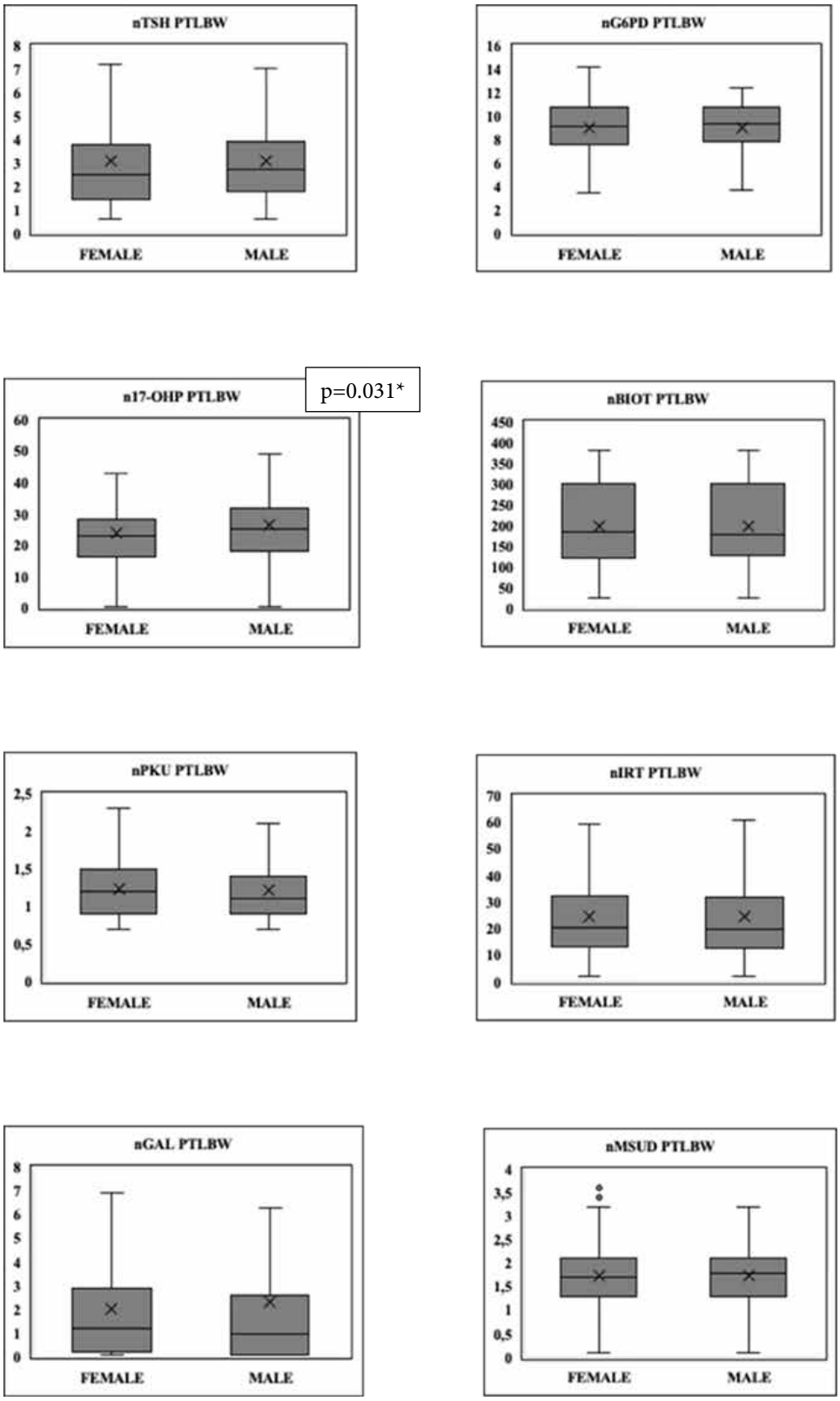

*denotes significance value of Mann-Whitney U test

In this group, the male newborns reported a median (range) value of 25.3 (142.8) nmol/L n17-OHP and females reported a value of 22.9 (72.3) nmol/L (p=0.031). The maximum valued detected in male and female newborns were 143.0 and 72.8 nmol/L, respectively.
The NBS parameters were also analysed for differences in values as per the gestational age and birth weight of the newborns included in the study, as illustrated in Figures 5,6. The median (range) nTSH showed significant differences among the term, moderate PT and very PT born newborns (p=0.012), as shown in Figure 5.

Figure 5: Distribution of NBS parameters as per the gestational age of the newborns in the study population.

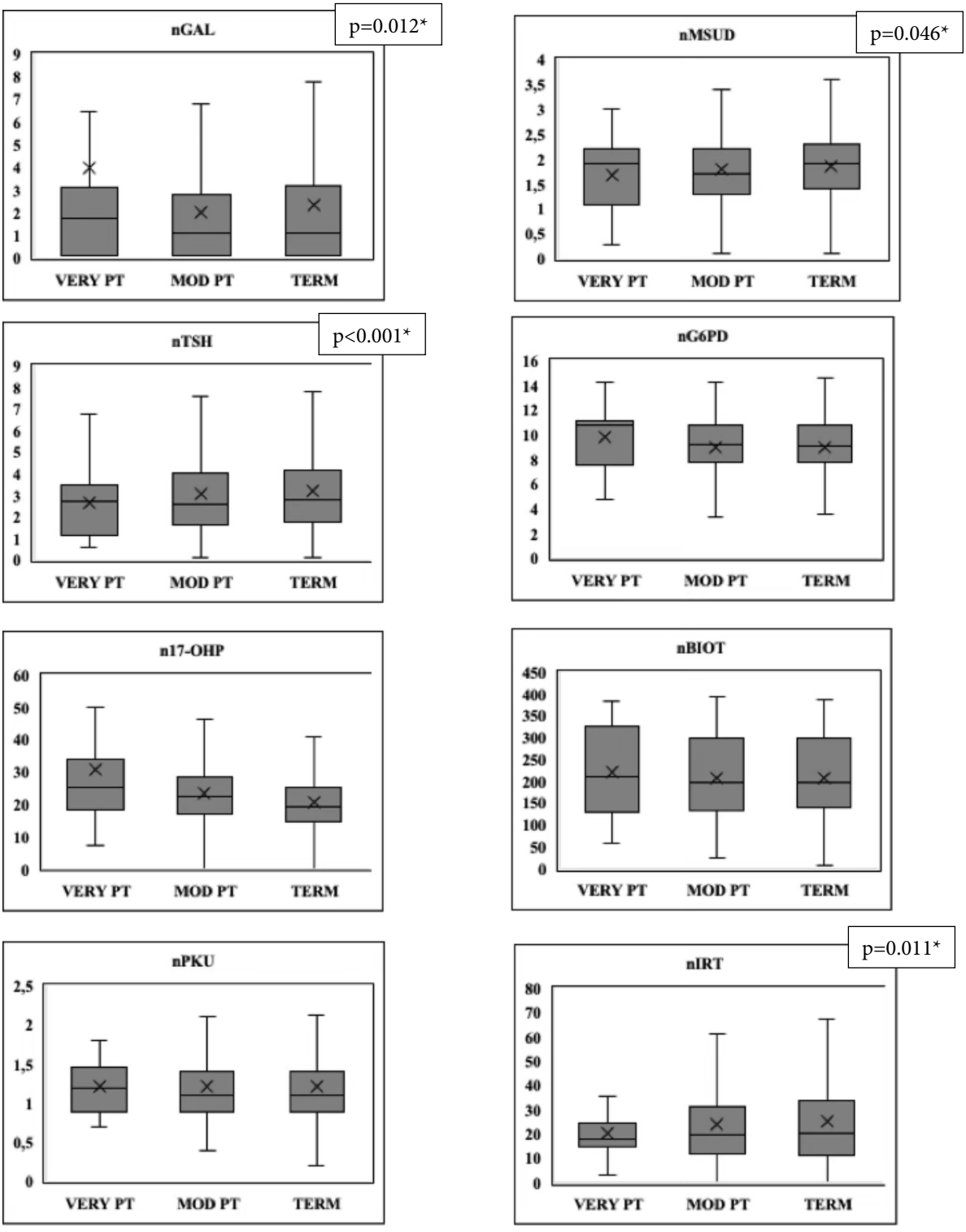

*denotes significance value of Independent-samples Kruskal-Wallis one way ANOVA test after Bonferroni correction for multiple tests

2.8 (16.8) mIU/L in term born was higher than 2.6 (16.8) mIU/L in moderate PT born (p=0.02). The median (range) in very PT was 2.7 (6.2) mIU/L. The nG6PD values varied as per the gestational age (p=0.046). The median (range) of 10.8 (9.4) IU/gHb observed in very PT was slightly higher than 9.1 (17.1) IU/gHb reported by term newborns (p=0.05) and 9.2 (14.0) IU/gHb reported by moderate PT (p=0.08). n17-OHP depicted significant variation as per the gestational age (p<0.001). Compared to the term born, the moderate PT (p<0.001) and very PT (p=0.016) recorded significantly higher levels. The median (range) values in term, moderate term, and very PT were respectively, 19.4 (86.8), 22.7 (78.6), and 25.2 (135.5) nmol/L. The respective nBIOT values were 196.9 (378.8), 196.1 (368.9), and 209.3 (322.8) U. For nPKU the levels were 1.1 (13.3), 1.1 (11.9), and 1.2 (1.6) mg/dL respectively. The nIRT values observed in the three groups were 20.2 (341.8), 19.7 (255.9), and 18.2 (46.0) µg/L. The respective values for nGAL were 1.1 (66.1), 1.1 (22.5), and 1.8 (66.1) mg/dL. No statistical differences were observed for nBIOT, nPKU, nIRT, and nGAL in the newborns as per their gestational age. nMSUD [1.9 (14.9) mg/dL] in term born was slightly higher than the moderate PT [1.7 (20.9) mg/dL] (p=0.011) born newborns. The value in very PT newborns was 1.9 (2.7) mg/dL. Distribution of NBS parameter according to their birth weight has been graphed in Figure 6.

Figure 6: Distribution of NBS parameters as per the birth weight of the newborns in the study population.

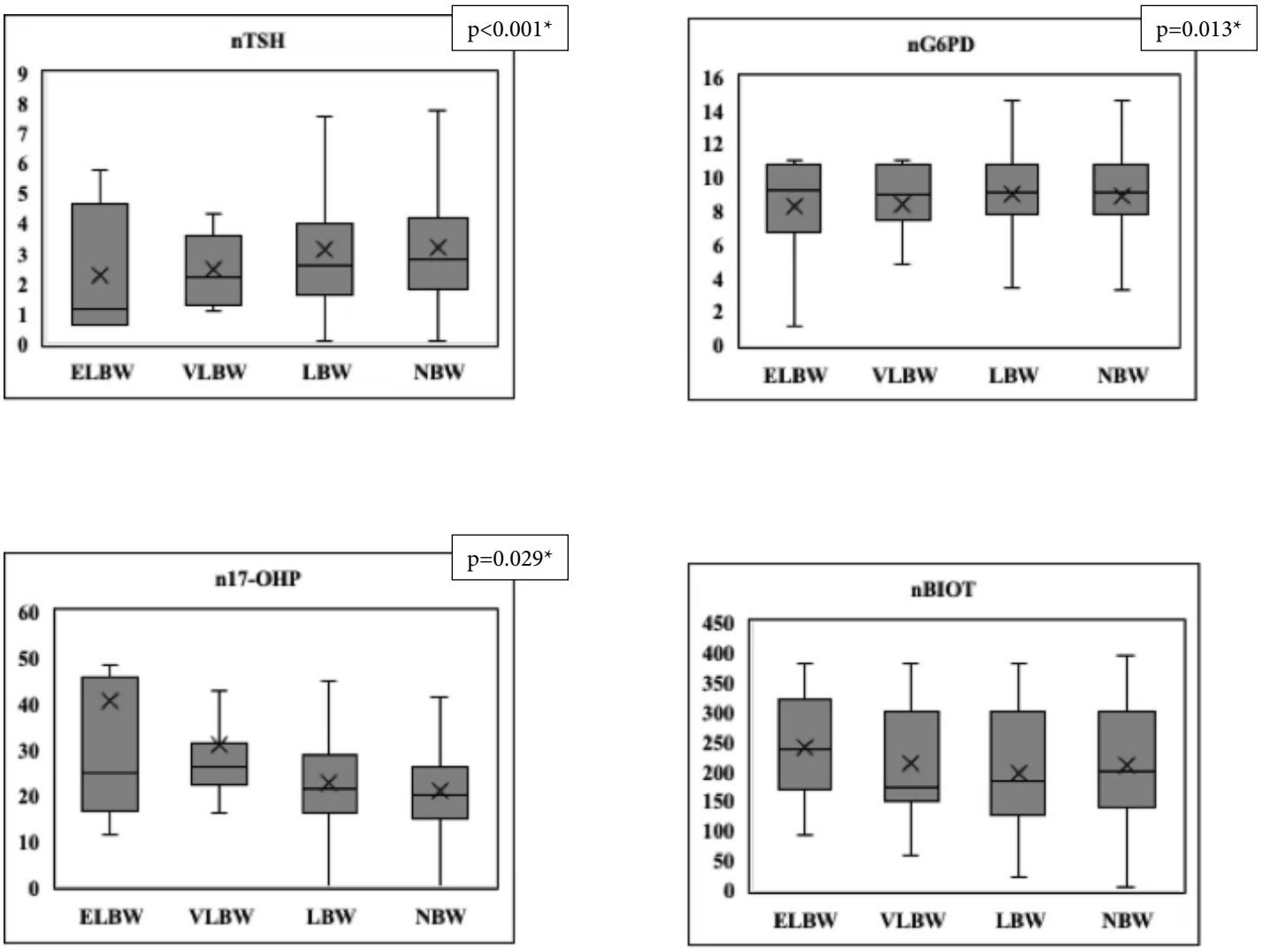

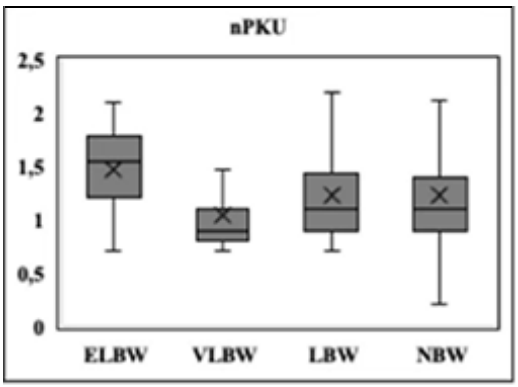

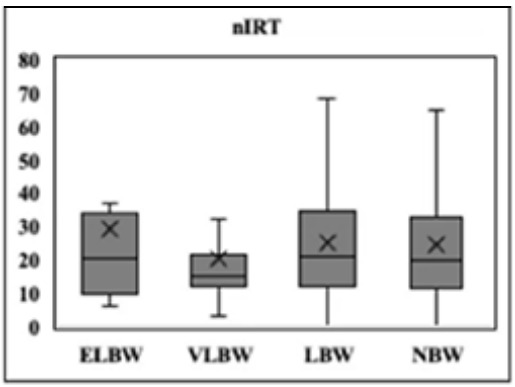

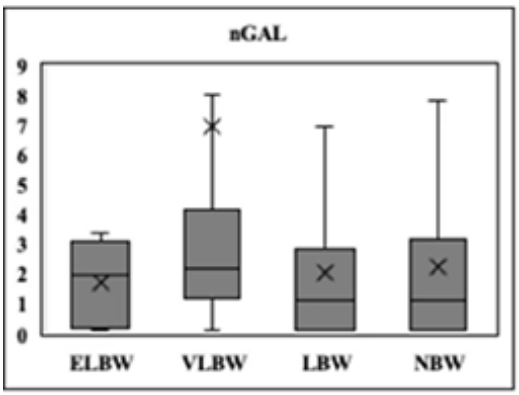

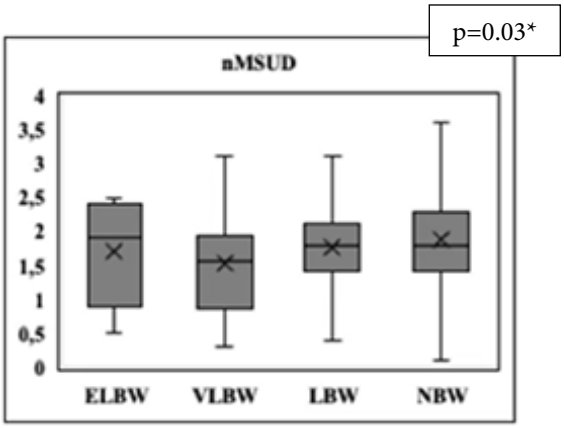

*denotes significance value of Independent-samples Kruskal-Wallis one way ANOVA test after Bonferroni correction for multiple tests

nTSH and nG6PD values did not vary significantly as per the birth weight of the newborns. The NBW, LBW, VLBW, and ELBW values for nTSH were 2.8 (16.8), 2.6 (16.8), 2.2 (3.2), and 1.2 (5.2) mIU/L respectively. The median (range) of nG6PD in these newborns were 9.1 (14.2), 9.1 (14.4), 9.0 (10.3), and 9.3 (10.0) IU/gHb, respectively. The respective levels for n17-OHP were 19.9 (86.8), 21.6 (75.6),26.0 (62.8), and 24.9 (131.6) nmol/L, respectively ($p<0.001$). VLBW newborns showed a higher value compared to LBW ($p=0.019$) and NBW (0.002). Similarly, in LBW newborns n17-OHP was higher than NBW ($p<0.001$). nBIOT median (range) value in NBW [201.3 (385.7) U] was significantly greater than 181.8 (358.5) U in LBW newborns($p=0.01$). The levels in VLBW and ELBW were 171.5 (324.6) and 236 (291.1) U. A lower nPKU level was observed in VLBW newborns compared to NBW ($p=0.023$), LBW ($p=0.019$), and ELBW ($p=0.004$). The nIRT median (range) values were 19.6 (255.9), 20.7 (341.8), 15.3 (62.5), 20.4 (102.6) µg/L in NBW, LBW, VLBW, and ELBW newborns respectively. The respective nGAL were 1.1 (66.1), 1.1 (19.8), 2.2 (66.1), and 2.0 (3.3) mg/dL. nIRT and nGAL showed no significant variations among the newborns as per their birth weight, but nMSUD did show differences ($p=0.03$). nMSUD in NBW newborns depicted a median (range) of 1.8 (20.9) mg/dL compared to LBW newborns 1.8 (3.6) mg/dL ($p=0.047$).

The percentile values of the NBS parameters have been detailed in Table 3.

Table 3: Percentile distribution of NBS parameters in the study groups.

	Study Groups	1.0th	2.5th	3.0th	99th
nTSH (mIU/L)					
	TERMNBW	0.6	0.6	0.7	9.2
	TERMLBW	0.5	0.6	0.6	10.6
	PTNBW	0.6	0.6	0.7	8.6
	PTLBW	0.6	0.6	0.6	16.9
nG6PD (IU/gHb)					
	TERMNBW	2	4.4	4.8	12.9
	TERMLBW	1.6	4.4	4.6	13.6
	PTNBW	1.4	2.8	4.1	13.2
	PTLBW	1.6	4.3	4.5	12.4
n17-OHP (nmol/L)					
	TERMNBW	0.9	6.4	7.3	48.6
	TERMLBW	0.7	6.9	8.2	48.6
	PTNBW	4.9	7.8	8	48.6
	PTLBW	1.1	5.7	6.5	70.2
nBIOT (U)					
	TERMNBW	52.7	63.7	66.7	382.5
	TERMLBW	55.3	62.7	65.3	382.5
	PTNBW	54.2	64.9	67.4	382.5
	PTLBW	48	57.9	58.9	382.4
nPKU (mg/dL)					
	TERMNBW	0.7	0.7	0.7	2.4
	TERMLBW	0.7	0.7	0.7	2.1
	PTNBW	0.7	0.7	0.7	2.3
	PTLBW	0.7	0.7	0.7	2.3
nIRT (µg/L)					
	TERMNBW	2	2	2.8	95
	TERMLBW	0.23	2	2	99.6
	PTNBW	1.2	2	2	72.8
	PTLBW	2	3.7	4.3	76
nGAL (mg/dL)					
	TERMNBW	0.1	0.1	0.1	14.9
	TERMLBW	0.1	0.1	0.1	18.4
	PTNBW	0.1	0.1	0.1	12.7
	PTLBW	0.1	0.1	0.1	14.3
nMSUD (mg/dL)					
	TERMNBW	0.2	0.4	0.5	3.6
	TERMLBW	0.3	0.4	0.5	3.5
	PTNBW	0.1	0.4	0.5	3.4
	PTLBW	0.3	0.5	0.6	3.4

The 99th URLvalue was considered the highest reference value for nTSH, n17-OHP, nPKU, nIRT, nGAL, and nMSUD because higher levels are considered as screening positive. The 1.0th LRL was taken as the lowest reference value for nG6PD and nBIOT where lower values are said to be positively screened for the disorders. The 99th URL of nTSH in TERMNBW was 9.2mIU/L. The same in TERMLBW, PTNBW, and PTLBW were 10.6, 8.6, and 16.9 mIU/L respectively. The 1.0th LRL

for nG6PD in the four groups were respectively, 2.0, 1.6, 1.4, and 1.6 IU/gHb. The 99th percentile newborns depicted a value of 48.6 nmol/L for n17-OHP in all groups except PTLBW in which the value was 70.2 nmol/L. The 1.0th LRL value of nBIOT in TERMNBW was 52.7 U, in TERMLBW was 55.3 U, in PTNBW was 54.2 U and PTLBW was 48.0 U. For nPKU, 99th URL value was close to 2.3 mg/dL. The same for nIRT in the four groups were respectively, 95.0, 99.6, 72.8, and 76.0 µg/L. The 99th URL for nGAL were 14.9 mg/dL for TERMNBW, 18.4 mg/dL for TERMLBW, 12.7 mg/dL for PTNBW, and 14.3 mg/dL for PTLBW. nMSUD values for the same were close to 3.5 mg/dL in the four groups.

Discussion

NBS is not widely accepted in Indian scenario compared to the western countries. Data regarding the cut-off range is not much studies in Indian hospital setup. Lack of awareness and lack of infrastructure are the most common causes to limit NBS testing. However, in recent years, lab clinicians have become active in establishing metabolic lab to aid the physicians in providing diagnostic set up for the inborn errors of metabolic disorders (IEMD). But till date, a defined reference value for NBS parameters is yet to be determined. It is high time to generated population-based reference value for these parameters. As per inclusion criteria, we evaluated 2860 newborns who have undergone NBS in our set up and had a confirmatory report for the parameter.

The TERMNBW group reflected higher median level than the other study groups (Table 2). Term born neonates depicted higher median than PT born neonates. Similarly, the levels were highest in NBW and lowest in ELBW neonates (Supplementary Table 1). Studies have depicted normal nTSH in the first sample of preterm and LBW newborns, but in later weeks the levels are elevated and returns back to normal term neonate level after 6-8 weeks [14]. Delayed TSH elevation, usually 11 – 176 days of birth, has been reported in LBW, VLBW, and ELBW in New England NBS Program and Wisconsin NBS program [15,16]. Most NBS program do not perform a second testing if nTSH in the first sample is within normal cut-off in preterm/LBW newborns. It is now recommended that a second specimen at 2 – 4 weeks is required is these newborns and sometimes a third sample also at 6 – 8 weeks of birth [17]. LaFranchi et al explained about reduced TSH surge in preterm babies than term babies due to immature hypothalamic-pituitary-thyroid (HPT) axis and slow recovery to normalization of this physiological axis. This axis starts maturing in later half of pregnancy, but normal feedback mechanism is not active until term gestation [18]. The highest reference value for cut-off (99th percentile) in TERMNBW was 9.2 mIU/L whereas for PTLBW was 16.9 mIU/L (Table 3). The lab cut-off value as per kit brochure was 10 mIU/L. Nascimento et al study on 74123 children in Santa Catarina, suggested to decrease the cut-off from 10 to 6 mIU/L for a better sensitivity for detecting the newborns with thyroid dysfunctions [19]. On the contrary, Verma et al study on 174000 neonates in various hospitals in North India reported an optimal cut-off value of ≥ 20 mIU/L for deciding further clinical evaluation, balancing the recall rate and false negativity [20]. The recall rate for nTSH screening increased by 2% when reference value was reduced from 20 mIU/L to 10 mIU/L [21]. The availability, affordability and awareness are the mainstay for NBS program to be a success. A very high recall rate (at a very low reference value of 6 mIU/L) might influence a high-cost burden on health system and a very low sensitivity (due to very high cut-off of 20 mIU/L) might lead to mis-diagnosis of thyroid disorder. Hence, it is suggested that a reference value of 10 mIUL should be considered as an optimal level for all categories of newborn. Due to a high dynamicity observed in nTSH levels in the first few weeks of birth, it is also recommended to adopt at least 2-screen settings at 4-6 weeks, especially PT and LBW newborns.

nGDPD in TERMNBW showed a higher median and range than the other study groups (Table 2). The levels in very PT and ELBW newborns were lowest with least range (Supplementary Table 2). Yang et al study reported the mean (SD) G6PD activity level in term infants under 30 days of age to be 13.6 (3.7) U/g Hb. The suggested cut-off value to differentiate normal from G6PD deficient heterozygotes in infants below 30 days of age was 9.35 U/g Hb. The implied cut-off to differentiate G6PD deficient female heterozygote and male hemizygote was 3.85 U/g Hb [22]. Algur et al performed the quantitative neonatal G6PD screening on healthy term newborns born to Sephardic Jewish mothers. The analysis was performed in umbilical cord sample and presented a median (range) value of 0.28 (0.01-6.2) U/g Hb in G6PD deficient male newborns and 18.76 (9.0-34.66) U/g Hb in normal male newborns. Similarly, the values were respectively 4.84 (0.06-6.96) and 18.36 (9.54-35.5) U/g Hb in deficient and normal female newborns. The study reported that the enzyme activity values were significantly lower in these newborns compared to African-American male neonates with G6PD variant [2.55 (2.15-3.05) U/g Hb, $p<0.001$], implying the role of ethnicity on different G6PD variants and severity (23). Mukherjee et al study on NBS for G6PD deficiency in Eastern India published a prevalence of 0.48% in term and late preterm newborns. The cut-off values used was 6.95 U/g Hb in the cord blood sample [24]. In the present study, the G6PD values differed significantly in newborns as per the gestational age ($p=0.046$, Supplementary Table 2), but not so considering their birthweight (Supplementary Table 2) or gender (Table 1). Our study presented a cut-off (1.0th percentile) of 2.0 U/g Hb in TERMNBW and 1.6 U/g Hb for others (Table 3). However, a genotype analysis for various G6PD variants would provide a more accurate insight regarding the type and severity.

Hayashi et al study observed the highest median (range) n17-OHP levels in newborns with BW ≤ 1500 g [38.7 (1.5-155.5) nmol/L] and the lowest in NBW neonates [15.6 (0.5-169) nmol/L]. The cut-off at 99.8th percentile determined for NBW was 60 nmol/L and 117 for LBW newborns [25]. van der Kamp

et al study suggested that the cut-off for n17-OHP should be based on BW and gestational age. The observed median (range) values in DBS samples in ELBW newborns was highest, 86 (9 – 603) nmol/L compared to newborns with higher BW. The lowest values were observed in newborns with BW ≥ 4000 g [17 (1-45) nmol/L]. Similarly, highest levels, 99 (9-603) nmol/L was seen in neonates ≤ 28 weeks of GA and lowest, 16 (2-32) nmol/L in those born ≥ 41 weeks. The study revealed a significant negative correlation between n17-OHP with BW and GA. However the regression model suggested GA be a better predictor for n17-OHP than BW because adrenal gland development is related to GA of fetus [26]. Choi et al study too noted significant inverse association of n17-OHP levels with GA and the number of false positive to be higher in PT born neonates [27]. Similar finding was also reported by Seeralar et al study [28]. Prasad et al study suggested a cut-off >30 nmol/L for term newborns, ≥ 40 nmol/L for PT newborns weighing <2500 g and ≥ 30 for PT weighing > 2500 g [1]. In agreement, we observed a significant negative correlation with GA and BW ($p<0.001$, data not shown). The present study figured out a cut-off of 48.6 nmol/L for the study population.

A noteworthy finding observed in the present study was the significant differences in 17-OHP values among the various study groups and subgroups. Studies have reported that newborn 17-OHP levels to be greatly influenced by various factors. The anxiety and trauma associated with child delivery leads to elevated physiological 17-OHP levels which gradually decreases in next 12-48 hours [29]. Similarly, higher values typically recorded in male newborns, PT babies, babies with LBW, babies exposed to stressful events during antenatal period [29,30]. Besides, the 17-OHP values are also influenced by the laboratory methodology used for screening, where presence of other steroids might show some degree of antibody cross reactivity [31]. Therefore, it is suggested that a careful consideration is required for interpreting the results. The laboratories should establish an adjusted cut-off value based upon time of collection of samples, baby's gender, gestational age, birth weight, antenatal history, and type of laboratory method, to minimize the false positives. A second-tier testing method like LCMS would increase the accuracy of diagnosis.

nBIOT levels depicted a significant difference among the study groups (Table 2), more so because the median (range) was significantly higher in NBW group than the LBW neonates (Supplementary Table 4). The biotinidase enzyme cleave the dietary biocytin to release biotin to be available for various enzymes involved in catalysing important metabolic reactions [1]. Semeraro et al study recorded a high incidence, 1:8797 of partial biotinidase deficiency in Italy, and carried 1330G>C (D444H) variant in the neonates. The false positive rate was 0.3% with a cut-off of 85 U/dL. The median (IQR) levels were lower in LBW [203.65 (75.75) U/dL] than NBW newborns ($p<0.05$) and in PT [213.7 (75.8) U/dL] than the term neonates ($p<0.05$). nBIOT values correlated positively with GA, BW and age of DBS specimen. Besides, the study also observed a seasonal variation of nBIOT levels with a significantly lower values in summer seasons. Hence it is recommended that each lab must set a cut-off value based on the GA and BW and season. A repeat specimen is suggested within 40 days of first NBS for a early diagnosis of partial biotinidase deficiency [32]. The cut-off value suggested by Prasad et al study was <58.5 U for term and PT newborns weighing >2500g, and <55 U for PT weighing <2500g (1). Considering the overall 1.0th percentile in all study groups and sub-groups, the present study considers 48 U, the 1.0th value in NBW group, as the cut-off value (Table Supplementary 4).

No significant differences in nPKU level were observed between the study groups (Table 2). However, the ELBW depicted a higher median level than the other sub-groups (Supplementary Table 5). The finding could be due to the fact that ELBW newborns are usually under parenteral preparations supplemented with essential amino acids or enteral feeding with fortified human or bovine milk [33]. This might be challenging in ELBW newborns and hence, need to be closely monitored.

Newborn screening for cystic fibrosis (CF) through measurement of IRT is crucial for early diagnosis and quality of life in affected patients. Arrundi-Moreno et al study obtained a cut-off value of 76.2 ng/mL for predicting CF with a sensitivity of 95.7% and specificity of 64.5%. The median nIRT values were higher in very PT (78.35 ng/mL) and late PT (73 ng/mL) newborns compared to term (70.12 ng/mL) newborns [34]. On the contrary, the values were lower in PT group in our study. Prasad et al study established a cut-off of >60 mg/mL based on the 98.5th and 99.6th percentiles for term and PT newborns [1]. The cut-off obtained for early diagnosis for our population was 72.8 µg/L for PT and 95 µg/L term newborns. Variation of nIRT in newborns requires more studies to determine the initial cut-off for screening CF.

Early diagnosis of galactosemia and restricted dietary content of galactose and lactose is crucial for preventing long term complications. It was observed that even in presence of residual galactose-1-uridyltransferase (GALT) activity, symptoms of galactosemia persists which might be due to different variants. Dilemma in determining factors and variants suggested a lower cut-off limit for NBS for TGAL [35]. Succoio et al published a total blood galactose (TGAL) cut-off of 7 mg/dL in 44334 newborns screened in Campania that led to 50% increase galactosemia cases [36]. Present study observed a cut-off of 14.9 mg/dL for term and 12.7 mg/dL for PT newborns (Table 3).

Children diagnosed with MSUD present with different symptoms and severity and thus diagnosing at an early age is indispensable to prevent neurological damage and its sequel [37]. The levels depicted significant differences between TERMNBW and PTLBW groups. PT newborns showed a wide range compared to others. Initiation of parenteral nutritional supplement with required amino acids in PT newborns might have influenced the results of MSUD in DBS specimen. A

value of 3.4 mg/dL might be considered as the cut-off level for MSUD cases. Hence, a judicious evaluation is required for PT newborns undergoing NBS testing.

The major limitation of the study is that sensitivity and specificity could not be determined for the cut-off values as recall were made for those who were screened positive in the initial screening. Secondly, genetic analysis was not performed for confirmation of the variants. However, the major strength of the study is the large sample size and the various study groups and sub-groups included such as LBW, VLBW, ELBW, Moderate PT and very PT in male and female newborns born in a tertiary centre in Central India. A detailed quantitative determination in so many groups for all the eight NBS parameters in Indian newborns yet to be published. Hence, the study provides a foundation for researchers from various other region to report the overall cut-off for their respective newborn population.

Conclusion

The study has provided a detailed comparison and reference values observed in various study groups and sub-groups. The findings suggest more accurate reference cut-off levels to determined considering the gestational age and birth weight of the newborns. More, so each lab must set up the cut-off levels based on their methodology and population inflow as significant variation across individuals might be there. Significant differences in 17-OHP values among the study groups and sub-groups was noteworthy indicating the need to establish an adjusted cut-off value based upon gender, birth weight, and gestational age. NBS is crucial for a newborn to have a healthy quality life. Genetic diversity might influence few parameters like G6PD, biotinidase and CF and thus there is need for improvising detection and genetic guidance to the parents. Future research is required to be undertaken in large cohort from different geographical regions of a country to have more accurate adjusted cut-offs and biological references for the NBS parameters in newborns.

Funding

The project was approved as intramural non-funded project. All tests undertaken for the research purpose were performed free of cost for the participants.

Ethical consideration

The study was reviewed and approved by the Institute Research Cell and Institute Ethics Committee and had been performed in accordance with the ethical standards described in an appropriate version of the 1975 Declaration of Helsinki, as revised in 2000. Written/verbal informed consent was taken from their legal representatives for the study.

Consent for publication

As per the IEC approved patient information sheet and informed consent, all participants have been explained that the research study shall be published in scientific meetings and journals and they were enrolled only after their consent. All authors have reviewed and agreed to the manuscript in the present form for submission.

Availability of data and material

The data is presently available with the principal investigator (Corresponding Author). It is not available in the public domain due to privacy or ethical restrictions. It be made available from the corresponding author upon reasonable request. The letter shall be reviewed and approved by all the authors and the Head of the Institution, following which it shall be made available.

Competing interests

The authors declare that they have no known competing financial interests or personal relationships that could have appeared to influence the work reported in this paper.

Authors contribution

SP, and RN developed the concept proposal. SP and EM formulated the study design. RN and EM provided intellectual content for the study. SP and SS performed the literature search. SP, NV, SS and RN performed data acquisition, sample collection and laboratory analyses. SP, NV and RN performed the statistical data analysis. SP and RN prepared the first draft of the manuscript. EM and SS performed the manuscript editing and all authors performed the final manuscript review. All authors read and approved the final manuscript.

Abbreviations

ACHDNC – Advisory Committee on Heritable Disorders in Newborn and Children
ANOVA – one way analysis of variance
BW – birth weight
CDC – Center of Disease Control
CF – cystic fibrosis
DBS – dried blood spot
ELBW – extremely low birth weight
ELISA – enzyme linked immunosorbent assay
GA – gestational age
GALT – galactose-1-uridyltransferase
HPT – hypothalamic-pituitary-thyroid
IEMD – inborn errors of metabolic disorders
IQR – Interquartile range
LBW – low birth weight
LCMS – liquid chromatography mass spectrometry
LRL – lower reference limit
n17-OHP – newborn 17-hydroxyprogesterone
nBIOT – newborn biotinidase
NBS – newborn screening
NBW – normal birth weight
nG6PD – newborn glucose 6-phosphate dehydrodenase
nGAL – newborn galactose
nIRT – newborn immunoreactive trypsinogen
nMSUD – newborn maple syrup urine disease
nPKU – newborn phenylketonuria
NSQAP – Newborn Screening Quality Assurance Program
nTSH – newborn thyroid stimulating hormone
PT – preterm

TGAL – total blood galactose
URL – upper reference limit
VLBW – very low birth weight

References

1. Prasad EM, Kinha R, Bendre R. Biological Reference Intervals for 17α-Hydroxyprogesterone Immunoreactive Trypsinogen, and Biotinidase in Indian Newborns. BioMed. 2024;4(3):268–276. DOI: 10.3390/biomed4030021.
2. Preterm birth. Fact sheets, World health Organization. 2023. Available from: https://www.who.int/news-room/fact-sheets/detail/preterm-birth
3. Beken S, Abali S, Yildirim Saral N, Guner B, Dinc T, Albayrak E, et al. Early Postnatal Metabolic Profile in Neonates With Different Birth Weight Status: A Pilot Study. Front Pediatr. 2021;9:646860. DOI: 10.3389/fped.2021.646860.
4. Sontag MK, Miller JI, McKasson S, Sheller R, Edelman S, Yusuf C, et al. Newborn screening timeliness quality improvement initiative: Impact of national recommendations and data repository. PloS One. 2020;15(4):e0231050. DOI: 10.1371/journal.pone.0231050.
5. NBS01 | Dried Blood Spot Specimen Collection for Newborn Screening. Available from: https://clsi.org/shop/standards/nbs01/
6. Kutar A, Ramanan PV, Eapen EK. Postnatal Growth at 64 Weeks Postmenstrual Age in Preterm Infants Delivered at ≤ 34 Weeks' Gestation: A Single Center Study. Indian Pediatr. 2024;61(6):540–544. URL: https://link.springer.com/10.1007/s13312-024-3203-3.
7. Girotra S, Mohan N, Malik M, Roy S, Basu S. Prevalence and Determinants of Low Birth Weight in India: Findings From a Nationally Representative Cross-Sectional Survey (2019-21). Cureus. 15(3):e36717. DOI: 10.7759/cureus.36717.
8. International Statistical Classification of Diseases and Related Health Problems. ICD10, Volume2_en_2010. World Health Organization. Available from: https://icd.who.int/browse10/Content/statichtml/ICD10Volume2_en_2010.pdf
9. Cutland CL, Lackritz EM, Mallett-Moore T, Bardají A, Chandrasekaran R, Lahariya C, et al. Low birth weight: Case definition & guidelines for data collection, analysis, and presentation of maternal immunization safety data. Vaccine. 2017;35(48Part A):6492–6500. DOI: 10.1016/j.vaccine.2017.01.049.
10. Ichihara K, Ozarda Y, Barth JH, Klee G, Qiu L, Erasmus R, et al. A global multicenter study on reference values: 1. Assessment of methods for derivation and comparison of reference intervals. Clin Chim Acta. 2017;467:70–82. DOI: 10.1016/j.cca.2016.09.016.
11. Khan AR, Alothaim A, Alfares A, Jowed A, Enazi SMA, Ghamdi SMA, et al. Cut-off values in newborn screening for inborn errors of metabolism in Saudi Arabia. Ann Saudi Med. 2022;42(2):107–118. DOI: 10.5144/0256-4947.2022.107.
12. Sadik I, Pérez de Algaba I, Jiménez R, Benito C, Blasco-Alonso J, Caro P, et al. Initial Evaluation of Prospective and Parallel Assessments of Cystic Fibrosis Newborn Screening Protocols in Eastern Andalusia: IRT/IRT versus IRT/PAP/IRT. Int J Neonatal Screen. 2019;5(3):32. DOI: 10.3390/ijns5030032.
13. Clerico A, Ripoli A, Masotti S, Musetti V, Aloe R, Dipalo M, et al. Evaluation of 99th percentile and reference change values of a high-sensitivity cTnI method: A multicenter study. Clin Chim Acta. 2019;493:156–161. DOI: 10.1016/j.cca.2019.02.029.
14. Herrick KA, Perrine CG, Aoki Y, Caldwell KL. Iodine Status and Consumption of Key Iodine Sources in the U.S. Population with Special Attention to Reproductive Age Women. Nutrients. 2018;10(7):874. DOI: 10.3390/nu10070874.
15. Mandel SJ, Hermos RJ, Larson CA, Prigozhin AB, Rojas DA, Mitchell ML. Atypical hypothyroidism and the very low birthweight infant. Thyroid Off J Am Thyroid Assoc. 2000;10(8):693–695. DOI: 10.1089/10507250050137770.
16. Kaluarachchi DC, Allen DB, Eickhoff JC, Dawe SJ, Baker MW. Increased Congenital Hypothyroidism Detection in Preterm Infants with Serial Newborn Screening. J Pediatr. 2019;207:220–225. DOI: 10.1016/j.jpeds.2018.11.044.
17. van Trotsenburg P, Stoupa A, Léger J, Rohrer T, Peters C, Fugazzola L, et al. Congenital Hypothyroidism: A 2020-2021 Consensus Guidelines Update-An ENDO-European Reference Network Initiative Endorsed by the European Society for Pediatric Endocrinology and the European Society for Endocrinology. Thyroid Off J Am Thyroid Assoc. 2021;31(3):387–419. DOI: 10.1089/thy.2020.0333.
18. LaFranchi SH. Thyroid Function in Preterm/Low Birth Weight Infants: Impact on Diagnosis and Management of Thyroid Dysfunction. Front Endocrinol. 2021;12:666207. URL: https://www.ncbi.nlm.nih.gov/pmc/articles/PMC8239410/.
19. Nascimento ML, Nascimento AL, Dornbusch P, Ohira M, Simoni G, Cechinel E, et al. Impact of the reduction in TSH cutoff level to 6 mIU/L in neonatal screening for congenital hypothyroidism in Santa Catarina: final results. Arch Endocrinol Metab. 2020;64:816–823. DOI: 10.20945/2359-3997000000299.
20. Verma P, Kapoor S, Kalaivani M, Vats P, Yadav S, Jain V, et al. An Optimal Capillary Screen Cut-off of Thyroid Stimulating Hormone for Diagnosing Congenital Hypothyroidism: Data from a Pilot Newborn Screening Program in Delhi. Indian Pediatr. 2019;56(4):281–286. DOI: 10.1007/s13312-019-1515-5.
21. Anne RP, Rahiman EA. Congenital hypothyroidism in India: A systematic review and meta-analysis of prevalence, screen positivity rates, and etiology. Lancet Reg Health Southeast Asia. 2022;5:100040. DOI: 10.1016/j.lansea.2022.100040.
22. Yang WC, Tai S, Hsu CL, Fu CM, Chou AK, Shao PL, et al. Reference levels for glucose-6-phosphate dehydrogenase enzyme activity in infants 7–90 days old in Taiwan. J Formos Med Assoc. 2020;119(1, Part 1):69–74. DOI:

10.1016/j.jfma.2019.03.010.
23. Algur N, Avraham I, Hammerman C, Kaplan M. Quantitative Neonatal Glucose-6-Phosphate Dehydrogenase Screening: Distribution, Reference Values, and Classification by Phenotype. J Pediatr. 2012;161(2):197–200. DOI: 10.1016/j.jpeds.2012.02.045.
24. Mukherjee S, Mallige A, Chowdhry A, Devgan A, Singh B, Mukherjee B, et al. Neonatal Screening for Glucose-6-Phosphate Dehydrogenase (G6PD) Deficiency in Eastern India. J Nepal Paediatr Soc. 2021;41(3):408–412. 10.3126/jnps.v41i3.37153.
25. Hayashi GY, Carvalho DF, de Miranda MC, Faure C, Vallejos C, Brito VN, et al. Neonatal 17-hydroxyprogesterone levels adjusted according to age at sample collection and birthweight improve the efficacy of congenital adrenal hyperplasia newborn screening. Clin Endocrinol (Oxf). 2017;86(4):480–487. DOI: 10.1111/cen.13292.
26. van der Kamp HJ, Oudshoorn CGM, Elvers BH, van Baarle M, Otten BJ, Wit JM, et al. Cutoff Levels of 17-α-Hydroxyprogesterone in Neonatal Screening for Congenital Adrenal Hyperplasia Should Be Based on Gestational Age Rather Than on Birth Weight. J Clin Endocrinol Metab. 2005;90(7):3904–3907. DOI: 10.5144/0256-4947.2022.107.
27. Choi YS, Lee BS, Kim KS, Kim EAR. Study of 17-alpha-hydroxy Progesterone in Preterm Infants. J Korean Soc Neonatol. 2012;19(2):77–83. URL: https://www.neo-med.org/journal/view.php?number=28.
28. Seeralar A, Jayachandran G, Srinivasan P. Interpretation of 17-hydroxyprogesterone levels in early neonatal period by dissociation-enhanced lanthanide fluorescent immunoassay technique in a tertiary care centre. Int J Res Med Sci. 2016;4(5):1522–1528. DOI: 10.18203/2320-6012.ijrms20161222.
29. Held PK, Bird IM, Heather NL. Newborn Screening for Congenital Adrenal Hyperplasia: Review of Factors Affecting Screening Accuracy. Int J Neonatal Screen. 2020;6(3):67. DOI: 10.3390/ijns6030067.
30. Pode-Shakked N, Blau A, Pode-Shakked B, Tiosano D, Weintrob N, Eyal O, et al. Combined Gestational Age- and Birth Weight-Adjusted Cutoffs for Newborn Screening of Congenital Adrenal Hyperplasia. J Clin Endocrinol Metab. 2019;104(8):3172–3180. DOI: 10.1210/jc.2018-02468.
31. Fingerhut R. False positive rate in newborn screening for congenital adrenal hyperplasia (CAH)-ether extraction reveals two distinct reasons for elevated 17alpha-hydroxyprogesterone (17-OHP) values. Steroids. 2009;74(8):662–665. DOI: 10.1016/j.steroids.2009.02.008.
32. Semeraro D, Verrocchio S, Di Dalmazi G, Rossi C, Pieragostino D, Cicalini I, et al. High Incidence of Partial Biotinidase Deficiency in the First 3 Years of a Regional Newborn Screening Program in Italy. Int J Environ Res Public Health. 2022;19(13):8141. DOI: 10.3390/ijerph19138141.
33. Zemanova M, Chrastina P, Sebron V, Prochazkova D, Jahnova H, Sanakova P, et al. Extremely low birthweight neonates with phenylketonuria require special dietary management. Acta Paediatr. 2021;110(11):2994–2999. DOI: 10.1111/apa.16035.
34. Arrudi-Moreno M, García-Romero R, Samper-Villagrasa P, Sánchez-Malo MJ, Martin-de-Vicente C. Neonatal cystic fibrosis screening: Analysis and differences in immunoreactive trypsin levels in newborns with a positive screen. An Pediatría Engl Ed. 2021;95(1):11–17. DOI: 10.1016/j.anpede.2020.04.022.
35. Kotb MA, Mansour L, Shamma RA. Screening for galactosemia: is there a place for it? Int J Gen Med. 2019;12:193–205. DOI: 10.2147/IJGM.S180706.
36. Succoio M, Sacchettini R, Rossi A, Parenti G, Ruoppolo M. Galactosemia: Biochemistry, Molecular Genetics, Newborn Screening, and Treatment. Biomolecules. 2022;12(7):968. DOI: 10.3390/biom12070968.
37. Liu Q, Li F, Zhou J, Liu X, Peng J, Gong L. Neonatal maple syrup urine disease case report and literature review. Medicine (Baltimore). 2022;101(50):e32174. DOI: 10.1097/MD.0000000000032174.

Supplementary Tables

Supplementary Table 1: Mean (SD) and median (range) and percentile values of the DBS nTSH (mIU/L) in the study groups.

	Study groups	Mean	SD	Median	Range	Min-Max	P value	1.0th
Gestational age							0.012*	
1	**Term**	3.2	2.1	2.8	16.8	0.1-16.9	1v2=0.02*	0.6
2	**Moderate PT**	3.1	2.2	2.6	16.8	0.1-16.9		0.6
3	**Very PT**	2.7	1.7	2.7	6.2	0.6-6.8		0.6
Birth weight							0.03*	
1	**NBW**	3.1	2.3	2.6	16.8	0.1-16.9		0.6
2	**LBW**	2.5	1.1	2.2	3.2	1.1-4.3		1.1
3	**VLBW**	2.5	1.1	2.2	3.2	1.1-4.3		1.1
4	**ELBW**	2.3	2.1	1.2	5.2	0.6-5.8		0.6

*denotes significance value of Independent-samples Kruskal-Wallis one way ANOVA test after Bonferroni correction for multiple tests;
PT denotes preterm; NBW denotes normal birth weight (BW); LBW denotes low BW; VLBW denotes very LBW; ELBW denotes extremely LBW; Term denotes > 37 gestational weeks (GW); Moderate PT denotes 32 to 37 GW; Very PT denotes 28 to <32 GW; NBW denotes BW ≥ 2500 g; LBW denotes BW 1500 to < 2500 g; VLBW denotes BW 1000 to <1500 g; ELBW denotes BW <1000 g.

Supplementary Table 2: Mean (SD) and median (range) and percentile values of the DBS nG6PD (IU/gHb) in the study groups.

	Study groups	Mean	SD	Median	Range	Min-Max	P value	1.0th	2.5th	3.0th	99th
Gestational age							0.046*				
1	**Term**	8.9	2	9.1	17.1	0.1-17.2	1v3=0.052*	1.9	4.4	4.8	13
2	**Moderate PT**	8.9	2.1	9.2	14	0.2-14.2		1.3	4	4.3	12.4
3	**Very PT**	9.8	2.3	10.8	9.4	4.8-14.2		4.8	4.8	4.8	4.8
Birth weight							0.77*				
1	**NBW**	9	1.9	9.1	14.4	0.2-14.6		2.7	4.4	4.8	12.4
2	**LBW**	8.4	2.9	9	10.3	0.8-11.1		0.8	0.8	0.8	
3	**VLBW**	8.4	2.9	9	10.3	0.8-11.1		0.8	0.8	0.8	
4	**ELBW**	8.3	3.4	9.3	10	1.1-11.1		1.1	1.1	1.1	

*denotes significance value of Independent-samples Kruskal-Wallis one way ANOVA test after Bonferroni correction for multiple tests, PT denotes preterm, NBW denotes normal birth weight (BW), LBW denotes low BW, VLBW denotes very LBW, ELBW denotes extremely LBW, Term denotes > 37 gestational weeks (GW), Moderate PT denotes 32 to 37 GW, Very PT denotes 28 to <32 GW, NBW denotes BW ≥ 2500 g, LBW denotes BW 1500 to < 2500 g, VLBW denotes BW 1000 to <1500 g, ELBW denotes BW <1000 g.

Supplementary Table 3: Mean (SD) and median (range) and percentile values of the DBS n17-OHP (nmol/L) in the study groups.

	Study groups	Mean	SD	Median	Range	Min-Max	P value	1.0th	2.5th	3.0th	99th
Gestational age							<0.001*				
1	**Term**	20.5	8.5	19.4	86.8	0.2-87.0	1v2<0.001*	0.9	6.6	7.3	48.6
2	**Moderate PT**	23.5	9.9	22.7	78.6	0.2-78.8	1v3=0.016*	1.6	6.3	7.9	48.6
3	**Very PT**	30.6	25.3	25.2	135.5	7.5-143.0		7.5	7.5	7.5	
Birth weight							<0.001*				
1	**NBW**	22.9	10.4	21.6	75.6	0.2-75.8	2v3=0.037*	1	6.1	7.2	48.9
2	**LBW**	30.8	15.8	26	62.8	16.0-78.8	1v3=0.002*	16	16	16	
3	**VLBW**	30.8	15.8	26	62.8	16.0-78.8	1v2<0.001*	16	16	16	
4	**ELBW**	40.6	43.1	24.9	131.6	11.4-143.0		11.4	11.4	11.4	

*denotes significance value of Independent-samples Kruskal-Wallis one way ANOVA test after Bonferroni correction for multiple tests, PT denotes preterm, NBW denotes normal birth weight (BW), LBW denotes low BW, VLBW denotes very LBW, ELBW denotes extremely LBW, Term denotes > 37 gestational weeks (GW), Moderate PT denotes 32 to 37 GW, Very PT denotes 28 to <32 GW, NBW denotes BW ≥ 2500 g, LBW denotes BW 1500 to < 2500 g, VLBW denotes BW 1000 to <1500 g, ELBW denotes BW <1000 g.

Supplementary Table 4: Mean (SD) and median (range) and percentile values of the DBS nBIOT (U) in the study groups.

	Study groups	Mean	SD	Median	Range	Min-Max	P value	1.0th	2.5th	3.0th	99th
Gestational age							0.74*				
1	**Term**	207.6	86.7	196.9	378.8	7.2-386.0		53.2	63.5	65.9	382.5
2	**Moderate PT**	207.4	88.8	196.1	368.9	24.0-392.9		51.7	59.6	63.3	382.5
3	**Very PT**	220.9	103.8	209.3	322.8	59.7-382.5		59.7	59.7	59.7	
Birth weight							0.006*				
1	**NBW**	198	86.9	181.8	358.5	24.0-382.5	1v2=0.005*	48	60.7	62.8	381.4
2	**LBW**	211.8	107.1	171.5	324.6	57.9-382.5		57.9	57.9	57.9	
3	**VLBW**	211.8	107.1	171.5	324.6	57.9-382.5		57.9	57.9	57.9	
4	ELBW	239.4	97.7	236.3	291.1	91.4-382.5		91.4	91.4	91.4	

*denotes significance value of Independent-samples Kruskal-Wallis one way ANOVA test after Bonferroni correction for multiple tests, PT denotes preterm; NBW denotes normal birth weight (BW), LBW denotes low BW, VLBW denotes very LBW, ELBW denotes extremely LBW, Term denotes > 37 gestational weeks (GW), Moderate PT denotes 32 to 37 GW, Very PT denotes 28 to <32 GW, NBW denotes BW ≥ 2500 g, LBW denotes BW 1500 to < 2500 g, VLBW denotes BW 1000 to <1500 g, ELBW denotes BW <1000 g.

Supplementary Table 5: Mean (SD) and median (range) and percentile values of the DBS nPKU (mg/dL) in the study groups.

	Study groups	Mean	SD	Median	Range	Min-Max	P value	1.0th	2.5th	3.0th	99th
"Gestational age"							0.83*				
1	**Term**	1.2	0.5	1.1	13.3	0.1-13.4		0.7	0.7	0.7	2.3
2	**Moderate PT**	1.2	0.6	1.1	11.9	0.1-12.0		0.7	0.7	0.7	2.3
3	**Very PT**	1.2	0.4	1.2	1.6	0.7-2.3		0.7	0.7	0.7	
"Birth											
weight"							0.68*				
1	**NBW**	1.2	0.6	1.1	11.3	0.7-12.0		0.7	0.7	0.7	2.2
2	**LBW**	1	0.4	0.9	1.6	0.7-2.3		0.7	0.7	0.7	
3	**VLBW**	1	0.4	0.9	1.6	0.7-2.3		0.7	0.7	0.7	
4	**ELBW**	1.5	0.4	1.5	1.4	0.7-2.1		0.7	0.7	0.7	

*denotes significance value of Independent-samples Kruskal-Wallis one way ANOVA test after Bonferroni correction for multiple tests, PT denotes preterm, NBW denotes normal birth weight (BW), LBW denotes low BW, VLBW denotes very LBW, ELBW denotes extremely LBW, Term denotes > 37 gestational weeks (GW), Moderate PT denotes 32 to 37 GW, Very PT denotes 28 to <32 GW, NBW denotes BW ≥ 2500 g, LBW denotes BW 1500 to < 2500 g, LBW denotes BW 1000 to <1500 g, ELBW denotes BW <1000 g.

Supplementary Table 6: Mean (SD) and median (range) and percentile values of the DBS nIRT (µg/L) in the study groups.

	Study groups	Mean	SD	Median	Range	Min-Max	P value	1.0th	2.5th	3.0th	99th
Gestational age							0.55*				
1	**Term**	25.3	20.7	20.2	341.8	0.1-341.9		2	2	2.5	95.3
2	**Moderate PT**	23.8	18.4	19.7	255.9	0.1-256.0		2	2	2	75.6
3	**Very PT**	20.3	10.6	18.2	46	3.4-49.4		3.4	3.4	3.4	
Birth weight							0.35*				
1	**NBW**	25.3	21.2	20.7	341.8	0.1-341.9		2	2	2	82.2
2	**LBW**	20.2	15.2	15.3	62.5	3.4-65.9		3.4	3.4	3.4	
3	**VLBW**	20.2	15.2	15.3	62.5	3.4-65.9		3.4	3.4	3.4	
4	**ELBW**	29.5	33.4	20.4	102.6	6.2-108.2		6.2	6.2	6.2	

*denotes significance value of Independent-samples Kruskal-Wallis one way ANOVA test after Bonferroni correction for multiple tests, PT denotes preterm, NBW denotes normal birth weight (BW), LBW denotes low BW, VLBW denotes very LBW, ELBW denotes extremely LBW, Term denotes > 37 gestational weeks (GW), Moderate PT denotes 32 to 37 GW, Very PT denotes 28 to <32 GW, NBW denotes BW ≥ 2500 g, LBW denotes BW 1500 to < 2500 g, LBW denotes BW 1000 to <1500 g, ELBW denotes BW <1000 g.

Supplementary Table 7: Mean (SD) a and median (range) and percentile values of the DBS nGAL (mg/dL) in the study groups.

	Study groups	Mean	SD	Median	Range	Min-Max	P value	1.0th	2.5th	3.0th	99th
Gestational age							0.51^				
1	**Term**	2.3	3.7	1.1	66.1	0.1-66.2		0.1	0.1	0.1	14.9
2	**Moderate PT**	1.9	2.7	1.1	22.5	0.1-22.6		0.1	0.1	0.1	12.8
3	**Very PT**	4	12.3	1.8	66.1	0.1-66.2		0.1	0.1	0.1	
Birth weight							0.13^				
1	**NBW**	2.1	2.9	1.1	19.8	0.1-19.9		0.1	0.1	0.1	13.9
2	**LBW**	6.9	16.5	2.2	66.1	0.1-66.2		0.1	0.1	0.1	
3	**VLBW**	6.9	16.5	2.2	66.1	0.1-66.2		0.1	0.1	0.1	
4	**ELBW**	1.7	1.4	2	3.3	0.1-3.4		0.1	0.1	0.1	

*denotes significance value of Independent-samples Kruskal-Wallis one way ANOVA test after Bonferroni correction for multiple tests, PT denotes preterm, NBW denotes normal birth weight (BW), LBW denotes low BW, VLBW denotes very LBW, ELBW denotes extremely LBW, Term denotes > 37 gestational weeks (GW), Moderate PT denotes 32 to 37 GW, Very PT denotes 28 to <32 GW, NBW denotes BW ≥ 2500 g, LBW denotes BW 1500 to < 2500 g, VLBW denotes BW 1000 to <1500 g, ELBW denotes BW <1000 g.

Supplementary Table 8: Mean (SD) and median (range) and percentile values of the DBS nMSUD (mg/dL) in the study groups.

	Study groups	Mean	SD	Median	Range	Min-Max	P value	1.0th	2.5th	3.0th	99th
"Gestational age"							0.011*				
1	**Term**	1.9	0.8	1.9	14.9	0.1-15.0	1v2=0.01*	0.2	0.4	0.5	3.6
2	**Moderate PT**	1.8	1	1.7	20.9	0.1-21.0		0.1	0.5	0.6	3.4
3	**Very PT**	1.7	0.7	1.9	2.7	0.3-3.0		0.3	0.3	0.3	
"Birth weight"							0.017*				
1	**NBW**	1.8	0.6	1.8	3.6	0.1-3.7	1v2=0.023*	0.3	0.5	0.5	4.5
2	**LBW**	1.5	0.8	1.6	2.8	0.3-3.1		0.3	0.3	0.3	
3	**VLBW**	1.5	0.8	1.6	2.8	0.3-3.1		0.3	0.3	0.3	
4	**ELBW**	1.7	0.8	1.9	2	0.5-2.5		0.5	0.5	0.5	

*denotes significance value of Independent-samples Kruskal-Wallis one way ANOVA test after Bonferroni correction for multiple tests, PT denotes preterm; NBW denotes normal birth weight (BW), LBW denotes low BW, VLBW denotes very LBW, ELBW denotes extremely LBW, Term denotes > 37 gestational weeks (GW), Moderate PT denotes 32 to 37 GW, Very PT denotes 28 to <32 GW, NBW denotes BW ≥ 2500 g, LBW denotes BW 1500 to < 2500 g, VLBW denotes BW 1000 to <1500 g, ELBW denotes BW <1000 g.

Research Article

Association of serum sortilin and insulin resistance in patients with gestational diabetes mellitus

Rupa Thakur[1], Leena Chand[1], Anjana Vinod[1*], Sowmya Krishnamurthy[1]

[1]*Department of Biochemistry, Sri Ramachandra Medical College and Research Institute, Chennai, India*

Article Info

[*]***Corresponding Author:***
Anjana Vinod
Assistant Professor, Department of Biochemistry
Sri Ramachandra Medical College & Research Institute, SRIHER, Chennai, India
Contact no: 9400918252
E-mail: anjanavinod1014@gmail.com

Keywords

Gestational Diabetes Mellitus, Insulin resistance, HOMA-IR, Sortilin

Abstract

Introduction: Gestational diabetes mellitus is a condition in which glucose intolerance develops during pregnancy. Sortilin is a type I transmembrane protein, that belongs to the VPS10 family of post-Golgi trafficking receptors that is involved in signaling, intracellular sorting, and transport of proteins. Sortilin is required for the storage of glucose and co-expressed with the glucose transporter GLUT4 in differentiated adipocytes. This study aimed to evaluate serum sortilin level in individuals with GDM and to elucidate its relation with insulin resistance.

Methodology: This was a case-control study. It involved 80 pregnant women, 40 with GDM (case group) and 40 healthy pregnant women (control group). Fasting blood glucose, HbA1c, insulin, HOMA-IR, and sortilin were analyzed in all the participants. Statistical analysis was performed with SPSS, version 26.0.

Results: Age, gestational week, and blood pressure showed no significant difference in both groups. Body mass Index (BMI), fasting blood glucose, glycated hemoglobin (HbA1c), fasting insulin, homeostasis model assessment of insulin resistance (HOMA-IR), and sortilin were significantly higher in the GDM group. Maternal serum sortilin showed a statistically significant positive correlation with BMI, fasting plasma glucose, serum insulin, HOMA-IR, and HbA1c. (r:0.37, p:<0.05; r:0.64, p:<0.001; r:0.38, p:<0.001; r:0.42, p<0.001, r:0.68, p<0.001 respectively). The Receiver Operating Characteristics (ROC) curve indicated sortilin as a potential biomarker for the prediction of cases with an area under a curve of 0.98 (p-value<0.001) and for the cut-off point value of >2.6ng/ml, the sensitivity was 97.5%, specificity was 97.5%, false negative rate was 2.5% and false positive rate was 2.5%. The Youden's index was 0.95, thus indicating the diagnostic accuracy of sortilin.

Conclusion: This study aimed to evaluate serum sortilin level in individuals with GDM and to elucidate its relation with insulin resistance. In this study, we observed that serum sortilin concentration was significantly higher in individuals with gestational GDM than in healthy pregnant women. Also, serum sortilin had a statistically significant positive correlation with fasting blood glucose, fasting insulin, HOMA-IR, and glycated hemoglobin. The area under the curve of ROC and the Youden's index shows the impeccable diagnostic accuracy of sortilin.

Introduction

Gestational diabetes mellitus is a condition in which glucose intolerance develops during pregnancy [1]. Globally, the prevalence of Gestational diabetes mellitus is around 14% of pregnancies. The prevalence of GDM in India is 0.80% of pregnancies in 2020 [2].

Several risk factors are implicated in the development of gestational diabetes mellitus namely, increased maternal age, obesity, family history of type 2 diabetes mellitus etc. In a normal gestation, the insulin sensitivity increases in the early gestation, but in the mid-2nd and 3rd trimester, the surge of local and placental hormones like oestrogen, prolactin, placental lactogen and growth hormone will elevate the blood glucose level. This increase in blood glucose level is associated with a compensatory increase in insulin secretion. The beta cells compensate for this increased metabolic demand by hypertrophy or hyperplasia. In gestational diabetes mellitus, the beta-cells inadequately compensates for the increased demand. Also, gestational diabetes mellitus is associated with decrease in insulin sensitivity of the tissues [3].

Previous studies have demonstrated a marked- reduction in insulin mediated glucose transport in the skeletal muscles of patients with gestational diabetes mellitus. This reduction in glucose transport is more severe in obese gestational diabetes mellitus individuals. Insulin mediates the transport of glucose across membranes via GLUT 4 transporters. GLUT 4 proteins are downregulated in the adipose tissue of pregnant women and this decrease is more profound in women with gestational diabetes mellitus. Also, the insulin induced translocation of GLUT4 to plasma membrane is abnormal in individuals with gestational diabetes mellitus [4].

Various proteins are involved in the translocation of GLUT 4 between the surface of plasma membrane and trans-Golgi network (TGN). The GLUT4 receptors from the plasma membrane are internalised into peripheral endosomes. From the peripheral endosomes, GLUT 4 is retrieved into trans-Golgi network, a perinuclear compartment. This prevents GLUT 4 from being degraded by the lysosomes [5]. Sortilin is a sorting protein which is involved in the export of GLUT4 from endosomes to TGN. It is a single-pass type 1 transmembrane glycoprotein encoded by the SORT1 gene. The luminal VPs 10 (vacuolar protein sorting 10 protein) domain of sortilin interacts with the first luminal loop of GLUT4, thereby rerouting it from entering the degradative pathway to recycling pathway. Hence sortilin plays an important role in insulin resistance. A case-control study done by Ozalp et al in 87 pregnant women showed an elevated level of serum sortilin in women with gestational diabetes mellitus [6,7,8,9].

This study was aimed to compare the level of serum sortilin between normal pregnant women and gestational diabetes mellitus women and to correlate the level of serum sortilin with insulin resistance. To our knowledge, this is the first study investigating sortilin levels specifically in an Indian ethnic population, highlighting its regional and demographic uniqueness compared to prior research on GDM.

Materials and Methods

Study design and Participants

This case-control study was conducted in the Department of Biochemistry & Department of Obstetrics & gynaecology, Sri Ramachandra Medical College & Research Institute, Chennai. The sample size was calculated with the power of 95% and α error of 5%. The study included 80 pregnant women of Indian ethnicity, with 40 healthy pregnant women above 18 years of age with singleton pregnancy in the control group and 40 women with GDM above 18 years of age with singleton pregnancy in the case group. The study was carried out over a one-year period, spanning from January 2023 to December 2023.

All the participants in the study underwent 75g oral glucose tolerance test between 24-28 weeks of gestation. The diagnostic criteria of International Association of Diabetes and Pregnancy Study Groups was used to interpret the oral glucose tolerance test. Pregnant women with hypertension, overt diabetes mellitus, multiple gestation, chronic hepatic, or renal diseases were excluded from the study. The study was conducted after obtaining ethical clearance from the Institutional Ethics Committee (REF: CSP/23/JUL/131/577).

Informed consent was obtained from all the participants. Baseline characteristics like age, gestational age, systemic blood pressure and body mass index were obtained from the study participants. Venous blood sampling was carried out by a trained phlebotomist. Blood samples for fasting blood glucose (Cobas e 6000 clinical chemistry analyser), glycated hemoglobin (Tosoh Automated Glycohemoglobin Analyzer HLC-723G8 analyser), serum insulin (Cobas e 602 immunoassay analyser) were processed within 3 hours of collection., and were processed in automated platforms. Serum samples for sortilin measurement were stored at –20°C and were analyzed collectively using a sandwich enzyme-linked immunosorbent assay (Human SORT1 ELISA Kit, catalogue number EH15347). The assay's detection range was 0.156–10 ng/mL, with a sensitivity of 0.094 ng/mL, and both intra-assay and inter-assay coefficients of variation were below 6%.

Statistical analysis

The statistical analysis was carried out by using the software

Statistical Package for the Social Science (SPSS) Version 26.0. The normality of the data was tested using Shapiro-wilk's test. Data showed normal distribution and hence was expressed as mean ± standard deviation. Independent sample t test was performed and a two-tailed p-value of <0.05 was considered statistically significant. The p-value for serum maternal sortilin levels was adjusted for BMI using regression analysis. Correlation analysis between the various parameters was assessed using Pearson's correlation.

Result

Table 1: Comparison of demographic and clinical characteristics between control (normal pregnant women) and case group (women with Gestational diabetes mellitus).

Parameters	Control group (n=40)	Case group (n=40)	p-value
Age	26.88±4.32	27.38±3.26	0.56
SBP (mmHg)	107.35±10.41	108.70±7.96	0.51
DBP (mmHg)	67.95±8.29	70.00±8.47	0.27
G. weeks	23.90±4.48	23.90±6.34	1
BMI (Kg/m2)	24.15±3.89	28.39±4.92	<0.001* *
FBG (mg/dL)	77.22±6.11	95.40±10.35	<0.001* *
HbA1c (%)	5.04±0.40	5.78±0.22	<0.001* *
Fasting Insulin (mU/ml)	10.30±5.60	24.11±19.26	<0.001* *
HOMA-IR	2.04±1.18	5.74±4.85	<0.001* *
Sortilin (ng/mL)	1.24±0.41	7.40±2.5	<0.001* *

Data represented as Mean ± standard deviation (SD). Comparison is done via independent sample t-test. * Statistically significant (p<0.05); * * Statistically significant (p<0.001)

BMI – body mass index; SBP – Systolic Blood pressure; DBP-Diastolic blood pressure; G. weeks- Gestational weeks; FBG – Fasting blood glucose; HbA1c – Glycated Hemoglobin; HOMA-IR: homeostatic model assessment of insulin resistance

Age, systemic blood pressure and gestational age did not show any statistically significant difference between the groups. But body mass index was significantly higher in women with gestational diabetes mellitus when compared with control group. Fasting blood glucose, HbA1c, fasting insulin, HOMA-IR and sortilin were significantly higher in women with gestational diabetes mellitus.

Table 2: Correlation of body mass index, HbA1c, fasting blood glucose, fasting insulin and HOMA-IR with sortilin.

Correlation coefficient (r value) with sortilin		P value
BMI	0.37	<0.05*
HbA1c	0.68	<0.001**
Fasting blood glucose	0.64	<0.001**
Fasting insulin	0.38	<0.001**
HOMA-IR	0.42	<0.001**

The correlation was done by using the Pearson correlation test

* Statistically significant (p<0.05)

* * Statistically significant (p<0.001)

Sortilin had a significant correlation with body mass index, glycated hemoglobin, fasting blood glucose, fasting insulin and HOMA-IR.

Figure 1: Scatter Plot Representing Correlation between HOMA-IR and Sortilin level in the case group.

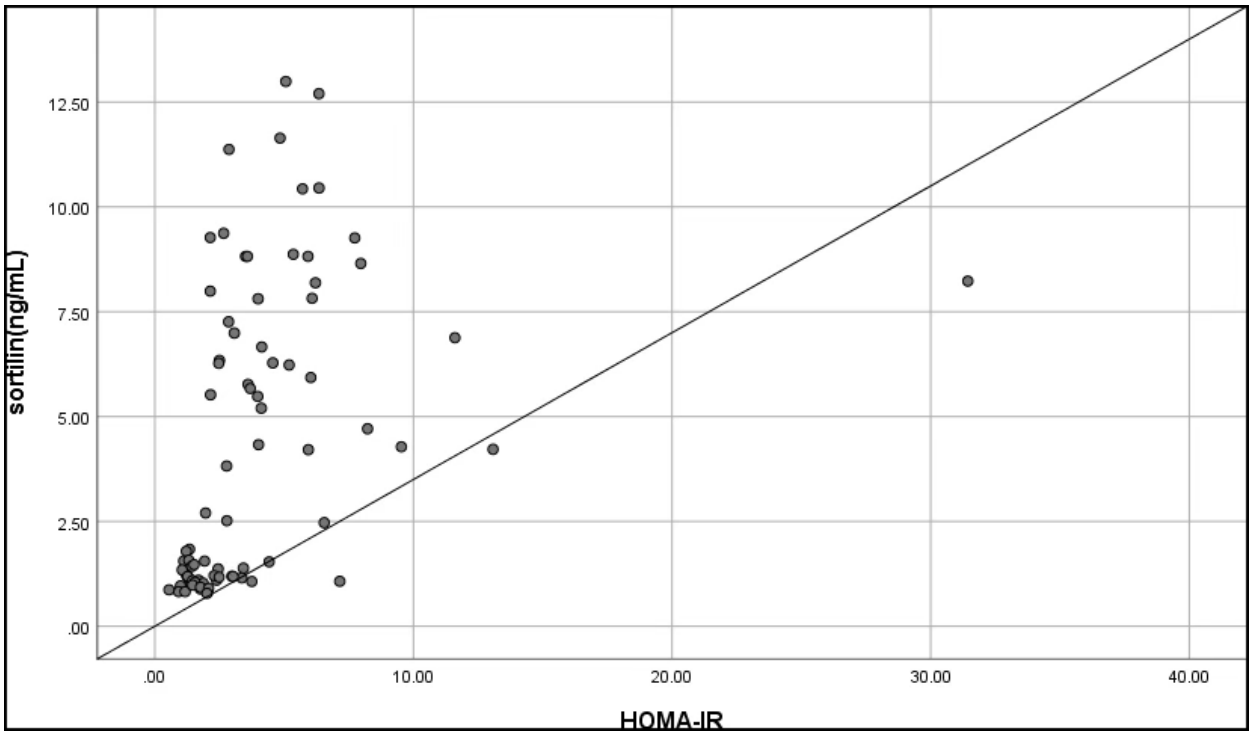

Sortilin level and HOMA-IR showed a strong positive association (correlation coefficient=0.42), which was statistically significant (p-value<0.001).

Figure 2: ROC curve of serum Sortilin.

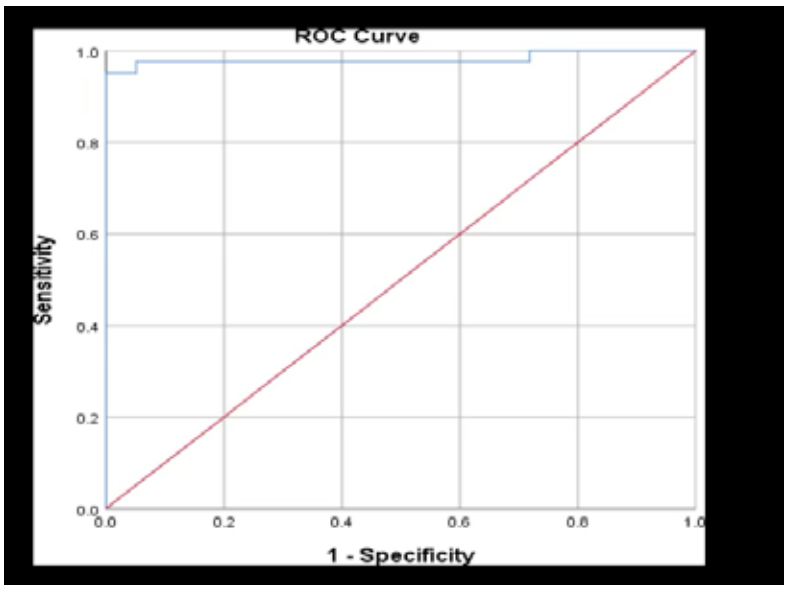

Table 3: ROC curve metrics.

Metrics	Value
Are under the curve (AUC)	0.98
Cut-off point value	>2.6 ng/mL
Youden's index	0.95
Sensitivity (2.6 ng/mL)	97.50%
Specificity (2.6 ng/mL)	97.50%

The Receiver Operating Characteristics (ROC) curve indicated sortilin as a potential biomarker with an area under a curve of 0.98 (p-value<0.001) and for the cut-off point value of >2.6ng/ml, the sensitivity was 97.5%, specificity was 97.5%, false negative rate was 2.5% and false positive rate was 2.5%. The Youden's index was 0.95, thus indicating the diagnostic accuracy of sortilin.

Table 4: 95% confidence interval for the ROC curve metrics.

Metrics	Value	95% confidence interval
Are under the curve (AUC)	0.98	0.95 – 1.00
Sensitivity (2.6 ng/mL)	97.50%	86.8% - 99.9%
Specificity (2.6 ng/mL)	97.50%	91.0% – 100%

Discussion

Sortilin is a post-Golgi trafficking receptor that is involved in signalling, intracellular sorting, and transport of proteins. It is highly expressed in metabolically active tissues such as the brain, liver, skeletal muscle, and adipose tissue. In adipocytes, sortilin plays an important role in the GLUT 4 pathway, affecting the peripheral transport of glucose into the cells [10,11].

In this study, BMI was significantly higher in the GDM group (p-value<0.001) with a mean of 28.39 kg/m2. Individuals with GDM have a higher body mass index when compared to healthy pregnant women. This is in consistent with the previously published studies [12]. The high pre-pregnancy BMI of the mother is an established risk factor for GDM (12). According to Lee et al, the prevalence of GDM was highest among Asian women with BMI ≥30 kg/m2 (13.8%) followed by women with BMI ≥25 kg/m2 (10.2%) [13]. Seshiah et al. also reported a significantly higher prevalence of GDM at higher BMI [14].

The significantly elevated fasting blood glucose and HbA1c level in this study are in alignment with Yanqin Lou et al., in which early-pregnancy FBG and HbA1c of pregnant women with GDM were higher when compared with the control group [15].

The fasting insulin and HOMA-IR level were significantly elevated in the GDM group when compared to the control group (p value<0.001). There is evidence to suggest that insulin and C-peptide values are good predictors of GDM [16]. The concentrations of fasting insulin and C-peptide are significantly higher in pregnant women with GDM than in healthy pregnant women [17].

Homeostatic model assessment for insulin resistance (HOMA-IR) is calculated from the values of fasting glucose and fasting insulin or C-peptide. The homeostatic model assessment for insulin resistance has mostly been reported to be significantly more abundant in pregnant women with GDM and is a good predictor of GDM [18].

However, some studies have downplayed the significance of HOMA-IR when compared to other parameters. Some studies have suggested that there is no difference in HOMA-IR between pregnant women with GDM and healthy pregnant women [19]. So, it can be concluded that the significance of HOMA-IR is questionable and HOMA-IR alone is insufficient for use as a predictive marker for GDM [20].

In early gestation, insulin sensitivity increases, promoting the uptake of glucose into adipose stores in preparation for the energy demands of later pregnancy. As the pregnancy progresses, there is an increase in local and placental hormones, namely estrogen, progesterone, leptin, cortisol, placental lactogen and placental growth hormone which together promote a state of insulin resistance. Also, the systemic and placental inflammatory responses associated with normal pregnancy are exaggerated by obesity. This is also reflected in elevated maternal circulating level of proinflammatory cytokines and increased mRNA expression of IL-1β, IL-8 and monocyte chemoattractant protein (MCP) 1 in the placenta. The increase in placental inflammatory mediators may be secondary to infiltration of maternal macrophages, which are elevated in the maternal circulation in obesity and known to release the proinflammatory cytokines IL-1, IL-6 and TNFα. [21].

Pro-inflammatory cytokines are known to impair insulin signalling and inhibit insulin release from β-cells. These factors induce insulin resistance either by diminishing insulin receptor (IR) tyrosine kinase activity, increasing serine phosphorylation of IRS-1, or through the STAT3-SOCS3 pathway, which degrades IRS-1. Hence, both increased concentration of placental hormones and inflammatory conditions together contribute to insulin resistance in GDM [21].

Sortilin had a normal distribution in the study and was expressed as mean and standard deviation. The mean Sortilin level in the control group was 1.24 ng/mL and, in the case, group was 7.40 ng/mL (Table 6). The Sortilin level was significantly higher in the GDM group when compared to the control group (p-value < 0.001). Also, sortilin had a statistically significant positive correlation with fasting blood glucose, insulin, HOMA-IR and HbA1c. This observation was consistent with already published articles. Mirac Ozalp et al. in their study revealed that serum sortilin level was significantly higher in the GDM group as compared to non-GDM [22].

This study also revealed that there was a positive correlation between serum sortilin, insulin, HOMA-IR and glycated hemoglobin.

On the contrary to the above-observed findings, Demir et al. compared the level of sortilin in newly diagnosed T2DM

patients with individuals having normal glucose tolerance and found that serum sortilin level were low in the T2DM group. Also, serum sortilin level are negatively correlated with fasting blood glucose, insulin, and HOMA-IR [23].

The differences between our findings and those of Demir et al. might be attributed to several factors. Variations in the characteristics of study populations, such as ethnicity, duration of diabetes, glycemic control, and presence of other health conditions, can influence serum sortilin levels differently. Additionally, methodological differences including assay types, sample storage, and timing of measurements may affect results. Sortilin is involved in diverse processes like lipid metabolism and inflammation, which might vary depending on the stage. Finally, disparities in study design, sample size, and statistical analysis could also contribute to the contrasting observations.

The relationship of sortilin with age, gestational age, BMI, FBG, HbA1c and HOMA-IR was analyzed in the GDM group. Sortilin did not show any statistically significant correlation with age or gestational age. However, sortilin had a statistically significant positive relationship with fasting blood glucose, HbA1c and HOMA-IR.

The Receiver Operating Characteristics (ROC) curve indicated sortilin as a potential biomarker for the prediction of cases with an area under a curve of 0.98 (p-value <0.001); and for the cut-off point value of >2.6ng/ml, the sensitivity was 97.5%, specificity was 97.5%, false negative rate was 2.5% and false positive rate was 2.5%. The Youden's index was 0.95, thus indicating the diagnostic accuracy of sortilin.

As sortilin plays an important role in this retrograde traffic of GLUT4 from endosomes and the reformation of IRVs; sortilin protein is a target of insulin signalling through the Insulin/PI3K/AKT signalling cascade and insulin increases sortilin protein expression.

Sortilin also plays an important role in intracellular lipid metabolism. In the hepatocytes, sortilin promotes the lipolysis of VLDL, through apolipoprotein B-100, resulting in elevated low-density lipoprotein concentration in the circulation. In the macrophages, it modulates the LDL uptake and foam cell formation, thereby playing an important role in atherosclerosis [24]. Sortilin is also linked to endothelial dysfunction and hypertension by exerting its effect through the S1P pathway; augmenting the production of Reactive Oxygen Species. This increased ROS production leads to impaired endothelium relaxation [25].

Conclusion

Hence, in this study, serum sortilin concentration was significantly higher in GDM individuals. The Receiver Operating Characteristics (ROC) curve indicated sortilin as a potential biomarker for the prediction of cases with an area under a curve of 0.98 (p-value<0.001) and a cut-off value of >2.6ng/ml. Also, serum sortilin had a statistically significant positive correlation with BMI, FBG, HbA1c and HOMA-IR, reflecting its role in the pathogenesis and later implication of GDM.

Limitations

The study was limited by its single-centre design, which may affect the wider applicability of the results. Additionally, the research included only participants of Indian ethnicity, restricting the generalizability to other populations. Furthermore, sortilin levels were not assessed during the postpartum period, leaving potential changes in this timeframe unexplored.

Author Contributations

Conceptualization: Rupa Thakur, Leena Chand, Anjana Vinod, K Sowmya; Methodology: Rupa Thakur, Leena Chand, Anjana Vinod, K Sowmya; Material preparation, data collection: Rupa Thakur, Leena Chand, Anjana Vinod, K Sowmya; Formal analysis and investigation: Rupa Thakur, Leena Chand, Anjana Vinod, K Sowmya; Writing - original draft preparation: Rupa Thakur, Leena Chand, Anjana Vinod, K Sowmya; Writing - review and editing: Rupa Thakur, Leena Chand, Anjana Vinod, K Sowmya; Resources: Rupa Thakur, Leena Chand, Anjana Vinod, K Sowmya; Supervision and final approval: Rupa Thakur, Leena Chand, Anjana Vinod, K Sowmya; Accountability for the research: Rupa Thakur, Leena Chand, Anjana Vinod, K Sowmya.

Ethics Approval

The study was approved by Sri Ramachandra Institute of Higher Education and Research Institutional Ethics Committee (CSP/23/JUL/131/577). This study was conducted in compliance with the ethical principles for medical research involving human subjects, in accordance with the Declaration of Helsinki.

Funding

No funding was received for the conduct of this project.

Data Availability

The datasets used and/or analysed during the current study are not available because of the Institutional policy.

Disclosure of Conflict of Interest

The authors declare that there is no conflict of interest concerning this study.

Acknowledgement

The authors like to express sincere gratitude to all participants who contributed to this study, and our Institution for providing the necessary facilities. Their invaluable support has been instrumental in the completion of this research.

References

1. Omazić J, Viljetić B, Ivić V, Kadivnik M, Zibar L, Müller A, et al. Early markers of gestational diabetes mellitus: what we know and which way forward? Biochem Med (Zagreb). 2021;31(3):030502. https://doi.org/10.11613/BM.2021.030502
2. Chakraborty A, Yadav S. Prevalence and determinants of gestational diabetes mellitus among pregnant women in India: an analysis of National Family Health Survey Data. BMC Womens Health. 2024;24(1):147. https://doi.org/10.1186/s12905-024-02936-0
3. Plows JF, Stanley JL, Baker PN, Reynolds CM, Vickers MH. The Pathophysiology of Gestational Diabetes Mellitus. Int J Mol Sci. 2018;19(11):3342 https://doi.org/10.3390/ijms19113342
4. Alesi S, Ghelani D, Rassie K, Mousa A. Metabolomic Biomarkers in Gestational Diabetes Mellitus: A Review of the Evidence. Int J Mol Sci. 2021;22(11):5512. https://doi.org/10.3390/ijms22115512
5. Shewan AM, van Dam EM, Martin S, Luen TB, Hong W, Bryant NJ, et al. GLUT4 recycles via a trans-Golgi network (TGN) subdomain enriched in Syntaxins 6 and 16 but not TGN38: involvement of an acidic targeting motif. Mol Biol Cell. 2003;14(3):973–986. https://doi.org/10.1091/mbc.e02-06-0315
6. Mazella J, Zsürger N, Navarro V, Chabry J, Kaghad M, Caput D, et al. The 100-kDa neurotensin receptor is gp95/sortilin, a non-G-protein-coupled receptor. J Biol Chem. 1998 Oct 9;273(41):26273–26276. https://doi.org/10.1074/jbc.273.41.26273
7. Petersen CM, Nielsen MS, Nykjaer A, Jacobsen L, Tommerup N, Rasmussen HH, et al. Molecular identification of a novel candidate sorting receptor purified from human brain by receptor-associated protein affinity chromatography. J Biol Chem. 1997;272(6):3599–3605. https://doi.org/10.1074/jbc.272.6.3599
8. Jacobsen L, Madsen P, Moestrup SK, Lund AH, Tommerup N, Nykjaer A, et al. Molecular characterization of a novel human hybrid-type receptor that binds the alpha2-macroglobulin receptor-associated protein. J Biol Chem. 1996;271(49):31379–31383. https://doi.org/10.1074/jbc.271.49.31379
9. Hermey G, Riedel IB, Hampe W, Schaller HC, Hermans-Borgmeyer I. Identification and characterization of SorCS, a third member of a novel receptor family. Biochem Biophys Res Commun. 1999;266(2):347–351. https://doi.org/10.1006/bbrc.1999.1822
10. Blondeau N, Béraud-Dufour S, Lebrun P, Hivelin C, Coppola T. Sortilin in Glucose Homeostasis: From Accessory Protein to Key Player? Front Pharmacol. 2018;9:1561. https://doi.org/10.3389/fphar.2018.01561
11. Ariga M, Nedachi T, Katagiri H, Kanzaki M. Functional role of sortilin in myogenesis and development of insulin-responsive glucose transport system in C2C12 myocytes. J Biol Chem. 2008;283(15):10208–10220. https://doi.org/10.1074/jbc.m710604200
12. Sun Y, Shen Z, Zhan Y, Wang Y, Ma S, Zhang S, et al. Effects of pre-pregnancy body mass index and gestational weight gain on maternal and infant complications. BMC Pregnancy Childbirth. 2020;20(1):390. https://doi.org/10.1186/s12884-020-03071-y
13. Lee KW, Ching SM, Ramachandran V, Yee A, Hoo FK, Chia YC, et al. Prevalence and risk factors of gestational diabetes mellitus in Asia: a systematic review and meta-analysis. BMC Pregnancy Childbirth. 2018;18(1):494. https://doi.org/10.1186/s12884-018-2131-4
14. Seshiah V, Balaji V, Balaji MS, Sanjeevi CB, Green A. Gestational diabetes mellitus in India. J Assoc Physicians India. 2004;52:707–711. https://pubmed.ncbi.nlm.nih.gov/15839447/
15. Lou Y, Xiang L, Gao X, Jiang H. Clinical Value of Early-Pregnancy Glycated Hemoglobin, Fasting Plasma Glucose, and Body Mass Index in Screening Gestational Diabetes Mellitus. Lab Med. 2022;53(6):619–622. https://doi.org/10.1093/labmed/lmac058
16. Clark CM, Qiu C, Amerman B, Porter B, Fineberg N, Aldasouqi S, et al. Gestational diabetes: should it be added to the syndrome of insulin resistance? Diabetes Care. 1997;20(5):867–871. https://doi.org/10.2337/diacare.20.5.867
17. Correa PJ, Vargas JF, Sen S, Illanes SE. Prediction of gestational diabetes early in pregnancy: targeting the long-term complications. Gynecol Obstet Invest. 2014;77(3):145–149. https://doi.org/10.1159/000357616
18. Rodrigo N, Glastras SJ. The Emerging Role of Biomarkers in the Diagnosis of Gestational Diabetes Mellitus. J Clin Med. 2018;7(6):120. https://doi.org/10.3390/jcm7060120
19. Andersson-Hall U, Carlsson NG, Sandberg AS, Holmäng A. Circulating Linoleic Acid is Associated with Improved Glucose Tolerance in Women after Gestational Diabetes. Nutrients. 2018;10(11):1629. https://doi.org/10.3390/nu10111629
20. Bonakdaran S, Khorasani ZM, Jafarzadeh F. Increased serum level of fgf21 in gestational diabetes mellitus. Acta Endocrinol (Buchar). 2017;13(3):278–281. https://doi.org/10.4183/aeb.2017.278
21. Aye ILMH, Lager S, Ramirez VI, Gaccioli F, Dudley DJ, Jansson T, et al. Increasing maternal body mass index is associated with systemic inflammation in the mother and the activation of distinct placental inflammatory pathways. Biol Reprod. 2014;90(6):129. https://doi.org/10.1095/biolreprod.113.116186
22. Özalp M, Akbaş H, Kızılırmak R, Albayrak M, Yaman H, Akbaş M, et al. Maternal serum sortilin levels in gestational diabetes mellitus. Gynecol Endocrinol. 2021;37(10):941–944. https://doi.org/10.1080/09513590.2021.1972966
23. Demir İ, Yildirim Akan O, Guler A, Bozkaya G,

Aslanipour B, Calan M. Relation of Decreased Circulating Sortilin Levels With Unfavorable Metabolic Profiles in Subjects With Newly Diagnosed Type 2 Diabetes Mellitus. Am J Med Sci. 2020;359(1):8–16. https://doi.org/10.1016/j.amjms.2019.10.003

24. Su X, Chen L, Chen X, Dai C, Wang B. Emerging roles of sortilin in affecting the metabolism of glucose and lipid profiles. Bosn J Basic Med Sci. 2022;22(3):340–352. https://doi.org/10.17305/bjbms.2021.6601
25. Varzideh F, Jankauskas SS, Kansakar U, Mone P, Gambardella J, Santulli G. Sortilin drives hypertension by modulating sphingolipid/ceramide homeostasis and by triggering oxidative stress. J Clin Invest. 2022;132(3):e156624. https://doi.org/10.1172/jci156624

Research Article

Enhancing Laboratory Quality: A Comprehensive Sigma Metric Analysis for Diverse Biochemical Parameters

Shobha C. Ramachandra[1], Kusuma K. Shivashankar[1], Akila Prashant[1], Swetha N. Kempegowda[1*]

[1]*Department of Biochemistry, JSS Medical College, JSS Academy of Higher Education & Research, Mysuru, India*

Article Info

[*]***Corresponding Author:***
Swetha N. Kempegowda
ORCID: https://orcid.org/0000-0002-3163-7405
Department of Biochemistry,
JSS Medical College, JSS Academy of Higher Education & Research, Mysuru, India
E-mail: swethank@jssuni.edu.in
Mobile: 9886403651

Keywords

Sigma metrics, Clinical chemistry, Quality control, Proficiency Testing

Abstract

Background: Ensuring quality in the analytical phase of clinical chemistry is paramount for accurate diagnosis and treatment. Sigma metrics offer a quantitative framework to assess and enhance laboratory performance. In this study, we intend to comprehensively assess diverse biochemical parameters using three different QC databases to determine their suitability and design a tailor-made QC plan based on this assessment.

Methods: This is a retrospective study, from an NABL-accredited laboratory. The coefficient of variation (CV) % was obtained from the IQC results and the Bias % from Proficiency Testing (PT) results. The Sigma value was calculated using the TEa from three different biological variation databases (EFLM database, Westgard database, CLIA database). QGI was calculated for parameters with a Sigma value <3.

Results: Around 28-33 parameters in different instruments showed a Sigma value <3 (poor performance). However, several parameters lack TEa values in the CLIA database, preventing their inclusion in assessments of acceptability.

Conclusion: By integrating Sigma calculations with established TEa standards, this study helped in identifying areas needing improvement. This comprehensive assessment ensured the evaluation of the performance of diverse analytes, thereby ensuring higher accuracy and reliability in patient test results.

Introduction

In the current era of evidence-based medicine, healthcare providers increasingly rely on laboratory investigations to guide patient management. Consequently, the demand on laboratories has intensified, necessitating the delivery of high-quality reports. Ensuring quality in laboratory processes has now become more crucial than ever, aiming to enhance the accuracy and timeliness of reports for better patient care. Laboratories must meticulously uphold the quality standards across the various phases of the testing process to ensure the accuracy of the test results [1].

Quality Control (QC) constitutes an integral component of the Total Quality Management system, encompassing all processes dedicated to upholding the quality of test results. Notably, this includes internal quality control (IQC) procedures executed prior to the analysis of patient samples. Regularly assessing the performance of QC is paramount for the success of any quality management system. Sigma metrics have emerged as a particularly effective tool in this regard, providing a simple and efficient means of evaluating IQC performance. Serving as a valuable guide, sigma metrics aid in planning corrective and preventive actions to enhance overall quality [2].

Sigma metrics serve as a quality management tool that delineates the defects per million opportunities (DPMO). The application of Six Sigma proves valuable in pinpointing error occurrences and shaping an effective strategy for enhancing quality. The scale of six sigma DPMO values spans from 0 to 6, where a sigma value surpassing 6 denotes excellent performance, while a sigma value less than 3 signifies below-par performance. Computation of sigma values involves factors like TEa, bias % and CV%. Numerous studies have leveraged the sigma metrics tool to evaluate their IQC performance for specific parameters, successfully identifying areas of poor performance and implementing corrective measures. However, the unavailability of total allowable error (TEa) values for all parameters poses a challenge. Studies have used either the The European Federation of Clinical Chemistry and Laboratory Medicine (EFLM) database or Biological variation from Westgard and Clinical Laboratory Improvement Amendment (CLIA) TEa for sigma values calculations [3,4].

Despite this, there is a scarcity of studies that assess the application of this tool in evaluating a majority of biochemical parameters such as immunoassays, blood gas parameters, and urine parameters. Hence, the current study intends to conduct a comprehensive sigma metric analysis across a diverse array of biochemical parameters to quantify performance errors accurately. Furthermore, a meticulous comparative analysis was undertaken using TEa values from all three QC databases to select the most suitable one for our laboratory setup. This analysis is intended to design a tailored quality control plan using the Sigma metric approach and thorough root cause analysis (RCA), ensuring the delivery of accurate results to the patient.

Methodology

This is a retrospective study, and data for the study were extracted between Jan 2023 to June 2023 from an NABL-accredited laboratory. The coefficient of variation(CV) % was obtained from the IQC results and the Bias % from Proficiency Testing (PT) results.

This study was done to assess the IQC performance of 90 biochemical parameters analysed on COBAS 6000 (c501, e601), COBAS 311(c 311), COBAS 411 (e411) fully automated Biochemistry analyzers, Radiometer Basic 800 series blood gas analyser, Gonotec OSMOMAT 3000 Osmometer and Bio-Rad D10 Haemoglobin system on a Sigma Scale by calculating the sigma metrics for each parameter.

The total TEa was obtained from three different biological variation databases:

1. CLIA Requirements for Analytical Quality-88 Proficiency Testing Criteria in terms of total allowable error “TEa” for acceptable performance for each analyte,
2. Desirable Biological Variation Database specifications, and
3. EFLM (desirable total error was taken into consideration) [5–7].

- CV% was calculated from BIORAD Internal QC for the parameters.

  $CV\% = (SD/mean) \times (100)$
- Bias percentage for each parameter was calculated from the PT results

  $Bias\% = (\text{Our EQAS result} - \text{peer group mean using the same instrument and method}) \times 100$

  Peer group mean using the same instrument and method
- Sigma metrics was calculated with the following formula:

  $Sigma = (TEa - Bias\%)/CV\%$ where Bias and CV% are the indicators of systematic and random errors respectively.

Sigma value was calculated for all the parameters using all three biological variation databases. However, TEa was not available for all the parameters in CLIA requirements for analytical quality and Desirable Biological Variation Database specifications, hence quality goal index (QGI) and QC plan was designed based on the EFLM database.

QGI was calculated for those parameters with Sigma value <3 (based on EFLM Sigma)

The QGI ratio was calculated using the following formula,

$QGI = Bias/1.5 \times CV\%$

The criteria used for interpreting QGI when test parameters fall short of Six Sigma is

<0.8 Imprecision, 0.8-1.2 Imprecision and inaccuracy, >1.2 Inaccuracy

Statistical analysis

Data collected were entered in MS Excel 2010. Descriptive analysis measures like Mean, SD and CV% were obtained from the IQC data. Bias%, Sigma and QGI values was calculated using the formulas as described in the methodology section. The TEa values were as per the guidelines described above.

Results

A total of 90 parameters analysed in the NABL-accredited clinical biochemistry lab were selected.

Table 1 depicts the performance of the parameters based on Sigma metrics. EFLM TEa, EFLM Sigma, and QGI calculated are depicted in Table 2. Table 3 depicts the Sigma Metric tools for QC design and frequency.

Table 4 depicts the QC plan (Control rules to be applied and QC frequency) was designed based on Sigma value calculated using the EFLM TEa%.

Table 1: Performance of the parameters based on Sigma metric analysis using three different TEa sources.

TEa Sources	Instrument	≥ 3Sigma	< 3 Sigma
EFLM- sigma	**Clinical Chemistry:** COBAS c501	Urea, triglyceride, LDL, Total Bilirubin, GGT, Creatine kinase, LDH, iron, amylase, CRP,	sodium, potassium, chloride, total protein, albumin, ALP (level 1), calcium, magnesium, cholinesterase.
		Glucose, creatinine, uric acid, total cholesterol, HDL, ALP (Level 2) AST, ALT, phosphorus, lipase, free kappa, free lambda	
	Clinical Chemistry: COBAS c311	Creatinine, uric acid, urea, total cholesterol, triglyceride, LDL, Total Bilirubin, AST, ALT, IgM,	Sodium, chloride, direct bilirubin, albumin, Calcium, beta 2 microglobulin
		Glucose, potassium, HDL, Total protein, Albumin, ALP, Phosphorus, D-dimer, IgA, IgG	
	Immunoassay: COBAS e601 & COBAS e411	Insulin, PSA, Testosterone	Ferritin, free T3, free T4, T3, PTH, T4, Vitamin D, Vitamin B12, beta HCG, C-peptide,
		Cortisol, folic acid, FSH, LH, prolactin, T3 (e411), TSH, Trop T, AFP, CA 19-9, CA 125, CEA	
	Others: Radiometer / BIORAD -D10 / Osmometer	PCO2, PO2	pH, HbA1c
BV-sigma	**Clinical Chemistry**: COBAS c501	Total Bilirubin, direct bilirubin, ALT, Creatine kinase, LDH, amylase, lipase, lactate, cholinesterase, iron	Uric acid, sodium, potassium, chloride, triglyceride, calcium, UIBC, total protein, albumin, Magnesium (level 1), urine creatinine, urine chloride.
		Glucose, creatinine, urea, total cholesterol, HDL, LDL,AST, , ALP, GGT, phosphorus, magnesium (level 2),CRP, free kappa, free lambda, G6PD, homocysteine, Urine albumin, potassium, sodium, protein & antiTPO	
	Clinical Chemistry: COBAS c311	Creatinine, urea, total cholesterol, LDL, Total Bilirubin, direct bilirubin, AST, ALT, IgA, IgM,	Uric acid, sodium, chloride, triglyceride, albumin (level 2), ALP, Calcium, ammonia, ADA, Beta2 microglobulin.
		Glucose, potassium , HDL, total protein, albumin (level1), phosphorus, D-dimer, IgG	

	Immunoassay: COBAS e601 & COBAS e411	C-peptide, Cortisol, Folic acid, FSH, insulin, prolactin, PTH, T3 (e411), TSH, testosterone, CKMB, Trop T, BNP, AFP, CA 19-9, CA-125, CEA, Vitamin B12, Anti TPO	Free T3, Free T4, T3 (Cobas 6000), T4
	Others: Radiometer / BIORAD -D10 / Osmometer	pH, PCO2, PO2 (level1, 2) Urine osmolality,	PO2 (level 3)
CLIA- sigma	**Clinical Chemistry**: COBAS c501	Creatinine, uric acid, triglyceride, total bilirubin, AST, ALT, ALP, Creatine kinase, LDH, Magnesium, iron	Potassium, chloride, HDL, LDL, Direct bilirubin, GGT, calcium, phosphorus, lipase, lactate, UIBC, cholinesterase
		Glucose, urea, sodium, total cholesterol, total protein, albumin, amylase	
	Clinical Chemistry: COBAS c311	Glucose, creatinine, uric acid, total cholesterol, triglyceride, Total Bilirubin, Total protein, AST, ALP, IgG	Potassium, HDL, LDL, Direct bilirubin, calcium, phosphorus, D-dimer, IgA, IgM
		Urea, sodium, chloride, Albumin, ALT	
	Immunoassay: COBAS e601 & COBAS e411	Cortisol, folic acid	FT3, FT4, beta HCG(level1,2), T3 (Cobas 6000), T3 (e411- level1), TSH, AFP (e411- level 1)
		Insulin, Beta HCG (level 3), T3 (e411), T4, AFP (e411- level 3)	
	Others: Radiometer / BIORAD -D10 / Osmometer	PCO2, PO2	pH

> 6 sigma > 3 < 6 sigma < 3 sigma

Table 2: Quality Goal Index based on European Federation for Laboratory Medicine TEa and Sigma.

Analyte	CV%	Bias %	EFLM-TEa	EFLM-Sigma	QGI	Imprecision/ Inaccuracy
HbA1c	2.62	-2.05	3.1	1.96	-0.52	Imprecision
	2.54	-2.05	3.1	2.02	-0.53	Imprecision
Beta 2 Microglobulin	2.394	5.69	6.4	0.29	1.58	Inaccuracy
	3.342	5.69	6.4	0.21	1.13	Inaccuracy
	3.212	5.69	6.4	0.22	1.18	Imprecision & Inaccuracy
Ferritin e601	4.544	11.4	13.8	0.53	1.67	Inaccuracy
	3.862	11.4	13.8	0.62	1.97	Inaccuracy
	3.954	11.4	13.8	0.61	1.92	Inaccuracy
Free T3 e411	5.286	13.19	6.5	-1.27	1.66	Inaccuracy
	4.576	13.19	6.5	-1.46	1.92	Inaccuracy
	4.122	13.19	6.5	-1.62	2.13	Inaccuracy
Free T4 e411	3.614	-1.775	6.3	2.23	-0.33	Imprecision
	3.942	-1.775	6.3	2.05	-0.3	Imprecision
	5.102	-1.775	6.3	1.58	-0.23	Imprecision

Intact Parathormone 601	5.932	5.75	20	2.4	0.65	Imprecision
	5.946	5.75	20	2.4	0.64	Imprecision
	6.968	5.75	20	2.05	0.55	Imprecision
Total T3 e601	4.33	-0.43	11.6	2.78	-0.07	Imprecision
Total T4 e601	4.394	-0.43	8.6	2.06	-0.07	Imprecision
	4.212	-0.43	8.6	2.14	-0.07	Imprecision
	4.088	-0.43	8.6	2.21	-0.07	Imprecision
Total T4 e411	4.96	1.53	8.6	1.43	0.21	Imprecision
	5.534	1.53	8.6	1.28	0.18	Imprecision
	4.726	1.53	8.6	1.5	0.22	Imprecision
25-OH Vitamin D-total e601	39.95	-1.59	12.4	0.35	-0.03	Imprecision
	9.53	-1.59	12.4	1.47	-0.11	Imprecision
	6.718	-1.59	12.4	2.08	-0.16	Imprecision
Sodiumc501	1.268	-0.41	0.7	0.88	-0.22	Imprecision
	1.356	-0.41	0.7	0.82	-0.2	Imprecision
Potassiumc501	1.752	0.97	4.8	2.19	0.37	Imprecision
	1.564	0.97	4.8	2.45	0.41	Imprecision
Chloridec501	1.84	1.33	1.3	-0.02	0.48	Imprecision
	1.694	1.33	1.3	-0.02	0.52	Imprecision
Total Proteinc501	1.674	-0.72	3.5	2.52	-0.29	Imprecision
	2.008	-0.72	3.5	2.1	-0.24	Imprecision
Albuminc501	1.706	0.37	3.4	1.78	0.14	Imprecision
	2.608	0.37	3.4	1.16	0.09	Imprecision
Alkaline Phosphatase c501	3.196	2.25	10.4	2.55	0.46	Imprecision
Calcium (Gen 2) c501	1.34	1.04	2.3	0.94	0.52	Imprecision
	1.192	1.04	2.3	1.06	0.58	Imprecision
Magnesium c501	2.772	-0.95	4	1.79	-0.23	Imprecision
	1.772	-0.95	4	2.79	-0.36	Imprecision
Cholinesterase c501	1.386	-0.71		0.51	-0.34	Imprecision
	1.016	-0.71		0.7	-0.47	Imprecision
Sodium c311	1.106	-0.84746	0.7	1.39	-0.51	Imprecision
	1.124	-0.84746	0.7	1.38	-0.5	Imprecision
Chloride c311	1.138	-1.1	1.3	2.11	-0.64	Imprecision
	1.184	-1.1	1.3	2.03	-0.62	Imprecision
Albumin c311	1.548	-1.08	3.4	2.89	-0.47	Imprecision
	1.866	-1.08	3.4	2.4	-0.39	Imprecision
Calcium (Gen 2) c311	1.486	1.33	2.3	0.65	0.6	Imprecision
	1.18	1.33	2.3	0.82	0.75	Imprecision

QGI <0.8: Imprecision, 0.8-1.2 Imprecision and inaccuracy, >1.2 Inaccuracy

Note: QGI could not be calculated for these parameters as EFLM value was not available: Osmolality serum and urine, Ammonia, Anti-TPO, AMH, G6PD, HCYS, ADA, CSF, and urine parameters, pH, pO2, Connecting-Peptide, ß- HCG, Vitamin B12, 25-OH Vitamin D-total, CKMB Mass, NT-Pro Brain Natriuretic Peptide

Table 3: Sigma Metric tools for QC design and frequency.

Sl. No	Sigma Metric	Control Rule	QC Frequency
1	Sigma ≥6	13s, N=2	1 per 1000 patient sample
2	Sigma 5 <6	1 3s/2 2s/R 4s, N = 2	1 per 450 patient samples
3	Sigma 4 < 5	1 3s/2 2s/R 4s /4 1s, N= 4	1 per 200 patient samples
4	Sigma 3 < 4	All Westgard rules as above including 10X, N = 6	1 per 45 patient samples
5	Sigma < 3	Maximum Westgard rules, N = 6	1 per 10 patient samples

Table 4: QC plan (Control Rule and QC frequency) based on Sigma metrics.

Sl. No	Sigma Metric	Control Rule	QC Frequency	Parameters
1	Sigma ≥6	$1_{3s,}$ N=2	1 per 1000 patient samples	**Roche Cobas 6000**: - Urea, Triglycerides, LDL Cholesterol, Total Bilirubin, Gamma-Glutamyl transferase, creatine kinase, LDH, Amylase, Iron, CRP, Insulin, Total Testosterone, Total PSA **Roche c311**- Creatinine, Urea, Uric acid, Total Cholesterol, Triglycerides, LDL Cholesterol, Total Bilirubin, Aspartate Transaminase, Alanine Transaminase, IgM **Roche e411**: Cortisol, FSH, Luteinizing Hormone, Prolactin, TSH, Total T3
2	Sigma 5 <6	$1_{3s}/2_{2}s/R_{4s}$, N = 2	1 per 450 patient samples	**Roche Cobas 6000**- Uric acid, HDL Cholesterol **Roche c311**- potassium, HDL Cholesterol, Phosphorus, D-Dimer, IgA
3	Sigma 4 < 5	$1_{3s}/2_{2s}/R_{4s}/4_{1s,}$ N= 4	1 per 200 patient samples	**Roche Cobas 6000**- Total Cholesterol, Aspartate Transaminase, Phosphorus, Lipase **Roche c311**- glucose, Potassium, Total Protein, Alanine Transaminase, IgG, ALP **Roche e411**: CA 19-9, CA 125, CEA **Radiometer**: pCO2
4	Sigma 3 < 4	All Westgard rules as above including 10X, N = 6	1 per 45 patient samples	**Roche Cobas 6000**- Glucose, hs Troponin T, Folic acid **Roche c311**- Free Kappa, Free Lambda **Roche e411**: Troponin T, AFP
5	Sigma < 3	Maximum Westgard rules, N = 6	1 per 10 patient samples	**Roche Cobas 6000**- Creatinine, Sodium, potassium, chloride, Total Protein, Albumin, ALP, Calcium, Magnesium, Cholinesterase, Ferritin, Total T3, Total T4 **Roche c311**- Sodium, Chloride, Direct Bilirubin, Albumin, Calcium, Beta 2 Microglobulin **Roche e411**: Free T3 and T4, Intact Parathormone, C peptide, Total T4, **Biorad D10**: HbA1c

Discussion

Quality Management (QM) in clinical laboratories encompasses the supervision of all tasks and activities necessary to maintain high standards of excellence. It involves establishing a quality policy, implementing quality assurance and planning, and continuously improving quality in the testing process. These components collectively form the foundation of Total Quality Management (TQM). Dr. James O. Westgard emphasized this by stating, "Quality is everyone's job"[8].

Six Sigma Metrics

The Greek letter Sigma in Six Sigma represents "Standard Deviation". "Six Sigma aims to maintain an error rate that is more than six standard deviations from the mean, indicating a process with minimal defects. The Six Sigma approach incorporates robust techniques such as Define-Measure-Analyze-Improve-Control (DMAIC) and RCA to identify and eliminate defects and variations within a process. Additionally, it offers an objective assessment of analytical techniques and equipment, alongside the strategic framework needed for practical implementation [9].

Globally, many laboratories design their IQC protocols based on their national standards. The frequency of QC runs per day is often determined by the daily sample load in the laboratory [10,11]. According to the National Accreditation Board for Testing and Calibration Laboratories (NABL 112) guidelines in India, it is recommended to run two levels of IQC before analyzing patient samples, followed by one level of IQC every eight hours to maintain laboratory quality. However, each laboratory should develop a unique, customized Individualized Quality Control Plan (IQCP) based on Six Sigma values. This approach, which ensures six standard deviations between the parameter mean and its control limits, is crucial in minimizing laboratory errors [2,12].

Principal Findings

Sigma Metrics: In this study, 27 parameters demonstrated a Sigma value less than 3 based on the EFLM database TEa values.

1. Using Desirable Biological Variation database specifications published on the Westgard website, 27 parameters showed a Sigma value less than 3.
2. Nearly 29 parameters demonstrated a Sigma value less than 3 from TEa values obtained from the CLIA database.

These findings suggest that several parameters lack TEa values in the CLIA database, preventing their inclusion in assessments of acceptability. Several studies[9–12] conducted earlier have evaluated the clinical chemistry and immunoassay analytes, while the analytes of Blood Gas analysis, HbA1c, Osmolality, Urine parameters and Tumour markers were not analysed in them. However, the present study is unique in that it has included all these analytes for Sigma Metric analysis along with the routine clinical chemistry and immunoassay analytes. A study conducted by Chinese Researchers [13] has made use of the TEa values derived from the EQA standard of China for all the urinary analytes as no other database has the TEa values for the Urinary Analytes.

Table 1 presents the aforementioned findings, while Table 2 details the QGI analysis based on TEa values from the EFLM database. QGI values help assess QC performance, identifying whether the issues are due to imprecision or inaccuracy or both. Most analytes exhibited either inaccuracy or imprecision, except Beta2-Microglobulin in c311 and Alkaline Phosphatase Level 2 in c501, which showed both. Addressing these issues will significantly enhance the quality of reports, thereby minimizing errors.

RCA was conducted for parameters with a Sigma value less than 3, highlighting imprecision or inaccuracy. Figure 1 illustrates the Fishbone diagram, which identifies potential issues in the laboratory that could lead to a lowered Sigma value. These issues may stem from materials, methods, equipment, processes, the environment, or personnel. Any deficiencies in these areas can affect Sigma metrics and result in errors in patient results. Therefore, it is critical to monitor Sigma metrics more frequently, rather than on a semi-annual or annual basis.

Figure 1: Root cause analysis for the analytes with poor performance (Sigma<3).

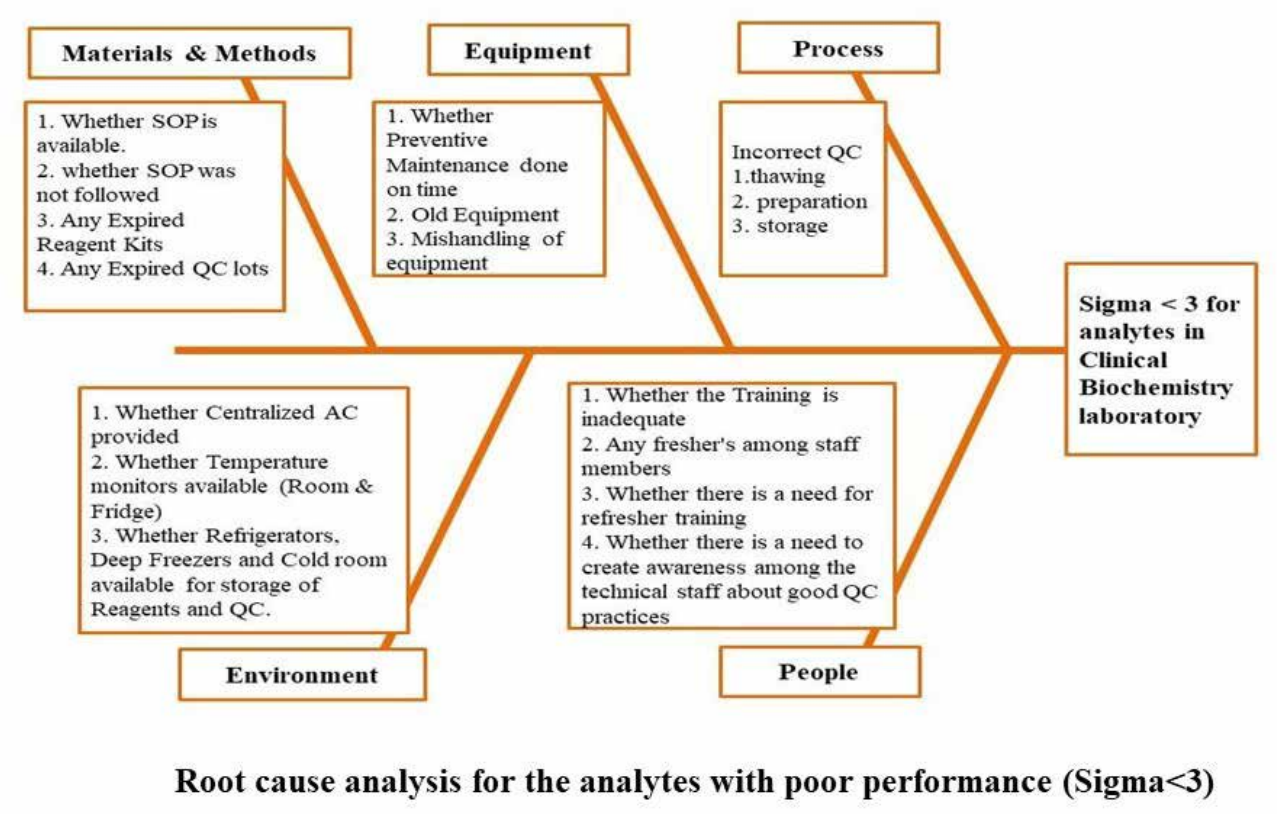

The practical application of Sigma Metrics in clinical biochemistry has direct implications for designing a QC program. Our study demonstrates that the Sigma metrics vary depending on the TEa guidelines used, with no universally accepted TEa guidelines currently available [4]. Various TEa guidelines/databases are utilized worldwide, including those from the College of American Pathologists (CAP), The Royal College of Pathologists of Australasia and the Australasian Clinical Biochemist Association Quality Assurance Program (RCPA), American Association of Bioanalysts (AAB), Desirable Quality Specifications based on Biological Variation (BV) on Westgard Website, Wadsworth Center of the New York State Department of Health (NYS), Wisconsin State Laboratory of Hygiene (WSLH), CLIA Amendments (CLIA), Canadian Fixed limits from the College of Physicians and Surgeons of Saskatchewan (CFX) and EFLM database

In the present study, TEa values from the CLIA, BV, and EFLM databases were used. It was observed that CLIA does not provide TEa for several Immunoassay and Chemistry parameters, while the BV and EFLM databases cover most analytes, except for ammonia, G-6PD, ADA, Homocysteine, CK-MB, NT-proBNP, C-peptide, Anti-TPO, Vit B12, Beta HCG, urine and CSF parameters. Among the three, EFLM database was the most stringent with narrower TEa values. The differences in Sigma values observed with different TEa guidelines showed that CLIA generally resulted in higher Sigma values compared to the BV and EFLM database for most of the analytes, though some analytes like Potassium, HDL, and Bilirubin, showed the opposite trend. Additionally, variations in Sigma values were noted between different instruments (e.g., c501 vs c311 and e601 vs e411) for different analytes. However, a previous study indicated that the Sigma variations across different TEa guidelines were more significant than the variations across different instruments using the same TEa guidelines [14].

A previous study conducted in North India [15] evaluated the Sigma metric values of HbA1c using the BIORAD-D10 instrument and reported Sigma values greater than 5 for both Level 1 and Level 2 Randox IQC, indicating excellent performance. In contrast, the present study, which used BIORAD QC for HbA1c, found Sigma values below 3. The Quality Goal Index (QGI) further indicated the presence of imprecision. This discrepancy underscores the potential impact on diabetic patient care if laboratory quality were assessed solely based on IQC or EQAS, without incorporating Sigma metric analysis.

The findings highlight the critical role of Sigma metrics, QGI, and RCA in ensuring accurate laboratory results. The RCA in this case suggested that the lower Sigma value (<3) for HbA1c may have resulted from improper handling of QC material, such as thawing or usage beyond the recommended 7-day period post-preparation. This issue was promptly communicated to laboratory technicians, emphasizing the need for strict adherence to QC handling protocols to avoid compromising

patient outcomes.
Additionally, a recent study from Libya published in Cureus [16] conducted Sigma metric analysis for blood gas analytes - pH, pO2, and pCO2 - across three different ABG analyzers. The study reported an unacceptable Sigma value (< 3) for pH, consistent with findings from the present study. However, both pO2 and pCO2 demonstrated marginal to excellent performance, with Sigma values ranging from 3 to 6, similar to the observations in our study. The RCA for the pH Sigma value being <3 indicated that samples analyzed on the Radiometer occasionally contained invisible clots. This was traced to a pre-analytical error - specifically, improper mixing of the blood sample at the time of collection. These tiny clots became lodged in the tubing near the electrode, compromising the accuracy of IQC, EQAS, and patient sample results. This finding reinforces the value of Sigma metric analysis in the early detection of such errors. In response, company personnel provided training to the nursing staff on proper techniques for blood sample collection, mixing, and transport to prevent recurrence.

QC frequency

The calculation of QC frequency, as shown in Table 3, [12,17] helps determine the number of QC runs required for different sample loads. QC frequency was planned based on the sigma metrics [17] and is summarized in Table 4. Planning and executing a QC plan based on the sigma metrics ensures the delivery of high-quality results to patients in a timely manner, consistent with the hospital's vision and mission.

The uniqueness of our study lies in its extensive analysis of a wide range of biochemical parameters using three different biological variation databases. This comprehensive analysis provides valuable insights into IQC performance across various parameters and has facilitated the implementation of appropriate corrective actions. However, the lack of TEa values for certain parameters across various biological variation databases was a limitation of our study. Our study emphasizes the need for standardization and harmonization of TEa models that are suitable for specific regions. However, achieving harmonization of TEa across laboratories remains a significant challenge, particularly in LMIC settings. Key barriers include the absence of standardized guidelines, weak regulatory frameworks for implementing TEa models, limited resources, economic constraints, inadequate training, variability in test methods, use of diverse testing platforms, and a general lack of prioritization for quality assurance protocols. Future large-scale, multi-centric collaborative approaches will be crucial in establishing uniform and standardized TEa models and quality control strategies.

Conclusion

Analytes with suboptimal performance require continuous monitoring by laboratory supervisors to ensure accurate and reliable reports. Laboratories are encouraged to explore the practical application and feasibility of integrating Sigma metrics into routine QC practices, particularly for analytes with a Sigma value below 3. Moreover, selecting appropriate TEa guidelines is critical when applying Sigma metrics to ensure accurate assessment of analyte performance.

Any conflict of interest

Authors declare no conflict of interest.

References

1. Badrick T. Evidence-Based Laboratory Medicine. Clin Biochem Rev 2013;34:43.
2. Kumar BV, Mohan T. Sigma metrics as a tool for evaluating the performance of internal quality control in a clinical chemistry laboratory. J Lab Physicians 2018;10:194–9. https://doi.org/10.4103/JLP.JLP_102_17
3. Luo Y, Yan X, Xiao Q, Long Y, Pu J, Li Q, et al. Application of Sigma metrics in the quality control strategies of immunology and protein analytes. J Clin Lab Anal 2021;35:e24041. https://doi.org/10.1002/JCLA.24041
4. van Heerden M, George JA, Khoza S. The application of sigma metrics in the laboratory to assess quality control processes in South Africa. Afr J Lab Med. 2022;11(1):1344. doi: 10.4102/ajlm.v11i1.1344.
5. Desirable Biological Variation Database specifications - Westgard n.d. https://westgard.com/clia-a-quality/quality-requirements/238-biodatabase1.html(Accessed on:10/07/2024)
6. CLIA Requirements for Analytical Quality - Westgard n.d. https://westgard.com/clia-a-quality/quality-requirements/125-clia.html (Accessed on:10/07/2024).
7. Six Sigma: Quality Design and Control Processes - Westgard n.d. https://westgard.com/lessons/advanced-quality-management-six-sigma/98-lesson67.html (Accessed on:10/07/2024).
8. Six Sigma - Westgard n.d. https://westgard.com/qc-applications/six-sigma-qc.html (Accessed on:10/07/2024)
9. S, Meera; K N N. Sigma metrics - A guide to quality control strategy in clinical Biochemistry laboratory. Int J Clin Biochem Res 2020;7:267–271. https://doi.org/10.18231/J.IJCBR.2020.058
10. Adiga US, Preethika A, Swathi K. Sigma metrics in clinical chemistry laboratory-A guide to quality control. Al Ameen J Med Sci 2015;8:4–5.
11. Raju Nilakantam S, Kasapura Shivashankar K, Prashant A, Dayananda M, Maduvanahalli Nataraj S, Authors Sathish Raju Nilakantam A, et al. Sigma-Metric Analysis to Evaluate Quality Management of Analytical Processes Using RCA and QGI in a Clinical Biochemistry Laboratory, South India. Int J Heal Allied Sci 2023;11:5. https://doi.org/10.55691/2278-344X.1035
12. Liu Q, Bian G, Chen X, Han J, Chen Y, Wang M, et

al. Application of a six sigma model to evaluate the analytical performance of urinary biochemical analytes and design a risk based statistical quality control strategy for these assays: A multicenter study. J Clin Lab Anal 2021;35:e24059. https://doi.org/10.1002/JCLA.24059

13. El Sharkawy R, Westgard S, Awad AM, Ahmed AOI, Iman EH, Gaballah A, et al. Comparison between Sigma metrics in four accredited Egyptian medical laboratories in some biochemical tests: an initiative towards sigma calculation harmonization. Biochem Medica 2018;28. https://doi.org/10.11613/BM.2018.020711
14. Mathew, Anisha, Debnath, Ekta, Chauhan, Preeti, Naik, Sanjukta and Singh R. Application of sigma metrics and method decision charts for assessment of quality assurance in BioRad D-10 HbA1c analyzer n.d. https://www.researchgate.net/publication/375074931_465_Application_of_sigma_metrics_and_method_decision_charts_for_assessment_of_quality_assurance_in_BioRad_D-10_HbA1c_analyzer#full-text
15. (Accessed on:10/07/2024)
16. Hamid H, Al-Wafi M, Ahmida MH, Elmansoury AM, Najah M. Beyond Total Error: An Observational Comparative Study of Sigma Metrics in Long-Term Arterial Blood Gas Analyzer Performance. Cureus 2025;17. https://doi.org/10.7759/CUREUS.77236
17. Zhou B, Wu Y, He H, Li C, Tan L, Cao Y. Practical application of Six Sigma management in analytical biochemistry processes in clinical settings. J Clin Lab Anal 2020;34. https://doi.org/10.1002/JCLA.23126.

Research Article

Anemia, Micronutrient Status, and Anthropometric Indicators in Undernourished Under-five Children: A Comprehensive Study on Nutritional Health

Aswanth KS[1], Nikhil Rajvanshi[1], Vinod Kumar[1], Swathi Chacham[1], Prashant Kumar Verma[1*]

[1]*Department of Pediatrics, All India Institute of Medical Sciences (AIIMS), Rishikesh, Uttarakhand, India*

Article Info

[*]***Corresponding Author:***
Prashant Kumar Verma
DM (Medical Genetics), Department of Pediatrics, All India Institute of Medical Sciences (AIIMS)
Rishikesh, Uttarakhand, India
Pin code: 249203
E-mail: 2004pkv@gmail.com
Mobile number: +91-9412592332
ORCID: 0000-0001-8929-5017

Keywords

Undernutrition, under-five, anemia, micronutrients, growth

Abstract

Introduction: Undernutrition in children is a serious global issue that adversely affects their physical and cognitive development. Anemia is a significant comorbidity contributing to increased mortality in undernourished children. However, it is not being addressed adequately. This study aims to evaluate the clinical and laboratory profile of anemia in undernutrition among under-five children.

Materials and methods: A cross-sectional study was conducted among children between six months to five years of age with undernutrition in a tertiary hospital in North India over a period of one year between December 2021 to December 2022. We observed the prevalence of anemia, its morphological type, micronutrient status, clinical features, and demographic parameters of these children.

Results: Of the 200 children who were enrolled in the study, 72% were found anemic with the proportion of mild, moderate, and severe anemia being 14%,33%, and 25% respectively. The most common type of anemia was microcytic (46.5%) followed by macrocytic (24.3%). Iron (68.7%) was the most common micronutrient deficient in these children with a significant number suffering from vitamin B12 (45.8%) deficiency. Mid-upper arm circumference, worm infestation, pica, and all serum-related parameters had statistical significance in comparison with the severity of anemia.

Conclusion: Despite the significant trend in various aspects of human development, undernutrition and anemia remain a formidable challenge, especially in developing countries. A high proportion of anemia in undernutrition indicates the gravity of the issue, yet not received the deserved attention.

Introduction

Adequate nutrition in early childhood is essential to ensure proper growth, organ development, and function. It is crucial for the effective immune system and neurological development as well. Undernutrition is one of the world's major health concerns, especially in developing countries. It continues to be one of the leading causes of under-five mortality accounting for 68·2% of the total under-5 mortality based on the 1990–2017 trends [1]. WHO defines undernutrition in children below five years in four forms: stunting [Length/height for age (L/HFA) below -2 Z], wasting [weight for height/length (WFH/L) below -2 Z], underweight [weight for age (WFA) below -2 Z], and micronutrient deficiencies. WHO recommends usage of WFH/L Z < -3Z and/or a mid-upper arm circumference (MUAC) value of <115 mm as an anthropometric parameter cut-off for defining children with severe acute malnutrition (SAM) and usage of WFH/L Z -2 Z to -3 Z and/or a MUAC of 115 to 125 mm for the diagnosis of moderate acute malnutrition (MAM) [2]. 149.2 million children were stunted and 45.4 million children were wasted as per 2021 WHO estimation [3]. According to NFHS-5 conducted in 2019-21, among children in India aged less than five years, 35.5% are stunted, 19.3% are wasted 7.7% are severely wasted, and 32.1% have underweight [4]. United Nations (UN) General Assembly on 1 April 2016 proclaimed the years between 2016 to 2025 as "The UN Decade of Action on Nutrition". Hence this decade is an unparalleled opportunity for addressing the issues related to undernutrition [3]. Undernutrition is associated with various comorbidities which have a significant effect on survival as well as long-term quality of life. Anemia is one such comorbidity. According to WHO, around 42% of children less than 5 years of age are anemic. The prevalence of anemia in Indian children aged 6 months to 5 years is 67.1% according to NFHS-5 which has increased from the NFHS-4 survey (58.6%) even after slight improvement in the under-five nutritional status [4]. Micronutrient deficiency remains a major issue in undernourished children. Though Iron is the most common micronutrient deficiency worldwide; vitamin B12 and folate deficiency also contribute to anemia in undernourished children significantly [5].

All management strategies by WHO and national guidelines recommend supplementing and replenishing micronutrients like Vitamin A, Iron, Magnesium, Potassium, etc. However, there is no clear-cut recommendation regarding vitamin B12 assessment and its supplementation in children with malnutrition. There is a lacuna in the literature regarding the anemia status of children with undernutrition. Therefore, this study was planned for estimating the proportion of anemia in children from six months to five years of age with undernutrition and their clinical profile, etiological factors along with micronutrient status with a special focus on iron, vitamin B12, and folic acid.

Materials and Methods

This was a hospital-based observational study done in the Department of Pediatrics of a tertiary care hospital in Northern India over 12 months from December 2021 to December 2022. The study was conducted after obtaining due clearance from the Institutional Ethics Committee (IEC/21/594) and performed in a manner to conform with the Helsinki Declaration of 1975, as revised in 2000 and 2008. As per WHO definitions, children with undernutrition between 6 months to five years of age who presented to outpatient and in-patient department of Pediatrics were enrolled [2]. As per Sarna et al., the prevalence of anemia was 40·5% among 1–4-year-olds [6]. The sample size calculated as per the formula $n=Z2P(1-P)/d2$ and obtained a number of 191. Hence, a convenient sample size of 200 was taken. Children with congenital anomalies, chronic systemic diseases, aplastic anemia, and hematological malignancies were excluded.

Detailed history and clinical examination were done for enrolled children. 1ml blood sample was taken in an EDTA vial and was processed by a five-part automated analyser, Sysmex XN1000 for hemogram. Age-based WHO cut-offs for hemoglobin were used to diagnose anemia. Peripheral smear examination along with serum iron, vitamin B12, and folate levels was done for all children with anemia. A 2 ml blood sample was collected in a plain vacutainer for serum iron, vitamin B12, and folate from which serum was separated. Serum iron was processed by a fully automated analyser, Beckman Coulter AU680. The ADVIA Centaur XP immunoassay system processed serum vitamin B12 and folate levels.

Statictical Analysis

Data collected was recorded in a predesigned data collection form and was stored in Microsoft Excel Sheet. IBM SPSS version 27.0 software was used for data analysis. Descriptive statistics were elaborated as mean/standard deviation or median/inter-quartile range for continuous variables, and frequency with percentage for categorical variables. Data were presented graphically wherever appropriate for data visualization using bar charts/pie charts for categorical data. Appropriate statistical tests were employed where applicable. The p-value of <0.05 was considered statistically significant.

Results

Baseline characteristics

A total of 200 children were enrolled, 117 of whom were males. The mean age of the study population was 2.03 ± 1.24 years. Table 1 represents baseline characteristics. 144 (72%) children had acute malnutrition, with 41.4% SAM and 58.6% MAM.

Table 1: Baseline characteristics of study cohort (N=200).

Parameter		Frequency (%)
Socioeconomic class (Modified Kuppusamy)	Upper	7 (3.5)
	Upper middle	23 (11.5)
	Lower middle	38 (19.0)
	Upper lower	81 (40.5)
	Lower	51 (25.5)
Duration of exclusive breastfeeding (<6 months)		136 (68.0)
Diet (Vegetarian)		104 (52.0)
Maternal education status	Illiterate	4 (2)
	Primary	18 (9)
	Secondary	108 (54)
	Graduate	70 (35)
Immunization status	Adequate	102 (52.0)
	Partial	74 (37.0)
	Unimmunized	24 (12.0)
Weight for age	Normal	20 (10.0)
	-2 to -3 Z	114 (57.0)
	<-3 Z	66 (33.0)
Height/length for age	Normal	51 (25.5)
	-2 to -3 Z	119 (59.5)
	<-3 Z	30 (15.0)
Weight for height/length	Normal	112 (56.0)
	-2 to -3 Z	58 (29.0)
	<-3 Z	30 (15.0)
Mid-upper-arm circumference	>12.5 cm	56 (28.0)
	11.5-12.5 cm	84 (42.0)
	<11.5 cm	60 (30.0)

Clinical features

The most common infection in undernourished children was respiratory (15.5%) followed by gastrointestinal (14%) infections. Frequently observed clinical parameters included pica (n=67, 33.5%), pallor (n=58, 29%), worm infestation (n=53, 26.5%), knuckle hyperpigmentation (n=46, 23%), and tremors (n=24,12%).

Anemia

144 (72%) children had anemia in our cohort. Among this, 66 (33%) had moderate anemia, 28 (14%) had mild, and 50 (25%) had severe anemia. The mean hemoglobin was 8.93 ± 2.71 g/dL. The mean values of RBC indices were 25.37 ± 3.56 fL (MCV), 25.37 ± 3.56 pg (MCH), and 28.38 ± 2.66 % (MCHC). The morphological classification of anemia is depicted in Figure 1.

Figure 1: Pie chart depicting the morphological classification of anemia.

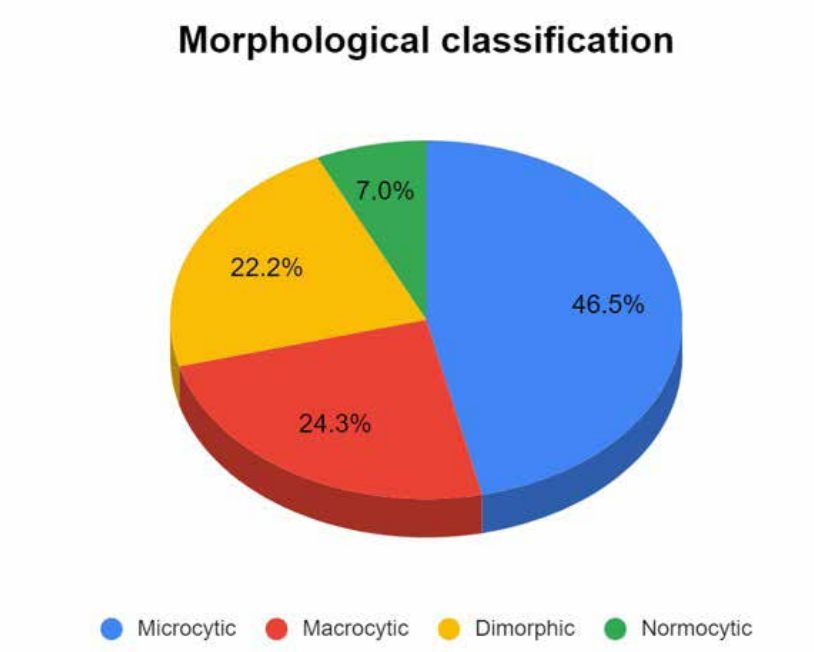

The most common micronutrient deficiency in anemic children was iron deficiency (n=99, 68.7%) followed by vitamin B12 (n=66,45.8%), and folic acid (n=15, 10.42%) deficiency. Of this, 33 (22.9%) children had concomitant iron and vitamin B2 deficiencies, 11 (7.6%) had combined folic acid and vitamin B12 deficiency and all three micronutrients were deficient in four (2.7%) children. None of the children had isolated folate deficiency or combined iron and folate deficiencies. The mean serum iron, vitamin B12, and folate values were 69.5 ± 29.48 mcg/dL, 252.6 ± 68.1 pg/mL, and 7.15 ± 3.28 ng/mL, respectively.

A comparison of sociodemographic, anthropometric parameters, and clinical features between anemic and non-anemic children is presented in Table 2. Anthropometric parameters and clinical features were also compared with the severity of anemia (Tables 3 and 4). Serum levels of all three micronutrients i.e., iron, Vitamin B12 and folate were significantly associated with the severity of anemia as represented in Table 5.

Table 2: Comparison of sociodemographic, anthropometric parameters, and clinical features of children with undernutrition with and without anemia (N=200).

Parameter		Anemic (n=144) [n (%)]	Non-anemic (n=56) [n (%)]	p-value*
Male		83 (57.6)	34 (60.7)	0.692
Socioeconomic class	Upper and upper middle	16 (11.1)	15 (26.8)	0.006**
	Lower middle	24 (16.7)	14 (25.0)	
	Upper lower	61 (42.4)	19 (33.9)	
	Lower	43 (29.9)	8 (14.3)	
Duration of exclusive breastfeeding (<6 months)		92 (63.9)	44 (78.6)	0.045**
Maternal education status	Illiterate	3 (2.08)	1 (1.79)	0.02**
	Primary	15 (10.42)	3 (5.36)	
	Secondary	85 (59.03)	23 (41.07)	
	Graduate	41 (28.47)	29 (51.78)	

Weight for age	Normal	13 (9.0)	7 (12.5)	0.722
	-2 to -3 Z	82 (56.9)	32 (57.1)	
	<-3 Z	49 (34.0)	17 (30.4)	
Length/height for age	Normal	34 (23.6)	17 (30.4)	0.616
	-2 to -3 Z	88 (61.1)	31 (55.4)	
	<-3 Z	22 (15.3)	8 (14.3)	
Weight for length/ height	Normal	31 (21.5)	12 (21.4)	0.907
	-2 to -3 Z	66 (45.8)	24 (42.9)	
	<-3 Z	47 (32.6)	20 (35.7)	
Mid-upper-arm circumference	>12.5 cm	26 (18.0)	30 (53.58)	<0.001**
	11.5–12.5 cm	67 (46.5)	17 (30.36)	
	<11.5 cm	51 (35.5)	9 (16.06)	
Worm infestation		53 (36.8)	2 (4.0)	<0.001**
Blood in stool		3 (2.0)	2 (4.0)	0.545
Tremors		16 (11.1)	8 (14.0)	0.535
Pedal edema		13 (9.0)	1 (2.0)	0.071

*Significance levels using the Chi-square test; ** p-value is significant

Table 3: Comparison of anthropometric parameters and severity of anemia (n=144).

Parameters	**Anemia**			**p-value***
	Mild (n=28) [n (%)]	**Moderate (n=66) [n (%)]**	**Severe (n=50) [n (%)]**	
Weight for age				
Normal (n = 13)	2 (15.4)	8 (61.5)	3 (23.1)	0.825
-2 to -3 Z (n = 82)	16 (19.5)	37 (45.1)	29 (35.4)	
<-3 Z (n = 49)	10 (20.4)	21 (42.9)	18 (36.7)	
Length/Height for age				
Normal (n = 34)	10 (29.4)	14 (41.2)	10 (29.4)	0.177
-2 to -3 Z (n = 88)	17 (19.3)	42 (47.7)	29 (33.0)	
<-3 Z (n = 22)	1 (4.5)	10 (45.5)	11 (50.0)	
Weight for height/length				
Normal (n = 74)	9 (12.2)	35 (47.3)	30 (40.5)	0.073
-2 to -3 Z (n = 48)	16 (33.3)	20 (41.7)	12 (25.0)	
<-3 Z (n = 22)	3 (13.6)	11 (50.0)	8 (36.4)	
Mid-upper-arm circumference				
>12.5 cm (n = 26)	10 (38.5)	11 (42.3)	5 (19.2)	0.03**

*Significance levels using the Chi-square test; ** p-value is significant

Table 4: Comparison of clinical features with severity of anemia (n=144).

Clinical features	Anemia			p-value*
	Mild (n=28) [n (%)]	Moderate (n=66) [n (%)]	Severe (n=50) [n (%)]	
Blood in stool/Malena	1 (33.3)	2 (66.7)	0 (0.0)	-
Worm infestation	7 (13.2)	20 (37.8)	26 (49.0)	0.019**
Pica	10 (14.9)	29 (43.3)	28 (41.8)	0.192
Tremors	4 (25.0)	9 (56.3)	3 (18.7)	0.362
Pallor	2 (3.5)	14 (24.1)	42 (72.4)	<0.001**
Pedal edema	5 (38.4)	4 (30.8)	4 (30.8)	0.179
Knuckle hyperpigmentation	12 (26.1)	20 (43.5)	14 (30.4)	0.372
Cheilosis/angular stomatitis	3 (14.3)	8 (38.1)	10 (47.6)	0.399

*Significance levels using the Chi-square test; ** p-value is significant

Table 5: Comparison of laboratory parameters and severity of anemia (n=144).

Parameter	Anemia			p-value*
	Mild (n=28) Mean (95% CI)	Moderate (n=66) Mean (95% CI)	Severe (n=50) Mean (95% CI)	
Iron (mcg/dL)	78.50 (47.0 to 97.0)	48.50 (37.0 to 88.0)	39.50 (23.25 to 67.75)	<0.001**
Vitamin B12 (pg/mL)	265.50 (243.0 to 297.0)	225.00 (175.0 to 264.0)	174.00 (134.0 to 244.0)	<0.001**
Folate (ng/mL)	7.00 (6.62 to 8.0)	6.45 (5.9 to 7.07)	6.30 (5.8 to 7.28)	0.026**

*Significance levels using the Chi-square test; ** p-value is significant

Discussion

According to our study, undernutrition affected males more than females, almost similar to previous studies [7-11]. Studies reported that immunity against infections is better in females than males due to the hormonal impact [12]. Thurstans S et al. in their systematic review stated that boys tend to be more undernourished than girls due to various biological and social mechanisms [13]. Even though undernutrition was expected to be maximum in the lower class, the majority belonged to upper-lower class. A possible explanation is the non-availing of health services by the lower class.

59.5% of children in our study had stunting and 15% had severe stunting. The proportion of wasting and severe wasting was 29% and 15%, respectively. Whereas underweight and severely underweight were 57% and 33%, respectively and 7% had edematous undernutrition. Among 200 enrolled children, 72% had acute malnutrition; out of which, 59% had MAM and 41% had SAM. This was much lower than the observations made by previous studies [10,14,15]. Undernutrition was detected in 11% of children who came for routine immunization. This shows the importance of regular growth monitoring.

The most common infection was found to be respiratory followed by gastrointestinal infections. This was similar in past studies as well [10,16]. However, Kumar R et al. and Garg M et al. reported a higher incidence of gastrointestinal infections than respiratory [14,15]. Hence, we emphasize steps like hygiene practices and immunization to prevent infections of these systems along with early treatment.

Pica and worm infestation were the most common symptoms in the study population. Their proportion was higher than previous studies [16,17]. Tremor as part of infantile tremor syndrome was present in 12% of children which was double the proportion reported by Yaikhomba et al [10]. This difference can be due to the increased number of vegetarian mothers in our study area. Pallor and knuckle hyperpigmentation were two common signs found in anemic children. Thakur et al. reported 33% of children with knuckle hyperpigmentation which was relatively higher than our study [11].

Anemia status

Anemia was found in 72% of undernourished children who participated in the study. Devi et al. reported 69.2% of children with undernutrition as anemic in the under-five population [16]. This was closest to our observation. Most of the other studies found a significantly higher proportion of anemia in under-five children [10,11,14]. The reason can be that most of the other studies were conducted on sick hospitalized children. In contrast, our study contained both in and out-patient children with simple ailments and those who even came for routine immunization. As per WHO classification, 14%

had mild anemia, 33%, and 25% had moderate and severe anemia, respectively. Kumar et al. and Garg M et al. also found moderate anemia more common than mild and severe anemia, similar to our study [13,14]. Whereas, according to certain other studies, undernourished children were found to be more severely anemic [10,11]. Morphologically, microcytic anemia was the most common type (46.5%) followed by macrocytic (24.3%) and dimorphic (22.2%). Thakur et al. also observed microcytic anemia as more prevalent than other types [11].

The proportion of normocytic anemia found in our study was considerably lower than what previous studies noted [10,11,18]. A possible explanation can be the exclusion of chronic diseases in our study which usually present as normocytic anemia.

Similar to our study, Thakur et al. also found iron as the predominant micronutrient deficient [11]. In contrast to this, Yaikhomba T et al. reported a higher proportion of vitamin B12 deficiency than that of iron and folate [10]. Most of the previous studies used serum ferritin to diagnose iron deficiency, which is also an acute inflammatory marker. Whereas in our study, we used serum iron levels. Hence, this can be one probable explanation for our study's increased proportion of iron deficiency. Dimorphic anemia is significantly high in our study population.

Limitations of our study include its single-center design, the inability to assess other iron profile parameters such as total iron-binding capacity and ferritin, and a limited evaluation of micronutrient deficiencies.

Conclusion

The study underscores the persistent challenge of undernutrition and anemia in under-five children, emphasizing its multifaceted clinical and laboratory profile. The study demonstrates a statistical relationship between MUAC, worm infestation, and serum micronutrient levels with anemia severity, providing an integrated perspective on nutritional deficiencies, clinical parameters, and anthropometric indices. This nuanced approach underscores the importance of including routine screening and management of vitamin B12 deficiency in malnutrition protocols, which is not currently a standard recommendation in many guidelines. The findings highlight the importance of comprehensive growth monitoring, micronutrient assessment, and targeted supplementation strategies, particularly in socioeconomically disadvantaged groups. Enhanced focus on early detection and intervention can significantly improve survival and developmental outcomes for this vulnerable population.

Declaration by authors

The manuscript has been read and approved by all the authors, the requirements for authorship, as stated earlier in this document, have been met, and each author believes that the manuscript represents honest work and the information is not provided in another form.

Ethical approval

Approved by Institutional Ethics Committee (IEC/21/594) and performed in a manner to conform with the Helsinki Declaration of 1975, as revised in 2000 and 2008.

Declarations

Funding

Nil.

Conflicts of interest

None declared.

Consent to participate

Signed informed consent obtained from patient.

Consent for publication

Signed informed consent obtained from patient.

References

1. Swaminathan S, Hemalatha R, Pandey A, Kassebaum NJ, Laxmaiah A, Longvah T, et al. The burden of child and maternal malnutrition and trends in its indicators in the states of India: The Global Burden of Disease Study 1990–2017. Lancet Child Adolesc Health. 2019;3(12):855–870 DOI: https://doi.org/10.1016/s2352-4642(19)30273-1
2. WHO child growth standards and the identification of severe acute malnutrition in infants and children [Internet]. [Accessed:20/01/2024]. Available from: www.who.int/childgrowth/standards
3. UNICEF/WHO/World Bank Joint Child Malnutrition Estimates, 2021 Edition. [Internet]. [Accessed:20/01/2024]. Available from: https://data.unicef.org/resources/jme-report-2021
4. National Family Health Survey (NFHS-5), 2019-21 for India [Internet]. [Accessed:20/01/2024]. Available from: https://main.mohfw.gov.in/sites/default/files/NFHS-5_Phase-II_0.pdf
5. WHO fact sheets, February 2025 [Internet]. [Accessed:20/06/2025]. https://www.who.int/news-room/fact-sheets/detail/anaemia
6. Sarna A, Porwal A, Ramesh S, Agrawal PK, Acharya R, Johnston R, et al. Characterisation of the types of anaemia prevalent among children and adolescents aged 1-19 years in India: a population-based study. Lancet Child Adolesc Health. 2020;4(7):515-525. DOI: https://doi.org/10.1016/s2352-4642(20)30094-8
7. Ambadekar NN, Zodpey SP. Risk factors for severe acute malnutrition in under-five children: a case-control study in a rural part of India. Public Health. 2017;142:136–143. DOI: https://doi.org/10.1016/j.puhe.2016.07.018
8. Mishra K, Kumar P, Basu S, Rai K, Aneja S. Risk factors for severe acute malnutrition in children below 5 y of age in India: A case-control study. Indian J Pediatr.

2014;81(8):762–765. DOI: https://doi.org/10.1007/s12098-013-1127-3

9. Murarkar S, Gothankar J, Doke P, Pore P, Lalwani S, Dhumale G, et al. Prevalence and determinants of undernutrition among under-five children residing in urban slums and rural areas, Maharashtra, India: a community-based cross-sectional study. BMC Public Health. 2020;20(1):1559. DOI: https://doi.org/10.1186/s12889-020-09642-0
10. Yaikhomba T, Poswal L, Goyal S. Assessment of iron, folate, and vitamin B12 status in severe acute malnutrition. Indian J Pediatr. 2015;82(6):511-514.DOI: https://doi.org/10.1007/s12098-014-1600-7
11. Thakur N, Chandra J, Pemde H, Singh V. Anemia in severe acute malnutrition. Nutrition. 2014;30(4):440-442.DOI: https://doi.org/10.1016/j.nut.2013.09.011
12. Muenchhoff M, Goulder PJ. Sex differences in pediatric infectious diseases. J Infect Dis. 2014;209 Suppl 3:S120-S126. DOI: https://doi.org/10.1093/infdis/jiu232
13. Thurstans S, Opondo C, Seal A, Wells J, Khara T, Dolan C, Briend A, Myatt M, Garenne M, Sear R, Kerac M. Boys are more likely to be undernourished than girls: a systematic review and meta-analysis of sex differences in undernutrition. BMJ Glob Health. 2020;5(12):e004030 DOI: https://doi.org/10.1136/bmjgh-2020-004030
14. Kumar R, Singh J, Joshi K, Singh HP, Bijesh S. Co-morbidities in hospitalized children with severe acute malnutrition. Indian Pediatr. 2014;51(2):125-127.DOI: https://doi.org/10.1007/s13312-014-0343-x
15. Garg M, Devpura K, Saini S. K, Kumara S. A hospital-based Study on Co-morbidities in children with severe acute malnutrition. J Pediatr Res.2017;4(1):82-88.DOI: https://doi.org/10.17511/ijpr.2017.01.16
16. Devi RU, Krishnamurthy S, Bhat BV, Sahai A. Epidemiological and Clinical Profile of Hospitalized Children with Moderate and Severe Acute Malnutrition in South India. Indian J Pediatr. 2015;82(6):504–510. DOI: https://doi.org/10.1007/s12098-014-1671-5
17. Mani Baskaran V, Naaraayan SA, Priyadharishini D. Comorbidities in children hospitalized with severe acute malnutrition. Indian J Child Health. 2018;5(8):530–532. DOI: https://doi.org/10.32677/IJCH.2018.v05.i08.005
18. Dwivedi D, Singh V, Singh J, Sharma S. Study of anemia in children with severe acute malnutrition. J Nepal Paediatr Soc. 2018;37(3):250–253. DOI: https://doi.org/10.3126/jnps.v37i3.18480

Review Article

Cardio-renal-metabolic laboratory profile: an integrated strategy for the prevention and management of chronic non-communicable diseases

Luis Figueroa Montes[1*]

[1]*Clinical Pathologist, Biochemistry Laboratory, Hospital III Suarez Angamos EsSalud, Lima, Peru*

Article Info

[*]***Corresponding Author:***
Luis Figueroa Montes
E-mail: patologoclinico@gmail.com
Biochemistry Laboratory, Hospital III Suarez Angamos EsSalud, Lima, Peru

Keywords

chronic kidney diseases of uncertain etiology, diabetes mellitus, obesity, cardiovascular diseases, metabolic syndrome

Abstract

Objective: This article emphasizes the need to integrate cardiovascular, renal, and metabolic assessments into routine clinical practice, with the aim of improving the prevention, diagnosis, and management of chronic non-communicable diseases (NCDs).

Methods: We conducted a comprehensive review of the current medical literature on cardio-renal-metabolic syndrome, alongside a critical analysis of traditional clinical profiles. Based on these findings, we propose a novel integrated laboratory profile that captures the interconnections between these systems, aiming to enhance diagnostic accuracy and patient management.
Results: Significant gaps in current fragmented assessments were identified, leading to the development of a profile that integrates key biomarkers from all three systems for a more comprehensive and accurate evaluation. This profile will be implemented according to the complexity of the care levels and according to the patient's stage of cardio-renal-metabolic syndrome.

Conclusion: Implementation of the new integrated cardiorenal-metabolic profile could likely optimize clinical care, reduce healthcare costs, and improve patient outcomes. However, its success will depend on the technical and logistical capabilities of clinical laboratory networks, as well as the stage of the patient's disease and the level of care at which it is implemented.

Introduction

The global rise in chronic non-communicable diseases (NCDs) - including cardiovascular, renal, and metabolic disorders - places an increasing strain on healthcare systems. These conditions share common pathophysiological mechanisms, such as chronic inflammation, oxidative stress, and insulin resistance, which drive their progression and interconnection [1].

Cardiovascular diseases (CVDs) are the leading cause of mortality worldwide, and their prevalence continues to increase due to population aging and unhealthy lifestyles, such as high-fat diet and sedentary lifestyle [2]. Furthermore, type 2 diabetes mellitus (DM) and obesity are key risk factors for the development of CVD, as well as for chronic kidney disease (CKD), which in turn exacerbates cardiovascular risk [3].

CKD, which affects 10% of the world's population and is associated with arterial hypertension and DM, underscores the importance of a comprehensive approach to the management of these conditions. Recent studies have shown that metabolic dysfunction, characterized by insulin resistance and hyperglycemia, not only drives the progression of CKD, but also increases the risk of adverse cardiovascular events [4].

In addition, the interconnection between these NCDs suggests the need for prevention and treatment strategies that address multiple conditions, with a focus on modifying common risk factors, such as diet, exercise, and glycemic control, but also with a comprehensive diagnosis from the clinical laboratory [5].

Traditional diagnostic profiles - such as lipid, renal, and metabolic panels - are typically ordered in isolation, which hinders a holistic understanding of NCD interconnections [1].

For example, the lipid profile, requested by the cardiologist, focuses on cardiovascular risk but does not evaluate markers of inflammation or endothelial dysfunction, which are key in the progression of renal and metabolic disease [6].

Similarly, the renal profile, ordered by the nephrologist, measures parameters such as creatinine and glomerular filtration rate (GFR), which does not include biomarkers of oxidative stress or insulin resistance, which are relevant for the assessment of cardiovascular and metabolic risk in patients with chronic kidney disease (CKD) [4].

On the other hand, the metabolic profile, ordered by the endocrinologist, focuses on glucose and lipids, but does not integrate markers of vascular or renal damage, which underestimates the risk of multi-organ complications in patients with DM [7].

These gaps highlight the urgent need for an integrated diagnostic laboratory profile that provides a more comprehensive assessment of NCDs. Traditional approaches that evaluate these conditions separately fail to account for their interconnections, resulting in fragmented patient care and suboptimal outcomes. A novel, integrated approach is needed - one that reflects the pathophysiological complexity of these conditions and enables more effective, prevention-focused management.

Objective

To address these diagnostic gaps, we propose an integrated cardio-renal-metabolic laboratory profile that unifies risk assessment and management strategies for chronic non-communicable diseases.

Methodology

Central question: What are the limitations of current diagnostic laboratory profiles (lipid, renal, metabolic) and how can an integrated profile improve the evaluation and management of NCDs?

Medical Literature Search: A recent review of medical literature related to the topic using databases including PubMed, Scopus, Web of Science, and the Cochrane Library. Keywords used in the search included "diagnostic profile", "chronic diseases", "cardio-renal-metabolic interface", "diabetes", "chronic kidney disease" and "cardiovascular disease", "cardiac injury", "heart failure", "metabolic syndrome", "liver fibrosis", "FIB-4", "HOMA-IR", "HOMA", "troponin", "high-sensitivity troponin", "natriuretic peptides".

Inclusion criteria: articles published from 2022 onwards. Original studies, systematic reviews, meta-analyses and clinical guidelines were included.

Exclusion criteria: outdated, non-peer-reviewed or methodology-poor studies.

Literature selection and critical appraisal: titles and abstracts were reviewed to select relevant articles. All studies included in this review involving human subjects complied with the ethical principles for medical research involving human subjects, in accordance with the Declaration of Helsinki and published in peer-reviewed journals.

Key findings were identified, such as proposed biomarkers, limitations of current profiles and evidence on the pathophysiological interface of NCDs.

Selecting laboratory tests for the new profile

The American Heart Association (AHA) in 2023, published "Cardiovascular, Renal, and Metabolic Health: An AHA Presidential Notice", which addresses the importance of integrating the assessment of cardiovascular, renal, and metabolic health due to the interconnection of these systems in the development of chronic diseases. Thus, the concept of cardio-renal-metabolic syndrome (CKM) is introduced, as a condition that reflects the interrelationship between these three areas and their impact on overall health [8].

CKM syndrome is classified into different stages, ranging from stage 0 (no risk factors) to stage 4 (established cardiovascular disease with renal or metabolic complications). The AHA emphasizes the need to identify and treat this syndrome early to prevent serious complications, such as heart failure, chronic kidney disease, and diabetes [8].

Different laboratory tests are recommended depending on the stage of CKM syndrome, specific laboratory tests to assess the risk and progression of the disease. These are:

- Cardiovascular markers: lipid profile (total cholesterol, LDL, HDL, triglycerides), high-sensitivity C-reactive protein (CRP) and natriuretic peptides (BNP/NT-proBNP).
- Renal markers: serum creatinine (GFR) and albuminuria (urine albumin-creatinine ratio).
- Metabolic markers: fasting plasma glucose, glycated hemoglobin (HbA1c), and insulin.
- Other markers: liver function tests, platelet count.

In addition, there are other non-laboratory variables that are measured, such as: coronary calcium concentration, ejection fraction, weight, BMI, others. Based on this evidence, I propose a new integrated cardio-renal-metabolic laboratory profile [8].

Profiles that exist to address NCDs in a disintegrated way

Currently, different specialties request laboratory test profiles to see in a disintegrated way the patient's clinical condition. In this part I will explain the different profiles used to see specific topics.

Lipid profile

The lipid profile (PL), is a blood test that measures the levels of specific lipids to assess cardiovascular risk and guide the treatment of dyslipidemia. Its main components include: total cholesterol, low-density lipoprotein cholesterol (LDL), high-density lipoprotein cholesterol (HDL), triglycerides. From these measurements, non-HDL cholesterol and very low-density lipoprotein (VLDL) can also be calculated [9,10].

PL is crucial for assessing a patient's lipid status, which plays an important role in the primary and secondary prevention of cardiovascular diseases (9,11). Currently, the therapeutic goal in the management of dyslipidemia is to reduce LDL cholesterol to levels appropriate for the patient's cardiovascular risk, through lifestyle changes and lipid-lowering drugs [9].

Renal Profile

Currently, the renal profile consists of two parts: the estimation of the glomerular filtration rate (eGFR) by measuring serum creatinine and the urine albumin/creatinine ratio (ACR) by measuring creatinine and albumin in random urine. The GFR assesses kidney function and the ACR assesses kidney damage. Let's look at both components.

Estimating the Glomerular Filtration Rate (GFR)

The eGFR is a fundamental component for assessing kidney function and is usually calculated using serum creatinine levels through validated equations. The most commonly used equation is the Chronic Kidney Disease Epidemiology Collaboration (CKD-EPI) equation, which has been updated to exclude race as a variable to promote health equity [12]. This equation is recommended for use in all US laboratories and is considered more accurate [13]. It should be noted that cystatin C is another marker used to estimate eGFR. Combining creatinine and cystatin C in eGFR may improve accuracy and support better clinical decision making compared to using either marker alone. The KDIGO 2024 guidelines suggest using either cystatin C-based eGFR (cys-based eGFR) or a combined creatinine and cystatin C-based eGFR (cr-cys-based eGFR) [12,14].

In pediatric patients, specific equations have been developed to account for age and sex differences, such as those proposed by the Chronic Kidney Disease in Children (CKiD) study. These equations are designed to reduce bias and improve accuracy in children and young adults [15,16].

Albumin-to-creatinine ratio (ACR)

The ACR is used to assess albuminuria, a marker of kidney damage and a predictor of cardiovascular risk. The ACR is calculated from a urine sample (preferably random) and provides a reliable estimate of daily albumin excretion, which is crucial for diagnosing and monitoring chronic kidney disease (CKD) and assessing cardiovascular risk, particularly in patients with diabetes [12,17].

The ACR has three levels: normal to mildly increased albuminuria (<30 mg/g), moderately increased (30-299 mg/g), and severely increased (≥300 mg/g) [14,18].

In patients with diabetes mellitus (DM), an elevated ACR is associated with an increased risk of major adverse cardiovascular events (MACE) and overall mortality, even when the ACR is within the normal range. Including the ACR in risk models improves the prediction of these outcomes [19,20]. Guidelines recommend annual ACR testing in adults with DM, with more frequent monitoring if eGFR is less than 60 mL/min/1.73 m² or if albuminuria exceeds 30 mg/g [18].

Metabolic profile

To understand more broadly, I will detail all the tests that allow us to have knowledge of the patient's metabolic homeostasis.

Diagnostic tests for diabetes mellitus (DM)

The diagnosis of DM is based on measuring plasma glucose levels and hemoglobin A1c (HbA1c or glycated hemoglobin). According to the American Diabetes Association (ADA) and other guidelines from societies and experts, they recommend the following tests to diagnose DM [18,21,22]:

- Fasting plasma glucose (FPG): measures blood glucose after an overnight fast of at least 8 hours. A glucose level ≥126 mg/dL (7.0 mmol/l) is diagnostic of diabetes.
- 2-hour plasma glucose (2hPG): During a 75-g oral glucose tolerance test (OGTT), blood glucose is measured 2 hours after ingesting a 75-gram anhydrous glucose solution. A

2hPG level ≥200 mg/dL (11.1 mmol/L) is diagnostic of diabetes.
- Hemoglobin A1c (HbA1c): This test reflects average glucose levels over the past 2 to 3 months. An HbA1c level ≥6.5% (48 mmol/mol) is diagnostic of DM. It is important that the HbA1c test be performed using a method certified by the National Glycohemoglobin Standardization Program (NGSP) and standardized according to the Diabetes Control and Complications Trial (DCCT).
- Random plasma glucose: In the presence of classic symptoms of hyperglycemia (polyuria, polydipsia, and unexplained weight loss) or a hyperglycemic crisis, a random glucose level ≥200 mg/dL (11.1 mmol/L) can be used to diagnose DM.

In the absence of unequivocal hyperglycemia, it is recommended that the diagnosis of diabetes is confirmed by repeat testing on a different day. In addition, if two different tests (e.g., FPG and HbA1c) are above their respective diagnostic thresholds, the diagnosis can be confirmed without repeat testing [21].

Diagnosis of metabolic syndrome (MS)

The diagnosis of MS involves identifying patients with at least three of five specific components. These components are elevated waist circumference, elevated serum triglycerides, reduced HDL cholesterol, elevated blood pressure, and elevated fasting plasma glucose. This diagnostic criterion is widely accepted and is based on the harmonized definition proposed by an international consortium of cardiovascular and DM organizations [23,24].

- Elevated waist circumference: This is a marker of abdominal obesity and is a critical component of MS. Specific cutoff values for waist circumference may vary based on ethnic and regional considerations. For example, the National Cholesterol Education Program (NCEP) Adult Treatment Panel III (ATP III) suggests a waist circumference >102 cm for men and >88 cm for women, while the International Diabetes Federation (IDF) provides ethnicity-specific cutoffs.
- Elevated triglycerides: A triglyceride level of ≥150 mg/dL is considered elevated.
- Reduced HDL: Low values <40 mg/dL for men and <50 mg/dL for women, contributing to the diagnosis of metabolic syndrome.
- Elevated blood pressure: Blood pressure is considered elevated if the systolic blood pressure is ≥130 mmHg or the diastolic blood pressure is ≥85 mmHg.
- Elevated fasting plasma glucose: A level ≥100 mg/dL is used as a threshold for this component (prediabetes).

The diagnosis of MS is important because it is associated with an increased risk of cardiovascular disease and type 2 DM. The prevalence of MS is increasing worldwide, driven by factors such as urbanization, sedentary lifestyles, and dietary changes [25].

Liver fibrosis profile

Liver fibrosis is a pathological process characterized by excessive accumulation of extracellular matrix (ECM) proteins in the liver, which occurs in response to chronic liver injury. This condition is a common consequence of several chronic liver diseases, including viral hepatitis, alcoholic liver disease, and nonalcoholic steatohepatitis (NASH) [26].

NASH is an inflammatory liver condition that is part of the spectrum of nonalcoholic fatty liver disease. It is a major clinical concern because it can progress to cirrhosis, liver failure, and hepatocellular carcinoma, and is a leading cause of liver transplantation in the United States [27,28,29].

The pathogenesis of NASH involves multiple factors, including lipotoxicity, oxidative stress, mitochondrial dysfunction, and inflammation. NASH is associated with MS, obesity, type 2 DM, and dyslipidemia, and its prevalence is increasing worldwide [30].

In order to assess the possibility of a patient having some degree of liver fibrosis, there is an easily calculated FIB-4 score. This is a non-invasive tool used to assess liver fibrosis, especially in patients with diseases such as NASH. The FIB-4 score is calculated using the following formula: [Age (years)×AST (IU/L)] / [PLT (109/L) × ALT 1/2 (IU/L)]

AST= aspartate transaminase enzyme, ALT= alanine transaminase enzyme, PLT= platelet count

On the interpretation of the FIB-4 score we have that [31,32]:

- The FIB-4 index is valued for its simplicity and cost-effectiveness, making it a useful initial screening tool, in primary care as well as in specialist settings [33].

Non-ischemic cardiac injury profile

The relationship between non-ischemic cardiac injury and high-sensitivity troponin is based on the ability of high-sensitivity troponin assays to detect very low levels of cardiac troponins, which are biomarkers of myocardial injury. Cardiac troponins, such as troponin I and T, are proteins that are released when myocardial injury occurs, such as in the case of a myocardial infarction (MI) or other forms of cardiac stress [34].

High-sensitivity troponin assays have improved analytical performance compared to previous generation assays. These assays can detect troponin levels in most healthy individuals, helping to identify even minor myocardial injuries that might not be detected with conventional assays [35].

The ability to detect small changes in troponin levels over time is crucial to distinguish between acute myocardial infarction and other causes of troponin elevation, as serial measurements can provide information on the kinetics of troponin release [34].

Heart failure profile

Natriuretic peptides (NPs), including atrial natriuretic peptide (ANP), B-type natriuretic peptide (BNP), and N-terminal pro-BNP (NT-pro-BNP), play a crucial role in the diagnosis, treatment, and pathophysiology of heart failure (HF). These peptides are produced by cardiomyocytes and are involved in the regulation of blood volume and sodium concentration, exerting effects such as natriuresis, diuresis, vasodilation, and inhibition of the renin-angiotensin-aldosterone system (RAAS) and sympathetic nervous system [36,37,38,39].

Elevated levels of BNP and NT-pro-BNP indicate increased cardiac stress and are used to diagnose HF, assess its severity, and predict prognosis. The FIB-4 score of <1.3 suggests a low risk of advanced fibrosis (F3-F4) and usually does not require immediate further investigation.

- A score between 1.3 and 2.67 is considered indeterminate and further evaluation is recommended, often using additional noninvasive tests such as measurement of liver stiffness, by transient elastography or enhanced liver fibrosis testing.

A score >2.67 indicates a high likelihood of advanced fibrosis, warranting referral to a hepatologist for further evaluation, which may include measurement of liver stiffness or liver biopsy to confirm the stage of fibrosis. These biomarkers have have a high negative predictive value, allowing to rule out HF in both emergency and outpatient settings when levels are below certain thresholds (e.g., BNP < 100 pg/ml, NT-proBNP < 300 pg/ml in emergency settings) [40,41].

Overall, NPs are central to the treatment of HF, providing diagnostic, prognostic, and therapeutic benefits, while highlighting the complex interplay of neurohormonal systems in cardiovascular homeostasis and disease progression [40,41].

Insulin resistance profile

The homeostatic model assessment index (HOMA) is a method used to estimate insulin resistance (HOMA-IR) and indirectly beta cell function from fasting plasma glucose and insulin levels. It is used in clinical and epidemiological studies due to its simplicity, with the minimal requirement of a single fasting blood sample for plasma glucose and insulin measurements [42].

The HOMA-IR index is calculated using the formula [43]:

HOMA-IR = (insulin × glucose) / 22.5*

(*) When glucose concentration is expressed in mmol/L, or:

HOMA-IR = (insulin × glucose) / 405**

(**) When glucose glycemia is expressed in mg/dL. In both cases, insulin is in mU/L.

This index provides an estimate of insulin resistance, which is a key feature in the pathophysiology of type 2 DM and MS. The HOMA-IR index has been validated against more complex methods of assessing insulin resistance and is frequently used in large-scale studies to assess the prevalence and risk factors associated with insulin resistance [44]. However, it is important to note that cut-off values for HOMA-IR may vary depending on the population and the specific clinical context [45].

Results

A list of laboratory tests is proposed that will comprehensively address cardio-renal-metabolic syndrome in patients. This list of laboratory tests can be requested according to the complexity of the health system and its work in laboratory networks, where priority is given to sending the sample and not the physical referral of the patient to the higher level of the health system. Table 1 details the list of laboratory tests by level of care for the Cardio-Renal-Metabolic Profile and Table 2 details the list of laboratory tests by stage of CKM syndrome.

Table 1: List of laboratory tests by level of care for the Cardio-Renal-Metabolic Profile.

Level of complexity of the health system	Proposed laboratory tests for the integrated Cardio-Renal-Metabolic Profile
First level of care	Cholesterol, HDL and triglycerides Glucose Serum creatinine (GFR) AST, ALT and platelet count (FIB-4)
Second level of care	Cholesterol, HDL and triglycerides Glucose, oral glucose tolerance test, glycated hemoglobin Serum creatinine (GFR) Albumin and creatinine in urine (ACR) AST, ALT and platelet count (FIB-4)

Third level of care	Cholesterol, HDL and triglycerides Glucose, oral glucose tolerance test, glycated hemoglobin Serum creatinine (GFR) Albumin and creatinine in urine (ACR) AST, ALT and platelet count (FIB-4) Insulin (HOMA index) High-sensitivity troponin Natriuretic peptides High-sensitivity CRP Lipoprotein(a) -Lp(a) Other tests

This tablet shows the different laboratory tests that must be implemented by level of complexity according to the health system.

Table 2: List of laboratory tests by stage of CKM syndrome for the Cardio-Renal-Metabolic Profi

Stage of cardio-renal-metabolic syndrome	Types of laboratory tests for the integrated Cardio-Renal-Metabolic Profile	Patient's clinical condition or risks	Findings
Stage 0 – Patients without risk factors	Perform laboratory tests according to age	Healthy patient	Normal BMI Normal ICC Fasting plasma glucose, 2-hour plasma glucose, HbA1c in normal values
Stage 1 – Excess adipose tissue dysfunction and dysglycemia	Glucose Hb A1c Oral glucose tolerance test	Overweight Obesity Prediabetes	Increased BMI Increased ICC Fasting plasma glucose, 2-hour plasma glucose, HbA1c in prediabetes values
Stage 2 – Metabolic risk factors (Metabolic syndrome)	Glucose Hb A1c Oral glucose tolerance test Cholesterol, HDL and triglycerides Serum creatinine (GFR) Urine albumin and creatinine (ACR)	Overweight Obesity Diabetes Dyslipidemia CKD	Increased BMI Increased WHR Fasting plasma glucose, 2-hour plasma glucose, HbA1c in diabetes values Hypertriglyceridemia Low HDL Hypertension CKD stage 3
Stage 3 – With subclinical atherosclerosis (Cardiovascular disease)	Glucose Hb A1c Oral glucose tolerance test Cholesterol, HDL and triglycerides Serum creatinine (GFR) Albumin and creatinine in urine (ACR) Insulin (HOMA index) AST, ALT and platelet count (FIB-4) High-sensitivity troponin Natriuretic peptides High-sensitivity CRP	Overweight Obesity Diabetes Dyslipidemia CKD Atherosclerosis in coronary arteries Decreased cardiac ejection fraction	Increased BMI Increased ICC Fasting plasma glucose, 2-hour plasma glucose, HbA1c in diabetes values Dyslipidemia Hypertension CKD stage 3

Stage 4 – With established cardio-renal-metabolic syndrome	Glucose Hb A1c Oral glucose tolerance test Cholesterol, HDL and triglycerides Serum creatinine (GFR) Albumin and creatinine in urine (ACR) Insulin (HOMA index) AST, ALT and platelet count (FIB-4) High-sensitivity troponin Natriuretic peptides High-sensitivity CRP Lipoprotein(a) -Lp(a) Other tests	Overweight Obesity Diabetes Dyslipidemia CKD Myocardial infarction Stroke Peripheral arterial disease Heart failure Atrial fibrillation	Increased BMI Increased ICC Fasting plasma glucose, 2-hour plasma glucose, HbA1c in diabetes values Dyslipidemia Hypertension CKD stage 4

This table details the type of laboratory tests that should be requested according to the stage of cardio-renal-metabolic syndrome and the clinical details presented at each stage.

Discussion

The proposed integrated Cardio-Renal-Metabolic Profile synergistically addresses the pathophysiological interconnection between cardiovascular, renal, and metabolic diseases. This unified approach improves the ability to identify cardio-renal-metabolic syndrome (CKM) early, facilitating risk stratification and personalization of clinical management [8].

An integrated healthcare approach coordinates multiple services to enhance patient outcomes, efficiency, and resource utilization [46].

For this reason, this approach is beneficial in the management of complex and chronic diseases, where patients often require services from multiple health care providers. Unlike the current fragmented approach, where lipid, renal, and metabolic profiles are ordered separately, this integrated profile provides a comprehensive analysis, capturing interactions between these systems. For example, the addition of biomarkers such as natriuretic peptides and high-sensitivity troponin at advanced levels provides an accurate assessment of cardiac stress and myocardial damage, which is not possible with traditional profiles that ignore these biomarkers [8].

In current models, the different profiles do not consider the coexistence and cross-impact between conditions such as DM and CKD on overall cardiovascular risk. This results in partial diagnoses and suboptimal therapeutic management. In addition, the duplication of tests generates an unnecessary increase in health care costs. Excessive laboratory testing negatively impacts patients and healthcare systems. The excessive use of medical tests is a recognized problem that can have physical, psychological and social consequences [47,48,49].

In contrast, an integrated profile not only optimizes resources, but also facilitates clinical adherence by avoiding multiple requests and repetitions of redundant tests. This proposal is adaptable to various healthcare settings in different health contexts. For example, in high-income countries, the profile can be integrated into advanced digital systems for automated analysis and continuous monitoring of CKM, with predictive analytics using artificial intelligence [5].

In low- and middle-income countries, the tiered design of the profile by level of care (first, second, and third level) ensures that basic tests such as serum creatinine and lipid profile are implemented at primary levels, while more complex biomarkers, such as high-sensitivity troponin and natriuretic peptides, are restricted to higher levels [50].

The possibility of scalability and customization of the implementation of the profile allows it to be adjusted according to the specific needs of the patient and the resources available in each health care setting, maintaining diagnostic quality in various health systems [50]. This new integrated profile is shown in the following figure.

Figure 1: New integrated Cardio-Renal-Metabolic Profile.

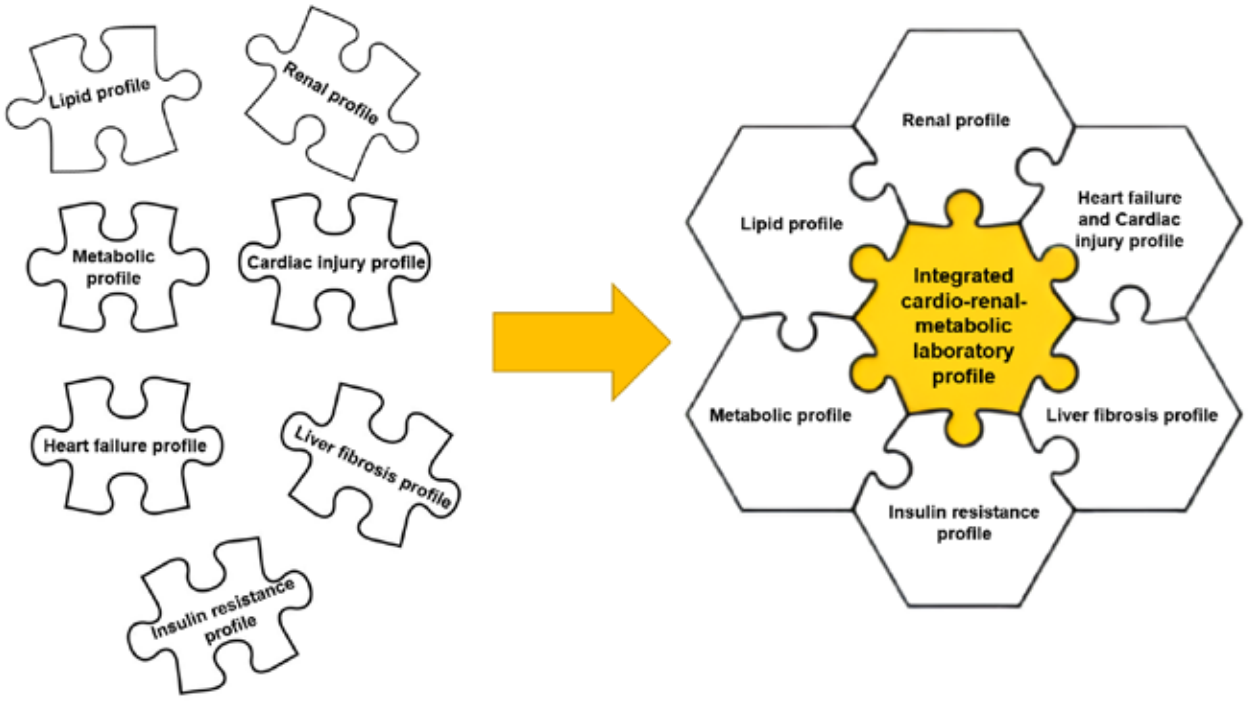

In this Figure we can observe how different laboratory profiles that are requested by different medical specialties could be integrated into a single CKM profile, well supported, seeking the timely prevention of this syndrome.

The implementation of improvements in health systems often faces a variety of barriers, which can be broadly classified into organizational, financial, human resources and technological areas [51]. Within their limitations, we can address some barriers, focused on initial and infrastructure costs, such as the acquisition of equipment and reagents for specialized laboratory tests, in clinical laboratories in countries with limited resources.

Another limitation would be that specialist physicians continue with disintegrated requests, as they are accustomed to requesting classic profiles and may show resistance in adopting this integrated approach [52]. It is important to highlight the need for validation in real conditions, with multicenter pilot studies being essential to evaluate their effectiveness, economic impact and operational viability in different scenarios [53]. Finally, the logistical work of laboratory networks, especially in countries with limited infrastructure, to ensure the adequate transport of samples for more complex tests at a higher care level.

One study shows an age-adjusted prevalence according to stages: stage 0 (11.2%), stage 1 (28.1%), stage 2 (47.4%), stage 3 (5.3%) and stage 4 (8.1%). The highest proportion of stage 4 was among adults ≥60 years old. Advanced stages 3 and 4 were associated with lower educational level, income and employment and higher mortality with a crude mortality rate of 188.8 per 1.000 person-years [54].

A cross-sectional study conducted in 29.722 American adults showed that unemployment, low family income, food insecurity and having 2 or more adverse social determinants of health were associated with a higher probability of advanced stages of CKM [55]. Other studies show that the higher the stage of CKM syndrome, the higher the risk of cardiovascular mortality, hence the importance of its early detection and stratification [56,57].

In conclusion, the proposal for an integrated cardio-renal-metabolic laboratory profile represents a paradigmatic advance in the diagnosis and management of NCDs. Its ability to offer a comprehensive and personalized assessment improves clinical decision-making, risk stratification, and health outcomes. Despite challenges related to cost, logistics, and healthcare infrastructure, the potential benefits strongly support adopting this profile as a standard of care. Validation through pilot studies will be crucial to establish its impact on different health systems, especially in low- and middle-income countries, where the burden of disease is greater and health budgets are strained. This profile not only reflects technical progress, but also an opportunity to transform laboratory medicine into a driver of prevention and health equity.

Author contribution

The author declares that he participated from the conception of the idea, drafting of the article, final editing, and approval of the final content.

Source of funding
Self-funded.

Conflicts of interest
The author declares that he has no conflict of interest related to this research study.

Acknowledgments
The author expresses his gratitude to Dr. Luis Fernando Hinojosa Baltierra of Mexico for his accurate and professional English translation, which ensured the clarity and intent of the original scientific text.

References

1. GBD 2019 Diseases and Injuries Collaborators. Global burden of 369 diseases and injuries in 204 countries and territories, 1990-2019: a systematic analysis for the Global Burden of Disease Study 2019. Lancet. 2020;396(10258):1204-1222. http://doi:10.1016/S0140-6736(20)30925-9.
2. Roth GA, et al. Global Burden of Cardiovascular Diseases and Risk Factors, 1990-2019: Update From the GBD 2019 Study. J Am Coll Cardiol. 2020;76(25):2982-3021. http://doi:10.1016/j.jacc.2020.11.010.
3. Alicic RZ, Rooney MT, Tuttle KR. Diabetic Kidney Disease: Challenges, Progress, and Possibilities. Clin J Am Soc Nephrol. 2017;12(12):2032-2045. http://doi:10.2215/CJN.11491116
4. Jager KJ, Kovesdy C, Langham R, Rosenberg M, Jha V, Zoccali C. A single number for advocacy and communication-worldwide more than 850 million individuals have kidney diseases. Kidney Int. 2019;96(5):1048-1050. http://doi:10.1016/j.kint.2019.07.012
5. WHO (Internet). WHO Discussion Paper on the development of an implementation roadmap 2023-2030 for the WHO Global Action Plan for the Prevention and Control of NCDs 2023-2030 (accessed:28/01/2025). Enlace web: https://www.who.int/publications/m/item/implementation-roadmap-2023-2030-for-the-who-global-action-plan-for-the-prevention-and-control-of-ncds-2023-2030
6. Arnett DK, et al. 2019 ACC/AHA Guideline on the Primary Prevention of Cardiovascular Disease: A Report of the American College of Cardiology/American Heart Association Task Force on Clinical Practice Guidelines. Circulation. 2019;140(11):e596-e646. http://doi:10.1161/CIR.0000000000000678
7. Ruiz-Ortega M, Rodrigues-Diez RR, Lavoz C, et al. Special Issue "Diabetic Nephropathy: Diagnosis, Prevention and Treatment". J Clin Med. 2023; 12(4): 1456. https://doi.org/10.1007/s11655-022-3591-y
8. Ndumele CE, et al; American Heart Association. Cardiovascular-Kidney-Metabolic Health: A Presidential Advisory From the American Heart Association. Circulation. 2023;148(20):1606-1635. http://doi:10.1161/CIR.0000000000001184
9. Parhofer KG, Laufs U. Lipid Profile and Lipoprotein(a) Testing. Dtsch Arztebl Int. 2023;120(35-36):582-588. http://doi:10.3238/arztebl.m2023.0150
10. Jacobson TA, et al; NLA Expert Panel. National Lipid Association Recommendations for Patient-Centered Management of Dyslipidemia: Part 2. J Clin Lipidol. 2015;9(6 Suppl):S1-S122.e1. http://doi:10.1016/j.jacl.2015.09.002.
11. De Vries M, Klop B, Castro Cabezas M. The use of the non-fasting lipid profile for lipid-lowering therapy in clinical practice - point of view. Atherosclerosis. 2014;234(2):473-475. http://doi:10.1016/j.atherosclerosis.2014.03.024
12. American Diabetes Association Professional Practice Committee. 11. Chronic Kidney Disease and Risk Management: Standards of Care in Diabetes-2024. Diabetes Care. 2024;47(Suppl 1):S219-S230. http://doi:10.2337/dc24-S011
13. Finelli A, et al. Management of Small Renal Masses: American Society of Clinical Oncology Clinical Practice Guideline. J Clin Oncol. 2017;35(6):668-680. http://doi:10.1200/JCO.2016.69.9645.
14. Kidney Disease: Improving Global Outcomes (KDIGO) CKD Work Group. KDIGO 2024 Clinical Practice Guideline for the Evaluation and Management of Chronic Kidney Disease. Kidney Int. 2024;105(4S):S117-S314. http://doi:10.1016/j.kint.2023.10.018
15. Pierce CB, Muñoz A, Ng DK, Warady BA, Furth SL, Schwartz GJ. Age- and sex-dependent clinical equations to estimate glomerular filtration rates in children and young adults with chronic kidney disease. Kidney Int. 2021;99(4):948-956. http://doi:10.1016/j.kint.2020.10.047
16. Miller WG. Perspective on New Equations for Estimating Glomerular Filtration Rate. Clin Chem. 2021;67(6):820-822. http://doi:10.1093/clinchem/hvab029.
17. Seegmiller JC, Bachmann LM. Urine Albumin Measurements in Clinical Diagnostics. Clin Chem. 2024;70(2):382-391. http://doi:10.1093/clinchem/hvad174.
18. Sacks DB, Arnold M, Bakris GL, Bruns DE, Horvath AR, Lernmark Å, Metzger BE, Nathan DM, Kirkman MS. Guidelines and Recommendations for Laboratory Analysis in the Diagnosis and Management of Diabetes Mellitus. Diabetes Care. 2023;46(10):e151-e199. http://doi:10.2337/dci23-0036.
19. Zeng C, Liu M, Zhang Y, Deng S, Xin Y, Hu X. Association of Urine Albumin to Creatinine Ratio With Cardiovascular Outcomes in Patients With Type 2 Diabetes Mellitus. J Clin Endocrinol Metab. 2024;109(4):1080-1093. http://doi:10.1210/clinem/dgad645
20. Hwang SW, Lee T, Uh Y, Lee JY. Urinary albumin creatinine ratio is associated with lipid profile. Sci Rep.

2024;14(1):14870. http://doi:10.1038/s41598-024-65037-w
21. American Diabetes Association Professional Practice Committee. 2. Diagnosis and Classification of Diabetes: Standards of Care in Diabetes-2025. Diabetes Care. 2025;48(Supplement_1):S27-S49. http://doi:10.2337/dc25-S002
22. Sacks DB, Arnold M, Bakris GL, Bruns DE, Horvath AR, Lernmark Å, Metzger BE, Nathan DM, Kirkman MS. Executive Summary: Guidelines and Recommendations for Laboratory Analysis in the Diagnosis and Management of Diabetes Mellitus. Diabetes Care. 2023;46(10):1740-1746. http://doi:10.2337/dci23-0048
23. Grundy SM, et al. 2018 AHA/ACC/AACVPR/AAPA/ABC/ACPM/ADA/AGS/APhA/ASPC/NLA/PCNA Guideline on the Management of Blood Cholesterol: A Report of the American College of Cardiology/American Heart Association Task Force on Clinical Practice Guidelines. J Am Coll Cardiol. 2019;73(24):e285-e350. http://doi:10.1016/j.jacc.2018.11.003.
24. Meschia JF, et al; American Heart Association Stroke Council; Council on Cardiovascular and Stroke Nursing; Council on Clinical Cardiology; Council on Functional Genomics and Translational Biology; Council on Hypertension. Guidelines for the primary prevention of stroke: a statement for healthcare professionals from the American Heart Association/American Stroke Association. Stroke. 2014;45(12):3754-832. http://doi:10.1161/STR.0000000000000046
25. Neeland IJ, Lim S, Tchernof A, Gastaldelli A, Rangaswami J, Ndumele CE, Powell-Wiley TM, Després JP. Metabolic syndrome. Nat Rev Dis Primers. 2024;10(1):77. http://doi:10.1038/s41572-024-00563-5
26. Akkız H, Gieseler RK, Canbay A. Liver Fibrosis: From Basic Science towards Clinical Progress, Focusing on the Central Role of Hepatic Stellate Cells. Int J Mol Sci. 2024;25(14):7873. http://doi:10.3390/ijms25147873
27. Sheka AC, Adeyi O, Thompson J, Hameed B, Crawford PA, Ikramuddin S. Nonalcoholic Steatohepatitis: A Review. JAMA. 2020;323(12):1175-1183. http://doi:10.1001/jama.2020.2298
28. American Diabetes Association Professional Practice Committee. 4. Comprehensive Medical Evaluation and Assessment of Comorbidities: Standards of Care in Diabetes-2024. Diabetes Care. 2024;47(Suppl 1):S52-S76. http://doi:10.2337/dc24-S004
29. Giashuddin S, Alawad M. Histopathological Diagnosis of Nonalcoholic Steatohepatitis (NASH). Methods Mol Biol. 2022;2455:1-18. http://doi:10.1007/978-1-0716-2128-8_1
30. Santos JPMD, et al. Non-Alcoholic Steatohepatitis (NASH) and Organokines: What Is Now and What Will Be in the Future. Int J Mol Sci. 2022;23(1):498. http://doi:10.3390/ijms23010498
31. Ouzan D, et al. Using the FIB-4, automatically calculated, followed by the ELF test in second line to screen primary care patients for liver disease. Sci Rep. 2024;14(1):12198. http://doi:10.1038/s41598-024-62549-3
32. Mignot V, et al. Early screening for chronic liver disease: impact of a FIB-4 first integrated care pathway to identify patients with significant fibrosis. Sci Rep. 2024;14(1):20720. http://doi:10.1038/s41598-024-66210-x.
33. Roh YH, Kang BK, Jun DW, Lee CM, Kim M. Role of FIB-4 for reassessment of hepatic fibrosis burden in referral center. Sci Rep. 2021;11(1):13616. http://doi:10.1038/s41598-021-93038-6.
34. Writing Committee; Kontos MC, de Lemos JA, Deitelzweig SB, Diercks DB, Gore MO, Hess EP, McCarthy CP, McCord JK, Musey PI Jr, Villines TC, Wright LJ. 2022 ACC Expert Consensus Decision Pathway on the Evaluation and Disposition of Acute Chest Pain in the Emergency Department: A Report of the American College of Cardiology Solution Set Oversight Committee. J Am Coll Cardiol. 2022;80(20):1925-1960. http://doi:10.1016/j.jacc.2022.08.750
35. Park KC, Gaze DC, Collinson PO, Marber MS. Cardiac troponins: from myocardial infarction to chronic disease. Cardiovasc Res. 2017;113(14):1708-1718. http://doi:10.1093/cvr/cvx183
36. Tsutsui H, et al. Natriuretic Peptides: Role in the Diagnosis and Management of Heart Failure: A Scientific Statement From the Heart Failure Association of the European Society of Cardiology, Heart Failure Society of America and Japanese Heart Failure Society. J Card Fail. 2023;29(5):787-804. http://doi:10.1016/j.cardfail.2023.02.009
37. Volpe M, Gallo G, Rubattu S. Endocrine functions of the heart: from bench to bedside. Eur Heart J. 2023;44(8):643-655. http://doi:10.1093/eurheartj/ehac759
38. Gallo G, Rubattu S, Autore C, Volpe M. Natriuretic Peptides: It Is Time for Guided Therapeutic Strategies Based on Their Molecular Mechanisms. Int J Mol Sci. 2023;24(6):5131. http://doi:10.3390/ijms24065131
39. Sangaralingham SJ, Kuhn M, Cannone V, Chen HH, Burnett JC. Natriuretic peptide pathways in heart failure: further therapeutic possibilities. Cardiovasc Res. 2023;118(18):3416-3433. http://doi:10.1093/cvr/cvac125.
40. Eltayeb M, Squire I, Sze S. Biomarkers in heart failure: a focus on natriuretic peptides. Heart. 2024;110(11):809-818. http://doi:10.1136/heartjnl-2020-318553
41. Vergani M, Cannistraci R, Perseghin G, Ciardullo S. The Role of Natriuretic Peptides in the Management of Heart Failure with a Focus on the Patient with Diabetes. J Clin Med. 2024;13(20):6225. http://doi:10.3390/jcm13206225
42. Wallace TM, Levy JC, Matthews DR. Use and abuse of HOMA modeling. Diabetes Care. 2004;27(6):1487-1495. http://doi:10.2337/diacare.27.6.1487
43. Matli B, et al. Distribution of HOMA-IR in a population-

based cohort and proposal for reference intervals. Clin Chem Lab Med. 2021;59(11):1844-1851. http://doi:10.1515/cclm-2021-0643
44. Diniz MFHS, et al. Homeostasis model assessment of insulin resistance (HOMA-IR) and metabolic syndrome at baseline of a multicentric Brazilian cohort: ELSA-Brasil study. Cad Saude Publica. 2020;36(8):e00072120. http://doi:10.1590/0102-311X00072120
45. Toin T, Reynaud Q, Denis A, Durieu I, Mainguy C, Llerena C, Pin I, Touzet S, Reix P. HOMA indices as screening tests for cystic fibrosis-related diabetes. J Cyst Fibros. 2022;21(1):123-128. http://doi:10.1016/j.jcf.2021.05.010
46. Foo C, et al. Integrating tuberculosis and noncommunicable diseases care in low- and middle-income countries (LMICs): A systematic review. PLoS Med. 2022;19(1):e1003899. http://doi:10.1371/journal.pmed.1003899
47. Korenstein D, Chimonas S, Barrow B, Keyhani S, Troy A, Lipitz-Snyderman A. Development of a Conceptual Map of Negative Consequences for Patients of Overuse of Medical Tests and Treatments. JAMA Intern Med. 2018;178(10):1401-1407. http://doi:10.1001/jamainternmed.2018.3573
48. Pennestrì F, Tomaiuolo R, Banfi G, Dolci A. Blood over-testing: impact, ethical issues and mitigating actions. Clin Chem Lab Med. 2024;62(7):1283-1287. http://doi:10.1515/cclm-2023-1227
49. Beriault DR, Gilmour JA, Hicks LK. Overutilization in laboratory medicine: tackling the problem with quality improvement science. Crit Rev Clin Lab Sci. 2021;58(6):430-446. http://doi:10.1080/10408363.2021.1893642
50. Fleming KA, et al. The Lancet Commission on diagnostics: transforming access to diagnostics. Lancet. 2021;398(10315):1997-2050. http://doi:10.1016/S0140-6736(21)00673-5
51. Durojaiye C, et al. Barriers and facilitators to high-volume evidence-based innovation and implementation in a large, community-based learning health system. BMC Health Serv Res. 2024;24(1):1446. http://doi:10.1186/s12913-024-11803-5
52. Deng W, Yang T, Deng J, Liu R, Sun X, Li G, Wen X. Investigating Factors Influencing Medical Practitioners' Resistance to and Adoption of Internet Hospitals in China: Mixed Methods Study. J Med Internet Res. 2023;25:e46621. http://doi:10.2196/46621
53. Pfeiffer RM, Chen Y, Gail MH, Ankerst DP. Accommodating population differences when validating risk prediction models. Stat Med. 2022;41(24):4756-4780. http://doi:10.1002/sim.9447.
54. Kim JE, Joo J, Kuku KO, Downie C, Hashemian M, Powell-Wiley TM, Shearer JJ, Roger VL. Prevalence, Disparities, and Mortality of Cardiovascular-Kidney-Metabolic Syndrome in US Adults, 2011-2018. Am J Med. 2025 Feb 3:S0002-9343(25)00063-4. http://doi:10.1016/j.amjmed.2025.01.031
55. Zhu R, Wang R, He J, Wang L, Chen H, Niu X, Sun Y, Guan Y, Gong Y, Zhang L, An P, Li K, Ren F, Xu W, Guo J. Prevalence of Cardiovascular-Kidney-Metabolic Syndrome Stages by Social Determinants of Health. JAMA Netw Open. 2024;7(11):e2445309. http://doi:10.1001/jamanetworkopen.2024.45309
56. Claudel SE, Schmidt IM, Waikar SS, Verma A. Cumulative Incidence of Mortality Associated with Cardiovascular-Kidney-Metabolic Syndrome. J Am Soc Nephrol. 2025 Feb 11. http://doi:10.1681/ASN.0000000637
57. Li N, Li Y, Cui L, Shu R, Song H, Wang J, Chen S, Liu B, Shi H, Gao H, Huang T, Gao X, Geng T, Wu S. Association between different stages of cardiovascular-kidney-metabolic syndrome and the risk of all-cause mortality. Atherosclerosis. 2024;397:118585. http://doi:10.1016/j.atherosclerosis.2024.118585

Case report

Metabolic and Cardiac Complications in a Case of Adrenal Carcinoma

Lechuang Chen[1], Jieli Li[2], Qing H. Meng[1*]

[1]Department of Laboratory Medicine, The University of Texas MD Anderson Cancer Center, Houston, USA
[2]Department of Pathology, The Ohio State University, Wexner Medical Center, Columbus, OH, USA

Article Info

[*]***Corresponding Author:***
Qing H. Meng
Department of Laboratory Medicine
The University of Texas MD Anderson Cancer Center
1515 Holcombe Blvd., Unit 37, Houston, TX 77030-4009.
Fax 713-792-4793
E-mail: qhmeng@mdanderson.org

Keywords

Adrenocortical carcinoma, Cushing syndrome, Cortisol, Electrolytes, Heart failure

Introduction

Adrenocortical carcinoma (ACC) is a very rare and aggressive cancer originating from the adrenal cortex. Most adrenal gland masses are benign, often discovered incidentally during medical imaging, affecting approximately 5–9% of adults. In contrast, malignant adrenal tumors such as ACC are extremely rare, with an estimated incidence of one case per million people per year [1]. These malignant tumors may be hormonally active (functioning), causing significant hormonal imbalance, or inactive (non-functioning), which typically remain symptom-free until the disease advances [2]. Current guidelines strongly recommend manage ACC by a multidisciplinary team, to effectively address its clinical challenges and enhance patient outcomes [3].

Functioning ACC tumors frequently produces excess cortisol, resulting in severe Cushing's syndrome. This hypercortisolism leads to special physical features including central obesity, facial rounding, easy bruising, muscle weakness, high blood pressure, and abnormal glucose metabolism [4]. Diagnosis involves clinical assessment, hormonal testing, and imaging studies to confirm adrenal gland pathology. Effective treatment typically requires surgical removal of the tumor (adrenalectomy), often preceded by medications like metyrapone to reduce cortisol levels preoperatively, improving patient outcomes [5].

The cardiovascular system is particularly vulnerable to the effects of elevated cortisol. Chronic hypercortisolism contributes significantly to metabolic disturbances such as hyperglycemia, high blood pressure, hypernatremia, and hypokalemia, all of which can severely exacerbate pre-existing heart conditions or even precipitate new cardiovascular disease [6]. The interaction between these metabolic abnormalities and cardiovascular health often leads to increased heart workload, fluid overload, reduced cardiac function, and elevated risk of heart failure and myocardial infarction [7]. Thus, effective metabolic and cardiac management remain crucial in improving survival and quality of life for patients.

Our case report emphasizes the complexities involved managing metabolic and cardiovascular complications in a patient with adrenocortical carcinoma and after adrenalectomy, highlighting the essential role of a coordinated multidisciplinary team.

Clinical-Diagnostic Case

A 65-year-old man was initially admitted to the hospital with symptoms including persistent hypertension (176/81 mmHg), facial rounding, easy bruising and was evaluated by our internal medicine and endocrinology teams. As his condition progressed, the patient developed congestive heart failure complicated by myocardial infarction, acute respiratory failure, hypokalemia, anemia, and pneumonia. Meanwhile, the patient had multiple chronic health conditions, including high cholesterol, diabetes, arthritis, osteoporosis, bone compression fractures, and acid reflux. During his hospital stay, the patient was diagnosed with adrenocortical carcinoma by imaging and histopathology. The patient received metyrapone, a medication used to reduce cortisol levels, correct metabolic disturbances, and reduce surgical risks. Subsequent surgical intervention included left adrenalectomy, partial exploration of the adrenal gland with excision of an adjacent retroperitoneal tumor, and complete splenectomy.

In the postoperative period, the patient's pre-existing heart failure remained unimproved, along with recurrent hypertension, atrial fibrillation, pulmonary edema, and infections, accompanied by nausea, weakness, confusion, and irritability. Postoperative vital signs included blood pressure 148/96 mmHg, pulse ranging from 63 to 103 beats per minute, and respiratory rates ranging from 14 to 21 breaths per minute. Physical examination revealed generalized weakness, diminished bilateral lung sounds, and mild abdominal distension with tenderness in the lower right quadrant. Additionally, the patient's extremities showed no signs of cyanosis or clubbing, but grade 2 bilateral upper- and lower-extremity edema was noted.

Laboratory tests performed during the patient's hospital stay showed his sodium levels were consistently high at 150 mmol/L, while potassium levels were decreased at 2.9 mmol/L, aligning with the typical electrolyte disturbances seen in similar cases (Table 1). Additionally, the total CO_2 level at 29 mmol/L and an arterial HCO_3 level of 32 mmol/L, along with a base excess of 6 mmol/L, were indicative of a metabolic alkalosis. Postoperative results showed a significant shift, with sodium levels reducing to 142 mmol/L and potassium levels increasing to 4.2 mmol/L. Notably, the postoperative total CO_2 decreased to 22 mmol/L and arterial HCO_3 decreased to 28 mmol/L, reflecting a correction towards normal acid-base balance. Endocrine function tests were critical considering the patient's adrenal pathology and surgery. Prior to surgery, the patient's cortisol and urine cortisol levels were significantly elevated at 82.7 µg/dL (8 am) and 800 µg/24 hr, respectively, with a corresponding glucose level of 170 mg/dL. Postoperatively, cortisol levels normalized to 14.2 µg/dL (with cortisol supplementation), and glucose levels also returned to the normal range. The adrenocorticotropic hormone (ACTH) levels were suppressed before surgery, at 5 pg/mL, but rebounded postoperatively to 31 pg/mL. Cardiac markers were continuously monitored due to the patient's history of heart failure. Troponin-T levels were elevated pre- and postoperatively, initially measuring 313 ng/L and peaking at 445 ng/L. NT-proBNP levels initially measured 13,432 pg/mL, remaining high at 12,617 pg/mL postoperatively. Postoperative cardiac imaging via X-ray and echocardiography revealed an ejection fraction of 35%, corroborating the diagnosis of congestive heart failure.

Table 1: Principal laboratory results.

Test	Pre-surgery1	Post-surgery2	Reference intervals (RI)
Sodium	150	142	136-145 mmol/L
Potassium	2.9	4.2	3.5-5.1 mmol/L
Chloride	107	112	98-107 mmol/L
Anion gap	9	13	4-14 mmol/L
Total CO_2	29	22	22-29 mmol/L
BUN	20	26	6-23 mg/dL
Creatinine	0.57	0.56	0.67-1.17 mg/dL
eGFRNAA	105	109	≥60 mL/min/1.73 m^2
Calcium	7.7	7.6	8.4-10.2 mg/dL
Magnesium	1.8	2.1	1.6-2.6 mg/dL
Phosphorus	2.7	4.1	2.5-4.5 mg/dL
Troponin-T (Gen 5)	313	445	≤18 ng/L
NT-proBNP	13,432	12,617	≤125 pg/mL

pH, arterial	7.41	7.38	7.35-7.45
pCO_2, arterial	50	35	35-45 mmHg
pO_2, arterial	39	118	83-108 mmHg
HCO_3	32	28	22-26 mmol/L
Base excess, arterial	6	0	-2-3 mmol/L
O_2 saturation, arterial	71	99	92-98%
Glucose	170	95	70-99 mg/dL
Cortisol (0800h)	82.7	14.2	4.8-19.5 µg/dL
Cortisol (U24h)	800	N/A	3.5-45 µg/24hr
ACTH	5	31	7-63 pg/mL

BUN, blood urea nitrogen; eGFRNAA, estimated glomerular filtration rate, non-African American; NT-proBNP, N-terminal pro b-type natriuretic peptide; ACTH, adrenocorticotropic hormone. Pre-surgery1: one week before the surgery; Post-surgery2: one week after the surgery.

The patient's postoperative treatment regimen addressed his adrenal insufficiency, cardiovascular conditions, and electrolyte imbalances. Hydrocortisone (20 mg), furosemide (Lasix; 40 mg), and carvedilol (Coreg; 25 mg) were administered daily to manage adrenal insufficiency, fluid retention, and heart failure, respectively. Losartan (Cozaar; 25 mg daily) was prescribed to manage hypertension, and potassium chloride (10 mmol/L daily) was given to correct hypokalemia. Additionally, low-dose aspirin (81 mg daily) was initiated, along with atorvastatin (Lipitor; 20 mg daily), to reduce the risk of further heart disease and stroke.

Discussion

Regulation of the hypothalamic-pituitary-adrenal axis

In this case study, a patient with endocrine disease progressed through three distinct clinical stages, each marked by significant changes in hormone levels and clinical symptoms. Initially, the patient's cortisol and urine cortisol levels were both markedly high, which are characteristic of Cushing syndrome. This condition, known as hypercortisolism, was consistent with the patient's clinical presentations, including hyperglycemia and suppressed levels of ACTH. Furthermore, the patient exhibited typical physical features of Cushing syndrome such as pronounced central obesity, facial rounding, and skin changes. The diagnosis of Cushing syndrome was further supported by the presence of hypertension, hypernatremia, hypokalemia, and metabolic alkalosis (Table 1).

Following surgical intervention, including adrenalectomy, the patient experienced a sharp decline in cortisol production due to the loss of adrenal gland function, disrupting the hypothalamic-pituitary-adrenal (HPA) axis (Figure 1). The HPA axis is a central regulatory system that manages the body's response to stress, regulates immune function, and maintains energy storage through the secretion of hormones, predominantly cortisol. This hormonal insufficiency led to a range of symptoms including general weakness, hypotension, and metabolic acidosis. Cortisol deficiency has been observed following adrenalectomy, even in patients with adequate preoperative adrenal function [8].

Figure 1: The hypothalamic-pituitary-adrenal axis under normal conditions and post-adrenalectomy.

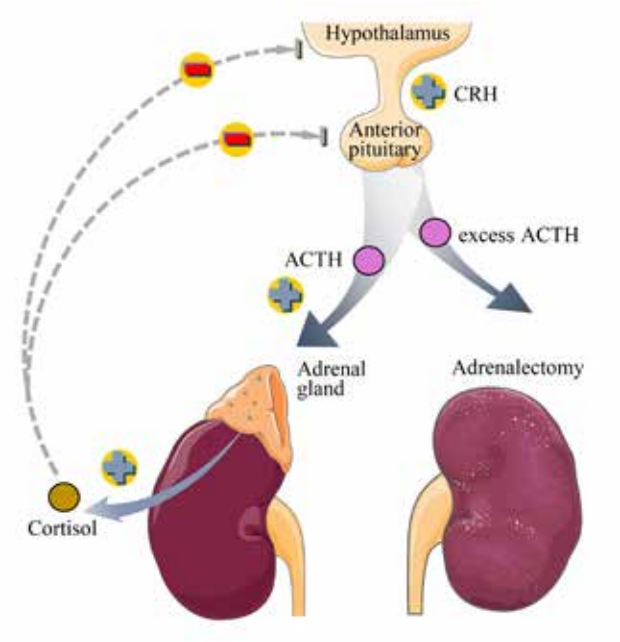

Under normal conditions (left), the hypothalamus releases corticotropin-releasing hormone (CRH), which stimulates the pituitary to secrete ACTH. ACTH further stimulates cortisol production from the adrenal glands, maintaining homeostasis through negative feedback. Adrenalectomy (right) eliminates cortisol, disrupting feedback, increasing ACTH and CRH as the body tries to stimulate the absent adrenal gland.

Postoperatively, the patient was immediately treated with steroid hormone therapy to mitigate the effects of adrenal insufficiency. Treatment with hydrocortisone (20 mg daily) effectively normalized his cortisol levels to 14.2 µg/dL and glucose levels to 95 mg/dL. Additionally, his ACTH levels returned to normal (31 pg/mL) within a week, indicating the partial restoration of HPA axis function. During the six-month follow-up, the patient improved in glucose control and cortisol levels, while he was still physical weakness and fatigue persisted. Concurrently, the patient continued to experience hypertension and episodes of atrial fibrillation, which were managed with adjustments to his cardiovascular medications. These conditions highlight the complex and long-lasting complications after adrenal surgery.

Metabolic disorder and cardiac complications

During his hospital stay, the patient's Troponin T levels remained elevated around 400 ng/L. Concurrently, NT-proBNP levels remained around 13,000 pg/mL, indicated significant cardiac distress exacerbated by fluid overload and metabolic disorders. The interplay between metabolic disturbances and cardiac dysfunction created a complex clinical situation.

The patient's Cushing syndrome, characterized by excessive cortisol secretion, contributes to multiple metabolic disturbances, including hyperglycemia, hypertension, and hypernatremia, all of them can exacerbate heart failure [9]. Cortisol promotes gluconeogenesis and induces insulin resistance, leading to persistent hyperglycemia, which contributes to endothelial dysfunction, increased oxidative stress, and myocardial energy dysregulation [4]. Additionally, cortisol enhances vascular sensitivity to catecholamines and stimulates sodium and water retention by activating mineralocorticoid receptors in the kidneys, mimicking aldosterone's effects. This leads to increased intravascular volume, elevated blood pressure, and heightened cardiac workload [6]. Hypernatremia can further exacerbate fluid retention by disrupting osmotic balance, drawing water into the intravascular space, and increasing plasma volume. This expansion of extracellular fluid places additional strain on the heart, promoting left ventricular hypertrophy and impairing diastolic relaxation [10]. As a result, the increased afterload and volume overload associated with Cushing's syndrome can accelerate the progression of heart failure by deteriorating myocardial oxygen demand, reducing cardiac efficiency, and predispose the heart to structural and functional deterioration.

Hypokalemia is a complication of both Cushing's syndrome and heart failure treatment, and it plays a critical role in cardiac function deterioration. Potassium is essential for maintaining myocardial excitability, and its depletion disrupts normal cardiac electrophysiology by prolonging repolarization and increasing the risk of arrhythmias, including ventricular tachycardia and fibrillation [7]. Hypokalemia also impairs myocardial contractility by reducing the activity of sodium-potassium ATPase, leading to inefficient cardiac muscle function. Furthermore, arterial blood gas analyses revealed metabolic alkalosis, with elevated total CO_2 and base excess.

Metabolic alkalosis in this patient was likely influenced by renal bicarbonate reabsorption and hydrogen ion loss in response to potassium depletion [11]. Metabolic alkalosis further compromises cardiac function by reducing ionized calcium levels, decreasing myocardial contractility, and exacerbating vasoconstriction, which can increase vascular resistance and further burden the failing heart.

Additional diagnostic considerations

To fully investigate the patient's metabolic disorder, it would be necessary to comprehensively evaluate his hormonal levels. According to the current clinical practice guidelines, a thorough assessment of cortisol levels requires repeated measurement of 24-hour urinary-free cortisol for assessing cortisol production postoperatively [12]. However, our patient did not have his postoperative 24-hour urinary-free cortisol levels measured. Obtaining this test would have helped evaluate the effectiveness of the adrenalectomy and monitor for any recurrence of hypercortisolism. Moreover, with persistent metabolic alkalosis, measuring serum aldosterone and plasma renin activity would have helped evaluate his mineralocorticoid status. Elevated aldosterone levels with plasma renin activity could indicate primary hyperaldosteronism, while low aldosterone levels might suggest other causes of mineralocorticoid excess or pseudo-hyperaldosteronism. An ACTH stimulation test could have provided valuable information about the residual function of the patient's remaining adrenal tissue. This test assesses the adrenal gland's ability to produce cortisol in response to exogenous ACTH, which is crucial in patient's post-adrenalectomy to determine the need for long-term glucocorticoid replacement therapy [13]. Regular monitoring of vital signs, electrolyte levels, renal function, and cardiac markers remained integral to managing the patient's complex metabolic state. For example, the patient's blood urea nitrogen levels increased from 20 mg/dL preoperatively to 32 mg/dL two months later, and his creatinine levels remained stable at 0.56 mg/dL, indicating the need for careful renal monitoring. The estimated glomerular filtration rate remained above 100 mL/min/1.73 m², suggesting preserved renal filtration but warranting vigilance due to potential prerenal azotemia from hypovolemia or heart failure [14].

Collaborative management involving endocrinology, cardiology, nephrology, and oncology specialists was essential to address the multifaceted challenges in this patient's care. Developing his treatment plan required an interdisciplinary approach to optimize outcomes and improve his quality of life.

Take home messages/Learning points

This case highlights that disruption of the hypothalamic-pituitary-adrenal (HPA) axis due to adrenocortical carcinoma significantly impacts endocrine and metabolic functions, leading to complex clinical challenges. It emphasizes the necessity of recognizing biochemical disturbances, including elevated cortisol levels, suppressed ACTH, electrolyte abnormalities (hypernatremia, hypokalemia, etc.), and metabolic alkalosis, typical in severe Cushing's syndrome. Clinicians must be aware of the disease process through hormonal assessment to provide appropriate treatment. Furthermore, electrolyte imbalances arising from endocrine dysfunction can severely worsen pre-existing cardiac conditions, highlighting the need for integrated endocrine and cardiac management. Finally, comprehensive postoperative hormonal monitoring is critical for detecting residual tumor activity or recurrence, ensuring effective long-term management, and improving patient outcomes.

Ethical approval and consent to participate

The IRB of The University of Texas MD Anderson Cancer Center determined that the study met the criteria for exemption under Category 4 (secondary research on data or specimens, no consent required), and a waiver of HIPAA authorization was granted for use of PHI.

Author contributions

All authors confirmed they have contributed to the intellectual content of this paper. Lechuang Chen: Writing – original draft, Investigation, Formal analysis, Data curation. Jieli Li: Writing – review & editing, Resources, Investigation, Data curation. Qing H. Meng: Writing – review & editing, Supervision, Resources, Project administration, Methodology, Investigation, Data curation, Conceptualization.

Disclosure statement

No potential conflict of interest was reported by the author(s).

Funding

This study received no external funding.

References

1. Fassnacht M, Libe R, Kroiss M, Allolio B. Adrenocortical carcinoma: a clinician's update. Nat Rev Endocrinol. 2011;7(6):323-335. https://doi.org/10.1038/nrendo.2010.235 (accessed: 10/28/2024)
2. Else T, Kim AC, Sabolch A, Raymond VM, Kandathil A, Caoili EM, et al. Adrenocortical carcinoma. 2014;35(2):282-326. https://doi.org/10.1210/er.2013-1029 (accessed: 10/28/2024)
3. Fassnacht M, Tsagarakis S, Terzolo M, Tabarin A, Sahdev A, Newell-Price J, et al. European Society of Endocrinology clinical practice guidelines on the management of adrenal incidentalomas, in collaboration with the European Network for the Study of Adrenal Tumors. 2023;189(1):G1-G42. https://doi.org/10.1093/ejendo/lvad066 (accessed: 10/28/2024)
4. Reincke M, Fleseriu M. Cushing syndrome: a review. JAMA. 2023;330(2):170-181. https://doi.org/10.1001/jama.2023.11305 (accessed: 10/28/2024)

5. Kamenicky P, Droumaguet C, Salenave S, Blanchard A, Jublanc C, Gautier JF, et al. Mitotane, metyrapone, and ketoconazole combination therapy as an alternative to rescue adrenalectomy for severe ACTH-dependent Cushing's syndrome. J Clin Endocrinol Metab. https://doi.org/10.1210/jc.2011-0536 2011;96(9):2796-2804. (accessed: 10/28/2024)
6. Mishra S, Kass DA. Cellular and molecular pathobiology of heart failure with preserved ejection fraction. Nat Rev Cardiol. 2021;18(6):400-423. https://doi.org/10.1038/s41569-020-00480-6 (accessed: 10/28/2024)
7. Felker GM, Ellison DH, Mullens W, Cox ZL, Testani JM. Diuretic therapy for patients with heart failure: JACC state-of-the-art review. J Am Coll Cardiol. 2020;75(10):1178-1195. https://doi.org/10.1016/j.jacc.2019.12.059 (accessed: 10/28/2024)
8. Fiore M, Baia M, Conti L, Piccioni F, Mariani L, Pasquali S, et al. Residual Adrenal Function After Multivisceral Resection With Adrenalectomy in Adult Patients. JAMA Surg. 2022;157(5):415-423. https://doi.org/10.1001/jamasurg.2021.7588 (accessed: 1/07/2025)
9. Gadelha M, Gatto F, Wildemberg LE, Fleseriu M. Cushing's syndrome. Lancet. 2023;402(10418):2237-2252. https://doi.org/10.1016/s0140-6736(23)01961-x (accessed: 1/07/2025)
10. Kamel KS, Schreiber M, Harel Z. Hypernatremia. JAMA. 2022;327(8):774-775. https://doi.org/10.1001/jama.2022.1376 (accessed: 1/07/2025)
11. Emmett M. Metabolic alkalosis: a brief pathophysiologic review. Clin J Am Soc Nephrol. 2020;15(12):1848-1856. https://doi.org/10.2215/cjn.16041219 (accessed: 1/07/2025)
12. Nieman LK, Biller BM, Findling JW, Murad MH, Newell-Price J, Savage MO, et al. Treatment of Cushing's syndrome: an endocrine society clinical practice guideline. J Clin Endocrinol Metab. 2015;100(8):2807-2831. https://doi.org/10.1210/jc.2015-1818 (accessed: 1/21/2025)
13. Prete A, Bancos I. Mild autonomous cortisol secretion: pathophysiology, comorbidities and management approaches. Nat Rev Endocrinol. 2024:1-14. https://doi.org/10.1038/s41574-024-00984-y (accessed: 1/21/2025)
14. Molitoris BA. Low-flow acute kidney injury: the pathophysiology of prerenal azotemia, abdominal compartment syndrome, and obstructive uropathy. Clin J Am Soc Nephrol. 2022;17(7):1039-1049. https://doi.org/10.2215/cjn.15341121 (accessed: 1/21/2025)

Case report

A rare combination of Hereditary folate malabsorption (SLC46A1 gene variant) and beta-thalassemia trait

Dolat Singh Shekhawat[1], Siyaram Didel[1*], Abhishek Purohit[2], Kuldeep Singh[1]

[1]*Medical Genetics, Department of Pediatrics, All India Institute of Medical Sciences, Jodhpur, India*
[2]*Department of Pathology and Lab Medicine, All India Institute of Medical Sciences, Jodhpur, India*

Article Info

[*]***Corresponding Author:***
Siyaram Didel, Associate Professor (Incharge PHO Div.)
Department of Pediatrics, All India Institute of Medical Sciences, Jodhpur, India
E-mail: drdsram2001@gmail.com

Keywords

Hereditary folate malabsorption disease, SLC46A1 gene, HBB, beta-thalassemia

Abstract

Background: Hereditary folate malabsorption is an autosomal recessive disorder caused by a pathogenic variant in SLC46A1, affecting proton-coupled folate transporter (PCFT) function. Infants with hereditary folate malabsorption often develop megaloblastic anemia and, without treatment, may experience serious neurodegenerative complications. Thalassemia is also an autosomal recessive genetic disorder. Major or compound heterozygous thalassemia is associated with severe complications and may require regular blood transfusions.

Case: A couple is seeking guidance on the recurrence risk of the condition that led to the loss of their two previous children. The second child's medical history and laboratory findings indicate a low vitamin B12 level 137.5 pg/mL, "reference range 211-911 pg/mL", elevated homocysteine 34.98 µmol/L, "reference range 3.7 -13.9 µmol/L", and ferritin levels at 1129 ng/mL "reference range 18.2 -341.2 ng/mL". Hematological results show a hemoglobin level of 6.4 g/dL, a total reticulocyte count of 3.39%, MCV of 82.7 fL, MCH of 26.9 pg, RDW of 19.0%, neutrophils at 27%, and lymphocytes at 42%. Hb-HPLC analysis revealed an HbA2 level of 4.6%. Whole-exome sequencing identified a homozygous pathogenic variant in the SLC46A1 gene (c.1127G>A), associated with hereditary folate malabsorption and a heterozygous pathogenic variant in the HBB gene (c.92+5G>C), linked to β-thalassemia. The first child's medical history also suggests low vitamin B12 levels and elevated homocysteine and ferritin levels. Hb-HPLC showed normal results, and genetic testing was not undertaken.

Conclusion: The homozygous SLC46A1 (c.1127G>A) variant is lethal, whereas a heterozygous state with SLC46A1 (c.1127G>A) and HBB (c.92+5G>C) may not be associated with complications like transfusion-dependent thalassemia.

Introduction

Hereditary folate malabsorption (HFM), or congenital folate malabsorption (OMIM#229050), is a rare autosomal recessive condition that can affect multiple organ systems and is potentially treatable. It results from homozygous or compound heterozygous variants in the SLC46A1 gene, which encodes the proton-coupled folate transporter (PCFT). Loss of function in this transporter impairs intestinal folate absorption and transport into the central nervous system. Importantly, HFM is a potentially treatable condition, making early diagnosis critical to prevent serious complications and optimize clinical outcomes [1]. This transporter is essential for folate absorption in the intestine and its transport across the choroid plexus. PCFT dysfunction causes folate deficiency in both serum and cerebrospinal fluid (CSF), manifesting as hematologic, immunologic, gastrointestinal, neurological symptoms and mitochondrial disease [2,3]. Intracranial calcifications are often observed in neuroimaging [4]. The diagnosis is established through various methods, including evidence of impaired absorption of an oral folate challenge[5], persistently low CSF folate levels despite corrected serum folate, or molecular genetic testing revealing pathogenic variants in SLC46A1. This report highlights the clinical presentation, biochemical profile, and genetic findings of a patient diagnosed with homozygous HFM and beta-thalassemia trait, representing the first documented case of its kind.

Case detail

A non-consanguineous couple visited the Hematology and Medical Genetics clinic seeking guidance on the recurrence risk of the condition that led to the loss of their two previous children. They expressed a desire to understand the underlying cause and explore preventive measures for future pregnancies. A detailed three-generation pedigree was constructed (Figure 1), and a comprehensive medical history was obtained.

The first child, a male, had a history of severe anemia, hepatosplenomegaly, and vitamin B12 deficiency (levels: 188 pg/mL, reference range 211-911 pg/mL) with hypersegmented neutrophils, elevated lactate dehydrogenase (LDH), and a fatal outcome at 2.5 years of age. Laboratory findings included ferritin levels of 900 ng/mL "reference range 18.2 -341.2 ng/mL", hemoglobin 6.2 g/dL, total reticulocyte count 2.39%, mean corpuscular volume (MCV) 72.7 fL, mean corpuscular hemoglobin (MCH) 25.9 pg, and red cell distribution width (RDW) 19.0%. Differential counts showed neutrophils at 22% (reference range 55–70%) and lymphocytes at 70% (reference range 20–40%). The Hb-HPLC profile was normal (Table 1). No genetic test was performed. These findings were suggestive of a complex underlying hematological and metabolic disorder requiring further investigation.

The second child, a male, was admitted to the Pediatric Intensive Care Unit (PICU) with severe anemia, congestive cardiac failure (CCF), mild tachypnea, severe acute respiratory distress syndrome (ARDS), and other complications. These included hyperglycemia (steroid-induced), hepatomegaly with the liver palpable 2 cm below the costal margin along the midclavicular line, splenomegaly with the spleen palpable 1 cm below the costal margin, thing, lusterless, and sparse hair. Despite these systemic manifestations, anthropometric measurements were normal. Laboratory findings indicated a low vitamin B12 level (137.5 µmol/L, reference range 211-911 pg/mL), elevated homocysteine (34.98 µmol/L, "reference range 3.7 -13.9 µmol/L"), and ferritin levels at 1129 ng/mL (reference range 18.2 -341.2 ng/mL). Hematological results showed hemoglobin at 6.4 g/dL, total reticulocyte count at 3.39%, MCV at 82.7 fL, MCH at 26.9 pg, RDW at 19.0%, neutrophils at 27% (reference 55–70%), and lymphocytes at 42% (reference 20–40%). Hb-HPLC showed HbA2 at 4.6%, with a maternal level of 4.2%, and normal findings for the father (Table 1). The neonatal, anthropometric, and clinical history, as documented in the medical records, is summarized in Table 2.

Suspecting an inborn error of metabolism (IEM) due to the clinical presentation and sibling history, further metabolic investigations, including tandem mass spectrometry (TMS), gas chromatography-mass spectrometry (GC-MS), amino acid, and acylcarnitine profiles, were performed but yielded normal results. After that, the family was advised to conduct further evaluation and clinical management based on the findings of the genetic report. Whole-exome sequencing (WES) identified a homozygous pathogenic variant in the SLC46A1 gene (c.1127G>A), a single heterozygous 5' splice variant in Intron 1 of the (c.92+5G>C), and a single heterozygous variant of uncertain significance in the KRT83 gene (c.950G>A). Unfortunately, the child succumbed on the 12th day of PICU admission due to multiple complications, including CCF, severe anemia, vitamin B12 deficiency, severe ARDS, stage 3 acute kidney injury (AKI), acute liver failure, and catecholamine-refractory septic shock.

The clinical and laboratory findings, along with the genetic data, strongly suggested that the deaths of both affected children were due to the same underlying condition. Genetic counseling was provided to the family, and WES was recommended for the parents to understand the recurrence risk better and to guide management in future pregnancies.

WES of the mother revealed a heterozygous pathogenic variant in the SLC46A1 gene (c.1127G>A), associated with HFM, and a heterozygous pathogenic variant in the HBB gene (c.92+5G>C), linked to beta-thalassemia. Additionally, a heterozygous missense variant of uncertain significance (VUS) in the KRT83 gene (c.950G>A) was identified, though its clinical relevance is unclear. WES of the father identified a heterozygous pathogenic variant in the SLC46A1 gene (c.1127G>A), as summarized in Table 3.

The second child harbored a homozygous SLC46A1 variant (c.1127G>A) inherited from both parents. Additionally, a heterozygous missense HBB variant (c.92+5G>C) was inherited from the mother.

The risks associated with genetic variations in future pregnancies were thoroughly explained. Each pregnancy carries a 25% risk of homozygous SLC46A1 gene variants. Additionally, there is a 25% chance of the fetus being heterozygous for SLC46A1 and heterozygous HBB gene variants.

Figure 1: Pedigree of the family.

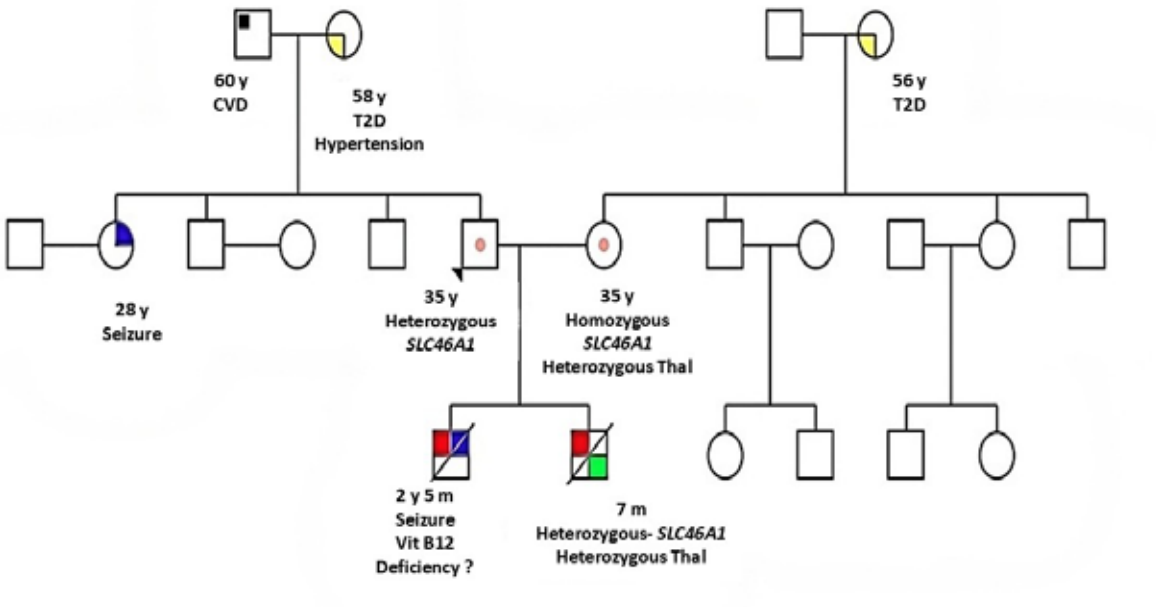

Table 1: Hb-HPLC profile of the couple and previous children.

Parameter	Second child (Ref.)	First child (Ref.)	Father (Ref.)*	Mother
HGB (g/dL)	6.4 (17-20)	6.2 (10.2-12.7)	14.3 (11-16)	10.7
RBC (109/L)	3.3 (3.5-7.5)	2.39 (4.1-6.7)	5.71 (3.5-5.5)	6
MCV (fL)	82.0 (95-125)	72.70 (80-96)	98.6 (82-100)	76.3
MCH (pg)	26.9 (30-42)	25.90 (27-31)	25.0 (27-34)	17.8
RDW-CV (%)	25.4 (11-16)	19.0 (10-15)	19.9 (11-16)	19
HPLC				
HbA (%)	88.8	92.1	92	91.4
HbA2 (%)	4	3.1	2.9	4.7
HbF (%)	1.6	0.9	0.9	0.7
P3 (%)	5.6	3.9	4.2	3.2

P3 – unknown peak at retention time 1.52 minute, Ref. -Reference range, (Ref.)* - reference range common for mother and father

Table 2: Development and clinical detail of sibling (as per available medical history).

Parameter	First child	Second child
Age of child at presentation	7 months	6 month
Birth history and anthropometry parameters at birth	Term, normal vaginal delivery; Birth Weight – 3.5 Kg	Term, normal vaginal delivery; Birth Weight – 3.2 Kg
Developmental history	Development as per the age	Development as per the age (sitting with own support, monosyllables, unidextrous reach, followed light and sound)
Anthropometry at presentation	Length – 68 cm (50th centile); Weight – 7.3 (3rd centile); Occipitofrontal Circumference – 44 cm (50th centile)	Length – 66 cm (25th centile); Weight – 6.7 (3rd centile); Occipitofrontal Circumference – 43 cm (40th centile)

Chief complaint at first presentation	Cough, low-grade fever, issues with feeding, significant pallor	Cough for one month (dry, non-spasmodic), low-grade fever for 2 days, difficulty in breathing, significant pallor
History of blood transfusion and treatment	Lowest Hb – 5.1 gm/dl; First transfusion at 6 months of age; Received – Vitamin B12, antibiotic, folate supplements	Lowest Hb – 4.1 gm/dl; First transfusion at 5 months of age; Received – Vitamin B12, folate supplements, antibiotics, immunoglobulin and antiviral
Final diagnosis made	As per available historical records – Pancytopenia under evaluation with B12 deficiency (166.9 µmol/L) with PBF s/o micro-ovalocytes, hypersegmented neutrophils and high LDH	Congestive cardiac failure, severe anemia, severe vitamin B12 deficiency (137.5 µmol/L) with hyperhomocysteinemia (34.98 µmol/L), severe ARDS (H1N1 Pneumonia), stage 3 acute kidney injury, acute liver failure, and catecholamine-refractory septic shock, multiple organ dysfunction, thalassemia minor
Cause of death	Death at the age of 2.5 years; 1a -??? Congestive cardiac failure; 1b - Severe anemia with ?? Systemic viral illness leading to decompensation	Death at the age of 8 months; 1a - Pulmonary Hemorrhage; 1b - Catecholamine refractory septic shock with respiratory distress syndrome; 1c - Severe H1N1 Pneumonia

Table 3: Findings of whole-exome sequencing in the father, mother, and child.

Subject	Gene	Zygosity	Genotype	Reference Sequence
Father	SLC46A1 Exon 3	Heterozygous	c.1127G>A, p.Arg376Gln	GRCh38
Mother	SLC46A1 Exon 3	Heterozygous	c.1127G>A, p.Arg376Gln	
	HBB Intron 1	Heterozygous	c.92+5G>C	
Second child	SLC46A1 Exon 3	Homozygous	c.1127G>A, p.Arg376Gln	
	HBB Intron 1	Heterozygous	c.92+5G>C	
First child	-	-	-	

The WES was performed using NovaSeq 6000 Illumina sequencing platform.

Discussion

A heterozygous missense variant in exon 3 of the SLC46A1 gene (chr17:g.28402276C>T) that results in the amino acid substitution of Glutamine for Arginine at codon 376 (p.Arg376Gln). The observed variant has previously been reported in patients affected with HNM and functional studies provide strong evidence that the variant has a damaging effect on the gene or gene product [6]. Clinical phenotype characterized by gastrointestinal, hematologic, immunologic, and neurological complications due to folate deficiency from the neonatal period onward. It is primarily caused by defective oral folate absorption and reduced CSF folate levels [2], highlighting the need to assess serum and CSF folate, including 5-methyltetrahydrofolate. Huddar et al. also reported a similar case of multisystem involvement with a severe phenotype and died undiagnosed without adequate health care at the age of 3 months [4]. In the present case, the second child died at 7 months of age, with the initial presentation occurring at 6 months. The suspected cause of death was multisystem involvement, possibly triggered by H1N1 pneumonia. The first child first presented with symptoms at 6 months of age and was diagnosed with vitamin B12 deficiency, for which treatment was initiated. However, the child passed away at 2.5 years of age despite ongoing management.

HFM is a treatable cause of neurological deterioration in children and should be considered in those presenting with concomitant megaloblastic anemia [7]. Diagnosis is confirmed by significantly low baseline serum folate levels (<0.1 ng/mL; normal range: 5–15 ng/mL) with minimal or no response to an oral 5-formyl-tetrahydrofolate load [8]. Studies suggest that

intramuscular folinic acid effectively restores CSF folate levels, whereas oral supplementation remains ineffective [5]. In the present case, folate level measurements were unavailable in the medical history of the deceased siblings. This case highlights the potentially fatal consequences when timely and appropriate treatment is not provided.

The reported genotype-phenotype associations of homozygous or compound heterozygous mutations in SLC46A1, resulting in loss of function of PCFT, suggest intracranial calcification [4], immunologic dysfunction, neurologic manifestations, and hematologic issues such as megaloblastic anemia and pancytopenia [9]. In the present case, the medical history of the second child indicates immunological dysfunction (H1N1 pneumonia), as well as hematological and gastrointestinal dysfunction. However, the medical history did not show episodes of seizures or other movement disorders in either sibling.

HFM results from homozygous or compound heterozygous variants in the SLC46A1 gene, with no reported cases involving heterozygous variants in both SLC46A1 and HBB. In this case, genetic analysis of the proband identified a homozygous pathogenic SLC46A1 variant (c.1127G>A) and a heterozygous HBB 5' splice site variant (c.92+5G>C). The clinical phenotype observed in deceased siblings may be attributed to the homozygous SLC46A1 variant or a possible compound heterozygous interaction with HBB.

Thalassemia major and intermedia, may experience folate deficiency due to increased folate utilization by the bone marrow during red blood cell production and ineffective erythropoiesis [10]. However, a recent case-control study suggests that individuals with β-thalassemia trait are not significantly more likely to exhibit folate deficiency compared to healthy controls [11]. In the present case, WES of the parents revealed that the mother carried heterozygous pathogenic variants SLC46A1 (c.1127G>A) and HBB (c.92+5G>C). However, genotype-phenotype correlation in the mother indicated an asymptomatic carrier. The presence of affected children in this context is particularly intriguing, especially considering that pathogenic variants in the SLC46A1 gene, encoding the proton-coupled folate transporter (PCFT), are typically associated with impaired folate absorption and related clinical manifestations.

Folate deficiency is central to HFM, resulting from impaired intestinal absorption and defective transport across the choroid plexus due to mutations in the SLC46A1 gene. In contrast, vitamin B12 deficiency is not intrinsically associated with HFM, as its absorption occurs via an independent pathway involving intrinsic factor and the terminal ileum [2]. However, serum vitamin B12 levels in reported HFM cases have shown considerable variability. For instance, Kumar M et al. [12] and Ahmad I et al. [7]documented elevated vitamin B12 levels as high as 2000 pg/mL, whereas Tan J et al.[13] and Sakurai Y et al.[14] reported markedly low levels of 105.48 pg/mL and 42 pg/mL, respectively. A case series by Manea E et al. [15] described both low and high vitamin B12 levels across different individuals, suggesting that vitamin B12 status in HFM patients may be influenced by factors such as nutritional intake, coexisting deficiencies, or supplementation history. In the present case, the patient exhibited a reduced vitamin B12 level (137.5 pg/mL).

Genetic counseling plays a crucial role in preventing genetic disorders [16]. HFM follows an autosomal recessive inheritance pattern, where each sibling of affected individuals has a 25% chance of being affected, a 50% chance of being a carrier, and a 25% chance of inheriting neither pathogenic variant if both parents are heterozygous for SLC46A1 [8]. Identifying both pathogenic variants within a family enables carrier screening for at-risk relatives and allows for prenatal and preimplantation genetic testing in high-risk pregnancies. In this case, the father was a carrier of SLC46A1 (c.1127G>A), while the mother was heterozygous for SLC46A1 (c.1127G>A) and HBB (c.92+5G>C). Both parents were healthy, with no history of illness. The deceased child was homozygous for SLC46A1 (c.1127G>A) and a carrier of HBB (c.92+5G>C). The likely cause of death was FHM, homozygous SLC46A1 (c.1127G>A) variant.

Conclusion

HFM is a treatable genetic disorder where early diagnosis is crucial. The homozygous SLC46A1 (c.1127G>A) variant is lethal, whereas a heterozygous state with SLC46A1 (c.1127G>A) and HBB (c.92+5G>C) is not associated with complications. Identifying both pathogenic variants in a family facilitates carrier screening for at-risk relatives and enables prenatal and preimplantation genetic testing in high-risk pregnancies.

Data Availability Statement

The data supporting this study's findings are available in this manuscript.

Ethical Approval and Consent

Consent was taken from both parents for this case report. All authors listed gave consent for the publication of this paper.

Conflicts of Interest

The authors declare no conflicts of interest.

Author Contributions

All authors contributed equally to the writing, development, and finalization of the case report.

Funding

None.

References

1. Zhan H-Q, Najmi M, Lin K, Aluri S, Fiser A, Goldman ID, et al. A proton-coupled folate transporter mutation

causing hereditary folate malabsorption locks the protein in an inward-open conformation. J Biol Chem 2020;295:15650–15661. https://doi.org/10.1074/jbc.RA120.014757.
2. Zhao R, Aluri S, Goldman ID. The proton-coupled folate transporter (PCFT-SLC46A1) and the syndrome of systemic and cerebral folate deficiency of infancy: Hereditary folate malabsorption. Molecular Aspects of Medicine 2017;53:57–72. https://doi.org/10.1016/j.mam.2016.09.002.
3. Serrano M, Pérez-Dueñas B, Montoya J, Ormazabal A, Artuch R. Genetic causes of cerebral folate deficiency: clinical, biochemical and therapeutic aspects. Drug Discovery Today 2012;17:1299–1306. https://doi.org/10.1016/j.drudis.2012.07.008.
4. Huddar A, Chiplunkar S, Nagappa M, Govindaraj P, Sinha S, Taly AB, et al. Child Neurology: Hereditary Folate Malabsorption. Neurology 2021;97:40–43. https://doi.org/10.1212/WNL.0000000000012083.
5. Lubout CMA, Goorden SMI, van den Hurk K, Jaeger B, Jager NGL, van Koningsbruggen S, et al. Successful Treatment of Hereditary Folate Malabsorption With Intramuscular Folinic Acid. Pediatr Neurol 2020;102:62–66. https://doi.org/10.1016/j.pediatrneurol.2019.06.009.
6. Mahadeo K, Diop-Bove N, Shin D, Unal ES, Teo J, Zhao R, et al. Properties of the Arg376 residue of the proton-coupled folate transporter (PCFT-SLC46A1) and a glutamine mutant causing hereditary folate malabsorption. Am J Physiol Cell Physiol 2010;299:C1153-1161. https://doi.org/10.1152/ajpcell.00113.2010.
7. Ahmad I, Mukhtar G, Iqbal J, Ali SW. Hereditary folate malabsorption with extensive intracranial calcification. Indian Pediatr 2015;52:67–68. https://doi.org/10.1007/s13312-015-0571-8.
8. Goldman I, Diop-Bove N, Kronn D, Mahadeo M K, Min Hee S, Sandoval C. Hereditary Folate Malabsorption. vol. 2008–2025. GeneReviews® [Internet]. Seattle (WA). University of Washington, Seattle; 1993-2023; n.d.
9. Goldman ID. Hereditary Folate Malabsorption. In: Adam MP, Feldman J, Mirzaa GM, Pagon RA, Wallace SE, Amemiya A, editors. GeneReviews®, Seattle (WA): University of Washington, Seattle; 1993.
10. Rivella S. Iron metabolism under conditions of ineffective erythropoiesis in β-thalassemia. Blood 2019;133:51–58. https://doi.org/10.1182/blood-2018-07-815928.
11. Thilakarathne S, Jayaweera UP, Herath TU, Silva R, Premawardhena A. Serum folate and dietary folate intake in beta thalassaemia trait: a case-control study from Sri Lanka. BMJ Open 2025;15:e086825. https://doi.org/10.1136/bmjopen-2024-086825.
12. Kumar M, Yoganathan S, Todari S, Suresh P, Chandran M, Danda S, et al. Hereditary Folate Malabsorption: A Rare Treatable Disorder with Hematological and Neurological Manifestations. Ann Indian Acad Neurol 2022;25:1238–1241. https://doi.org/10.4103/aian.aian_1118_21.
13. Tan J, Li X, Guo Y, Xie L, Wang J, Ma J, et al. Hereditary folate malabsorption with a novel mutation on SLC46A1: A case report. Medicine (Baltimore) 2017;96:e8712. https://doi.org/10.1097/MD.0000000000008712.
14. Sakurai Y, Toriumi N, Sarashina T, Ishioka T, Nagata M, Kobayashi H, et al. An infantile case of hereditary folate malabsorption with sudden development of pulmonary hemorrhage: a case report. J Med Case Rep 2022;16:268. https://doi.org/10.1186/s13256-022-03448-x.
15. Manea E, Gissen P, Pope S, Heales SJ, Batzios S. Role of Intramuscular Levofolinate Administration in the Treatment of Hereditary Folate Malabsorption: Report of Three Cases. JIMD Rep 2018;39:7–12. https://doi.org/10.1007/8904_2017_39.
16. Resta R, Biesecker BB, Bennett RL, Blum S, Estabrooks Hahn S, Strecker MN, et al. A New Definition of Genetic Counseling: National Society of Genetic Counselors' Task Force Report. Journal of Genetic Counseling 2006;15:77–83. https://doi.org/10.1007/s10897-005-9014-3.

Case report

Spontaneous expulsion and compositional analysis by infrared spectroscopy of a parotid sialolith: a case report

Abdelaali Belhachem[1,2,4*], Mustapha Zendjabil[3], Amina Amiar[2,4], Fatma Boudia[2,4], Houari Toumi[2,4]

[1]*Pharmaceutical Inorganic Chemistry Laboratory, Faculty of Medicine, University of Bechar, Bechar, Algeria*
[2]*Pharmacovigilance department, University Hospital Establishment of Oran (EHU-O), Oran, Algeria*
[3]*Department of Biochemistry, Oran University Hospital, Oran, Algeria.*
[4]*Pharmaceutical Development Research Laboratory, University of Oran 1, (LRDP-O), Oran, Algeria*

Article Info

[*]***Corresponding Author:***
Abdelaali Belhachem
Pharmaceutical Inorganic Chemistry Laboratory
Faculty of Medicine, University of Bechar, Algeria
Phone No: 00213559587473
E-mail: belhachem.ali87@gmail.com

Keywords

Sialolithiasis, Salivary stone, FTIR-ATR, Biochemical composition

Abstract

Introduction: Sialolithiasis, or salivary gland stone formation, is a condition characterized by mineralized deposits in the salivary ducts. This case report highlights the clinical presentation, spontaneous expulsion, and compositional analysis of a salivary stone in a 35-year-old North African male.

Case Presentation: A patient with no significant medical history or dental issues presented with a spontaneously expelled salivary stone during a salty meal. The stone, measuring 13 mm and weighing 0.52 g, caused mild pain in the left parotid gland during salty and sour meals. Laboratory tests revealed normal calcium and electrolyte levels. The stone was examined using optical microscopy and Fourier transform infrared spectroscopy (FTIR-ATR), confirming its composition as carbonated apatite with minor organic content.

Discussion: The formation of sialoliths is attributed to salivary stasis and altered salivary composition, promoting calcium phosphate precipitation. FTIR-ATR analysis demonstrated a structure composed of concentric layers of carbonated apatite, indicating progressive mineralization. Smoking and glandular physiology, including higher calcium content and pH in parotid saliva, were likely contributors. Management strategies for sialolithiasis emphasize conservative measures, with surgical intervention reserved for larger stones.

Conclusion: This case underscores the complex interplay of local and systemic factors in sialolith formation. The detailed compositional analysis enhances understanding of pathogenesis, aiding in improved diagnostic and therapeutic approaches for salivary stones.

Introduction

Sialolithiasis is the most common disorder of the salivary glands, affecting approximately 1.2% of the adult population, with a slight male predominance. This condition is characterized by the formation of calcified deposits, known as sialoliths, within the ductal system or parenchyma of the salivary glands, most frequently in the submandibular gland (80% of cases). Sialoliths can obstruct salivary flow, leading to painful swelling, particularly during mealtime, due to increased intraglandular pressure. The typical size of sialoliths ranges from 1 mm to 1 cm, with rare instances exceeding 1.5 cm, and even fewer documented cases reaching the size threshold of 3.5 cm or larger [1] [2]. The rarity of giant sialoliths makes them significant in clinical practice, as they can present unique challenges in diagnosis, treatment, and management.

Salivary stones typically appear yellow or yellow-brown and can vary significantly in both size and weight, ranging from 1 mg to nearly 6 g, with an average weight of approximately 300 mg. Submandibular stones are generally larger than those found in the parotid gland. The shape of a sialolith often depends on its origin; stones from the ductal system tend to be elongated, while those from the hilus or gland are more rounded or oval. Additionally, submandibular stones usually have a smoother surface, whereas parotid stones are often more irregular in shape [3] [4].

Sialoliths are composed of both organic and inorganic materials, with a variable ratio between the two. Unlike submandibular stones, which expel more frequently due to anatomical factors, parotid stones rarely expel spontaneously, occurring in less than 10–15% of cases. The majority of parotid stones must be removed surgically or by sialendoscopic means. The organic matrix, which constitutes 23-100% of the stone, is primarily located in the nucleus and outer shell. Inorganic components are predominant, particularly in submandibular stones, where they account for 70-80% of the composition, compared to approximately 50% in parotid stones [4] [2]. Mineralization increases with stone size, indicating a gradual accumulation of minerals within the organic matrix. Hydroxyapatite ($Ca_5(PO_4)_3OH$) is universally present in submandibular stones, often accompanied by whitlockite ($Ca_3(PO_4)_2$), which is commonly found in stones from Wharton's duct. Parotid stones also consistently contain hydroxyapatite, with whitlockite and octacalcium phosphate observed more frequently than in submandibular stones [5] [6].

Case report

A 35-year-old North African male patient, with no significant medical or dental history, presented with a body mass index (BMI) of 26.37 (height: 172 cm, weight: 78 kg), categorizing him as overweight. The patient spontaneously expelled a salivary stone while consuming a salty meal, with the calculus migrating through the left parotid duct due to the pressure from saliva secretion. Post-expulsion imaging (Figure 1) revealed dilation of the affected duct. Laboratory analyses were within the reference interval levels in plasma of calcium, potassium, sodium, magnesium, phosphate, creatinine, and urea. The patient's history indicated that he is a smoker and reported experiencing intermittent pain in the left parotid gland, particularly during the consumption of salty or sour foods. A follow-up consultation three months later with an otolaryngologist revealed no clinical signs of sialolith formation or infection in the parotid region. Notably, the patient reported complete resolution of symptoms, including the absence of pain during sour food consumption. These findings, along with normal blood laboratory results, suggest spontaneous elimination of the salivary stone.

Figure 1: Post-elimination dilation of the left salivary parotid duct.

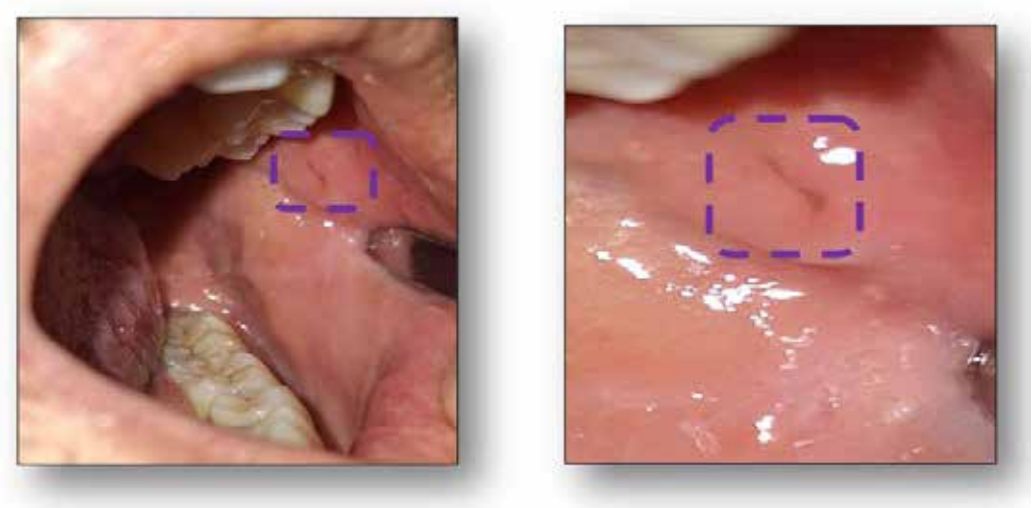

The stone weighed 0.52 g and measured 13 mm. It was observed under an optical microscope (Gx10x40) to examine the morphology of its surface and section, as shown in (Figure 2).

Figure 2: Surface and section of the stone under optical microscope (10*40).

The sialolith exhibits an oval to rounded shape with a nodular surface texture, indicative of mineral deposition. Its color ranges from white to yellowish, with a beige to pink central hue. Internally, the stone displays concentric layers that resemble rings, suggesting a gradual accumulation of minerals over time. These concentric formations are characteristic of the stone's progressive growth. The center, often referred to as the nucleation point, presents a distinct texture and color, representing the initial site of formation where mineralization commenced. Overall, the texture of the stone is smooth.

The infrared spectra were obtained using Fourier transform infrared spectroscopy coupled with attenuated total reflection (FTIR-ATR) (PerkinElmer, Shelton, CT, USA). The stone was first rinsed with distilled water to remove surface contaminants, then air-dried at room temperature. Using an agate mortar and pestle, the dried sample was ground into a consistent powder. To guarantee spectral reproducibility and accuracy, three consecutive scans were averaged for each measurement, and spectra were recorded in the 4000–500 cm^{-1} range with a spectral resolution of 4 cm^{-1}.

The FTIR-ATR spectrum of sialolith reveals key features characteristic of its composition. A broad peak at 3284 cm^{-1} corresponds to hydroxyl group stretching (–OH), while a peak at 2909 cm^{-1} suggests the presence of trace organic material (C–H). The strong peak at 1642 cm^{1} indicates bending vibrations of molecular water, highlighting hydration. Peaks at 1412 cm^{1} and 872 cm^{1} are attributed to carbonate ions (CO_3^{2-}), confirming the carbonated nature of the apatite. Additionally, prominent peaks at 1012 cm^{-1}, 599 cm^{1}, and 569 cm^{1} represent phosphate ion (PO_4^{3-}) vibrations typical of biological apatite. These spectral features confirm the stone's composition as carbonated apatite, with hydration and minor organic content, consistent with sialolith formation via mineral precipitation and organic matrix incorporation in the salivary ducts (Figure 3).

Figure 3: FTIR-ATR spectrums of the salivary stone.

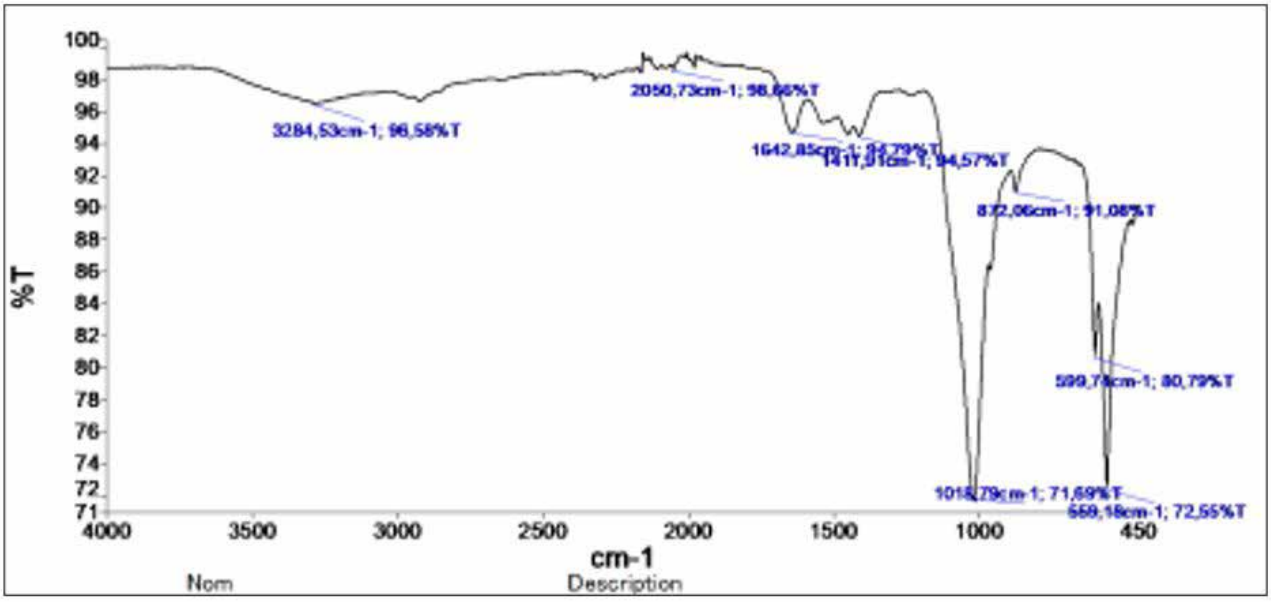

Discussion

The clinical formation of this salivary stone composed of carbonated apatite, as confirmed by FTIR-ATR analysis, aligns with the typical pathogenesis of sialoliths [2]. The process begins with salivary stasis or reduced salivary flow within the ducts, often caused by inflammation, ductal obstruction, or altered salivary composition [7]. This stagnation facilitates the precipitation of calcium and phosphate ions, which combine to form hydroxyapatite [8]. In biological systems, carbonate ions frequently substitute into the hydroxyapatite lattice, resulting in carbonated apatite, a mineral commonly found in salivary stones [9].

The nucleation of a stone begins around an organic core, typically composed of mucus, cellular debris, or bacterial colonies, which serves as a scaffold for mineral deposition. Over time, layers of carbonated apatite accumulate concentrically, as indicated by the FTIR-ATR spectrum [10]. Hydration and minor organic components further promote the growth and stabilization of the stone. The formation of these stones reflects a combination of local environmental changes in the salivary ducts and systemic factors that influence mineral metabolism [11].

Parotid saliva has a higher pH and contains twice the amount of calcium compared to saliva from other glands, both of which support mineralization [12]. The elevated pH reduces the solubility of calcium phosphate, promoting the formation of a mucoid gel that can calcify within the ductal system [7]. This mineralization can obstruct the duct, leading to pain, swelling, and decreased saliva production, with symptoms often worsening during meals [13]. The accumulation of saliva can lead to infection and inflammation of the gland, a condition known as sialadenitis. Treatment options may include hydration, gland massage, or, if conservative methods prove ineffective, surgical removal of the stone [14].

The formation of sialolithiasis is influenced by both local and systemic factors. Altered saliva composition, characterized by increased protein content, viscosity, and calcium concentration, along with reduced levels of crystallization inhibitors such as phytate, magnesium, and citrate, plays a critical role in promoting mineralization [15]. Systemic factors such as gout and the use of diuretics, which decrease salivary flow, further predispose individuals to the formation of stones [13]. Smoking may exacerbate bacterial colonization and inflammation; however, its role in the development of salivary stones remains uncertain [16]. Interestingly, the relationship between salivary stones and systemic conditions such as diabetes, hypertension, kidney stones, and gallstones is inconsistent, warranting further investigation [17]. Structurally, sialoliths consist of a mineralized core surrounded by concentric layers of organic and inorganic materials, with their formation likely occurring intermittently [18]. The biochemical composition reveals a predominance of calcium phosphates in the inorganic matrix, while the organic matrix comprises proteins, lipids, and carbohydrates. Notably, submandibular stones exhibit distinct differences in the proportions of organic materials compared to parotid stones [19]. Our results were contrasted with comparable cases reported in the literature, such as a 4 mm stone extruded via skin ulceration and an 11 mm parotid stone expelled through a cutaneous fistula Furthermore, thorough FTIR-ATR analysis yielded accurate compositional insights that had not been documented in earlier research [13].

Management of sialolithiasis focuses on preserving gland function and minimizing discomfort. Small, ductal stones are often treated conservatively through gland massage, sialogogues, and irrigation, while larger or more complex stones may require transoral surgical removal or advanced techniques such as lithotripsy or sialoendoscopy [14]. Post-treatment care, including gland massage and a sour diet, is essential for stimulating salivary flow and reducing recurrence rates, which remain low at 1–10% [8]. The ability of glands to recover function post-treatment depends on factors such as infection, stone size, and patient age [20]. Despite advances in minimally invasive procedures, further research into the mechanisms of stone formation and tailored treatment approaches could enhance patient outcomes.

Conclusion

This case highlights the spontaneous elimination of a salivary stone in a 35-year-old male patient, offering valuable insights into the pathogenesis, composition, and management of sialolithiasis. The stone, composed of carbonated apatite, exemplifies the typical structural and biochemical characteristics of salivary stones, including concentric layers and a hydrated organic matrix, as confirmed by FTIR-ATR analysis. Local factors, such as elevated salivary pH and calcium concentration in the parotid gland, along with systemic influences like smoking, likely contributed to its formation. Management in this case was non-invasive, with spontaneous stone expulsion facilitated by salivary stimulation during a salty meal. This outcome underscores the potential of conservative measures for small ductal stones while emphasizing the necessity of regular follow-up to monitor gland function and prevent recurrence. The findings further support ongoing research into the multifactorial mechanisms of sialolith formation and the development of optimized, patient-specific treatment protocols.

Statements and Declarations

Funding

No funding was obtained for this research.

Competing interests

The authors declare that they have no competing interests.

Author contributions
AAB, MZ and AA carried out the study, designed and conducted all laboratory analyses, interpreted experimental results, and prepared the manuscript. FB and HT supervised the study.

Consent for publication
All authors read and approved the final manuscript.

Ethical approval and Consent to Participate
It was not required for this salivary stone analysis as it involved the use of previously collected and anonymized clinical data. The research that involves the analysis of existing, de-identified data, without any direct patient interaction or intervention, does not necessitate ethical approval.

Consent to participate
Informed consent was obtained from the patient included in the study.

Consent to publish
The authors affirm that human research participant provided informed consent for publication of the images in Figures 1, 2 and 3.

Clinical trial number
Not applicable.

Acknowledgements
Authors would like to thank the team of Pharmacovigilance department of EHU-ORAN, and the pharmaceutical development research laboratory, University Oran 1-Algeria.

Code Availability
This study did not use any custom code or software.

Availability of data and materials
NA.

Declaration
During the preparation of this work, the authors used OpenAI's language model (ChatGPT and WordVice) in order to enhance the clarity and coherence of the manuscript. After using this tool, the authors reviewed and edited the content as needed and takes full responsibility for the content of the publication.

References
1. Ledesma-Montes, C., et al., Giant sialolith: case report and review of the literature. Journal of oral and maxillofacial surgery, 2007;65(1):128-130. doi:10.1016/j.joms.2005.10.053 https://www.joms.org/article/S0278-2391(06)01228-6/abstract (accessed: 08/07/2025)
2. Kraaij, S., et al., Salivary stones: symptoms, aetiology, biochemical composition and treatment. British dental journal, 2014;217(11):E23-E23. DOI: 10.1038/sj.bdj.2014.1054 https://pubmed.ncbi.nlm.nih.gov/25476659/ (accessed: 08/07/2025)
3. Gupta, A., D. Rattan, and R. Gupta, Giant sialoliths of submandibular gland duct: report of two cases with unusual shape. Contemporary clinical dentistry, 2013;4(1): 78-80. DOI: 10.4103/0976-237X.111599 https://pubmed.ncbi.nlm.nih.gov/23853458/ (accessed: 08/07/2025)
4. Sarıkaya, E.R., et al., Rare Cases Of Giant Sialoliths: 4 Case Reports. International Dental Journal, 2024;74:S60. Doi: 10.1016/j.identj.2024.07.751 https://pubmed.ncbi.nlm.nih.gov/37621584/ (accessed: 08/07/2025)
5. Arslan, S., et al., Giant sialolith of submandibular gland: report of a case. Journal of surgical case reports, 2015. 2015(4): p. rjv043. Doi: 10.1093/jscr/rjv043 https://academic.oup.com/jscr/article/2015/4/rjv043/2412696 (accessed: 08/07/2025)
6. Faklaris, I., N. Bouropoulos, and N. Vainos, Composition and morphological characteristics of sialoliths. Crystal Research and Technology, 2013;48(9):632-640. doi: 10.1002/crat.201300201 https://onlinelibrary.wiley.com/doi/abs/10.1002/crat.201300201 (accessed: 08/07/2025)
7. Schapher, M., et al., Neutrophil extracellular traps promote the development and growth of human salivary stones. Cells, 2020;9(9):2139. doi: org/10.3390/cells9092139 https://pubmed.ncbi.nlm.nih.gov/32971767/ (accessed: 08/07/2025)
8. Chen, T., R. Szwimer, and S.J. Daniel, The changing landscape of pediatric salivary gland stones: a half-century systematic review. International Journal of Pediatric Otorhinolaryngology, 2022;159:111216. doi: 10.1016/j.ijporl.2022.111216. https://pubmed.ncbi.nlm.nih.gov/35777140/ (accessed: 08/07/2025)
9. Heidari, A., et al., Investigation of the frequency of salivary gland stones in corpses referred to forensic medicine in Fars province: a cross-sectional study in the years 2020-2021. Pars Journal of Medical Sciences, 2023;21(1):45-52. Doi: 10.22034/pjms.2023.706815. https://jmj.jums.ac.ir/article_706815.html?lang=en (accessed: 08/07/2025)
10. Enax J, Fandrich P, Schulze zur Wiesche E, Epple M. The Remineralization of Enamel from Saliva: A Chemical Perspective. Dentistry Journal. 2024;12(11):339. doi: 10.3390/dj12110339 https://pubmed.ncbi.nlm.nih.gov/39590389/ (accessed: 08/07/2025)
11. Schicht, M., et al., The translational role of MUC8 in salivary glands: A potential biomarker for salivary stone disease? Diagnostics, 2021;11(12):2330. doi: 10.3390/diagnostics11122330. https://pubmed.ncbi.nlm.nih.gov/34943565/ (accessed: 08/07/2025)
12. Birkhed, D. and U. Heintze, Salivary secretion rate, buffer capacity, and pH, in Human Saliva, Volume I., CRC press. 2021;1:25-74. doi: 10.1201/9781003210399-2. https://www.taylorfrancis.com/chapters/edit/10.1201/9781003210399-2/salivary-secretion-rate-buffer-capacity-ph-dowen-birkhed-ulf-heintze (accessed: 08/07/2025)
13. Kraaij, S., et al., Lactoferrin and the development of

salivary stones: a pilot study. Biometals, 2023;36(3):657-665. Doi: 10.1007/s10534-022-00465-7. https://pubmed.ncbi.nlm.nih.gov/36396778/ (accessed: 08/07/2025)
14. Lysenko, A., et al., The first clinical use of augmented reality to treat salivary stones. Case Reports in dentistry, 2020. 2020(1): 5960421. Doi: 10.1155/2020/5960421. https://pubmed.ncbi.nlm.nih.gov/32695526/ (accessed: 08/07/2025)
15. Proctor, G. and A. Shaalan, Disease-induced changes in salivary gland function and the composition of saliva. Journal of dental research, 2021;100(11):1201-1209. Doi: 10.1177/00220345211004842. https://pubmed.ncbi.nlm.nih.gov/33870742/ (accessed: 08/07/2025)
16. Pakdel, F., et al., Evaluation of the Relation of Smoking, Gallstones, and Renal Stones With Sialolithiasis in Patients Referred to Oral Medicine and ENT Department of Tabriz University of Medical Sciences. Avicenna Journal of Dental Research, 2021;13(4):124-129. doi: 10.34172/ajdr.2021.24. https://ajdr.umsha.ac.ir/FullHtml/ajdr-415 (accessed: 08/07/2025)
17. Nematollahi, M., B. Keshavarzi, and S. Hashemi, Occurrence, physicochemical properties and clinical symptoms of salivary stones (Sialoliths). Armaghane Danesh, 2024;29(4):524-541. Doi: 10.61186/armaghanj.29.4.524. https://armaghanj.yums.ac.ir/article-1-3660-en.html (accessed: 08/07/2025)
18. Barrueco, A.S., et al., Sialolithiasis: Mineralogical composition, crystalline structure, calculus site, and epidemiological features. British Journal of Oral and Maxillofacial Surgery, 2022;60(10):1385-1390. Doi: 10.1016/j.bjoms.2022.08.005. https://pubmed.ncbi.nlm.nih.gov/36109276/ (accessed: 08/07/2025)
19. Park, J., et al., Microbiomic association between the saliva and salivary stone in patients with sialolithiasis. Scientific Reports, 2024;14(1):9184. Doi: 10.1038/s41598-024-59546-x. https://www.nature.com/articles/s41598-024-59546-x (accessed: 08/07/2025)
20. Jadaun, G., et al., Sialolithiasis: an unusually large submandibular salivary stone. Cureus, 2023;15(7):345-346. Doi: 10.7759/cureus.41859. https://pubmed.ncbi.nlm.nih.gov/37583739/ (accessed: 08/07/2025)

Editorial letter

CLAIR 2025: Artificial Intelligence as a Catalyst for the Future of Laboratory Medicine

Bernard Gouget*, Swarup Shah, IFCC ETD Executive Committee

*Corresponding Author:
Bernard Gouget IFCC-ETD Executive Committee
Via Carlo Farini 81, 20159 Milano, Italy
E-mail: b.gouget@icloud.com

Keywords

Artificial Intelligence, Laboratory Medicine, Clinical Decision Support, Emerging Technologies

The Clinical Laboratories Artificial Intelligence Revolution (CLAIR) 2025 symposium, held in Belgrade on March 28, 2025, marked an important milestone in shaping the global dialogue around artificial intelligence (AI) in laboratory medicine. Initiated by the IFCC Division of Emerging Technologies, in collaboration with the Serbian Society for Clinical Laboratory Medicine and Science (SCLM) and the University Clinical Center of Serbia/Center for Medical Biochemistry, the symposium was designed not only as a scientific gathering but also as a forward-looking forum to envision how AI will transform diagnostics, patient care, and healthcare systems in the years to come.

At the heart of CLAIR 2025 was a clear call for innovation with future oriented vision. The opening keynote by Damien Gruson emphasized that AI has already moved beyond pilot projects and experimental phases to become a genuine driver of transformation. No longer a distant possibility, AI now requires strategic integration into laboratory workflows and healthcare systems.

The program was structured around three forward-looking axes:

1. Data as the foundation of AI: Speakers highlighted that high-quality, standardized, and interoperable datasets are indispensable for reliable AI solutions. Presentations by Sanja Stankovic, and Anna Carobene underscored the critical role of data governance, normalization, and quality assurance.
2. AI in clinical decision support: Case studies in endocrinology, cardiology, and oncology, together with contributions from Sarina Yang and colleagues, illustrated how AI tools can integrate laboratory and imaging data to support diagnosis, personalize treatments, and improve clinical workflows.
3. Future perspectives: Forward-looking talks addressed exposomics, generative AI, and the profound challenges of cybersecurity and privacy. These discussions confirmed that the scope of AI extends far beyond technical processes, encompassing the broader health ecosystem.

While technological innovation dominated the program, equity, ethical and governance issues were never far

from the debate. Anna Carobene eloquently reminded the audience that algorithmic bias, inequitable access, and lack of transparency risk undermining the promise of AI if not addressed. Echoing these concerns, Alexander Haliassos and colleagues warned that cybersecurity threats and data privacy breaches represent existential challenges for laboratories adopting cloud-based AI platforms. A recurrent message was that AI must be guided by principles of fairness, accountability, and transparency. This requires international collaboration and harmonization of standards, ensuring that AI tools not only improve efficiency but also protect patient dignity and equity.

The CLAIR initiative highlights the leadership role of the IFCC Emerging Technologies Division. By launching this symposium, the Division reaffirmed its mission to anticipate technological disruptions and to equip laboratories with the knowledge, infrastructure, and governance models needed for responsible adoption. The Division's proactive vision goes beyond assessing tools; it encompasses fostering multidisciplinary collaboration, promoting digital literacy among laboratory professionals, and building bridges between technology developers, clinicians, regulators, and patients. By positioning CLAIR as a global platform, the Division aims to ensure that AI is not just implemented but implemented responsibly and inclusively.

The vision that emerged from CLAIR 2025 is unambiguous: AI will become an indispensable partner in laboratory medicine. Its transformative potential spans early error detection, predictive diagnostics, real-time decision support, and more sustainable resource management. Yet, harnessing this potential requires collective effort. Looking ahead, laboratories and scientific societies must take the lead in shaping AI for meaningful, human-centered healthcare. This means aligning innovation with ethical responsibility, ensuring equitable access to technology, and maintaining strong human oversight in all clinical applications. CLAIR 2025 was not a conclusion but a beginning, a foundation on which to build a global, collaborative effort to shape the role of AI in laboratory medicine. The IFCC Emerging Technologies Division invites the international community to join in this endeavor, ensuring that AI serves not only science and medicine but also society at large.

Rapid Communication

A Present Where AI is Enhancing Laboratory Medicine, A Future Where It Redefines Healthcare

Damien Gruson[1,2,3*]

[1]*Department of Laboratory Medicine, Cliniques Universitaires St-Luc and Université Catholique de Louvain, Brussels, Belgium.*
[2]*Pôle de recherche en Endocrinologie, Diabète et Nutrition, Institut de Recherche Expérimentale et Clinique, Cliniques Universitaires St-Luc and Université Catholique de Louvain, Brussels, Belgium.*
[3]*IFCC Division on Emerging Technologies*

Article Info

[*]***Corresponding Author:***
Prof. Damien Gruson
Department of Laboratory Medicine,
Cliniques Universitaires St-Luc and Université Catholique de Louvain
10 Avenue Hippocrate, B-1200 Brussels, Belgium
Phone +32-(0)2-7646747
fax +32-(0)2-7646930
E-mail: damien.gruson@uclouvain.be
ORCID: 0000-0001-5987-4376

Abstract

Artificial Intelligence (AI) has transitioned from a technological concept to a foundational component of healthcare innovation. In laboratory medicine, it is no longer a question of whether AI will play a role, but rather how it will be responsibly integrated to amplify clinical value, operational efficiency, and equitable patient care. This article explores the current and future impact of AI across diagnostic workflows, clinical decision-making, personalized prevention strategies, and hospital governance. It also highlights the ethical, legal, and sustainability considerations critical to ensuring AI supports a smarter, fairer, and more sustainable healthcare system.

Keywords

Artificial intelligence, automation, sustainability, clinical decision support system, workflow, equity

Introduction

Laboratory medicine stands at a transformative crossroads. Just as Moore's Law once defined computational growth, Huang's Law now marks the explosive evolution of AI processing power, driving unprecedented breakthroughs in healthcare. Between 2016 and 2024, AI computing power surged by over 1000x - an acceleration that is reshaping how we screen, diagnose, and manage diseases [1,2]. In this context, laboratory professionals are uniquely positioned to integrate AI to transform diagnostics, patient pathways, and population health. This short article presents a comprehensive view of how AI is currently enhancing laboratory medicine and outlines a vision of how it will redefine healthcare in the future. It draws on multidisciplinary insights to propose a collaborative and ethical path forward for laboratories worldwide.

The Evolution of AI in Healthcare

AI in healthcare now encompasses machine learning, generative AI, natural language processing, and multimodal models capable of integrating text, images, sensor data, and audio signals. Applications range from triaging patients in resource-limited settings to early detection of cardiovascular deterioration through smart wearables and remote sensors [2–4].

Recent studies show that generative AI can improve communication by offering culturally sensitive, emotionally aware support for patients, helping close gaps in health literacy and engagement [2,5]. AI also enables behavioral health interventions, such as using personalized avatars and visuals to enhance emotional regulation in pediatric or chronic care settings [6].

The Patient-Centered AI Landscape

AI holds promise in making healthcare more personalized and responsive. For patients with chronic diseases such as heart failure (HF) - particularly in those with diabetes, where HF may be the first sign of cardiovascular disease - AI can enhance follow-up and monitoring [2,7]. By integrating real-time data from wearables and digital health records, AI facilitates early intervention and dynamic care plans tailored to individual risk profiles [2,8]. AI can also act as a "health literacy bridge" by translating complex medical terminology into understandable, personalized insights, thus ensuring that patients are not only monitored but also empowered [2,9].

Empowering Clinicians with AI Tools

From the perspective of general practitioners (GPs), AI is reshaping the clinical workflow. Speech-based AI tools detect subtle cardiovascular changes, while language models help synthesize patient histories and suggest differential diagnoses [5]. Physicians increasingly rely on AI for administrative efficiency - automating documentation and reducing cognitive burden - thereby allowing more time for patient care [5,10]. AI also enhances medical education by standardizing case evaluations and promoting adaptive learning. As a decision-support system, it fosters earlier disease recognition, augments diagnostic accuracy, and bolsters continuity of care.

AI in Laboratory Operations

AI is revolutionizing every phase of the laboratory process [3,11,12]:

- **Pre-analytical**: Predictive AI detects potential sample anomalies before testing.
- **Analytical**: AI-powered instruments optimize calibration, reduce errors, and accelerate interpretation through pattern recognition.
- **Post-analytical**: AI assists in generating actionable insights and interpreting complex datasets, including omics-level information.

Laboratory automation is evolving toward hyperautomation where integrated AI systems orchestrate tasks, monitor quality in real-time, and anticipate resource demands [3,11]. Personalized proficiency testing is emerging, enabling labs to receive tailored assessments based on their test portfolios, improving targeted quality improvement [3].

Hospital Leadership and AI Strategy

AI is not just a clinical tool - it's a strategic asset for hospital directors. Predictive analytics help optimize bed management, staffing, and supply chain logistics. Hospitals that integrate AI report not only reduced operational costs but also improved patient throughput and satisfaction [13]. At the governance level, however, AI implementation must navigate challenges of interoperability with legacy systems, regulatory constraints, and the "hype vs. reality" gap. Successful strategies depend on interdisciplinary alignment - where clinicians, IT professionals, and administrators co-design AI integration [2,7].

Integrating Environmental and Social Determinants: The Role of Exposomics

AI is also enabling "precision exposomics" by merging environmental data (e.g., air quality, urbanization, socioeconomic factors) with health records to predict disease patterns and outcomes. For example, convolutional neural networks analyzing over 500000 Google Street View images in U.S. cities successfully predicted coronary heart disease (CHD) prevalence and explained 63% of variation across geographic areas [14].

This reinforces the importance of integrating environmental data in cardiovascular prevention and health policy planning. Exposomics, coupled with metabolomics and AI, represents a frontier in personalized risk assessment [15,16].

Ethical, Legal, and Environmental Challenges

The widespread use of AI in healthcare raises critical ethical and legal questions [12,17]:

- **Accountability**: Who is liable if AI makes a diagnostic error? The developer, the clinician, or the institution?
- **Transparency**: AI systems can produce "hallucinations"

or misleading outputs. Ensuring interpretability is key.
- **Bias and Equity**: Algorithms must be trained on diverse datasets to avoid reinforcing disparities.
- **Privacy**: Data governance must protect patient confidentiality while enabling secure AI training.

AI training models also consume substantial energy. The environmental impact of large-scale models has prompted calls for sustainable AI development, with best practices including model efficiency, transparent reporting, and carbon offsetting [17,18].

A Framework for Responsible Innovation

To fully realize AI's potential in laboratory medicine, we must align innovation with responsibility. A proposed action plan includes:

1. **Embrace Innovation Responsibly**
   Leverage AI to enhance diagnostics and precision medicine, while maintaining human oversight.
2. **Commit to Sustainable AI**
   Advocate for transparent reporting of AI energy consumption and develop energy-efficient algorithms.
3. **Navigate Ethical and Legal Frontiers**
   Support international consensus on AI liability, data standards, and patient autonomy.
4. **Foster Multidisciplinary Collaboration**
   Bring together clinicians, data scientists, policymakers, and patients to shape inclusive AI use cases.
5. **Act Now**
   Start piloting AI innovations in laboratory workflows to gain experience and refine governance strategies.

Conclusion

AI is already enhancing laboratory medicine - from diagnostics to workflow automation. Its future lies not just in innovation, but in responsible transformation. Developed and governed with care, AI will not only make laboratories smarter and more efficient, but also more sustainable, ethical, and aligned with the needs of patients and healthcare professionals (Figure 1). As laboratory medicine evolves, it must not merely adopt AI - it must shape it. With great computational power comes the responsibility to guide AI toward meaningful, equitable, and human-centered healthcare.

Figure 1: AI's evolving role in laboratory medicine: from current impact to future transformation.

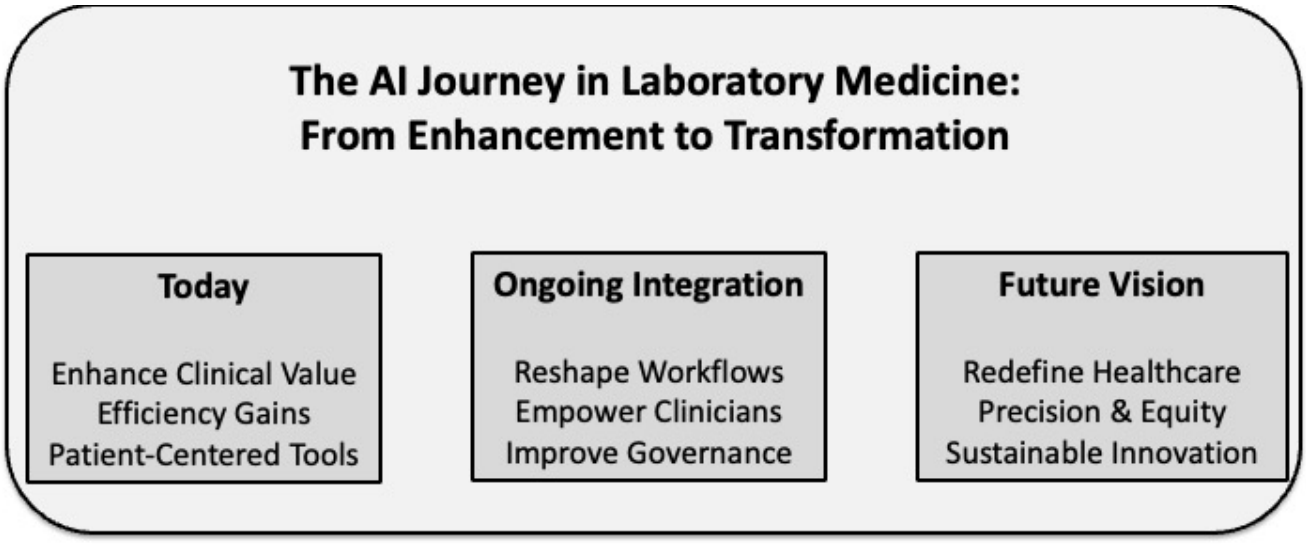

Funding Statement

The authors received no specific funding for this work.

Declaration of Conflicts of Interest

The authors declare no conflicts of interest related to this publication.

Ethical Approval Statement

This article does not contain any studies with human participants or animals performed by any of the authors. Therefore, ethical approval was not required. The article is in compliance with the ethical principles for medical research involving human subjects, in accordance with the Declaration of Helsinki.

Author Contributions

Damien Gruson conceived, wrote, and reviewed the manuscript.

Credit Author Statement

Damien Gruson: Conceptualization, Writing - original draft, Writing - review & editing, Supervision.

Data Availability Statement

No datasets were generated or analyzed during the current study.

References

1. Video Shows How Engineers Fuel Huang's Law | NVIDIA Blogs [Internet]. [ci. Available from: https://blogs.nvidia.com/blog/huangs-law-dally-hot-chips/ (Accessed: 15/07/2025)
2. Lüscher TF, Wenzl FA, Ascenzo FD, Friedman PA, Antoniades C. Artificial intelligence in cardiovascular medicine: clinical applications. Eur Heart J. 2024;45(40):4291–4304.
3. Kim S, Min WK. Toward High-Quality Real-World Laboratory Data in the Era of Healthcare Big Data. Ann Lab Med. 2025;45(1):1–11.
4. Gruson D, Kemaloğlu Öz T. Trends in Healthcare and Laboratory Medicine: A Forward Look into 2025. Balkan Med J. 2025 Mar 24
5. Elvas LB, Almeida A, Ferreira JC. The Role of AI in Cardiovascular Event Monitoring and Early Detection: Scoping Literature Review. JMIR Med Inform. 2025;13.
6. Mansoor M, Hamide A, Tran T. Conversational AI in Pediatric Mental Health: A Narrative Review. Children. 2025;12(3):359.
7. Thangaraj PM, Benson SH, Oikonomou EK, Asselbergs FW, Khera R. Cardiovascular care with digital twin technology in the era of generative artificial intelligence. Eur Heart J. 2024;45(45):4808–4821.
8. Monzo L, Bresso E, Dickstein K, Pitt B, Cleland JGF, Anker SD, et al. Machine learning approach to identify phenotypes in patients with ischaemic heart failure with reduced ejection fraction. Eur J Heart Fail. 2024
9. Johnson KB, Horn IB, Horvitz E. Pursuing Equity with Artificial Intelligence in Health Care. JAMA Health Forum. 2025;6(1):e245031–e245031.
10. Vrdoljak J, Boban Z, Vilović M, Kumrić M, Božić J. A Review of Large Language Models in Medical Education, Clinical Decision Support, and Healthcare Administration. Healthcare. 2025;13(6):603.
11. Gruson D, Magalhaes T, Ruszanov A, Granaldi C, Bernardini S, Buttigieg SC. Hyperautomation in Healthcare: Perspectives from a Joint IFCC – EHMA Session. EJIFCC. 2023;34(4):284.
12. Gruson D, Gruson D, Macq B. The Next Clinical Decision Frontier: How to Efficiently and Safely Combine Machine Learning and Human Expertise. Clin Chem. 2023; Nov 29
13. Maleki Varnosfaderani S, Forouzanfar M. The Role of AI in Hospitals and Clinics: Transforming Healthcare in the 21st Century. Bioengineering. 2024;11(4):337.
14. Chen Z, Dazard JE, Khalifa Y, Motairek I, Al-Kindi S, Rajagopalan S. Artificial intelligence-based assessment of built environment from Google Street View and coronary artery disease prevalence. Eur Heart J. 2024;45(17):1540–1549.
15. Gruson D, Fux E, Kemaloğlu Öz T, Gouget B, Lee W, Shah S, et al. Contribution of laboratory medicine and emerging technologies to cardiovascular risk reduction via exposome analysis: An opinion of the IFCC Division on Emerging Technologies. Clin Chem Lab Med. 2024 Sep 2
16. Khera R. Artificial intelligence-enhanced exposomics: novel insights into cardiovascular health. Eur Heart J. 2024;45(17):1550–1552.
17. Gonzalez A, Crowell T, Lin SYT. AI Code of Conduct - Safety, Inclusivity, and Sustainability. JAMA Intern Med. 2025;185(1):12–13.
18. COLLECTIVE ACTION FOR RESPONSIBLE AI IN HEALTH. 2024 ; Available from: http://www.oecd.org/termsandconditions. (Accessed: 15/07/2025)

Review Article

The Challenges of Data Privacy and Cybersecurity in Cloud Computing and Artificial Intelligence (AI) Applications for EQA Organizations

Alexander Haliassos[1*], Dimitrios Kasvis[2], Serafeim Karathanos[1]

[1]*ESEAP & GSCC-CB, Athens, Greece*
[2]*HeadWay Consultants, Athens, Greece*

Article Info

[*]***Corresponding Author:***
Alexander Haliassos
ESEAP & GSCC-CB, Athens, Greece
E-mail: haliassos@moleculardiagnostics.gr

Keywords

Cybersecurity, Data Privacy, Cloud Computing, artificial intelligence, AI, EQA, PT

Abstract

Background: The adoption of cloud computing and Artificial Intelligence (AI) technologies offers significant advantages for External Quality Assessment (EQA) providers, including scalability, cost efficiency, and broader accessibility. However, these benefits come with substantial cybersecurity and data privacy challenges.

Methodology: We performed a systematic literature review on cybersecurity risks in healthcare cloud computing, consulted experts in bioinformatics and cybersecurity, and analyzed real-world hacking incidents targeting EQA organizations. A risk-focused framework was developed to outline key challenges and best practice mitigation strategies.

Results: Ten key challenges were identified: 1. data breaches and unauthorized access, 2. compliance with regulations such as HIPAA and GDPR, 3. data sovereignty and jurisdictional issues, 4. shared infrastructure vulnerabilities, 5. insider threats, 6. data loss and availability concerns, 7. inadequate security measures by cloud providers, 8. application vulnerabilities, 9. limited visibility and control, and 10. the complexity of cloud security management.

Conclusion: To fully benefit from cloud computing and AI, EQA providers must implement robust security practices, ensure regulatory compliance, and continuously monitor their environments. Proactive cybersecurity strategies are essential to safeguarding sensitive laboratory data and maintaining operational continuity and accreditation.

Introduction

External Quality Assessment (EQA) schemes have long served as critical tools in maintaining the reliability, accuracy, and comparability of laboratory testing worldwide. Firstly, implemented in limited, often local settings with a small number of participants performing interlaboratory comparison of results on shared samples, EQA schemes have evolved significantly over the past decades [1]. The increasing complexity of laboratory diagnostics, combined with globalization and regulatory demands, has led to a dramatic rise in the number of participating laboratories and the volume of data generated during each EQA cycle. As a result, EQA providers have turned to cloud computing and, more recently, artificial intelligence (AI) technologies to efficiently manage, analyze, and report these large-scale data sets.

Cloud computing offers a scalable, cost-effective, and collaborative environment that supports real-time data access, centralized data storage, automated workflows, and streamlined communication between EQA providers and participant laboratories [2,3]. Similarly, AI technologies, including adaptive machine learning algorithms, natural language processing, and data mining, are increasingly used to automate result evaluations, detect errors, provide personalized feedback, and identify performance trends across laboratories. These innovations enable more dynamic and responsive EQA processes that better support continuous quality improvement in diagnostic testing.

However, as EQA operations become more digitally interconnected, the nature and severity of cybersecurity risks escalate. The sensitive nature of laboratory data that contains patient-related or institution-specific identifiers, combined with the widespread distribution of EQA participants across different countries and regulatory environments, makes EQA platforms attractive targets for cyberattacks. Additionally, the reliance on third-party cloud service providers raises critical questions about data governance, regulatory compliance (e.g., GDPR), and risk ownership in the event of a security breach.

The growing sophistication of cyber threats, ranging from ransomware and phishing campaigns to advanced persistent threats, highlights the urgent need for robust data protection mechanisms and proactive cybersecurity strategies. For EQA providers, ensuring data privacy and system integrity is not merely a technical challenge but a fundamental requirement for maintaining trust, safeguarding accreditation processes, and protecting the broader public health landscape [3].

This paper aims to explore the current and emerging challenges related to data privacy and cybersecurity in the context of cloud computing and AI adoption among EQA providers. Through case examples, risk analysis, and discussion of regulatory frameworks, we aim to provide actionable insights for EQA organizations seeking to navigate the complex digital ecosystem while upholding the highest standards of quality and data protection.

Methodology

Our approach included a comprehensive literature review of recent publications indexed in PubMed, Scopus, IEEE Xplore, and ScienceDirect, as well as reports from cybersecurity authorities such as ENISA and the CVE (Common Vulnerabilities and Exposures) database. The references included in this study (1–16) were identified using the following search terms and combinations: “cybersecurity healthcare”, “cloud computing data breach”, “EQA cybersecurity risks”, “AI in EQA”, “cybersecurity”, and “healthcare ransomware attacks”.

We analyzed real-life cases of cyberattacks on healthcare systems and EQA platforms. In addition, we gathered more information through targeted consultations with three experts in the field. These discussions were based on open-ended questions designed to understand emerging threats, common vulnerabilities, and potential mitigation strategies. The findings from the literature review, case studies, and expert input were synthesized to develop a comprehensive framework outlining the main challenges and recommended countermeasures for EQA organizations.

Results

1. Data Breaches and Unauthorized Access

Unauthorized access to sensitive laboratory or participant data is one of the most critical cybersecurity concerns for EQA providers operating within cloud-based environments. EQA workflows, which involve the submission, processing, and evaluation of diagnostic data from multiple laboratories, inevitably generate large volumes of potentially identifiable information. When hosted in the cloud, data becomes vulnerable to exploitation through weak credentials, misconfigured access policies, lack of encryption, or insufficient activity monitoring [4].

To mitigate these risks, EQA providers should implement a multilayered security strategy that begins with robust user authentication. Multi-factor authentication (MFA) must be used at all access points, especially for administrative and evaluator roles, to help prevent unauthorized access. MFA requires users to verify their identity with at least two independent credentials, usually something they know (like a password) and something they have (such as a one-time code, hardware token or an authenticator app on their phones). This approach lowers the chance of unauthorized access, even if passwords are stolen or credentials are compromised [5,6].

Equally important is implementing strict role-based access control (RBAC), which ensures that users only access data and system functions necessary for their defined responsibilities. The principle of least privilege should drive all access permissions, with temporary elevation of rights used only in exceptional cases. Such segmentation significantly limits the potential damage in case of account compromise, minimizing the impact of the attack [7].

Encryption constitutes another fundamental safeguard. All

EQA-related data stored in cloud infrastructure should be encrypted at rest using industry-standard algorithms such as AES-256. Also, data in transit must be protected with a secure communication protocol, preferably TLS version 1.2 or higher, to prevent interception or tampering during upload, retrieval, or analysis [8].

2. Compliance with Regulations

EQA organizations that manage laboratory and healthcare-related data in the cloud must ensure compliance with national and international data protection frameworks. Among the most prominent regulations are the Health Insurance Portability and Accountability Act (HIPAA) in the United States and the General Data Protection Regulation (GDPR) in the European Union. These frameworks impose strict requirements on how personal information is stored, accessed, and transmitted, making regulatory compliance not only a legal obligation but also a crucial component of maintaining trust and integrity within the EQA ecosystem [9].

Ensuring compliance in cloud environments presents particular challenges, as control over the underlying infrastructure is often limited. Cloud service providers may not consistently meet all regulatory requirements and consequently EQA providers must take an active role by confirming that their chosen cloud platforms offer the necessary technical and organizational safeguards.

There are cloud providers that offer a range of tools to support compliance management. Platforms such as AWS Artifact, Microsoft Azure Compliance Manager, and Google Cloud's compliance resource center provide documentation, risk assessment templates, and automated controls aligned with regulatory standards.

Beyond the documentation and controls, real-time monitoring of data handling practices is essential. EQA systems should be configured to log all access and activity related to sensitive datasets, including uploads, downloads, modifications, and user authentication events. Audit tools such as AWS CloudTrail, Azure Monitor, and Google Cloud Audit Logs enable continuous surveillance and traceability, which are critical for identifying compliance gaps and responding to incidents [10].

For EQA organizations, failure to comply can lead to significant financial penalties, reputational damage, and loss of credibility among participating laboratories and accreditation bodies.

3. Data Sovereignty and Jurisdictional Issues

Another highly important cloud computing risk for EQA providers is the issue of data sovereignty. As EQA applications increasingly rely on global cloud infrastructures, the potential for laboratory or patient data to be stored or transferred across multiple jurisdictions raises serious compliance and governance concerns as it becomes subject to the laws and political dynamics of the host countries and sometimes outside the control or awareness of the data owner.

A critical risk arises when cloud infrastructure is managed or controlled by entities based in a single country. In the case of geopolitical tensions, sanctions, or policy shifts, that country could stop or restrict service provision to other regions.

To mitigate such risks, EQA organizations must implement strict data residency controls. Many platforms offer options to select specific geographic regions for data storage. These tools allow organizations to restrict data within legally permitted areas. Additionally, geofencing mechanisms can be configured to restrict data flows and processing to pre-approved areas, reducing the risk of non-compliant cross-border transfers [9,10].

Regular consultation with legal and compliance specialists ensures that storage and processing strategies are aligned with applicable local regulations, especially when operating in multiple countries or handling data from multinational laboratory networks.

4. Shared Infrastructure Vulnerabilities

Cloud environments typically operate on shared infrastructure, where multiple tenants utilize the same underlying hardware through virtualization technologies. While this model enables scalability and cost efficiency, it also introduces risks. A failure in isolation mechanisms through hypervisor exploits, container escape vulnerabilities, or misconfigured virtual machines could result in unauthorized access to sensitive data hosted by other tenants.

To address these concerns, EQA organizations should enforce strict workload isolation by deploying services within dedicated virtual private clouds (VPCs) or segmented virtual networks. Network segmentation using firewalls, subnets, and security groups adds further restriction. Ensuring hypervisors and container runtimes are regularly patched is essential, along with leveraging hardware-level virtualization protections such as Intel VT-x or AMD-V [11,12].

5. Insider Threats

In addition to external cyberattacks, internal threats raise a significant risk to data confidentiality. Cloud service provider employees could theoretically have access to underlying systems, and without strong internal safeguards, this access could be used to retrieve or manipulate sensitive EQA or healthcare data.

To mitigate this risk, EQA organizations should implement strict access control frameworks, including just-in-time (JIT) provisioning and immediate revocation of access when no longer required. In addition, monitoring all administrative activities using cloud-based tools, such as AWS CloudWatch, Azure Security Center, or Google Cloud Security Command Center, can identify mishandling and enforce accountability.

Most importantly, by using customer-managed encryption keys (CMKs), organizations retain exclusive control over the encryption and decryption of their data, thereby minimizing the risk of unauthorized access even at the provider level [13].

6. Data Loss and Availability Concerns
Service outages, accidental deletions, or even data corruption can also occur in cloud-based systems and seriously impact the continuity of EQA operations and the availability of critical laboratory information. Without robust backup and recovery strategies, such events can lead to irreversible data loss or extended downtime that put at risk the reporting schedules and stakeholder trust.
In order to avoid these risks, EQA organizations should adopt automated backup procedures, ensuring that backups are encrypted and distributed across multiple regions to protect against localized failures. Disaster recovery plans must be routinely tested to validate their effectiveness in real-world scenarios. Additionally, designing infrastructure with built-in redundancy, such as deploying applications across multiple availability zones or regions, enhances resilience. High-availability database services like AWS RDS Multi-AZ, Azure SQL Database with geo-replication, or Google Cloud Spanner can further support business continuity during unexpected outages [14].

7. Inadequate Security Measures by Cloud Providers
Not all cloud providers implement the same security practices, and some may not implement basic protections such as strong encryption, intrusion detection systems, or application-level firewalls. For EQA organizations handling sensitive laboratory data, blindly relying on a provider's default controls can leave critical assets exposed to cyberthreats.
For this reason, organizations should perform rigorous and detailed search before selecting a provider by evaluating security certifications (e.g., ISO 27001, SOC 2), independent audit reports, and compliance documentation. Once committed, they should leverage the provider's advanced platform security services, such as AWS GuardDuty, Azure Defender, or Google Cloud Security Scanner. Importantly, cloud-based security should be reinforced with third-party tools such as endpoint protection platforms, intrusion detection/prevention systems (IDS/IPS), and web application firewalls (WAFs), offering an additional layer of defense beyond the provider's basic level [15].

8. Application Vulnerabilities
EQA applications hosted in the cloud may be vulnerable due to insecure code, misconfigured Application Programming Interfaces (APIs), or outdated components. Such weaknesses can be exploited by hackers to gain unauthorized access, manipulate data, or disrupt services.
To address this risk, organizations must integrate secure development practices throughout the software lifecycle. This includes applying static and dynamic security testing (SAST/DAST), conducting regular code reviews, and performing security audits before deployment. Particular attention should be paid to API security, as exposed interfaces are common attack vectors. APIs should be protected with protocols like OAuth 2.0, governed by rate-limiting policies, and managed through API gateways. Additionally, strict input validation and sanitization must be enforced to prevent injection attacks [11,16].

9. Limited Visibility and Control
A common challenge in cloud-based environments is the limited visibility that organizations have over their own data, infrastructure, and security configurations. For EQA providers, this lack of transparency can hinder timely detection of threats, delay incident response, and complicate compliance monitoring.
To overcome these limitations, organizations should implement centralized logging and monitoring using platforms like AWS CloudWatch, Azure Monitor Logs, or third-party tools such as Splunk or the ELK Stack. These solutions enable real-time visibility across distributed systems. Additionally, deploying Cloud Security Posture Management (CSPM) tools such as AWS Config, Azure Policy, or Prisma Cloud, helps maintain continuous oversight of configuration drift and policy violations. When integrated with Security Information and Event Management (SIEM) systems, these tools provide a comprehensive view of security events and support rapid threat detection and remediation across the cloud environment [16].

10. Complexity of Cloud Security
In contrast to traditional systems, cloud infrastructures are highly dynamic, involve numerous interdependent services, and require specialized expertise. Without proper controls and up-to-date knowledge, misconfigurations or overlooked vulnerabilities can create critical security gaps.
To manage this complexity, EQA organizations should adopt Infrastructure as Code (IaC) tools - such as Terraform, AWS CloudFormation, or Azure Resource Manager - that enable consistent and automated implementation of secure configurations. Regular security audits and vulnerability assessments, using tools like Nessus, Qualys, or native cloud scanners, are essential to proactively identify risks. Equally important is investing in ongoing training for technical staff, ensuring that both development and operations teams are trained and familiar with current best practices and awareness of evolving cloud threats.

Discussion
Examples from real-world incidents reinforce the criticality of addressing these challenges. The 2019 AMCA breach, affecting nearly 20 million patients, was caused by insufficient encryption practices. Cloud outages like AWS S3's 2017 downtime highlighted the need for resilient disaster recovery plans [17].
Countermeasures must combine technical, procedural, and legal elements. Technologies such as MFA, CMKs, SIEM, VPC segmentation, and automated configuration management significantly reduce risk. At the organizational level, training,

strict access policies, and legal compliance frameworks must be maintained.

In Figure 1, a flowchart summarizing the recommended security measures provides a systematic approach to securing cloud-based EQA infrastructures, beginning from basic access control to advanced threat detection and automated audits.

Figure 1: Security measures for cloud-based EQA infrastructures.

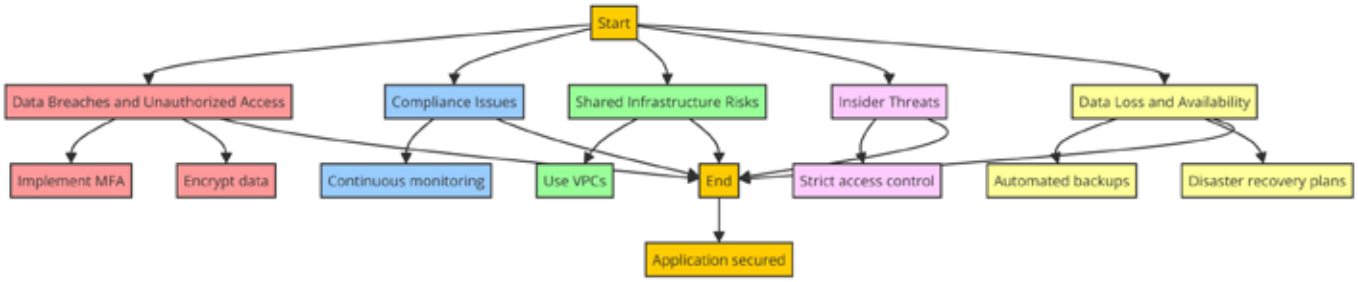

In Figure 2, we present interwoven the solutions to all possible security issues that lead to our ultimate goal, the security of healthcare and EQA applications on the net.

Figure 2: Solutions to all possible security issues.

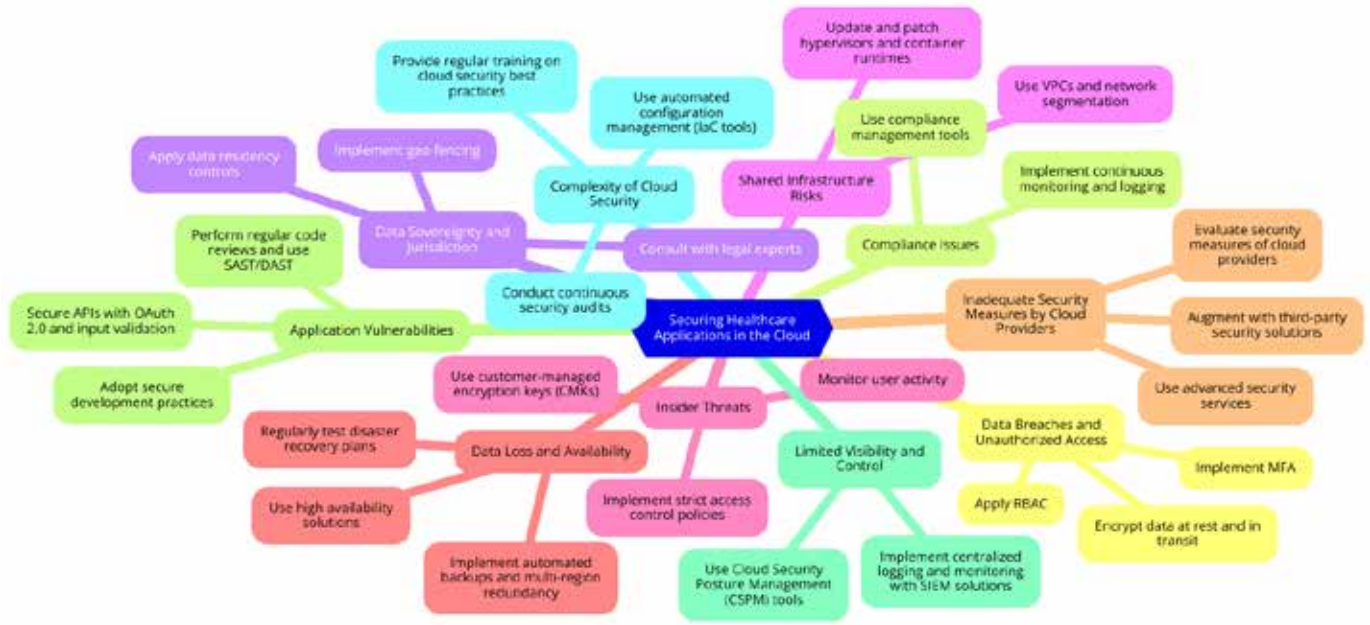

References

1. Buchta C, Marrington R, De la Salle B, Albarède S, Badrick T, Bietenbeck A, et al. Behind the scenes of EQA – characteristics, capabilities, benefits and assets of external quality assessment (EQA) Part I – EQA in general and EQA programs in particular. Clin Chem Lab Med. 2025;63(5):844–858. doi:10.1515/cclm-2024-1289.
2. Sobeslav V, Maresova P, Krejcar O, Franca TCC, Kuca K. Use of cloud computing in biomedicine. Journal of Biomolecular Structure and Dynamics. 2016;34(12):2688–2697. doi:10.1080/07391102.2015.1127182
3. Al-Issa Y, Ottom MA, Tamrawi A. EHealth Cloud Security Challenges: A Survey. Journal of Healthcare Engineering. 2019;2019:7516035. doi:10.1155/2019/7516035.
4. Seh AH, Zarour M, Alenezi M, Sarkar AK, Agrawal A, Kumar R, et al. Healthcare data breaches: Insights and implications. Healthcare (Switzerland). 2020;8:100. doi:10.3390/healthcare8010100.
5. De Carvalho Junior MA, Bandiera-Paiva P. Health Information System Role-Based Access Control

Current Security Trends and Challenges. Journal of Healthcare Engineering. 2018;2018:6510249. doi:10.1155/2018/6510249.
6. Williamson J, Curran K. The Role of Multi-factor Authentication for Modern Day Security. Semiconductor Science and Information Devices. 2021;3(1):16–23. doi:10.30564/ssid.v3i1.3152.
7. Saffarian M, Sadighi B. Owner-based role-based access control OB-RBAC. In: ARES 2010 - 5th International Conference on Availability, Reliability, and Security. (ARES). 2010;236-241. doi:10.1109/ARES.2010.94.
8. Mohamed NN, Othman H, Isa MAM, Noor NAM, Hashim H. A secure communication in location based services using AES256 encryption scheme. In: ISCAIE 2017 - 2017 IEEE Symposium on Computer Applications and Industrial Electronics. Institute of Electrical and Electronics Engineers (ISCAIE). 2017;163-167. doi:10.1109/ISCAIE.2017.8074970.
9. Rose RV, Kass JS. Mitigating Cybersecurity Risks. Continuum. 2017;23(2):553–556. doi:10.1212/CON.0000000000000442.
10. Ng MY, Helzer J, Pfeffer MA, Seto T, Hernandez-Boussard T. Development of secure infrastructure for advancing generative artificial intelligence research in healthcare at an academic medical center. J Am Med Inform Assoc. 2025;32(3):586–588. doi:10.1093/jamia/ocaf005.
11. Schabacker DS, Levy LA, Evans NJ, Fowler JM, Dickey EA. Assessing cyberbiosecurity vulnerabilities and infrastructure resilience. Front Bioeng Biotechnol. 2019;7. doi:10.3389/fbioe.2019.00061.
12. Regola N, Chawla NV. Storing and using health data in a virtual private cloud. J Med Internet Res. 2013;15(3). doi:10.2196/jmir.2548.
13. Alsowail RA, Al-Shehari T. Techniques and countermeasures for preventing insider threats. PeerJ Comput Sci. 2022;8:e964. doi:10.7717/peerj-cs.964.
14. Miller AR, Tucker CE. Encryption and the loss of patient data. J Policy Anal Manage. 2011;30(3):534–556. doi:10.1002/pam.20590.
15. Whaiduzzaman M, Gani A. Measuring security for cloud service provider: A third-party approach. In: 2013 International Conference on Electrical Information and Communication Technology (EICT). IEEE; 2014. doi:10.1109/EICT.2014.6777855.
16. González-Granadillo G, González-Zarzosa S, Diaz R. Security information and event management (SIEM): Analysis, trends, and usage in critical infrastructures. Sensors. 2021;21(14):Article/status. doi:10.3390/s21144875.
17. Alder S. Multistate settlement resolves 2019 American Medical Collection Agency data breach investigation. HIPAA Journal [Internet]. 2021 Mar 12 [cited 2025 Aug 20]. Available from: https://www.hipaajournal.com/multistate-settlement-resolves-2019-american-medical-collection-agency-data-breach

Author Comment

Tribulations, Triumphs, and Governance: Shaping the Future of Artificial Intelligence in Healthcare

Anna Carobene[1*]

[1]IRCCS Ospedale San Raffaele, Milan, Italy

Article Info

[*]***Corresponding Author:***
Anna Carobene
Address: IRCCS Ospedale San Raffaele
Via Olgettina 60, 20132 Milan, Italy
E-mail: carobene.anna@hsr.it

Keywords

Artificial Intelligence, Machine Learning, Laboratory Medicine, Ethics and Governance, Health Equity

Abstract

Artificial intelligence (AI) is driving a profound transformation across the healthcare landscape, with the potential to enhance diagnostic accuracy, optimize clinical decision-making, improve resource allocation, and advance personalized medicine. In public health, AI is redefining infectious disease epidemiology by enabling outbreak forecasting, genomic surveillance, and data-driven policy support, even in the presence of incomplete information. Within clinical laboratories, AI plays a pivotal and expanding role. It facilitates automation of complex workflows, supports diagnostic interpretation, and contributes to analytical performance improvements. Particularly promising is its integration into point-of-care testing, enabling decentralized diagnostics and broader access to timely care, especially in resource-constrained settings.

However, these advancements are not without challenges. Concerns regarding algorithmic bias, lack of data representativeness, and risks to privacy and transparency must be carefully addressed. Moreover, the ethical and societal implications of AI are increasingly central. As emphasized by Pope Francis, while AI may accelerate access to knowledge and innovation, it also risks deepening global disparities and promoting a "throwaway culture" that undermines human dignity. His appeal for a "culture of encounter" rooted in equity, justice, and inclusion aligns with the mission of public health and laboratory medicine. This paper, based on the invited lecture delivered at the Clinical Laboratories Artificial Intelligence Revolution (CLAIR) 2025 conference, explores these themes through a critical lens. International scientific societies such as the IFCC are called to foster equitable implementation of AI by promoting access to training, infrastructure, and governance frameworks thus ensuring that AI contributes meaningfully to global health solidarity and equity.

Introduction

Artificial intelligence (AI) is rapidly transforming the landscape of healthcare delivery [1]. AI technologies are poised to revolutionize clinical workflows, ranging from early diagnosis and risk stratification to the tailoring of personalized treatment plans, however, such transformation remains largely prospective, as many models still require extensive external validation and performance monitoring before they can be integrated reliably into routine care. In the field of laboratory medicine, AI is gaining prominence as a tool to automate interpretation, detect anomalies, and integrate complex biological data to support evidence-based decision-making [2]. These advances reflect wider movements in digital health, such as the integration of precision medicine approaches, the adoption of interoperable electronic health records, and the decentralization of diagnostic services through point-of-care technologies. However, the pace and extent of these transformations vary significantly across regions, particularly where resource constraints or infrastructural gaps limit digital readiness. Bridging this global divide remains a critical challenge for equitable AI deployment.

Yet, the advancement of AI technologies in healthcare is not without significant challenges. Technical concerns such as algorithmic bias, data quality, and lack of interoperability intersect with profound ethical and legal questions. Issues related to patient autonomy, data privacy, transparency, and accountability have gained increasing attention, especially in light of the opaque "black box" nature of many AI models. These concerns are further compounded in low- and middle-income countries, where limited digital infrastructure may widen health disparities unless addressed by equitable AI deployment strategies. As emphasized by Bouderhem, the future of AI in healthcare hinges not only on technological capability, but also on the development of adequate regulatory, ethical, and governance frameworks [1].

The World Health Organization (WHO), in its reports and position papers, has stressed the importance of adopting legally binding norms to govern AI applications in health [3, 4] while the European Union's AI Act aims to provide a harmonized legal model grounded in human rights and safety standards [5].

At the same time, global voices such as Pope Francis have drawn attention to the broader societal risks of AI. In the document Antiqua et Nova: Note on the Relationship Between Artificial Intelligence and Human Intelligence [6] and in his address at the G7 session on artificial intelligence held in Italy in 2024 [7], the Pope warned of the dangers of a "throwaway culture" driven by efficiency at the expense of human dignity and advocated instead for a "culture of encounter" that promotes fairness, inclusion, and justice.

Such a perspective underscores the moral urgency of inclusive technological development.

In this context, laboratory medicine emerges not only as a technical domain but also as a strategic platform for fostering equitable AI integration. International scientific bodies such as the International Federation of Clinical Chemistry and Laboratory Medicine (IFCC) play a critical role in promoting standards, infrastructure, and training to ensure responsible adoption.

This article contributes to the ongoing discourse by providing a critical overview of both the achievements and the unresolved questions surrounding the implementation of AI in healthcare. It is based on the lecture presented by the author at Clinical Laboratories Artificial Intelligence Revolution, March 28th, 2025, Belgrade, Serbia (CLAIR 2025), under the title: "Tribulations, Triumphs, and Governance: Shaping the Future of AI in Healthcare".

Triumphs of AI in Healthcare

AI is achieving transformative success across the healthcare ecosystem, extending far beyond diagnostic imaging. In addition to surpassing or equaling expert performance in interpreting radiological images such as chest X-ray (CXR), computed tomography (CT), and magnetic resonance imaging (MRI) scans, AI is reshaping core clinical processes and public health strategies [1].

Beyond radiology, AI is driving major advances in the management of chronic diseases such as cardiovascular conditions and diabetes, which continue to burden global health systems. Most machine learning (ML) applications to date have focused on diagnostic decision support in these areas, enabling earlier detection, risk stratification, and individualized management. In nephrology, for instance, AI systems have been implemented to detect chronic kidney disease, predict renal function decline, and anticipate acute kidney injury. Similarly, predictive algorithms in primary care settings support early intervention and resource optimization. However, existing studies underscore the need for rigorous model transparency, robust external validation, and comprehensive lifecycle reporting, including ongoing performance monitoring after clinical deployment [8].

The role of AI in public health is rapidly expanding, particularly in infectious disease epidemiology.

Recent advances published in Nature illustrate how AI models significantly improve traditional epidemiological approaches by accelerating forecasting, managing incomplete surveillance data, and supporting timely policy interventions. The integration of empirical data, computational modelling, and real-time policy feedback represents a paradigm shift in epidemic response systems [9].

AI is also contributing to precision medicine and clinical pharmacology. In clinical trials, AI facilitates more efficient patient stratification and recruitment, supports adaptive protocol design, and enables real-time analysis of interim results,

contributing to faster, more cost-effective, and targeted trial execution. AI-enhanced tools can reduce sample sizes, shorten trial durations, and increase the probability of regulatory success, particularly in oncology and rare diseases [10].

The breadth of AI's clinical application is reflected in a recent scoping review of randomized controlled trials (RCTs), which underscores both the promise and limitations of current evidence. Gastroenterology emerged as the most represented specialty, followed by radiology, cardiology, surgery, and oncology, highlighting a concentration of AI research in a few clinical domains, with limited exploration across others. Geographically, the United States and China are the leading contributors, each responsible for nearly one-third of the trials. Notably, while studies from the United States span various specialties, the majority of Chinese trials were focused on gastroenterology. Most RCTs were conducted in a single country and at a single center, with only a small fraction involving multinational collaborations, predominantly within Europe. This pattern reveals a critical gap in demographic representation and multicenter validation, underscoring the need for cross-regional cooperation and broader evaluation strategies [11].

Generative AI is further expanding the scope of these advancements by enhancing diagnostic accuracy, automating complex workflows, and streamlining scientific processes. In healthcare, these models have been applied to tasks such as drug–drug interaction identification, clinical decision support, and pharmacovigilance, demonstrating promise in early detection and management of adverse drug events [12]. In research, generative AI is accelerating hypothesis generation, optimizing study design, and assisting with scientific writing. These advancements underscore the transformative potential of generative AI in improving patient outcomes and expediting scientific discoveries. However, this rapid integration also raises important ethical concerns, particularly regarding authorship, transparency, and the preservation of scientific integrity, calling for clear guidelines and human oversight in AI-assisted scholarly communication [13].

Applications in Laboratory Medicine

AI is playing an increasingly transformative role in laboratory medicine, enhancing quality, efficiency, and clinical impact across the entire total testing process, from pre-analytical to post-analytical phases. While early applications focused on tasks such as automated microscopy and sediment analysis, recent progress has shifted toward deep learning models that support complex classification, real-time quality control, and integrative diagnostic support [14, 15].

- **In the pre-analytical phase**: AI tools have demonstrated the ability to mitigate frequent sources of error. ML algorithms have been developed to detect inappropriate test requests [16], identify mislabeled or misidentified samples (e.g., wrong blood in tube) [17], and flag potential pre-analytical inconsistencies through pattern recognition and delta checks [18]. These solutions contribute to reducing unnecessary testing, increasing patient safety, and optimizing resource utilization [19].
- **In the analytical phase**: AI-based approaches, such as Patient-Based Real-Time Quality Control (PBRTQC), enhance error detection by monitoring longitudinal trends and identifying analytical shifts that would be undetectable through conventional internal quality control methods [20, 21]. Additionally, AI supports the interpretation of complex datasets, such as those from mass spectrometry and flow cytometry, improving both speed and consistency. However, most of these tools have been developed and tested in isolated settings, and few have undergone multicenter validation. As such, their true impact on error reduction and quality assurance in routine clinical environments remains to be conclusively demonstrated [22].
- **In the post-analytical phase**: AI is increasingly used for diagnostic and prognostic applications [23-25]. Machine learning models have shown high predictive accuracy for hematological conditions such as hemoglobinopathies, based on routine laboratory parameters like complete blood count (CBC) data [26], classifying neoplastic cell types from blood films [27], and stratifying patients with suspected urinary tract infections through interpretable decision-tree algorithms [28]. AI has also been applied to stratify diabetes subtypes [29] and predict outcomes in acute leukemia and sepsis using laboratory data alone [30-32].

These models improve diagnostic precision and facilitate early detection and patient risk stratification, thereby providing clinically actionable insights that surpass the interpretive capacity of conventional laboratory reporting.

Furthermore, AI holds significant promise in point-of-care testing (POCT) by enabling decentralized diagnostics through image-based interpretation and smartphone-enabled tools, offering new opportunities to expand access to testing in remote and underserved settings [33, 34].

Despite these advances, the majority of models remain at early stages of clinical translation. Widespread implementation is constrained by limited multicenter validation, real-world testing, and the need for standardized reporting frameworks to ensure reproducibility and comparability [35, 36]. Many proposed applications remain at a conceptual or prototype stage, with limited demonstration of clinical utility in real-world workflows. Moreover, several initiatives are restricted to isolated environments, lacking generalizability and standardization. These limitations must be addressed before AI can be safely and meaningfully integrated into routine laboratory practice. Nevertheless, laboratory medicine, with its structured and high-throughput data environment, represents an ideal setting for the continued integration of AI to support clinical decision-making, enhance quality assurance, and

advance personalized healthcare [2, 37, 38].
One example of successful clinical application within laboratory medicine is the use of machine learning models for sepsis detection based solely on hematological parameters, including complete blood count and monocyte distribution width. These models have undergone multicenter development and external validation, demonstrating performance comparable to more invasive and resource-intensive approaches [32]. Importantly, the integration of AI in laboratory medicine within low-resource settings remains particularly challenging. Barriers include inadequate digital infrastructure, lack of trained personnel, and limited access to validated tools. While AI-powered POCT solutions may offer opportunities to improve access, their success depends on affordability, local capacity-building, and strong governance mechanisms tailored to contextual realities.

Generative Artificial Intelligence in Laboratory Medicine
Beyond traditional machine learning, the adoption of generative AI and large language models (LLMs), such as ChatGPT, offers new possibilities in report generation, natural language explanation, and interactive clinical decision support. These systems can support interpretive comments in laboratory reports, enhancing communication with clinicians and improving the integration of laboratory findings into the broader clinical picture [39, 40].

One example involves the use of LLMs to predict hemoglobinopathies from CBC data, achieving up to 76% accuracy. However, these models showed limitations in handling negative cases and demonstrated a tendency for false positives, reinforcing the need for expert supervision [41]. Importantly, these models have shown a tendency toward elevated false-positive rates and inconsistent performance in handling negative or borderline cases, which may jeopardize clinical decision-making if left unchecked. Without robust validation, continuous performance tracking, and transparent reporting of error rates, the integration of generative AI into laboratory practice may pose significant risks rather than benefits [42]. Chatbots have also been tested on complex diagnostic scenarios, including recommendations on the utility of CK-MB in myocardial infarction, where they occasionally generate outdated or incomplete information, thus reinforcing the importance of human validation [43]. While generative AI can streamline documentation, extract structured information from unstructured reports, and support educational and research tasks, its current performance remains inconsistent in clinical environments where contextual understanding and nuanced reasoning are essential. For this reason, a cautious and critical integration into laboratory workflows is essential [44, 45]. Despite these constraints, supervised use of generative AI can improve text summarization, support structured data extraction from unstructured reports, and even assist in educational tasks such as generating questions or synthesizing scientific literature, potentially streamlining laboratory workflows, and fostering broader access to advanced data tools [46]. Moreover, LLMs can assist in generating standardized interpretive commentaries, simulating patient scenarios for training purposes, and flagging inconsistencies across multiple test results. These capabilities may enhance efficiency in high-volume laboratories while offering scalable tools for settings with limited specialist access.

Tribulations: Ethical and Technical Challenges
The increasing reliance on AI systems in healthcare introduces a range of ethical, technical, and regulatory vulnerabilities that must be addressed to ensure responsible innovation [47]. Among the foremost concerns is the quality and representativeness of the data used to train AI models. Algorithms trained on biased, incomplete, or non-representative datasets may inadvertently amplify pre-existing healthcare disparities, thereby entrenching structural inequities and compromising the generalizability of clinical insights. This concern is particularly pronounced in real-world healthcare settings, where heterogeneity in data quality, inconsistencies in clinical documentation, and variable measurement standards complicate the development of robust, transferable AI models. Recent updates to the Declaration of Helsinki (10th revision, October 2024) explicitly address these emerging ethical concerns in AI and big data research [48, 49]. The revised guidelines reaffirm core ethical principles while explicitly addressing emerging challenges in AI and big data research, including requirements for algorithmic transparency, data protection, and equitable technology deployment. Key updates include:

- **Emphasis on data protection and AI ethics**: Research involving AI must adhere to strict ethical, legal, and regulatory standards. Informed consent is required for the use of health-related big data, and compliance with data privacy laws is mandatory.
- **Capacity building within ethical review boards**: Ethics committees are now encouraged to include expertise in AI and machine learning to appropriately assess the risks and methodological soundness of studies involving these technologies.
- **Commitment to equity**: AI applications in healthcare must not exacerbate social or geographic inequalities. Researchers are urged to ensure algorithmic fairness and facilitate integration of AI tools into healthcare systems globally, including in low-resource settings.
- **Transparency and bias monitoring**: The Declaration highlights the need for ongoing surveillance of AI systems to detect hidden biases and prevent undue influence from commercial interests.

The increasing complexity of AI technologies underscores the urgent need for explainability to ensure transparency, trust, and safe clinical integration. Clinicians are often reluctant to

adopt systems whose decision-making processes are opaque or unverifiable.

Explainability must operate at both the local level clarifying individual predictions, and the global level, illuminating overall model behavior. Without such clarity, trust in clinical implementation cannot be sustained.

Crucially, the deployment of AI systems in healthcare must not compromise patient safety, which depends on sustained clinician oversight. AI output, particularly those derived from non-transparent models, can carry significant clinical consequences if misinterpreted or accepted uncritically. Thus, robust safeguards, including human-in-the-loop designs and clinical validation protocols, are essential to prevent harm and ensure accountability.

In a recent interdisciplinary "manifesto of open challenges" in explainable AI (XAI), Longo et al. identify 28 pressing research challenges grouped into nine thematic areas [50]. These encompass technical and conceptual aspects, including the need for interpretable generative models, collaborative learning frameworks, and clearer definitions of trust in XAI. The authors call for rigorous quantitative and qualitative evaluation of explanations to ensure they promote genuine understanding rather than superficial interpretability. The manifesto emphasizes the societal imperative of fostering human-centered AI systems that are not only technically sound but also aligned with principles of fairness, inclusivity, and democratic oversight. This entails shifting from mere interpretability to genuine epistemic transparency and user-centered design.

In his recent reflections on AI, Pope Francis warns that technological advancement devoid of ethical guidance may foster a "throwaway culture" that subordinates human dignity to efficiency. In the Vatican's Antiqua et Nova document, he advocates for an 'epistemology of care' that situates human dignity, social justice, and ethical responsibility as foundational elements in the development and deployment of AI technologies - particularly in healthcare, where algorithmic decisions bear direct implications for human well-being [6]. These principles are especially vital in healthcare, where decisions driven by algorithms must never eclipse the intrinsic value of each human life.

This ethical framework compels us to view AI not merely as a technical solution but as a social intervention - one that must reflect values of solidarity, transparency, and inclusivity. To that end, a "culture of encounter" is needed, fostering inclusive dialogue among technologists, clinicians, ethicists, and patients, and ensuring that the benefits of AI do not remain the privilege of the few but are extended universally. These principles were echoed in recent international policy discussions, including the Vatican's statement at the G7 Summit (2024), emphasizing the dual promise and peril of AI [7]. While AI may democratize knowledge and automate arduous labor, it may also deepen social injustices and foster a culture of exclusion rather than inclusion.

Data privacy and accountability remain critical concerns. Health data are intrinsically sensitive, and their misuse, whether inadvertent or deliberate, can lead to serious ethical, legal, and reputational consequences. Many jurisdictions have yet to establish comprehensive frameworks for determining liability in cases of AI-related harm or data breaches.

Finally, the limited AI literacy among members of ethics committees and regulatory authorities constitutes a significant barrier to responsible governance. Targeted training and interdisciplinary collaboration are urgently required to equip regulatory bodies and ethics committees with the skills necessary to evaluate algorithmic systems, assess risks, and enforce compliance with evolving legal and ethical standards.

Governance and Regulation

A coherent governance model is urgently required to guide the safe and equitable integration of AI in healthcare. This includes the development of standards for algorithm validation, implementation, and post-market surveillance. Such a model must ensure not only technical robustness but also ethical alignment and societal trust.

Key principles for effective AI governance include:

- **Multistakeholder Involvement:** Ensure inclusive participation of clinicians, laboratory professionals, data scientists, ethicists, patients, and regulatory authorities throughout the design, validation, and oversight phases of AI integration.
- **Clinical Validation and Continuous Monitoring:** Require thorough validation across diverse populations and enforce post-deployment surveillance to detect algorithm drift and performance degradation.
- **Equity-Focused Regulation**: Assess the societal impact of AI tools and mitigate risks of exacerbating health disparities, particularly in under-resourced settings.
- **Transparency and Accountability**: Mandate full disclosure of model architecture, training datasets, and decision-making processes to support auditability and clinician trust.
- **Ethical Oversight:** Align AI applications with bioethical principles and international declarations, including the revised 2024 Declaration of Helsinki and the Declaration of Taipei.

The revised 2024 Declaration of Helsinki, along with the Declaration of Taipei, underscores the need for consistent ethical oversight in AI-related research, particularly in the use of large health datasets [43]. However, divergent data governance regimes across jurisdictions, such as General Data Protection Regulation (GDPR) in the EU versus fragmented policies in the U.S., emphasize the urgent necessity

for harmonizing international legal and ethical standards, particularly in light of cross-border data use, divergent regulatory landscapes, and the global nature of AI innovation [51].

The European Union's (EU) AI Act, finalized in early 2024, establishes a comprehensive risk-based framework that mandates transparency, human oversight, and third-party conformity assessment for high-risk AI systems in health [52]. It allows for real-world testing under strict conditions and encourages the use of regulatory sandboxes to safely innovate while protecting fundamental rights. The Act is expected to serve as a global benchmark, analogous to the GDPR in data protection. Its tiered approach, pre-market conformity assessments, and regulatory sandbox provisions aim to balance innovation with patient safety, offering a model for international cooperation. Nevertheless, without coordinated investment in capacity-building - particularly in low-resource settings - and without mechanisms to enforce cross-border accountability, these efforts risk reinforcing existing global inequities. Equitable AI governance must include training programs, infrastructure support, and shared oversight models that protect patient rights across jurisdictions, not only where technological leadership is concentrated.

At the institutional level, emerging models of AI governance emphasize the importance of continuous evaluation and adaptive oversight [53].

Moreover, the WHO has called for the establishment of binding international standards to ensure equitable AI deployment across healthcare systems. While current guidance remains largely aspirational, efforts are underway to reform the International Health Regulations (IHR) to include digital and AI health governance [1]. Until such frameworks are adopted globally, regional legislation such as the EU AI Act may serve as de facto blueprints for responsible innovation.

The Role of Laboratory Medicine Societies

Scientific societies in laboratory medicine are uniquely positioned to lead the responsible integration of AI into clinical practice. Their contributions should encompass:

- **Knowledge Dissemination:** Provide training and educational resources on AI fundamentals for laboratory professionals. Notably, the Italian Society of clinical chemistry and laboratory medicine (SIBioC) Working Group on Big data and Artificial Intelligence has recently launched two national training programs: "Understanding Generative AI and Its Applications" and "Introduction to Machine Learning in Laboratory Medicine" [54]. These initiatives reflect a broader commitment to professional capacity building and equitable technological adoption, especially in settings lacking dedicated data science support. Such initiatives are particularly critical for addressing disparities in access to AI training and infrastructure, which affect many professional communities in low- and middle-income countries. Strengthening international cooperation and resource-sharing is essential to prevent technological exclusion and promote equitable capacity development.
- **Interdisciplinary Collaboration:** Foster dialogue between laboratory scientists, clinicians, data scientists, and engineers. The IFCC, through its Task Force on Ethics [55], has undertaken a timely and relevant survey investigating the real-time electronic disclosure of laboratory results in ambulatory settings. The survey, which closed on March 17, 2025, seeks to identify prevailing practices and ethical concerns, ultimately informing the development of international guidance to ensure transparency, patient autonomy, and responsible data sharing.
- **Regulatory Advocacy and Ethical Oversight:** Participate in national and international policymaking to ensure that laboratory-specific considerations are included in AI governance. The IFCC has also issued 15 key recommendations for the development of machine learning in laboratory medicine, with the first underscoring the imperative to "involve diverse stakeholders to develop clinically useful, practical, and ethical models" [56]. This principle captures the essence of ethical AI development: it must be inclusive, transparent, and continuously validated to remain trustworthy and clinically relevant. Ethics in AI is not only about minimizing bias but also about ensuring replicability, workflow integration, and patient-centered impact.
- In support of these principles, a recent publication in Clinical Chemistry emphasizes the need to go beyond initial model validation [57]. The authors call for comprehensive lifecycle oversight, including performance tracking in real-world settings and revalidation as clinical conditions evolve.
- **Consensus Development and Infrastructure:** Generate position papers, best practice guidelines, and frameworks for data quality and governance. The European Federation of Clinical Chemistry and Laboratory Medicine (EFLM) Working Group on Artificial Intelligence has made substantial contributions in this area, including a European survey that maps current AI adoption, identifies structural and educational barriers, and calls for targeted investment in infrastructure to support effective AI integration [37]. An additional contribution from the EFLM underscores the critical role of metadata and peridata in laboratory data management, offering a structured methodology to improve AI-driven applications through enhanced data standardization and interoperability [58]. Indeed, a thorough understanding of metadata and peridata - including analytical and biological sources of variation - enables the appropriate use of laboratory data along with its intrinsic "noise", a form of uncertainty that only domain experts such as clinical laboratorians can correctly interpret and integrate into AI workflows to enhance robustness and contextual validity [36, 59].

These collective efforts underscore the strategic and operational role of laboratory medicine societies in shaping an ethically sound, scientifically robust, and socially responsible future for AI in healthcare. By investing in education, governance, data quality, and international dialogue, these organizations ensure that the transformative potential of AI is directed toward improving patient care and advancing health equity.

Conclusion

Artificial intelligence offers unprecedented opportunities to reshape healthcare delivery, public health infrastructure, and laboratory medicine. However, realizing its full potential requires a deliberate and ethically grounded approach to its design, validation, and implementation. The promise of technical innovation must be matched by ethical vigilance, legal coherence, and inclusive governance that bridges diverse clinical contexts and global disparities. This imperative is especially acute in low-resource environments, where AI has the potential to either narrow or widen health inequities depending on how inclusively it is designed, validated, and deployed.

Laboratory medicine, with its structured data environment and central role in clinical decision-making, is uniquely positioned to lead this transformation. Professional societies, including IFCC, EFLM, and national organizations like SIBioC, are critical to this effort, advancing AI literacy, fostering interdisciplinary collaboration, and shaping international standards for responsible innovation.

As underscored in this manuscript, the challenges of data representativeness, explainability, and global regulatory fragmentation remain formidable.

Yet they also present a pivotal opportunity: to develop a global framework grounded in accountability, transparency, and justice—ensuring that AI evolves as a catalyst for health equity rather than a vector of new disparities. Clinician oversight must remain central to all AI-enabled processes to ensure that safety, accountability, and clinical judgment are never subordinated to algorithmic convenience.

To translate these reflections into actionable guidance, the responsible integration of AI in laboratory medicine should rest on several key pillars:

1. Rigorous model validation across diverse settings;
2. Clinician oversight to safeguard patient safety;
3. Equitable access to AI education and infrastructure;
4. Alignment with evolving ethical and legal frameworks;
5. Continuous performance monitoring and quality assurance.

These principles should guide professional societies, developers, and policymakers alike as they shape the future of AI in healthcare.

Pope Francis's appeal for a "culture of encounter" reminds us that technological advancement must never eclipse human dignity. Rather, it must be anchored in solidarity, inclusion, and global cooperation. The future of AI in healthcare is therefore not merely a matter of technological advancement, it is a shared societal responsibility, entrusted to clinicians, scientists, regulators, and the communities they serve.

Abbreviations List

AI	Artificial Intelligence
CBC	Complete Blood Count
CLAIR	Clinical Laboratories Artificial Intelligence Revolution
CT	Computed Tomography
EFLM	European Federation of Clinical Chemistry and Laboratory Medicine
EU	European Union
GDPR	General Data Protection Regulation
IFCC	International Federation of Clinical Chemistry and Laboratory Medicine
IHR	International Health Regulations
LLM	Large Language Models
ML	Machine Learning
MRI	Magnetic Resonance Imaging
PBRTQC	Patient-Based Real-Time Quality Control
POCT	Point-of-Care Testing
RCTs	Randomized Controlled Trials
SIBioC	Italian Society of Clinical Chemistry and Laboratory Medicine
WHO	World Health Organization
XAI	Explainable Artificial Intelligence
CXR	Chest X-ray

Declaration of generative AI and AI-assisted technologies in the writing process

During the preparation of this manuscript, the author utilized ChatGPT-4o (OpenAI) to assist with language refinement and rephrasing. The content generated was subsequently reviewed, edited, and validated by the author, who assumes full responsibility for the final version of the work.

Conflicts of interest

The author declares no conflicts of interest.

Funding Statement

This work did not receive any specific grant from funding agencies in the public, commercial, or not-for-profit sectors.

Data Availability Statement

No datasets were generated or analyzed during the current study.

References

1. Bouderhem R. Shaping the future of AI in healthcare through ethics and governance. Humanit Soc Sci Commun. 2024;416. https://doi.org/10.1057/s41599-024-02894-w.
2. Plebani M, Cadamuro J, Vermeersch P, Jovičić S, Ozben T, Trenti T, et al. A vision to the future: value-based laboratory medicine. Clin Chem Lab Med. 2024;62:2373-2387.

doi: 10.1515/cclm-2024-1022.
3. WHO (2023) Regulatory considerations on artificial intelligence for health. World Health Organization. Available from: https://iris.who.int/handle/10665/373421 (Accessed 02/03/2025).
4. WHO (2021) Report, Ethics and governance of artificial intelligence. Available from: https://www.who.int/publications/i/item/9789240029200 (Accessed 02/03/2025).
5. EU Council, Artificial Intelligence Act 2024. Text of the Provisional Agreement, 2 February 2024. Available from: https://data.consilium.europa.eu/doc/document/ST-5662-2024-INIT/en/pdf (Accessed 05/01/2025).
6. ANTIQUA ET NOVA: Note on the Relationship Between Artificial Intelligence and Human Intelligence. Available at: https://press.vatican.va/content/salastampa/it/bollettino/pubblico/2025/01/28/0083/01166.html#ing
7. G7 Session on Artificial Intelligence. Address of His Holiness Pope Francis. Available from: https://www.vatican.va/content/francesco/en/speeches/2024/june/documents/20240614-g7-intelligenza-artificiale.html (Accessed 02/03/2025).
8. Rakers MM, van Buchem MM, Kucenko S, de Hond A, Kant I, van Smeden M, et al. Availability of Evidence for Predictive Machine Learning Algorithms in Primary Care: A Systematic Review. JAMA Netw Open. 2024;7:e2432990. doi: 10.1001/jamanetworkopen.2024.32990.
9. Kraemer MUG, Tsui JL, Chang SY, Lytras S, Khurana MP, Vanderslott S, et al. Artificial intelligence for modelling infectious disease epidemics. Nature. 2025;638:623-635. doi: 10.1038/s41586-024-08564-w.
10. Askin S, Burkhalter D, Calado G, El Dakrouni S. Artificial Intelligence Applied to clinical trials: opportunities and challenges. Health Technol (Berl). 2023;13:203-213. doi: 10.1007/s12553-023-00738-2.
11. Han R, Acosta JN, Shakeri Z, Ioannidis JPA, Topol EJ, Rajpurkar P. Randomised controlled trials evaluating artificial intelligence in clinical practice: a scoping review. Lancet Digit Health. 2024;6:e367-e373. doi: 10.1016/S2589-7500(24)00047-5.
12. Ong JCL, Chen MH, Ng N, Elangovan K, Tan NYT, Jin L, et al. A scoping review on generative AI and large language models in mitigating medication related harm. NPJ Digit Med. 2025;8:182. doi: 10.1038/s41746-025-01565-7.
13. Carobene A, Padoan A, Cabitza F, Banfi G, Plebani M. Rising adoption of artificial intelligence in scientific publishing: evaluating the role, risks, and ethical implications in paper drafting and review process. Clin Chem Lab Med. 2023;62:835-843. doi: 10.1515/cclm-2023-1136.
14. Hou H, Zhang R, Li J. Artificial intelligence in the clinical laboratory. Clin Chim Acta. 2024;559:119724. doi: 10.1016/j.cca.2024.119724.
15. Carobene A, Gruson D, Cadamuro J, Cabitza F, Agnello L, Campagner A, Padoan A. The role of artificial intelligence in the clinical laboratory: challenges and opportunities. Biochimica Clinica. 2025;49. doi: 10.23736/S0393-0564.24.00007-0
16. Kumar Ashwin PSS, Yuvaraj D, Kaur R, Kayathri S, Dhamotharan KA, Patil N. Artificial Intelligence in Clinical Biochemistry Is Designed To Prevent Unnecessary Routine Testing In the Pre-Analytic Phase. Bulletin of Environment, Pharmacology and Life Sciences Bull. Env. Pharmacol. Life Sci. 2022;11: 207-212. https://bepls.com/april_2022/38.pdf (Accessed 02/01/2025).
17. Farrell CJ, Makuni C, Keenan A, Maeder E, Davies G, Giannoutsos J. A Machine Learning Model for the Routine Detection of "Wrong Blood in Complete Blood Count Tube" Errors. Clin Chem. 2023;69:1031-1037. doi: 10.1093/clinchem/hvad100.
18. Seok HS, Yu S, Shin KH, Lee W, Chun S, Kim S, et al. Machine Learning-Based Sample Misidentification Error Detection in Clinical Laboratory Tests: A Retrospective Multicenter Study. Clin Chem. 2024;70:1256-1267. doi: 10.1093/clinchem/hvae114.
19. Lippi G, Mattiuzzi C, Favaloro EJ. Artificial intelligence in the pre-analytical phase: State-of-the art and future perspectives. J Med Biochem. 2024;43:1-10. doi: 10.5937/jomb0-45936.
20. Duan X, Zhang M, Liu Y, Zheng W, Lim CY, Kim S, et al. Patient-Based Real-Time Quality Control Working Group of the Asia Pacific Federation of Clinical Biochemistry and Laboratory Medicine. Next-Generation Patient-Based Real-Time Quality Control Models. Ann Lab Med. 2024;44:385-391. doi: 10.3343/alm.2024.0053.
21. Lorde N, Mahapatra S, Kalaria T. Machine Learning for Patient-Based Real-Time Quality Control (PBRTQC), Analytical and Preanalytical Error Detection in Clinical Laboratory. Diagnostics (Basel). 2024;14:1808. doi: 10.3390/diagnostics14161808.
22. Duan X, Wang B, Zhu J, Shao W, Wang H, Shen J, Wu W, Jiang W, Yiu KL, Pan B, Guo W. Assessment of patient-based real-time quality control algorithm performance on different types of analytical error. Clin Chim Acta. 2020;511:329-335. doi: 10.1016/j.cca.2020.10.006.
23. Famiglini L, Campagner A, Carobene A, Cabitza F. A robust and parsimonious machine learning method to predict ICU admission of COVID-19 patients. Med Biol Eng Comput. 2022:1–13. doi: 10.1007/s11517-022-02543-x.
24. Campagner A, Carobene A, Cabitza F. External validation of Machine Learning models for COVID-19 detection based on Complete Blood Count. Health Inf Sci Syst. 2021;9:37. doi: 10.1007/s13755-021-00167-3.
25. Carobene A, Milella F, Famiglini L, Cabitza F. How is test laboratory data used and characterised by machine learning models? A systematic review of diagnostic and prognostic models developed for COVID-19 patients using only laboratory data. Clin Chem Lab Med. 2022;60:1887-1901. doi: 10.1515/cclm-2022-0182.
26. Schipper A, Rutten M, van Gammeren A, Harteveld CL, Urrechaga E, Weerkamp F, et al. Machine Learning-Based

Prediction of Hemoglobinopathies Using Complete Blood Count Data. Clin Chem. 2024;70:1064-1075. doi: 10.1093/clinchem/hvae081.
27. Zini G, Mancini F, Rossi E, Landucci S, d'Onofrio G. Artificial intelligence and the blood film: Performance of the MC-80 digital morphology analyzer in samples with neoplastic and reactive cell types. Int J Lab Hematol. 2023;45:881-889. doi: 10.1111/ijlh.14160.
28. Yildirim M, Bingol H, Cengil E, Aslan S, Baykara M. Automatic Classification of Particles in the Urine Sediment Test with the Developed Artificial Intelligence-Based Hybrid Model. Diagnostics (Basel). 2023;13:1299. doi: 10.3390/diagnostics13071299.
29. Mizani MA, Dashtban A, Pasea L, et al. Identifying subtypes of type 2 diabetes mellitus with machine learning: development, internal validation, prognostic validation and medication burden in linked electronic health records in 420 448 individuals. BMJ Open Diab Res Care. 2024;12:e004191. doi:10.1136/bmjdrc-2024-004191.
30. Alcazer V, Le Meur G, Roccon M, Barriere S, Le Calvez B, Badaoui B, et al. Evaluation of a machine-learning model based on laboratory parameters for the prediction of acute leukaemia subtypes: a multicentre model development and validation study in France. Lancet Digit Health. 2024;6:e323-e333. doi: 10.1016/S2589-7500(24)00044-X.
31. Agnello L, Vidali M, Padoan A, Lucis R, Mancini A, Guerranti R, et al. Machine learning algorithms in sepsis. Clin Chim Acta. 2024;553:117738. doi: 10.1016/j.cca.2023.117738.
32. Campagner A, Agnello L, Carobene A, Padoan A, Del Ben F, Locatelli M, et al. Complete Blood Count and Monocyte Distribution Width-Based Machine Learning Algorithms for Sepsis Detection: Multicentric Development and External Validation Study. J Med Internet Res. 2025;27:e55492. doi: 10.2196/55492.
33. Han GR, Goncharov A, Eryilmaz M, Ye S, Palanisamy B, Ghosh R, et al. Machine learning in point-of-care testing: innovations, challenges, and opportunities. Nat Commun. 2025;16:3165. doi: 10.1038/s41467-025-58527-6.
34. Khan AI, Khan M, Khan R. Artificial Intelligence in Point-of-Care Testing. Ann Lab Med. 2023;43:401-407. doi: 10.3343/alm.2023.43.5.401.
35. Carobene A, Cabitza F, Bernardini S, Gopalan R, Lennerz JK, Weir C, et al. Where is laboratory medicine headed in the next decade? Partnership model for efficient integration and adoption of artificial intelligence into medical laboratories. Clin Chem Lab Med. 2022;61:535-43. doi: 10.1515/cclm-2022-1030. Erratum in: Clin Chem Lab Med. 2023;61:1359. doi: 10.1515/cclm-2023-0352.
36. Cabitza F, Campagner A, Soares F, García de Guadiana-Romualdo L, Challa F, Sulejmani A, et al. The importance of being external. methodological insights for the external validation of machine learning models in medicine. Comput Methods Programs Biomed. 2021;208:106288. doi: 10.1016/j.cmpb.2021.106288.
37. Cadamuro J, Carobene A, Cabitza F, Debeljak Z, De Bruyne S, van Doorn W, et al. A comprehensive survey of artificial intelligence adoption in European laboratory medicine: current utilization and prospects. Clin Chem Lab Med. 2024;63:692-703. doi: 10.1515/cclm-2024-1016.
38. Bellini C, Padoan A, Carobene A, Guerranti R. A survey on Artificial Intelligence and Big Data utilisation in Italian clinical laboratories. Clin Chem Lab Med. 2022;60:2017-2026. doi: 10.1515/cclm-2022-0680.
39. Yang, He S., Li, Jieli, Yi, Xin and Wang, Fei. Performance evaluation of large language models with chain-of-thought reasoning ability in clinical laboratory case interpretation. Clin Chem Lab Med. 2025. doi: 10.1515/cclm-2025-0055. Epub ahead of print.
40. Cadamuro J, Cabitza F, Debeljak Z, De Bruyne S, Frans G, Perez SM, et al. Potentials and pitfalls of ChatGPT and natural-language artificial intelligence models for the understanding of laboratory medicine test results. An assessment by the European Federation of Clinical Chemistry and Laboratory Medicine (EFLM) Working Group on Artificial Intelligence (WG-AI). Clin Chem Lab Med. 2023;61:1158-1166. doi: 10.1515/cclm-2023-0355.
41. Kurstjens S, Schipper A, Krabbe J, Kusters R. Predicting hemoglobinopathies using ChatGPT. Clin Chem Lab Med 2023;62:e59–61.
42. Rashidi HH, Pantanowitz J, Chamanzar A, Fennell B, Wang Y, Gullapalli RR, Tafti A, Deebajah M, Albahra S, Glassy E, Hanna MG, Pantanowitz L. Generative Artificial Intelligence in Pathology and Medicine: A Deeper Dive. Mod Pathol. 2025;38:100687. doi: 10.1016/j.modpat.2024.100687.
43. Wu AH, Jaffe AS, Peacock WF, Kavsak P, Greene D, Christenson RH. The Role of Artificial Intelligence for Providing Scientific Content for Laboratory Medicine. J Appl Lab Med 2024;9:386–393.
44. Plebani M. ChatGPT: angel or Demon? Critical thinking is still needed. Clin Chem Lab Med 2023;61:1131–1132.
45. Del Ben F, Galozzi P, Lucis R, Cabitza F, Carobene A. Generative artificial intelligence in laboratory medicine: innovations, limitations, and ethical considerations. Biochimica Clinica 2025;49:75-84. doi: 10.23736/S0393–0564.24.00003-0.
46. Van Noorden R, Perkel JM. AI and science: what 1,600 researchers think. Nature 2023;621:672–675.
47. Pennestri F, Banfi G. Artificial intelligence in laboratory medicine: fundamental ethical issues and normative key-points. Clin Chem Lab Med. 2022;60:1867-1874. doi: 10.1515/cclm-2022-0096.
48. World Medical Association. World Medical Association Declaration of Helsinki: Ethical Principles for Medical Research Involving Human Participants. JAMA. 2025;333:71-74. doi: 10.1001/jama.2024.21972.
49. Shaw JA. The Revised Declaration of Helsinki-Considerations for the Future of Artificial Intelligence in Health

and Medical Research. JAMA. 2025;333:26-27. doi: 10.1001/jama.2024.22074.
50. Longo L, Brcic M, Cabitza F, Choi J, Confalonieri R, Del Ser J, et al. Explainable Artificial Intelligence (XAI) 2.0: A manifesto of open challenges and interdisciplinary research directions. Information Fusion 106. 2024:102301. doi: 10.1016/j.inffus.2024.102301.
51. Aidun E. Associate Member, University of Cincinnati Law Review Vol. 93 Data Privacy in the Digital Age: A Comparative Analysis of U.S. and EU Regulations. Available from: https://uclawreview.org/2025/03/05/data-privacy-in-the-digital-age-a-comparative-analysis-of-u-s-and-eu-regulations
52. Schmidt J, Schutte NM, Buttigieg S, Novillo-Ortiz D, Sutherland E, Anderson M, et al. Mapping the regulatory landscape for artificial intelligence in health within the European Union. NPJ Digit Med. 2024;7:229. doi: 10.1038/s41746-024-01221-6.
53. Saenz AD; Mass General Brigham AI Governance Committee; Centi A, Ting D, You JG, Landman A, Mishuris RG. Establishing responsible use of AI guidelines: a comprehensive case study for healthcare institutions. NPJ Digit Med. 2024;7:348. doi: 10.1038/s41746-024-01300-8. Erratum in: NPJ Digit Med 2025;8:70. doi: 10.1038/s41746-025-01445-0.
54. Carobene A, Padoan A. Esplorando l'Intelligenza Artificiale in medicina di laboratorio e nella ricerca scientifica: tra sfide e nuove opportunità l'importanza di un approccio proattivo. Editorial. Biochim Clin. 2024;48:111-114. doi: 10.19186/BC_2024.022
55. https://ifcc.org/taskforceethics/ (Accessed 02/03/2025).
56. Master SR, Badrick TC, Bietenbeck A, Haymond S. Machine Learning in Laboratory Medicine: Recommendations of the IFCC Working Group. Clin Chem. 2023;69:690-698. doi: 10.1093/clinchem/hvad055.
57. Spies NC, Farnsworth CW, Wheeler S, McCudden CR. Validating, Implementing, and Monitoring Machine Learning Solutions in the Clinical Laboratory Safely and Effectively. Clin Chem. 2024;70:1334-1343. doi: 10.1093/clinchem/hvae126.
58. Padoan A, Cadamuro J, Frans G, Cabitza F, Tolios A, De Bruyne S, et al. Data flow in clinical laboratories: could metadata and peridata bridge the gap to new AI-based applications? Clin Chem Lab Med. 2024;63:684-691. doi: 10.1515/cclm-2024-0971.
59. Campagner A, Famiglini L, Carobene A, Cabitza F. Everything is varied: The surprising impact of instantial variation on ML reliability Applied Soft Computing, 2023, 146, 110644.

Letter to the Editor

Implementing Machine Learning in the Clinical Laboratory: Opportunities and Challenges

He Sarina Yang[1*]

[1]*Department of Pathology and Laboratory Medicine, Weill Cornell Medicine, New York, USA*

Article Info

[*]***Corresponding Author:***
He Sarina Yang, PhD, MBBS, DABCC
Associate Professor
Department of Pathology and Laboratory Medicine
Weill Cornell Medicine
525 E. 68th St, New York, NY, 10065
E-mail: hey9012@med.cornell.edu

Keywords

Machine learning, clinical laboratory, generalizability, reproducibility, fairness

In recent years, the Laboratory Medicine field's strong interest in the potential application of artificial intelligence (AI) and machine learning (ML) has been reflected in the substantial growth of publications. A number of reported studies have explored the applications of AI/ML across the four phases of the total testing process, such as improving test utilization [1], detecting pre-analytical errors [2, 3], enhancing analytical efficiency [4], and interpreting complex laboratory panels [5-7]. In addition, machine learning-based clinical decision supporting tools have been used to predict the onset, progression, subtypes, and outcome of diseases, such as sepsis [8], acute kidney injury [9], and COVID-19 [10]. Compared to the traditional clinical algorithm or scoring systems, ML can ingest far larger, richer dataset, automatically flag subtle variables that manual scores miss, and generate more accurate predictions of disease diagnosis and prognosis.

Data generated from the clinical laboratory is largely composed of discrete numerical or categorical values in a structured format, and the number of tests ordered for each patient makes these datasets inherently high-dimensional [11]. Clinical laboratory data has several noteworthy characteristics: first, test values can vary across instrument platforms and analytical methodologies, and their corresponding reference ranges can differ as well. Therefore, integrating data from different sources must begin with careful normalization. Second, clinical datasets may contain missing values and outliers. Missing values stem from systematic missingness and random missingness. Systematic missingness, i.e., laboratory tests are not always ordered on a regular basis for all patients in clinical practice, especially with different institutional practice, reflecting institution-specific ordering patterns. On the other hand, random missingness could occur when a test is ordered but cannot be completed due to pre-analytical or analytical errors. When processing a clinical dataset, we should determine if it is reliable to impute the missing values from the remaining results using imputation techniques. In addition, outliers in laboratory data can occur due to analytical or pre-analytical errors, or true pathological reasons. The causes of outliers should be investigated to determine whether they should be included or excluded from the data analysis. Informative outliers can be accommodated with techniques like robust loss functions, whereas erroneous ones should be removed. Last but not least, unreported data, such as hemolysis, icterus, and lipemia index, are kept in the middleware, but not transmitted to EHR, yet these data may be valuable for ML analysis.

A successful ML pipeline in Laboratory Medicine begins with robust data collection: assemble a large, high-quality dataset that represents the target population; Next comes data preprocessing and method development, which includes normalization, handling of missing values and outliers, feature engineering, optimization of hyperparameters, and selection of appropriate model architecture. Once a candidate model is locked, rigorous evaluation of its performance on an internal hold-out test set and independent external datasets are needed to detect overfitting [12]. If a model is successfully developed and demonstrates strong promise during retrospective analysis, several checkpoints are still needed before it can be integrated into clinical workflow:

1. Assess a model's generalizability and transportability – the model should perform reliably on independent, unseen data collected from different geographic or demographic patient populations or different hospital settings. In the laboratory setting, factors, such as sample handling protocol, instrument platforms, methodologies, send-out laboratories, and regional patient characteristics, can shift data distributions and impact a model's performance. External validation on datasets that capture these variations is therefore indispensable as it tests a model's real-world utility, uncovers hidden biases, and confirms a model's robustness [13].
2. Demonstrate a model's interpretability. Physicians and laboratory professionals are more likely to accept a model that is comprehensible and aligned with their clinical knowledge. Most conventional ML models, such as logistic regression and decision tree, are self-interpretable due to their linear or rule-based nature. In contrast, more complicated ML models, such as deep learning networks, are largely "black boxes". While some research has shown that accuracy sometimes trumps interpretability, the assumption is that such accuracy should be widely tested and proven to be generalizable, which is challenging in many clinical scenarios. For "black box models", post-hoc methods can translate its input-output behavior into a simpler surrogate (e.g., a decision tree) or quantify each feature's influence. The Shapley additive explanations (SHAP) technique, for instance, decomposes the model's prediction for each sample as an additive integration of the contributions from each individual feature, and thus, can show how features act as force to push the model to make positive or negative predictions.
3. Evaluate a model's fairness. Since clinical decisions guided by ML may influence diagnostics, treatments, and resource allocation, we should make sure that a model does not systematically over- or under- predict risk for certain races, sexes, or socioeconomic groups. A model's fairness can be evaluated using metrics including disparate impact (the probabilities of the positive outcome for the two groups), equal opportunity difference (the difference in true positive rates between two groups), the predictivity parity difference (the difference in positive predictive values), with the White race being the privileged group. A model's performance should be assessed retrospectively and prospectively across demographic groups to detect any disparities that could introduce or perpetuate bias.
4. Involve clinical teams in the development and deployment pipeline. Evaluating an ML model is not just a data-science exercise, it requires frontline clinical insight [14]. Clinical teams should be involved and provide insights on how, where, and by whom the tool would be used – alert fatigue, hand-off timing, and documentation burden often make or break adoption. The clinicians can map model outputs to actionable decisions, e.g. ordering confirmatory tests or adjusting medication, and estimate the downstream impact on patient outcomes.

Despite the buzz around AI, clinically deployed AI/ML tools in the clinical laboratory remain limited. Compared to Radiology which has over 700 AI-based technologies approved by FDA, Laboratory Medicine only has a combined total of 37 AI applications across clinical chemistry, immunology, hematology and microbiology [15].

Translating a proof-of-concept model into measurable clinical benefit requires rigorous validation and a well-designed implementation strategy, as well as interdisciplinary collaboration. Several huddles slow the pipeline from model development to deployment [16]:

1. lack of data infrastructure that supports ML validation implementation;
2. lack of informatics personnel to conduct data extraction, model deployment, and ongoing maintenance;
3. limited knowledge and experience among laboratorians, leaving many unfamiliar with how to validate, monitor, and trouble-shoot ML outputs,
4. lack of guidelines or expert consensus on best practice for ML implementation in the clinical laboratory.

Our field urgently needs more success stories of integrating ML into clinical workflow, along with practical guidelines on how to validate and implement various types of AI/ML applications. Machine learning won't replace seasoned laboratorians, but laboratories that harness ML thoughtfully will outperform those who don't – catching errors earlier, improving laboratory efficiency, freeing humans for higher-order tasks, and delivering more precise care. The opportunity is huge; the challenge is to move beyond proof-of-concepts into regulated, reproducible, and equitable practice. With the right guidelines and a collaborative mindset, the clinical laboratory can become a flagship environment where AI proves its value.

References

1. H.S. Yang, W. Pan, Y. Wang, M.A. Zaydman, N.C. Spies, Z. Zhao, T.A. Guise, Q.H. Meng, F. Wang, Generalizability of a Machine Learning Model for Improving Utilization of Parathyroid Hormone-Related Peptide Testing across Multiple Clinical Centers, Clin Chem 2023;69(11): 260-1269.
2. C.J. Farrell, C. Makuni, A. Keenan, E. Maeder, G. Davies, J. Giannoutsos, A Machine Learning Model for the Routine Detection of "Wrong Blood in Complete Blood Count Tube" Errors, Clin Chem 2023;69(9):1031-1037.
3. B.V. Graham, S.R. Master, A.E. Obstfeld, R.B. Wilson, A Multianalyte Machine Learning Model to Detect Wrong Blood in Complete Blood Count Tube Errors in a Pediatric Setting, Clin Chem 2025;71(3): 418-427.
4. H.S. Seok, S. Yu, K.H. Shin, W. Lee, S. Chun, S. Kim, H. Shin, Machine Learning-Based Sample Misidentification Error Detection in Clinical Laboratory Tests: A Retrospective Multicenter Study, Clin Chem 2024;70(10):1256-1267.
5. E.H. Wilkes, G. Rumsby, G.M. Woodward, Using Machine Learning to Aid the Interpretation of Urine Steroid Profiles, Clin Chem 2018;64(11):586-1595.
6. E.H. Wilkes, E. Emmett, L. Beltran, G.M. Woodward, R.S. Carling, A Machine Learning Approach for the Automated Interpretation of Plasma Amino Acid Profiles, Clin Chem 2020;66(9):1210-1218.
7. F. Chabrun, X. Dieu, M. Ferre, O. Gaillard, A. Mery, J.M. Chao de la Barca, A. Taisne, G. Urbanski, P. Reynier, D. Mirebeau-Prunier, Achieving Expert-Level Interpretation of Serum Protein Electrophoresis through Deep Learning Driven by Human Reasoning, Clin Chem 2021;67(10):1406-1414.
8. H.S. Yang, Machine Learning for Sepsis Prediction: Prospects and Challenges, Clin Chem 2024;70(3):465-467.
9. A.U. Rehman, J.A. Neyra, J. Chen, L. Ghazi, Machine learning models for acute kidney injury prediction and management: a scoping review of externally validated studies, Crit Rev Clin Lab Sci 2025:1-23.
10. H.S. Yang, Y. Hou, L.V. Vasovic, P.A.D. Steel, A. Chadburn, S.E. Racine-Brzostek, P. Velu, M.M. Cushing, M. Loda, R. Kaushal, Z. Zhao, F. Wang, Routine Laboratory Blood Tests Predict SARS-CoV-2 Infection Using Machine Learning, Clin Chem 2020;66(11):1396-1404.
N.C. Spies, C.W. Farnsworth, S. Wheeler, C.R. McCudden, Validating, Implementing, and Monitoring Machine Learning Solutions in the Clinical Laboratory Safely and Effectively, Clin Chem 2024;70(11): 1334-1343.
12. H.S. Yang, D.D. Rhoads, J. Sepulveda, C. Zang, A. Chadburn, F. Wang, Building the Model, Arch Pathol Lab Med (2022).
13. F. Cabitza, A. Campagner, F. Soares, L. Garcia de Guadiana-Romualdo, F. Challa, A. Sulejmani, M. Seghezzi, A. Carobene, The importance of being external. methodological insights for the external validation of machine learning models in medicine, Comput Methods Programs Biomed 2021;208:106288.
14. F. Wang, A. Beecy, Implementing AI models in clinical workflows: a roadmap, BMJ Evid Based Med (2024).
15. F. Del Ben, Beyond test results: the strategic importance of metadata for the integration of AI in laboratory medicine, Clin Chem Lab Med 2025;63(4):653-655.
[16] J. Cadamuro, A. Carobene, F. Cabitza, Z. Debeljak, S. De Bruyne, W. van Doorn, E. Johannes, G. Frans, H. Ozdemir, S. Martin Perez, D. Rajdl, A. Tolios, A. Padoan, C. European Federation of Clinical, I. Laboratory Medicine Working Group on Artificial, A comprehensive survey of artificial intelligence adoption in European laboratory medicine: current utilization and prospects, Clin Chem Lab Med 63(4) (2025) 692-703.

Review Article

Leveraging AI to enhance electronic health records

Sanja Stankovic[1,2*]

[1]University Clinical Center of Serbia, Center for Medical Biochemistry, Belgrade, Serbia
[2]University of Kragujevac, Faculty of Medical Sciences, Kragujevac, Serbia

Article Info

[*]***Corresponding Author:***
Sanja Stankovic
University Clinical Center of Serbia, Center for Medical Biochemistry, Belgrade, Serbia
University of Kragujevac, Faculty of Medical Sciences, Kragujevac, Serbia
E-mail: sanjast2013@gmail.com
ORCID: https://orcid.org/0000-0003-0890-535X
Telephone: +381 113615631
Fax number: +381 113615631
Address: University Clinical Center of Serbia, Pastrova 2, 11000 Belgrade, Serbia

Keywords

artificial intelligence, electronic health record, healthcare, medicine

Abstract

The artificial intelligence (AI) integration in the medical field benefits both clinicians and patients. One of the most exciting applications of AI in healthcare is its role in electronic health records (EHRs). Leveraging AI to enhance EHR holds incredible potential for streamlining processes and reducing errors, enhancing clinical decision support and improving interoperability, contributing to more accurate, personalized, and effective healthcare, improved patient outcomes and quality of life. This article provides an overview of the role of AI in EHR, illustrates several examples of how AI incorporation into EHRs transforms healthcare delivery, illustrates how AI-powered EHRs impact healthcare stakeholders, and highlights the challenges and barriers of AI adoption in EHR systems.

Introduction

Electronic Health Record (EHR), essential part of modern healthcare systems, is comprehensive digitalized patient-centred record, that gives information instantly and securely to multiple healthcare care providers and healthcare organizations. EHRs contain a wide variety of data types. The main types of EHRs data that AI can analyse could be classified in: structured, semi-structured and unstructured data. Structured data are well-organized, easily quantifiable, often stored in predefined format and structure. They include demographics (age, gender, ethnicity, address, insurance status), as well as weight/height, heart rate, blood pressure, blood group, laboratory test results, medication records (current prescriptions, dosage, timing, history of use), diagnoses and codes, procedure codes, immunization records (vaccination type, dates), allergies, metadata, and information related to generation of data. Semi-structured data are more flexible compared with structured data, mainly as a text describing smoking status, chronic disease, examination results, etc. Unstructured data, the most detailed form of data, lacks a defined structure, and includes clinical notes, surgical notes, radiology reports, audio, and video recordings [1, 2].

The history of EHRs is a story of gradual adoption over the last sixty years, accompanied by significant technological, financial, and policy-driven changes. EHRs have evolved significantly from simple data sources to integral components of the healthcare system, offering a lot of opportunities to enhance collaborative care, promote patient active engagement in their health management, and facilitate clinical research [3,4]. The projected global EHR market is $93 billion by 2035, with compound annual growth rate of 8.6% from 2024 to 2035. Growth is a consequence of increased adoption of EHR systems, rising demand for efficient healthcare data management, and integration of technologies [5]. The combination of AI with the wealth of data stored in EHR redefines its role, enabling greater benefits from digital records to improve diagnostic accuracy, reshape patient care strategies, support clinical decision-making to streamline operations, and enhance healthcare outcomes across various medical fields.

Role of AI in EHRs

Leveraging AI in EHRs improves it in different segments [6-10]

- Data entry: AI can automatically enter data into EHR by extracting information from scanned documents, clinical notes, voice recordings, saving time, reducing manual effort, and improving quality of patients' records, reducing errors.
- Data organization: AI can help sort and organize data efficiently. It can categorize patient information, making it easier to access specific details (lab results, prescriptions, or medical histories), prioritize urgent tasks.
- Virtual medical assistant is able to send reminders, answer simple patient questions.
- Automating billing/coding: AI can automatically identify the correct codes based on clinical notes and test results, reducing human error and speeding up reimbursements.
- Claims management: AI can also help in managing insurance claims by analysing patterns in rejected claims and helping healthcare providers to take proactive steps to avoid claim denials.
- Data Analysis: AI models can analyse large volumes of EHR data, and can identify patterns and trends in patient data that are not immediately obvious to clinicians and help in patient's diagnosis and management.
- Predictive Analytics: AI models can analyse EHRs historical data and risk factors, with the aim to predict a patient's likelihood of developing some disease/outcome, prioritizing the decision on the appropriate management
- Natural language processing (NLP) helps extract valuable insights from unstructured data in EHRs, such as physician notes, discharge summaries, and patient narratives; assist with the automation of medical coding by interpreting physician notes and accurately applying ICD-10 codes; Improve the accuracy of clinical documentation by identifying missing information and suggesting relevant additions or corrections.
- Automated Image and Signal Analysis: AI-driven EHRs can help in analysis of X-rays, MRIs, or CT scans, ECGs
- Clinical Decision Support: AI-powered EHRs can issue clinicians with real-time evidence-based recommendations, assist in diagnosis, provide tailored recommendations and treatment plans, analysing patient data (medical history, genetics, lifestyle factors), flag potential drug interactions, adverse drug reactions.
- Personalized Medicine: AI-driven EHR analyse clinical, genomic, proteomic data to give accurate diagnosis, optimize treatment strategies, predict drug responses, with the aim to reduce adverse reactions, improve patient outcomes personalizing care for every individual.
- Reducing Healthcare Costs: AI/EHR integration can help reduce costs by reducing readmission rates (AI can predict readmission risks based on EHR data, allowing healthcare providers to take preventive action) and optimizing resource allocation (AI can help identify underused resources, optimize staffing, and streamline hospital workflows based on patient data).

AI can help manage and streamline EHRs by automating administrative tasks and improving administrative efficiency. Streamlining administrative tasks, actually reducing healthcare workers′ burnout induced by increased administrative burden, "computer fatigue" and stress, EHRs that are not user/friendly, lack of adequate training, disruptions in patient-provider interaction, increase in workload outside of office hours, cognitive load and multitasking (interacting with patients, managing EHRs, reviewing laboratory results, etc.).

Application of AI in EHRs

The application of AI in EHR requires four steps that are important in preparing data for processing with AI [11]:

- Data collection -AI for extracting data from different healthcare providers
- Data cleaning - AI corrects errors (missing values, removes duplicates, fix inconsistencies)
- Normalisation and standardisation- AI models normalize and standardize quantitative data with the aim to adjust data to a standard scale for the purpose of comparability
- Data preservation- AI helps monitor and secure data throughout the process with the aim to enable data integrity/confidentiality.

AI-powered EHR impact on healthcare stakeholders

The impact of AI-powered EHRs spans across a variety of stakeholders (patients, healthcare providers, administrators, insurers, and policymakers). Here's a breakdown of how each is affected [12]:

- Patients benefit from improved diagnosis and treatment, faster service, reduced errors, better engagement
- Healthcare professionals' benefits from reducing administrative burden, clinical decision support, workflow optimisation
- Hospital/Clinic Administrators- benefits from improvement in operational efficiency, financial performances, quality metrics
- Developers of EHR Software - responsibility for creating systems, development, maintenance, and utilisation in clinical practice, compliance with regulative.

Integration of AI to EHR-based models: real-word implementation

There are several real-world examples of how AI is integrated with EHRs, specifically in cardiology field during last few years.

Recent evidence showed that AI tools applied to EHR data analysis enhanced accurate cardiovascular risk assessments, enable earlier interventions and personalized patients′ management, but also have implications for clinical trial design. It seems that AI models offer superior results compared with traditional risk algorithms for prediction of atherosclerotic cardiovascular disease risk, and overperformed cardiology trainees in the correct interpretation of ECG abnormalities. Literature data shows that coronary artery disease (CAD) prediction score using EHR clinical features (EHR score) predict CAD risk one year prior to diagnosis in health system [13]. Wu et al. [14] discovered the potential of natural language processing to improve the detection and diagnosis of heart failure (HF) with preserved ejection fraction patients from unstructured EHR data. It is very important because this is the predominant form of HF that is still underdiagnosed in clinical environment and connected with elevated mortality.

Using deep neural network, Raghunath et al. [15] created AI model that can predict one-year all-cause mortality from large subset of ECG voltage–time traces, even in patients whose ECG was interpreted as normal. Further, they discovered that a deep neural network could predict new-onset AF in patients without a history of atrial fibrillation, from the resting 12-lead ECG, and that this prediction may help identify those at risk of atrial fibrillation-related stroke and prevent it [16]. A novel machine learning platform that uses 12-lead electrocardiogram data, age and sex was developed to identify patients with high risk of undiagnosed structural heart disease with excellent performance, i.e., any one of seven structural heart diseases that are diagnosable by echocardiography [17]. The first report on using machine learning and EHR data to predict EF changes across a large cohort of HF patients from three academic medical centers was recently published [18]. It was shown that EHR-based deep learning model can assist clinicians in early identification patients with HF who are at risk of severe decompensation or death, and help in decision about advanced HF surgical interventions [19].

Yang et al. [20] showed that AI based on EHRs can be useful for cancer care in neoplasm categorization, methods/algorithms, application in cancer care, and data/data sets. NLP has shown significant potential in cancer research using EHRs and clinical notes, especially in breast, lung, and colorectal cancers [21]. Integration of AI with EHRs, can contribute to the quick and precise recruitment of patients in clinical trial (monitoring patients' data and determine eligibility), that can influence the effectiveness of clinical trials and receiving new cancer therapies [22].

Sarwal et al. [23] developed NLP algorithm that with high sensitivity automatically identify familial and genetic risk of pancreatic cancer from unstructured clinical notes within the EHR, that can contribute. This algorithm is the first step in identification high-risk patients who will benefit from risk-based PC screening in early, asymptomatic stage that can positively impact survival rates. Li et al. [24] established the first deep learning application to predict brain metastases in lung cancer patients diagnosed on the basis of EHR data. Last month, a new machine learning model developed to enhance prostate cancer screening by predicting the likelihood of an abnormal prostate MRI using EHR, was announced. The model analyses factors from EHR including age, prostate-specific antigen levels, prostate size (volume), and body mass index. At the same time, this model can potentially optimize the MRI utilization, potentially reducing wait times and minimizing unnecessary biopsies [25].

One of the newest applications of AI is in cardio-oncology, focused on the identification of patients at high risk for cardiovascular problems during cancer treatment who need timely to refer to cardio-oncologists and expand access to appropriate cardiovascular care. Using a large dataset of deidentified EHRs of patients with breast, kidney, B-cell lymphoma cancers and patients who receive immunotherapy,

Al-Droubi et al. [26] trained/tested the machine learning model to identify oncology patients who are at risk for cardiovascular problems during cancer treatment.
Machine learning models that use EHRs' clinical data can predict the risk of sepsis before the onset of symptoms, in early detection, diagnosis, subtyping analysis, prognosis assessment, and management of treatment [27,28]. The observational study that included non-ICU patients revealed that a machine learning causal probabilistic network algorithm model can predict sepsis within 48 hours using EHR data [29] . Nemati et al. [30] constructed a deep learning model to predict sepsis 4 hours in advance using EHR data together with high-resolution time series dynamics of heart rate and blood pressure.
In the past couple of years, studies about rare diseases and AI have the potential to significantly enhance the management of rare diseases by improving early and more accurate detection, personalizing treatment, optimizing care, predicting the progression of the disease and supporting clinical research. The integration of AI into EHR systems offers a comprehensive approach to managing these complex, multi-system disorders, ultimately improving patient outcomes and quality of life.
As EHRs are wide, precious source of information it can be used to develop and evaluate ML-based screening and NLP methods to identify rare diseases. Phenotypes and clinical signs are extracted from EHRs, and obtained data are processed to calculate phenotypic distances. Rare disease expert physicians decide whether or not to perform complementary tests to confirm the diagnosis. The rapid redirection of patients to rare disease experts via chatbots, and consultations via telemedicine should ensure faster management. The emergence of large language models opens new perspectives for the reuse of textual data that are still unexplored [31].
About fourteen EHR-based familial hypercholesterolemia screening algorithms and/or tools have described to enhance identification of familial hypercholesterolemia. Although there is no sufficient evidence supporting the use of this algorithms/ tools, they show the potential for improving population-level detection and management of patients with familial hypercholesterolemia [32].

Challenges and barriers to AI adoption in EHR
While the integration of EHRs and AI offers many benefits, there are still several challenges ranging from technical to organizational issues [11]:

- Data Privacy and Security: EHRs contain sensitive patient information, and patients′ data should always be protected according to the regulations like HIPPA and GDPR.
- Interoperability: Integration with existing systems often requires substantial technical upgrades which are expensive and time-consuming;
- Bias in AI models: In the case the AI model is trained on incomplete or non-representative dataset, it can influence the effectiveness of AI algorithms, and influence clinical decisions;
- Workforce trust, training and adaptation-Healthcare workers must be adequately trained on user-friendly interfaces and convinced that AI is a helpful tool rather than a replacement, which may require overcoming resistance to change. demystify the processes behind AI applications and build a foundation of trust and confidence.

Conclusion
The use of artificial intelligence is shaping electronic health records, paving the way for improved clinical practice and better patient outcomes.

Data Availability Statement
Data will be provided on request.

Declaration of conflict of interest
The author of this article declares that there is no conflict of interest with regard to the content
of this manuscript.

Funding
None.

Submission declaration
The work described has not been published previously in this form. The article is not under consideration for publication elsewhere.

References
1. Lee S, Kim HS. Prospect of Artificial Intelligence Based on Electronic Medical Record. J Lipid Atheroscler. 2021;10(3):282-290. doi: 10.12997/jla.2021.10.3.282.
2. Paraschiv E, Cîrnu, C, Vevera, A. (2024). Integrating Artificial Intelligence and Cybersecurity in Electronic Health Records: Addressing Challenges and Optimizing Healthcare Systems. . In: Parimala VK. Electronic Health Records - Issues and Challenges in Healthcare Systems. IntechOpen 2024. p. 1-24. doi:10.5772/intechopen.1007041
3. Kim E, Rubinstein SM, Nead KT, Wojcieszynski AP, Gabriel PE, Warner JL. The Evolving Use of Electronic Health Records (EHR) for Research. Semin Radiat Oncol. 2019;29(4):354-361. doi: 10.1016/j.semradonc.2019.05.010. PMID: 31472738.
4. Cowie MR, Blomster JI, Curtis LH, Duclaux S, Ford I, Fritz F, et al. Electronic health records to facilitate clinical research. Clin Res Cardiol. 2017;106(1):1-9. doi: 10.1007/s00392-016-1025-6.
5. Roots Analysis business research & consulting. Electronic Health Records Market. Available from: https://www.rootsanalysis.com/reports/electronic-health-records-market.html (accessed: 12/06/2025)
6. Madden A, Bekker A. Artificial intelligence for EHR: use cases, costs, challenges. ScienceSoft Healthcare. Available from: https://www.scnsoft.com/healthcare/ehr/artificial-

intelligence. (accessed 24/06/2025)
7. Tuan J. Role of AI in Electronic Health Records: Insights for Transforming Healthcare Delivery. Topflight. Available from: https://topflightapps.com/ideas/ai-in-ehr/. (accessed: 20/06/2025)
8. Munivel R. How Artificial Intelligence is Revolutionizing EHR/EMR Systems in Modern Healthcare. Kanini. Available from: https://kanini.com/blog/ai-in-ehr/. (accessed: 24/06/2025)
9. Chauhan A. AI-Driven EHR: Transforming Healthcare with Intelligent Data Solutions. Techahead. Available from: https://www.techaheadcorp.com/blog/ai-driven-ehr-transforming-healthcare-with-intelligent-data-solutions/. (accessed: 24/06/2025)
10. Parekh AE, Shaikh OA, Simran, Manan S, Hasibuzzaman MA. Artificial intelligence (AI) in personalized medicine: AI-generated personalized therapy regimens based on genetic and medical history: short communication. Ann Med Surg (Lond). 2023;85(11):5831-5833. doi: 10.1097/MS9.0000000000001320.
11. Chen YM, Hsiao TH, Lin CH, Fann YC. Unlocking precision medicine: clinical applications of integrating health records, genetics, and immunology through artificial intelligence. J Biomed Sci. 2025;32(1):16. doi: 10.1186/s12929-024-01110-w.
12. Chanallawala M. How AI-Powered EHR Systems Are Shaping the Future of Healthcare
author image. Healthray. https://healthray.com/blog/ehr/impact-ai-ehr-hospital-systems-patient-outcomes/ (accessed: 22/06/2025)
13. Petrazzini BO, Chaudhary K, Márquez-Luna C, Forrest IS, Rocheleau G, Cho J, et al. Coronary Risk Estimation Based on Clinical Data in Electronic Health Records. J Am Coll Cardiol. 2022;79(12):1155-1166. doi: 10.1016/j.jacc.2022.01.021
14. Wu J, Biswas D, Ryan M, Bernstein BS, Rizvi M, Fairhurst N, et al. Artificial intelligence methods for improved detection of undiagnosed heart failure with preserved ejection fraction. Eur J Heart Fail. 2024;26(2):302-310. doi: 10.1002/ejhf.3115.
15. Raghunath S, Ulloa Cerna AE, Jing L, vanMaanen DP, Stough J, Hartzel DN, et al. Prediction of mortality from 12-lead electrocardiogram voltage data using a deep neural network. Nat Med. 2020;26(6):886-891. doi: 10.1038/s41591-020-0870-z.
16. Raghunath S, Pfeifer JM, Ulloa-Cerna AE, Nemani A, Carbonati T, Jing L, et al. Deep Neural Networks Can Predict New-Onset Atrial Fibrillation From the 12-Lead ECG and Help Identify Those at Risk of Atrial Fibrillation-Related Stroke. Circulation. 2021;143(13):1287-1298. doi: 10.1161/CIRCULATIONAHA.120.047829.
17. Ulloa-Cerna AE, Jing L, Pfeifer JM, Raghunath S, Ruhl JA, Rocha DB, et al. rECHOmmend: An ECG-Based Machine Learning Approach for Identifying Patients at Increased Risk of Undiagnosed Structural Heart Disease Detectable by Echocardiography. Circulation. 2022;146(1):36-47. doi: 10.1161/CIRCULATIONAHA.121.057869.
18. Adekkanattu P, Rasmussen LV, Pacheco JA, Kabariti J, Stone DJ, Yu Y, et al. Prediction of left ventricular ejection fraction changes in heart failure patients using machine learning and electronic health records: a multi-site study. Sci Rep. 2023;13(1):294. doi: 10.1038/s41598-023-27493-8.
19. McGilvray MMO, Heaton J, Guo A, Masood MF, Cupps BP, Damiano M, et al. Electronic Health Record-Based Deep Learning Prediction of Death or Severe Decompensation in Heart Failure Patients. JACC Heart Fail. 2022;10(9):637-647. doi: 10.1016/j.jchf.2022.05.010.
20. Yang X, Mu D, Peng H, Li H, Wang Y, Wang P, et al. Research and Application of Artificial Intelligence Based on Electronic Health Records of Patients with Cancer: Systematic Review. JMIR Med Inform. 2022;10(4):e33799. doi: 10.2196/33799.
21. Bilal M, Hamza A, Malik N. NLP for Analyzing Electronic Health Records and Clinical Notes in Cancer Research: A Review. J Pain Symptom Manage. 2025;69(5):e374-e394. doi: 10.1016/j.jpainsymman.2025.01.019.
22. Nashwan AJ, Hani SB. Transforming cancer clinical trials: The integral role of artificial intelligence in electronic health records for efficient patient recruitment. Contemp Clin Trials Commun. 2023;36:101223. doi: 10.1016/j.conctc.2023.101223. PMID: 38034843; PMCID: PMC10682526.
23. Sarwal D, Wang L, Gandhi S, Sagheb Hossein Pour E, Janssens LP, Delgado AM, et al. Identification of pancreatic cancer risk factors from clinical notes using natural language processing. Pancreatology. 2024;24(4):572-578. doi: 10.1016/j.pan.2024.03.016.
24. Li Z, Li R, Zhou Y, Rasmy L, Zhi D, Zhu P, et al. Prediction of Brain Metastases Development in Patients With Lung Cancer by Explainable Artificial Intelligence From Electronic Health Records. JCO Clin Cancer Inform. 2023;7:e2200141. doi: 10.1200/CCI.22.00141.
25. NYU Langone urologists present at AUA's 2025 annual meeting. News release. NYU Langone Health. April 25, 2025. Available from: https://tinyurl.com/563jhau6 (accessed: 24/06/2025)
26. Al-Droubi SS, Jahangir E, Kochendorfer KM, Krive M, Laufer-Perl M, Gilon D, et al. Artificial intelligence modelling to assess the risk of cardiovascular disease in oncology patients. Eur Heart J Digit Health. 2023;4(4):302-315. doi: 10.1093/ehjdh/ztad031.
27. Yang J, Hao S, Huang J, Chen T, Liu R, Zhang P, et al. The application of artificial intelligence in the management of sepsis. Med Rev (2021). 2023;3(5):369-380. doi: 10.1515/mr-2023-0039.
28. Islam KR, Prithula J, Kumar J, Tan TL, Reaz MBI, Sumon MSI, et al. Machine Learning-Based Early Prediction of Sepsis Using Electronic Health Records: A Systematic Review. J Clin Med. 2023;12(17):5658. doi: 10.3390/jcm12175658.
29. Valik JK, Ward L, Tanushi H, Johansson AF, Färnert A, Mogensen ML, et al. Predicting sepsis onset using a machine learned causal probabilistic network algorithm based on

electronic health records data. Sci Rep. 2023;13(1):11760. doi: 10.1038/s41598-023-38858-4.
30. Nemati S, Holder A, Razmi F, Stanley MD, Clifford GD, Buchman TG. An Interpretable Machine Learning Model for Accurate Prediction of Sepsis in the ICU. Crit Care Med. 2018;46(4):547-553. doi: 10.1097/CCM.0000000000002936.
31. Germain DP, Gruson D, Malcles M, Garcelon N. Applying artificial intelligence to rare diseases: a literature review highlighting lessons from Fabry disease. Orphanet J Rare Dis. 2025;20(1):186. doi: 10.1186/s13023-025-03655-x.
32. Osei J, Razavi AC, Otchere B, Bonful G, Akoto N, Akyea RK, et al A Scoping Review of Electronic Health Records-Based Screening Algorithms for Familial Hypercholesterolemia. JACC Adv. 2024;3(12):101297. doi: 10.1016/j.jacadv.2024.101297.

Thank you for all Reviewers in 2025 year!

Abdel Gounni, University of Manitoba Investigator, Children's Hospital Research Institute of Manitoba, Department of Immunology, Manitoba
Ádám Balogh, Debrecen, Hungary
Adil I. Khan, Temple University, Department of Pathology and Laboratory Medicine, USA
Admir Nake, University of Medicine, Tirana, Albania
Afif Ba, Military Hospital of Instruction of Tunis: Hopital Militaire Principal d'Instruction de Tunis, Department of Biochemistry Laboratory, Tunisia
Altaf Ahmad Mir, All India Institute of Medical Sciences, Department of Biochemistry, Raebareli, India
Angela W.S. Fung, The University of British Columbia, Department of Pathology and Laboratory Medicine, Canada
Anikha Bellad, Institute of Bioinformatics, Department of Proteomics, Bengaluru, India
Anisha Mathew, Lady Hardinge Medical College, Department of Biochemistry, Moti Nagar, New Delhi
Arshiya Anjum, BIACH&RI: Basavatarakam Indo-American Cancer Hospital and Research Institute, Department of Clinical Biochemistry, India
Ashishkumar Mohanbhai Agravatt, Biochemistry Department PDU Medical College Rajkot, Gujarat, India
Ayan Banerjee, Department of Physical Sciences, Center of Excellence in Space Sciences, Kolkata, India
Aysha Habib, The Aga Khan University Hospital, Pathology and Laboratory Medicine, Karachi, Pakistan
Barna Vásárhelyi, Semmelweis Egyetem, Department of Laboratory Medicine, Budapest, Hungary
Béla Nagy, University of Debrecen, Faculty of Medicine, Debrecen, Hungary
Bettina Chale-Matsau, University of Pretoria and National Health Laboratory Service, Department of Chemical Pathology, South Africa
Bianka Hoxha, Catholic University Our Lady of Good Counsel: Universita Cattolica Nostra Signora Del Buon Consiglio, Department of Chemical - Pharmaceutical and Biomolecular Technologies, Albania
Bremansu Osa-Andrews, University of Florida, Department of Pathology, USA
D.V Satyamurthy G, AIIMS Madurai: All India Institute of Medical Sciences Madurai, Department of Biochemistry, India
David Alter, Emory University School of Medicine, Department of Pathology and Laboratory Medicine, USA
Deepak Parchwani, All India Institute of Medical Sciences, Department of Biochemistry, Rajkot, Gujarat, India
Dipuo Dephney Motshwari, SAMRC: South African Medical Research Council, South Africa
Edgard Delvin, CHU Sainte-Justine Research Center, Montréal, Québec, Canada
Eiman Shahrour, Tishreen University, Department of Laboratory diagnosis, Syrian Arab Republic
Ekta Debnath, Lady Hardinge Medical College, Department of Biochemistry, Moti Nagar, New Delhi
Ellis Jacob, EJ Clinical Consulting, LLC, USA
Eloisa Urrechaga, Hospital Galdakao-Usansolo, Galdakao, Bizkaia, Spain
Farhan Javed Dar, International Medical Center, Department of Pathology, Laboratory Medicine & Blood Bank, Saudi Arabia
Gábor Nagy, University of Debrecen, Faculty of Medicine, Debrecen, Hungary
George Abdo, Poria Medical Center, The Baruch Padeh Medical Center Poriya, Central Laboratory, Nofhagalil, Isreal
Harjit Pal Bhattoa, Department of Laboratory Medicine, University of Debrecen, Hungary
Hicham Chemsi, Hassan II University, Faculty of Medecine and Pharmacy, Department of Biochemistry Laboratory, Casablanca, Morocco
Indika Neluwa-Liyanage, University of Sri Jayewardenepura Faculty of Medical Sciences, Deparment of Biochemistry, Nugegoda, Sri Lanka
János Kappelmayer, University of Debrecen, Faculty of Medicine, Debrecen, Hungary
Jayesh Warade, Meenakshi Labs Madurai GH in Shenoy Nagar, Madurai, India
Jayson Pagaduan, Intermountain Health, Department of Central Laboratory, USA
Joe Wiencek, Vanderbilt University School of Medicine, Pathology, Microbiology, and Immunology, USA

John Anetor, University of Ibadan, Chemical Pathology, Nigeria
Juan Carlos Gomez de la Torre, Faculty of Chemical Sciences, Universidad Autónoma de San Luis Potosí, Mexico
Judit Bedekovics, University of Debrecen, Department of Pathology, Debrecen, Hungary
Julia Peacock, SUNY Broome: SUNY Broome Community College, USA
K ArulJothi, SRM Institute of Science and Technology (Deemed to be University), Department of Genetic Engineering, India
Karthick E, Sri Ramachandra Medical College and Research Institute: Sri Ramachandra Institute of Higher Education and Research (Deemed to be University), Department of Biochemistry, India
Katia Al-Sawalha, American University of Madaba, Department of Medical Laboratories, Madaba, Jordan
Keerthy Rethinam, Sri Ramachandra Institute of Higher Education and Research (Deemed to be University), Department of Biochemistry, Tamil Nadu, India
Laura Sciacovelli, Padua University Hospital: Azienda Ospedale Universita Padova, Padova, Italy
Luis Edgardo Figueroa Montes, Hospital III Suarez Angamos - Seguridad Social , Lima-Peru / Expresidente Asociacion Medica Peruana de Patologia Clinica, Department of Clinical Pathology, Lima, Peru
Lydia Peris, Vall d'Hebron Hospital, Hospital Universitari Vall d'Hebron, Department of Clinical Biochemistry, Spain
Maria del Carmen Pasquel Carrera, Centro Especializado de Analisis, Pichincha, Ecuador
Meita Hendrianingtyas SpPK(K), Clinical Pathology Study Program, Faculty of Medicine, Diponegoro University, Indonesia
Mihilie Sathira Kulasinghe, Lady Ridgeway Hospital for Children, Department of Chemical Pathology, Gampaha, Sri Lanka
Morley Hollenberg, University of Calgary, Department of Physiology and Pharmacology, Canada
Mithu Banerjee, All India Institute of Medical Sciences - Jodhpur, India
Mohammad Imteyaz Ahmad, Dubai Hospital, Department of Laboratory Medicine and Pathology, United Arab Emirates
Moslem Jafarisani, Shahroud University of Medical science, Faculty of Medicine, Iran
Naciye Leyla Acan, Hacettepe Universitesi Tip Fakultesi, Department of Medical Biochemistry, Ankara, Türkey
Nafija Serdarevic, Depatment of Clinical Biochemistry, Clinical Center, Sarajevo, Bosnia and Herzegovina
Nayab Afzal, Aga Khan University Hospital, Pathology and Laboratory Medicine, Karachi, Pakistan
Nilda Fink, Fundacion Bioquimica Argentina, Programa PROES, Buenos Aires, Argentina
Péter Antal-Szalmás, University of Debrecen, Faculty of Medicine, Debrecen, Hungary
Pradeep Kumar Dabla, Department of Biochemistry, GB Pant Institute of Postgraduate Medical Education & Research (GIPMER), India
Rahinaz Usman Bedrabettu, Yenepoya University, Department of Biochemistry, India
Rajlaxmi Tiwari, Siksha O Anusandhan University Institute of Medical Sciences and SUM Hospital, Deparment of Biochemistry, Odisha, India
Raúl Héctor Girardi, Fundación Bioquímica Argentina, Un Programa de Evaluación Externa de la Calidad (PEEC), Buenos Aires, Argentina
Robin Williams, WA Health, Government of Western Perth, Australia
Roshnara Puthan Peedikakkal, RajaRajeswari Medical College & Hospital, Department of Biochemistry, India
Sándor Baráth, University of Debrecen, Faculty of Medicine, Debrecen, Hungary
Sathya Selvarajan, MGM Healthcare, Tamil Nadu, India
Seema Bhargava, Sir Ganga Ram Hospital, Department of Biochemistry, India
Shanel Raghubeer, Cape Peninsula University of Technology, Biomedical Sciences, South Africa
Shivani Singh, Dr Ram Manohar Lohia Institute of Medical Sciences, Department of Biochemistry, India
Shubha Jayaram, Mysore Medical College and Research Institute, Depatment of Biochemistry, Karnataka, India
Sibtain Ahmed, The Aga Khan University Hospital, Pathology and Laboratory Medicine, Pakistan
Sindhu Harish, Kasturba Medical College Mangalore, Department of Biochemistry, India
Som Dev, All India Institute of Medical Sciences, Depatment of Biochemistry, Kalyani, India
Sukhes Mukherjee, AIIMS Bhopal, Department of Biochemistry, India
Sutirtha Chakraborty, Fonna Hospital Trust, Department of Laboratory Medicine, Rogaland, Norway
Terry Gbaa, JB Consulting Limited, Department of Clinical Biochemistry, UK
Thathsarani Pathirana, Teaching Hospital Badulla, Department of Chemical Pathology, Badulla, Sri Lanka
Udara Dilrukshi Senarathne, University of Sri Jayewardenepura Faculty of Medical Sciences, Biochemistry, Nugegoda, Sri Lanka
Wasan A.M. Al Taie, American University of Ras Al Khaimah School of Arts and Science, Department of Mathematics and Natural Sciences, Ras Al Khaimah, United Arab Emirates
Xavier Arus Morato, Ace Alzheimer Center Barcelona, Barcelona, Spain
Yenice Sedef, Group Florence Nightingale Hospital, Grup Florence Nightingale Hastaneleri, Department of Biochemistry, Istanbul, Türkey

Publisher: IFCC Communications and Publications Division (IFCC-CPD)

The eJIFCC is a member of the **Committee on Publication Ethics (COPE).**

The eJIFCC (Journal of the International Federation of Clinical Chemistry)
is an electronic journal with frequent updates on its home page. Our articles, debates, reviews and editorials are addressed to clinical laboratorians. Besides offering original scientific thought in our featured columns, we provide pointers to quality resources on the World Wide Web.

Published by:

IFCC International Federation of Clinical Chemistry and Laboratory Medicine

www.ifcc.org